



Universiteit
Leiden
The Netherlands

Control of replication associated DNA damage responses by Mismatch Repair

Ijsselsteijn, R.

Citation

Ijsselsteijn, R. (2023, October 26). *Control of replication associated DNA damage responses by Mismatch Repair*. Retrieved from <https://hdl.handle.net/1887/3655391>

Version: Publisher's Version

License: [Licence agreement concerning inclusion of doctoral thesis in the Institutional Repository of the University of Leiden](#)

Downloaded from: <https://hdl.handle.net/1887/3655391>

Note: To cite this publication please use the final published version (if applicable).

Control of replication associated DNA damage responses by Mismatch Repair

Robbert Ijsselsteijn

ISBN: 978-94-6483-285-3

© Copyright 2023 by Robbert Ijsselsteijn. All rights reserved

Cover design & layout: Robbert Ijsselsteijn

Printed by: Ridderprint, www.ridderprint.nl

No part of this thesis may be reprinted, reproduced or transmitted in any form or by any means without the expressed, written consent of the author or, if applicable, of the publisher of the article(s)

Control of replication associated DNA damage responses by Mismatch Repair

Proefschrift

ter verkrijging van

de graad van doctor aan de Universiteit Leiden,
op gezag van rector magnificus prof. dr. ir. H. Bijl,
volgens besluit van het college voor promoties
te verdedigen op donderdag 26 oktober 2023
klokke 11.15 uur

door

Robbert Ijsselsteijn
geboren te Gouda
in 1992

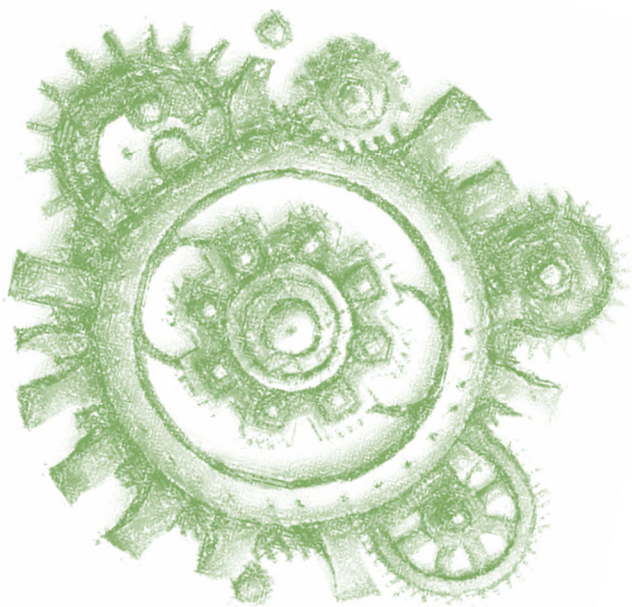
Promotor: Prof. dr. M. Tijsterman

Co-promotor: Dr. J. G. Jansen

Leden promotiecommissie: Prof. dr. ir. S. M. van der Maarel
Prof. dr. T. K. Sixma, Nederlands Kanker Instituut
Dr. H. Vrieling
Dr. J. H. G. Lebbink, Erasmus MC

Table of Contents:

Chapter 1	General Introduction	5
Chapter 2	DNA mismatch repair-dependent DNA damage responses and cancer	29
Chapter 3	Characterizing the role of mismatch repair components in the ultraviolet light-induced post-translesion synthesis repair pathway	43
Chapter 4	Elucidating the genetic entanglement of translesion synthesis and mismatch repair during the ultraviolet light-induced DNA damage response	79
Chapter 5	Induction of mismatch repair deficiency, compromised DNA damage signaling and compound hypermutagenesis by a dietary mutagen in a cell-based model for Lynch syndrome	107
Chapter 6	Discussion and future perspectives	143
Appendices	Summary	159
	Samenvatting	
	Curriculum Vitae	
	Dankwoord	





Chapter 1: General introduction



General Introduction:

The integrity of our genomic DNA is essential for a healthy life, but is continuously threatened upon exposure to DNA damaging agents that are omnipresent; the oxygen we breath, the sunlight we often enjoy and the food we eat can result in damage to the DNA of our cells (1). DNA damage alters the structure of the DNA and as such it interferes with the work of DNA and RNA polymerases (1, 2). Persistent damage can ultimately result in genomic instability which, in germ cells, positively contributes to evolution, but can also lead to heritable diseases. In somatic cells mutagenesis is mainly known for its role in cancer. To mitigate the harmful effects of DNA damage cells activate DNA damage responses, including cell cycle arrest, activation of DNA repair pathways, senescence and apoptosis (3).

Understanding the control of DNA damage-induced mutagenesis may contribute to the treatment or prevention of cancer. This chapter describes factors that control the DNA damage response, including DNA damage signaling and mutagenesis, with particular attention to DNA damage induced by ultraviolet light (UV) and by 2-Amino-1-methyl-6-phenylimidazo(4,5-b)pyridine (PhIP), two genotoxic agents related to cancer formation in the skin and the gastro-intestinal tract, respectively. The final part of this chapter deals with DNA mismatch repair (MMR), a pathway which main function is thought to be the correction of misincorporations by DNA polymerases. However, MMR may also play an important role in the cellular response to DNA damage.

The risk of being a carnivore on a sunny day: cancer

For diurnal life one of the most common sources of DNA damage is UV radiation from sunlight. Although limited sunlight exposure seems beneficial for human health (4), too much exposure is correlated with skin cancer development (5). Globally, the incidence of skin cancer was over 1.5 million in 2020 (6) and over the years incidence has been rising steadily (5). Skin cancer is a heterogeneous disease and can be divided based on the cell type of origin; basal cell carcinomas, squamous cell carcinomas, sebaceous carcinomas and melanocyte originated melanomas (7, 8). The different skin cancer types have different mortality rates, with melanomas being the most lethal and non-melanoma skin cancers being relatively harmless, if diagnosed early on (5). The difference in mortality may be explained by the propensity of melanomas to invade and metastasize, whereas the non-melanoma skin cancers remain more localized (9). Skin cancer incidence is markedly different between different population groups, with skin cancer being the most common cancer in Caucasians (5). White skin contains the least amount of melanin and provides the least protection against sunlight highlighting the importance of UV-radiation as the driving etiological factor in skin cancer (10). UV-light is divided into three groups, UVA (320-400 nm), UVB (280-320 nm) and UVC (200-280 nm). Wavelengths under 315 nanometer are effectively filtered by the ozone layer and thus skin tissue is mostly exposed to UVA and UVB wavelengths (11). UVA is weakly mutagenic and produces both oxidative lesions and low levels of cyclobutane pyrimidine dimers (CPD) (12), while UVB is more mutagenic and produces high levels of CPD and lower levels of 6-4 photoproducts (6-4PP) (11). Following a 30 minutes exposure to sunlight on a clear day, skin cells accumulate nearly two hundred thousand CPD per genome, which lesion frequency is approximately 5-fold higher than the number of endogenous DNA lesions occurring in each human cell during a whole day (13, 14). Photolesions are formed by direct absorption of UV light by DNA resulting in intrastrand crosslinks between two adjacent pyrimidines, but CPD only mildly distort the DNA helix structure, whilst 6-4PP heavily distort the DNA helix (11). This results in 6-4PP being recognized by DNA repair mechanisms more rapidly than CPD (15). As such, sunlight-induced mutagenesis mostly comes from CPD produced by exposure to UVB radiation (16). UVB-induced CPD lesions in human skin are found most often at thymidine-thymidine dimers followed by thymidine-cytosine dimers, whilst cytosine-thymidine and cytosine-cytosine dimers are found least often (17). Curiously, the mutational signature of skin tumors is characterized by mutations on cytosines, specifically cytosine to thymidine transitions and not by mutations on the more commonly induced thymidine CPD (18). This may be explained by deamination of cytosine CPD adducts and the subsequent replication of these deaminated cytosines resulting in aforementioned C>T transitions (18). Moreover, replication of thymidine CPD is a relatively error-free process whereas replication of cytosine CPD more often results in replication errors (19).

Another common source of DNA damage is the diet and this is often associated with the development of colorectal cancer (CRC) (20, 21). CRC is the third most common cancer type world-wide, with nearly 2 million new cases in 2020 and a mortality of

nearly 1 million (6). Moreover, incidence is significantly higher in developed countries, such as those in North America and Western Europe, while the lowest incidence is found in countries found on the African continent (6). Importantly, in developing countries, such as those found in Eastern Europe and Eastern Asian regions, CRC incidence is strongly on the rise (20). The most likely explanation for these geographic difference in CRC incidence are life-style factors such as a diet, consisting of high caloric intake and red meat, and reduced amounts of physical activity, which is more often observed in rapidly developing and wealthy countries (21, 22). Mortality, however, is declining in developed countries as gastro-intestinal screening procedures have been implemented for those at highest risk, due to age or genetic background (23).

It is long known that life-style factors influence CRC development and more than a few DNA damaging compounds have been identified in the diet. Nitrosamines found in, amongst others, processed/cured meats and smoked/salted fish is thought to damage the DNA by forming toxic aldehydes inducing alkylation damage (24). Other dietary mutagens are primary aromatic amines, found in certain food packaging that can subsequently transfer into the food. Moreover, smoking meat can also result in the formation of polycyclic aromatic hydrocarbons, chemical compounds that are associated with CRC as well (25). Another group of common mutagens that are associated with CRC development are the heterocyclic amines (HCA). It has been shown that especially grilling meat at high temperatures results in increased generation of HCA which differs per preparation method and meat type (Table 1). Of all the various HCA, PhIP is the most abundant and seems to be the most mutagenic in mammalian cells (26). PhIP only becomes mutagenic when metabolically activated by the liver after which PhIP is actively transported to the intestines for clearance. Here, PhIP metabolites can react with DNA of intestinal (stem) cells (26, 27). Indeed, measurements of PhIP adducts in human colorectal mucosa show the presence of several PhIP adducts per 10^8 bases (27). In detail, PhIP damages the DNA by binding to the C8-position of guanines resulting in cellular toxicity and increased mutagenesis (28). Not surprisingly, spectra of mutations induced by PhIP consist of mutations specifically on guanines which mostly are guanine to thymidine transversions and guanine to adenine transitions (26). Spectra of PhIP-induced mutations most resemble the COSMIC mutagenic signatures SBS4, SBS18 and SBS29 (29). Interestingly, these signatures do not seem to overlap one-to-one with the CRC mutational signatures. This may be explained by the fact that, unlike skin cancer, where sunlight exposure results in an easy to interpret mutational spectrum, the mutational spectrum of CRC is influenced by many sources and types of DNA damaging agents resulting in scattered mutational signatures. A total of 8 different mutational signatures are found in CRC samples with etiologies ranging from age, defective DNA repair, defective replication proofreading and tobacco chewing (30). A definitive diet-related signature has yet to be uncovered, but epidemiological studies paint a clear picture: there is a significant correlation between intake of DNA damaging agents and colon cancer (21, 31, 32).

Table 1:

Concentrations of PhIP (ng/g) in types of meat at various stages of doneness and preparation methods. Adapted from Gibis *et al.* (133).

Meat:	Temperature (°C)	Time (min)	PhIP (ng/g)
Ground beef patties (fried)	150	4-20	nd-1.8
	230	4-20	1.3-3.2
	277	12	68
Chicken (pan fried)	197-221	14-36	12-70
Chicken (roasted)	175-240	24-40	nd
Pork patties (pan-fried)	177-225	9-21	0.3-10.5
Pork patties (broiled)	177-225	9-21	nd-2.7
Bacon (oven-broiled)	175	7.5	15.9
Bacon (pan-fried)	176	16.1	4.9

Replication fork stalling and the activation of DNA damage signaling

An important line of defense against DNA damage is the activation of DNA damage signaling. When DNA damage stalls the replication machinery it generates single stranded (ss)DNA due to the uncoupling of DNA polymerases and helicases (33). ssDNA is inherently fragile and may break causing toxic double stranded DNA breaks (DSB). To prevent this from happening ssDNA is coated with heterotrimeric Replication Protein A (RPA) to stabilize it (33). This coating also attracts the kinase Ataxia Telangiectasia and Rad3 related (ATR) via its binding partner ATR-Interacting Protein (ATRIP) (34). In parallel, at 3' junctions of ssDNA and dsDNA, the Rad9-Rad1-Hus1 complex is loaded leading to the recruitment of TopBP1 that can also activate the ATR kinase (35). The activation of ATR, in turn, is an important event branching out in the activation multiple downstream effectors (36), the most well-known being Checkpoint Kinase 1 (CHK1). ATR phosphorylates CHK1 at serines 317 and 345 resulting in cell cycle arrest, transcription - and replication regulation and promotion of DNA repair.

DNA damage can also result in DSB, which upon processing activates DNA damage signaling. Two apical kinases are activated upon DSB generation, namely DNA-dependent Protein Kinase catalytic subunit (DNA-PKcs), which is recruited by Ku80 and is mainly involved in DSB repair, and Ataxia Telangiectasia Mediated (ATM), which has a wide-array of downstream effectors (36). In vitro, ATM is recruited and activated by members of the Mre11-Rad50-Nbs1 (MRN) complex at the site of damage (37, 38), although there is some MRN-independent activation reported (36). ATM in turn can activate the tumor suppressor p53 responsible for cell cycle arrest, senescence or apoptosis (36). Moreover, ATM is known to phosphorylate H2AX, a modification known as γH2AX, which triggers a chromatin-based signaling cascade that may amplify the DSB signaling and promote repair (39). Chromatin is also modified by KAP-1 which relaxes chromatin formation and promotes DSB repair upon phosphorylation by ATM

(40, 41). Finally, ATM also stimulates DSB repair by promoting DSB end resection, exposing stretches of ssDNA that are required for the DSB repair pathway homologous recombination (HR) (36).

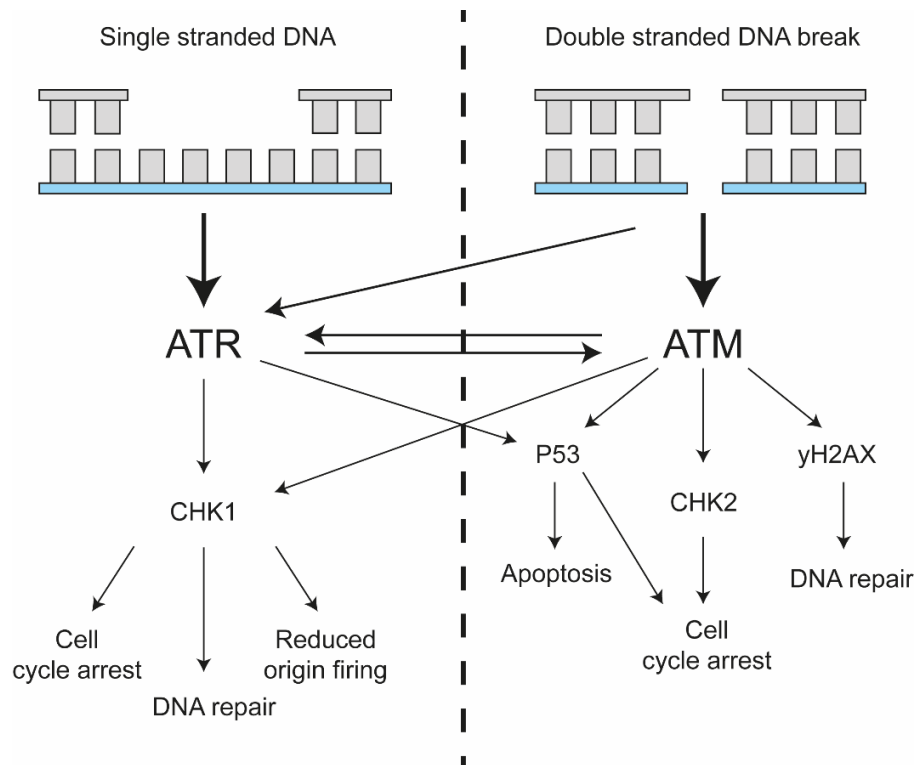


Figure 1: Simplified overview of the ATR/ATM DNA damage signaling axes

Persistent single stranded DNA (ssDNA) formations can activate ATR to induce a range of protective responses. The main effector kinase of ATR is CHK1 and activation of CHK1 can result in reduced origin firing, cell cycle arrest and increased DNA repair. Double stranded DNA breaks (DSB) can activate both ATR and ATM. Both pCHK2 and P53 can induce cell cycle arrest, phosphorylated H2AX can stimulate (DSB) DNA repair and apoptosis can be triggered via P53. ATM and ATR display overlapping substrate specificities, for instance ATR can activate P53 and ATM may activate CHK1.

Obviously, the ATR/ATM signaling axes are intermingled: ATR, activated by ssDNA, can be recruited to a DSB after resection (42, 43) and ATM can be recruited to DSB formed when ssDNA formations break (36, 44). Moreover, there also seems to be significant overlap between the substrates of ATM and ATR: both ATM and ATR can activate p53 as well as CHK1 (Fig. 1) (36, 45, 46).

DNA repair pathways to prevent genome instability

One of the outcomes of DNA damage signaling is the promotion of the various DNA repair pathways (36). DNA damage comes in many forms, such as the aforementioned DSB, intrastrand crosslinks (such as those induced by UV), helix-distorting DNA lesions (such as those induced by PhIP), interstrand crosslinks and adducts resulting from exposure to alkylating and oxidating agents. Moreover, many of these lesions stall the replication machinery leading to formation of ssDNA. Each DNA lesion type is associated with one or more DNA repair pathways that are able to remove the damage

and restore the normal DNA structure (Table 2), thereby preventing mutagenesis. Therefore, loss of any of these pathways often results in cancer formation. For instance, loss of HR is often found in breast cancer (47) and loss of nucleotide excision repair (NER), which repairs bulky and helix-distorting lesions like those induced by UV, results in skin cancer and other skin-associated malignancies (48). When a DNA lesion goes unrepaired it may lead to different outcomes based on lesion type and lesion density. For instance, DNA damage from alkylation and oxidation are sometimes still instructive and mis-instruct DNA polymerases during replication leading to point mutations (49, 50). The more toxic lesion types such as bulky and DNA helix distorting adducts always stall the replication machinery, resulting in stretches of ssDNA that can become DSB (44, 51, 52). DSB can cause large genomic rearrangements, especially when they are repaired by error-prone end joining pathways (53). Loss of one copy of a segment of DNA, also known as loss of heterozygosity (LOH), is a term closely associated with cancer, as LOH is an important genetic event contributing to the loss of tumor suppressor genes (54). LOH is especially dangerous for individuals that have inherited a dysfunctional copy of a tumor suppressor gene, for instance inheritance of a faulty copy of *BRCA2*, an important gene in the aforementioned HR DNA repair pathway. Indeed, these *BRCA2*-heterozygous cells become HR-deficient more easily, thus resulting in a predisposition for cancer (55).

Table 2: The varying types of DNA damage are caused by different sources, repaired by specialized DNA repair pathways and replicated by different polymerases. Abbreviations: BER (Base Excision Repair), MMR (Mismatch Repair), NER (Nucleotide Excision Repair), FA (Fanconi Anemia), HR (Homologous Recombination), alt/canonical NHEJ (alt/canonical Non-Homologous End Joining), SSBR (single strand break repair).

DNA damage type:	Example sources:	DNA Repair Pathways:	Polymerases:
Alkylating	Diet, Bile, cytostatic drugs (134-136)	Methyltransferases, BER, NER (50)	Replicative/TLS (137)
Oxidating	Mitochondria, inflammation (138, 139)	BER, MMR, NER (140)	Replicative/TLS (141-143)
Helix distorting	Diet, UV (11, 133)	NER (144, 145)	TLS (62)
Interstrand crosslinks	Diet, cytostatic drugs (146)	FA, NER, HR (146)	TLS (147)
Double stranded DNA break	Ionizing radiation, stalled replication forks, repair intermediates (148)	alt/canonical NHEJ, HR (149, 150)	Replicative/TLS (150, 151)
Single stranded DNA break	Repair intermediates, Oxidation (152, 153)	SSBR (152, 153)	Replicative/PolB (152, 153)

When DNA damage persists: DNA damage tolerance

In replicating cells, DNA lesions that escape repair can result in stalling and eventual collapse of the replication fork which results in the generation of DSB (44). To prevent DSB-associated mutagenicity and toxicity the cell activates DNA damage tolerance (DDT) mechanisms that allow replication of a damaged DNA template (56). Two major pathways for DDT have so far been uncovered: an error free pathway called template switching and translesion synthesis (TLS), an inherently error-prone pathway (56). Coordination which pathway performs the bypass seems to be directed post-translational modifications at the ring-forming, homotrimeric Proliferating Cell Nuclear Antigen (PCNA). The PCNA ring encircles DNA, keeps DNA polymerases on the DNA and acts as a sliding clamp during DNA replication. PCNA mono-ubiquitination by Rad18 at lysine 164 is suggested to trigger TLS bypass (57), although TLS may also be activated independently from PCNA ubiquitination (58, 59). Conversely, template switching seems to be activated in vitro by SUMOylation or polyubiquitination at lysine 164 of PCNA (57, 60, 61), however in vivo data for template switching and its biological relevance is scarce. So far two modes of action have been postulated for template switching: recombination-mediated template switching, in which the replicating strand invades the already synthesized sister chromatid and template switching by fork reversal (56). Fork reversal occurs upon annealing of the nascent DNA strands and reannealing of the parental strands of a replication fork resulting in a four-way “chicken foot” structure. Both of these mechanisms are best explained visually and Chang et al. have published a clear picture of how this may work (56).

TLS does not require a sister chromatid and bypasses the damage by replicating the damaged nucleotides directly. TLS is comprised of specialized DNA polymerases that, as compared with replicative DNA polymerases, have a more relaxed open catalytic domain that can more easily encompass damaged nucleotides (62). Moreover, TLS polymerases contain no proofreading domains, allowing for the bypass without getting stuck on probable mis-incorporations (62). TLS is split into two main families, the Y-family polymerases (REV1, Eta/η, Iota/ι, Kappa/κ) and the B-family polymerase Polζ (63). Generally speaking, a Y-family polymerases performs the initial nucleotide insertion opposite the damaged nucleotide and the B-family polymerase extends past the damaged nucleotide before replicative polymerases can take over. However, studies have shown that TLS is more complex, for instance, Polk can also perform the extension step at certain lesions in vitro (64, 65). Moreover, PrimPol, a member of the archaeal eukaryotic primases is important in restarting replication downstream of the lesion (66), but also displays polymerase activity and can bypass oxidative and UV lesions in human cells (67-69). Lastly, Polymerase Theta, a member of the A-family of DNA polymerases, has also been shown to perform TLS in human fibroblasts (70, 71).

Due to a more relaxed catalytic domain and lack of proofreading, TLS is a relatively error-prone process and can sometimes be inefficient, however, this differs per lesion and polymerase (72). For instance, the bypass of T-T CPD lesions by Polη is efficient and relatively error-free, whereas deficiency for Polη results in error-prone bypass by Polk, Polι or Polζ and increased UV-sensitivity in both mouse embryonic fibroblasts

and human cells (19, 73, 74). Conversely, C-C CPD is bypassed in an error-prone manner by Pol η due to the deamination of cytosine to uracil. Uracil originating from cytosine CPD is bypassed “correctly” by Pol η and matched with adenine, thus resulting in the well-known C>T mutations that are found in UV-induced skin cancers (75). Furthermore, in MEF, the strongly helix-distorting 6-4PPs depend on TLS polymerases Rev1/Pol ζ for bypass (76) and not on Pol η . Another type of bulky lesions often found in human DNA will be those induced by the diet related chemical PhIP. The dG-C8-PhIP adduct is mostly bypassed by Rev1 in vitro, and the subsequent extension reaction is performed by Pol κ (64). The bypass by Rev1 is also relatively error-free, as Rev1 exclusively incorporates cytosines opposite the damage (77).

Importantly, the bypass of DNA lesions by TLS results in quenching of DNA damage signaling, as the replication fork is no longer stalled and patches of ssDNA are converted to dsDNA (78). This prevents replication fork collapse, DSB formation, persistent signaling and apoptosis. As such control of TLS is key in the balance between mutagenesis and apoptosis; too much error-prone bypass can lead to DNA-associated diseases such as cancer, but too little leads to excessive apoptosis and senescence resulting in rapid aging syndromes and developmental issues as is seen in mice with TLS defects (79, 80).

Control of TLS

Control of TLS is important to minimize the negative effects of this pathway. TLS is controlled on multiple levels: the expression levels of TLS polymerases, post-translational modifications, recruitment of TLS polymerases to the lesion and competition with other DNA polymerases. Expression levels of TLS polymerases during different phases of the cell cycle have been measured in mammalian cells and no significant differences were found for most TLS pols tested, except for Pol η which is slightly higher expressed in G2 (81). Also, the overall mutagenicity of TLS opposite 6-4PP or (+)-trans benzo(a)pyrene diolepoxide N2 guanine (N(2)-BPDE-dG), an important food and tobacco smoke adduct, is similar between the different cell cycle stages, however there is a cell stage specific mutagenic signature (81). This may highlight two different modes of TLS-mediated bypass. When a mildly distorting lesion such as a CPD is encountered it may be bypassed directly, also known as “on the fly”, without repriming of the replication machinery (Fig.2). In contrast, when a lesion is strongly DNA helix distorting, such as a 6-4PP, the replication machinery reprimates downstream of the lesion (82) (Fig. 2) leaving a ssDNA gap. At a later stage these ssDNA gaps are likely filled in, in a more error-prone fashion, dependent on Pol ζ and Rev1 (76). Moreover, microRNA is shown to regulate TLS activity further by directly inhibiting the expression of Rev1 or by regulating the expression of Rad18, thus affecting TLS recruitment (83). The activity of TLS polymerases is also regulated by post-translational modifications. For instance, using a cell-free model with purified human proteins, it was shown that phosphorylation of Pol η results in release of sequestration by PDIP38 and an increase in its binding strength to PCNA (84). Moreover, in yeast, Rev1 is phosphorylated in response to DNA damage and this

phosphorylation is, at least in a NER-deficient background, required for proficient TLS (85, 86).

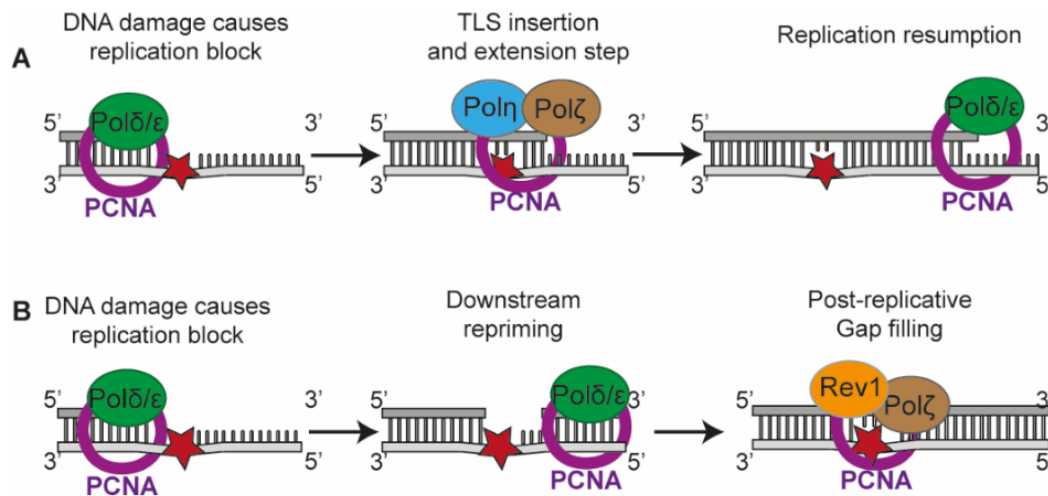


Figure 2: Modes of action for TLS

TLS can be performed in two ways: either “on the fly” during replication or post-replicative gap filling. A: After a replication block at a DNA lesion (asterisk) an inserter TLS polymerase is recruited (like Pol η) to replicate the DNA lesion followed by extension by an extender polymerase (for instance Pol ζ). Lastly, replicative polymerases can take over again and proceed replicating the DNA. B: During persistent replication blockage the replication machinery can also be reprimed downstream of the lesion to continue DNA synthesis. Afterwards post-replicative TLS gap filling takes place dependent on TLS polymerases Rev1 and Pol ζ .

How polymerases are chosen and compete with each other is still a matter of debate. One theory is the model of a “molecular toolbelt” in which PCNA is a kind of polymerase hub that binds multiple TLS polymerases directly or via the “molecular bridge” Rev1. Most TLS polymerases actually have binding domains specifically for PCNA in support of this idea (87). Thus, when PCNA stalls on a lesion, replicative polymerases are replaced by TLS polymerases until the bypass is completed before switching back. Moreover, Pol ζ shares the subunits Pol31 and Pol32 with Pol δ . These subunits are important for PCNA-mediated TLS. Pol32 interacts with PCNA, thus it seems likely that Pol ζ and Pol δ compete directly for access to the PCNA sliding clamp (88). Mono-ubiquitination of PCNA has been suggested to play a major role here, which stimulates the activity of TLS polymerases and allows them to outcompete replicative polymerases (87). Yet, studies in mammalian cells have shown that PCNA mono-ubiquitination is not always essential for TLS bypass. For instance, binding of Pol η to PCNA does not require PCNA mono-ubiquitination in human cells (58). Moreover, in MEF mutated to prevent PCNA mono-ubiquitination, approximately 30% of TLS activity remains (59). This shows that PCNA mono-ubiquitination is important for regulating TLS, but not essential.

Mutagenicity of TLS polymerases might also be controlled more directly. Although TLS polymerases do not exhibit proofreading activity themselves, they may be assisted by

replicative DNA polymerases that can proofread. In yeast it has been shown that Pol α errors may be corrected by Pol δ (89).

Moreover, simultaneous loss of both proofreading activities of Pol δ and Pol ϵ resulted in mutagenesis higher than the sum of loss of the single proofreading activities, suggesting in trans proofreading (90). As such Pol δ or Pol ϵ may also proofread TLS errors to minimize the mutagenicity of lesion bypass. In fact, in human cells it has been shown that when Pol η creates a mismatch further extension from this mismatched terminus becomes much slower allowing for proofreading by Pol δ or Pol ϵ (91). However, further research has to be done to show this for other TLS polymerases, too.

MMR and the control of replication errors

The bulk of the DNA is undamaged and is replicated by the replicative polymerases. In short Pol α creates template primers and the replicative polymerases Pol δ /Pol ϵ start replicating from these primers and do so either in a continuous manner during leading strand synthesis (Pol ϵ) or discontinuous during lagging strand synthesis (Pol δ) (92). DNA replication on undamaged templates has a very low error-rate with approximately 1 error per billion bases (63). This high fidelity can be attributed to three factors: (I) the tight catalytic domain steering proper base pairing, (II) the proofreading domain that identifies and allows for the removal of mismatches and (III) post-replicative MMR (63). The MMR pathway is able to identify and excise misincorporations that slip through proofreading thereby increasing the fidelity of DNA replication by a factor between hundred to thousand-fold and protecting cells from mutagenesis (63, 93). The MMR pathway was first identified in the 1970s in prokaryotes (94, 95) and was soon after studied in one of the simpler eukaryotic systems, *Saccharomyces cerevisiae*, before ultimately being translated to humans. A simple description of eukaryotic MMR follows four steps: (I) identification of a mismatch by MSH2/MSH6 (MutS α) or MSH2/MSH3 (MutS β), (II) nicking of the daughter strand by MLH1/PMS2 (MutL α), (III) removal of the misincorporation by exonucleases and (IV) resynthesis of the excised strand and ligation (96) (Fig. 3). However, the molecular mechanisms of MMR are complex, especially in eukaryotes and the next sections will discuss MMR step-by-step in detail.

For the recognition step eukaryotes express two heterodimers with slightly overlapping functionality, MSH2/MSH6 and MSH2/MSH3, also known as MutS α and MutS β , respectively. MutS α is mainly involved in the recognition of base:base mismatches and small insertion deletion (indel) loops (Fig. 2), whereas MutS β is involved in MMR for larger indel loops (97). MutS α can recognize mispairs by slightly bending the DNA duplex to monitor its rigidity. In the case of a mismatch, the DNA duplex bends further compared to correctly paired DNA, allowing for better interaction with MutS α catalytic sites (98). Interestingly, not every mismatch is recognized with similar efficiency. Many fundamental studies use the G-T mismatch to investigate which proteins might play a role in MMR and with good reason as the G-T mismatch is recognized 8-fold more often than, for instance, a C-A mismatch in vitro (99). Moreover, not only mismatches on undamaged DNA templates are recognized, but DNA lesions are recognized as well. Several studies using human (cancer) cells have shown that MutS α is able to

recognize a wide variety of DNA lesions, including O⁶-methylguanine, the cisplatin d(GpG) intrastrand crosslink (100), UV-induced photolesions (101), aminofluorene - and acetylaminofluorene adducts (102) and benzo[c]phenanthrene adenine adducts (103). The recognition of a misincorporation opposite a DNA lesion is also important in suppressing mutagenesis stemming from DNA damaging agents in mammalian cells, as loss of MutS α results in DNA damage-induced hypermutagenesis (1, 104, 105). Mismatch recognition by MutS α of mismatches opposite damaged nucleotides seems to be similar to misincorporations opposite undamaged nucleotides: in the case of a O⁶-methylguanine-thymidine mismatch the structure is remarkably similar to an undamaged G-T mismatch (98). However, how MutS α might recognize a misincorporation opposite a bulky DNA lesion remains to be determined. After successful recognition MutS α exchanges ADP for ATP to trigger a conformational change in MutS α , that allows for the recruitment of proteins involved in the next step: the nicking of the newly synthesized daughter strand.

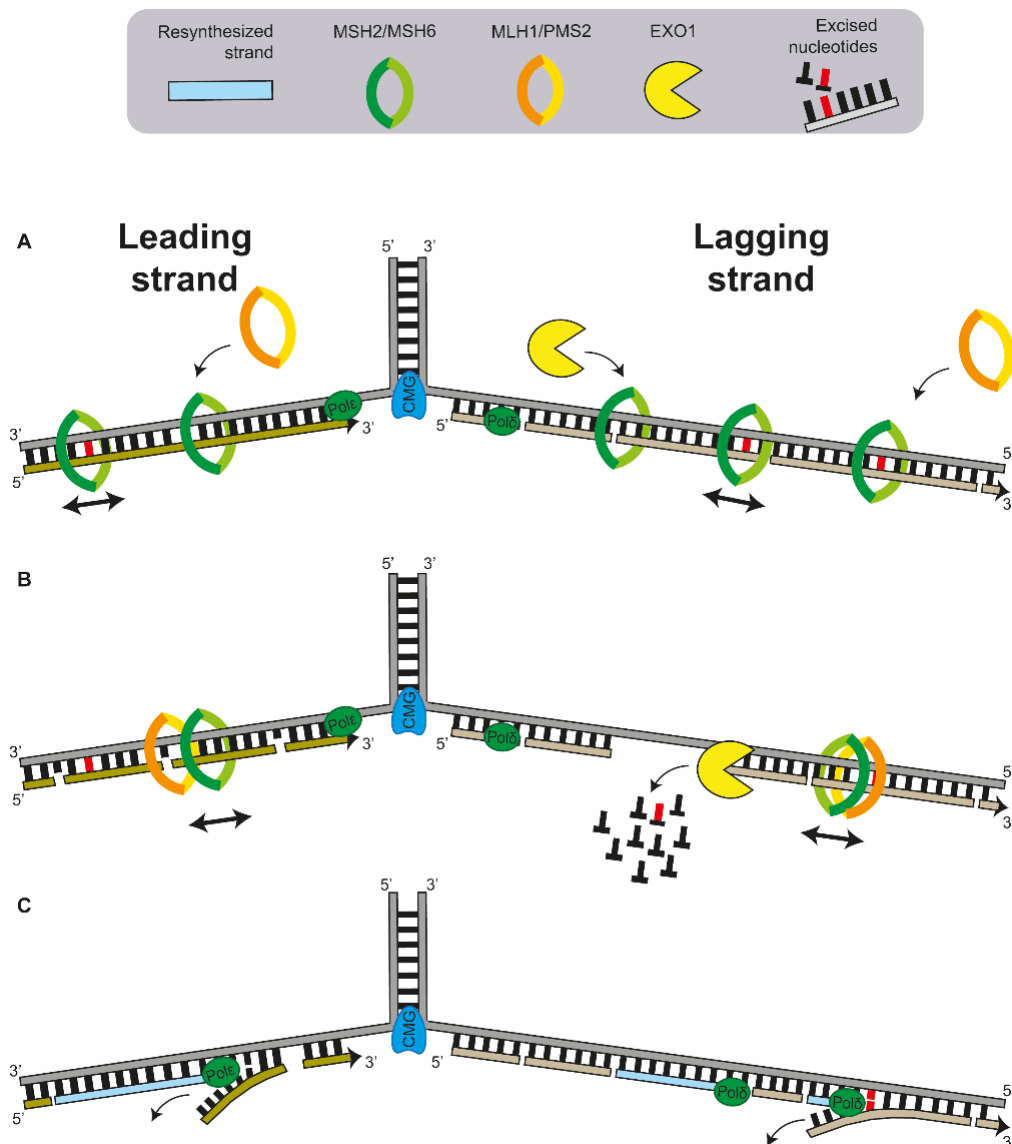


Figure 3: Eukaryotic Mismatch Repair on lagging and leading strands

A: Mismatch repair starts by recognition of a mismatched base (■) by MSH2/MSH6 which forms a sliding clamp. This allows for the activation of multiple MSH2/MSH6 complexes and triggers the recruitment of MLH1/PMS2 or EXO1 depending on strand and directionality. B: MLH1/PMS2 also slide over the DNA and can be activated by PCNA (not shown) to make multiple incisions. EXO1 degrades the daughter strand nucleotide by nucleotide, including the mismatch, which may occur on both strands. C. Replicative polymerases can resynthesize the strand thereby either displacing the still present daughter strand, including the mismatch, or simple gap filling if there was exonuclease activity.

The recognition of the daughter strand by MMR is a topic that is markedly different between eukaryotes and prokaryotes. For instance, during *E. Coli* MMR the newly synthesized daughter strand is recognized by the methylation status of the strand (106). In eukaryotes strand discrimination may be directed by how PCNA is loaded at nicks by clamp loaders. Its orientation allows for a way to discriminate the template strand from the daughter strand (107). As such PCNA is able to steer the endonucleolytic heterodimer MLH1/PMS2, also known as MutL α , to the daughter strand to create a nick which provides an entrance for the subsequent excision step (108). However, nicking may not always be essential due to the presence of nicks due to unligated Okazaki fragments in the lagging strand that may also serve as an entry for excision (96) (Fig. 3).

Excision of the daughter strand is often described to be performed by the exonuclease EXO1 in eukaryotic MMR. EXO1 acts in 5'-3' direction and in mismatch repair excises a stretch of the newly synthesized strand including the mismatch (Fig. 3) (109). Curiously, although EXO1 is important for MMR *in vitro*, Exo1 deficiency only displays a weak mutator phenotype in mice (110), which may hint at other exonucleases that play a role in MMR as well. Indeed, some overlap between exonuclease functionality has been proposed, as mutant Exo1 MEF upregulate the exonucleases Artemis, Mre11 and Fan1, which contributes to restoring MMR activity (111). Interestingly, in human cells, FAN1 and MRE11 are able to bind to MLH1 providing additional evidence for their role in MMR (112, 113). Studies using mammalian cells have shown that cells deficient for both FAN1 and EXO1 have significantly decreased MMR efficiency compared to either EXO1 or FAN1 single mutants, indeed suggesting a genetic redundancy between the two exonucleases (114). Conversely, FAN1 is also reported to frustrate MMR rather than act as a backup for EXO1 by sequestering MLH1 and thereby preventing the binding of MLH1 to MutS β and possibly MutS α (115). Moreover, exonuclease-independent pathways exist (Fig. 3) that rely on continued endonucleolytic degradation performed by MutL α followed by unwinding by the replicative polymerases (116). After excision the ssDNA is coated by RPA for stability until the daughter strand is resynthesized and the remaining nicks are ligated (96).

Apart from the MMR genes described, two MMR homologs may also play a minor role during MMR, namely MLH3 and PMS1, which can both bind to MLH1. MLH3 shares some sequence homology with PMS2 and contains an endonuclease domain (117). MLH3 has a clear role in meiosis, where its endonuclease activity is important for cleaving recombination intermediates (118). During MMR in somatic cells, however,

MLH3 is suggested to be a very limited backup of PMS2 as demonstrated by both in vitro and in vivo experiments with single and double knock-out mice (119, 120). In contrast to MLH3, PMS1 does not have an endonuclease domain and the MLH1/PMS1 complex is considered an accessory factor (121). In yeast, scMLH2 (the ortholog of human PMS1) prevents excessive genomic rearrangements during meiotic recombination. Moreover, the scMLH1/scMLH2 complex is also recruited to mismatches, but its role in MMR remains unclear (122).

MMR and cancer

Loss of the MMR pathway results in increased mutagenesis and is therefore associated with cancer (123). This can occur either spontaneously during life, resulting in MMR-deficient tumors, or by inheritance of the MMR-defects. MMR is mainly associated with colorectal cancer (CRC) as most MMR-deficient tumors are found in that tissue. In fact, of all CRC, approximately 15% have a defect in MMR (124). Moreover, approximately 3% of CRC is caused by a heterozygous defect in one of four core genes involved in MMR: MSH2, MSH6, MLH1 and PMS2, known as Lynch syndrome (LS) (125).

LS mainly gives rise to tumors in the colorectum and endometrium and displays a high mutational burden, partly caused by microsatellite instability (MSI) (126, 127). DNA polymerases often “slip” over these microsatellites (small repeated DNA motifs) creating small indel loops that are normally repaired by MMR, preventing mutagenesis (128). This high mutation frequency accelerates carcinogenesis with a tumor developing from a colonic adenoma in less than 3 years in LS, down from the 6-10 years seen in sporadic CRC (126). Interestingly, the high mutational burden also attracts immune cells and thus the prognosis of a patient with an MMR-deficient tumor is distinctly better than the MMR-proficient counterpart (23, 129). LS is also associated with a younger age of onset, as the first tumor develops typically in patients younger than 50 years old (126), which is significantly earlier than the age of onset of sporadic CRC, which is approximately 70 years (23). This younger age of onset may be explained by the fact that LS patients, heterozygous for one of the four core MMR genes, only need to lose the remaining wild-type MMR allele, whereas a healthy individual needs to lose both alleles of a core MMR gene (126).

The age of onset also depends on which MMR gene is mutated. Patients carrying germline mutations in MLH1 and MSH2 show a lower age of onset than carriers with mutations in MSH6 or PMS2 (126). This may possibly be explained by the functional redundancies in the MMR pathway. As discussed above MSH2/MSH3 and MLH1/MLH3 may also contribute to repair of various mismatches and indel loops and these heterodimers are still formed in individuals that have lost MSH6 or PMS2 (97, 119). However, MSH3 or MLH3 are not considered as “LS genes” and are hardly associated with increased risk of developing cancer. The type of cancer caused by MMR defects partly depends on which MMR gene is mutated. For instance, MSH6+/- carriers more often develop endometrial cancer, sometimes without MSI, possibly due to the redundancy with MSH2/MSH3. MSH2+/- and MLH1+/- carriers typically develop

CRC, but MSH2+/- is also associated with extracolonic tumors. PMS2 mutations are also associated with CRC, but sometimes without family history (126). Interestingly, deletions in the EPCAM gene may also lead to LS, specifically the development of CRC, due to the close proximity of this gene to the MSH2 locus (130). Mutations in MSH2 are also most often associated with Muir-Torre, a variant of LS that causes cancer predominantly in the sebaceous glands of the skin (131).

In rare cases it can occur that not one, but two faulty copies of an MMR gene are inherited, giving rise to constitutional MMR deficiency (cMMRd) syndrome. These individuals develop tumors early in life, often before the age of 10, and they no longer predominantly develop CRC, but also tumors in tissues that are associated with rapidly dividing cells during early development, like the brain and the hematopoietic system (132). This tragic syndrome raises an important question: why is cMMRd associated with tumors in all rapidly dividing tissues, but does LS predominantly cause CRC? Moreover, why is sporadic loss of MMR often found in the gastro-intestinal (GI) tract? The answers to these questions will be addressed in this thesis.

In conclusion, both misincorporations generated by replicative DNA polymerases on undamaged DNA and error-prone TLS at bulky or helix-distorting nucleotide lesions contribute to mutagenesis related to cancer formation. Mammalian cells minimize mutagenesis (i) by activating post-replicative MMR, which removes misincorporations that have escaped the proofreading activity of replicative DNA polymerases, and (ii) by activating DNA damage signaling and checkpoint pathways following induction of bulky or helix-distorting nucleotide lesions. The latter will result in inhibition of DNA replication, induction of cell cycle arrests and activation of DNA repair to remove nucleotide lesions prior to DNA replication. If DNA lesions are persistent, they will be replicated by TLS, an inherently error-prone process. How error-prone TLS is controlled remains to be determined. However, scant experimental evidence indicates that some MMR proteins may contribute not only in the activation of DNA damage responses, but also in suppressing DNA damage-induced mutagenesis.

Aim and outline of the thesis

Aim:

This thesis aims to investigate the role of core MMR factors Msh6, Mlh1 and Pms2, MMR homologs Mlh3 and Pms1, and exonucleases Exo1 and Fan1 in protecting mammalian cells from the genotoxic effects of UVC light and the dietary carcinogen PhIP, which induce bulky and helix-distorting DNA lesions. This analysis will contribute to better comprehend the cellular response to bulky and helix-distorting DNA lesions and may help in understanding the cancer tropism found in LS patients who carry a heterozygous defect in one of the four core MMR genes.

Outline:

Chapter 2 of this thesis provides an in-depth overview of the various ways MMR and DNA damage intertwines. In this chapter the role of MMR in suppressing mutagenesis resulting from the four main types of damage, namely methylating, oxidating, helix-distorting and interstrand crosslinks, is reviewed. Moreover, the clinical implications of MMR loss are discussed, how this affects the use of generic cancer treatments for MMR-deficient tumors and what role DNA damage plays in generating a specific gastro-intestinal cancer tropism associated with loss of the MMR genes. **Chapter 3** studies in detail how MMR can suppress mutagenesis in mammalian cells following exposure to UVC light as a prototypic DNA damaging agent. Using mouse embryonic stem cells, multiple MMR and MMR-associated genes are investigated with respect to their role in UV-induced damage signaling and control of mutagenesis, including analyses of spectra of mutations in Mlh1-deficient and Msh6-deficient cells. **Chapter 4** describes studies on the intertwinement between TLS and MMR by making use of MMR and Pol η knock-out and double-knockout cells. This study tests the hypothesis that MMR proteins suppress mutagenesis by removing TLS errors post-replicatively, a pathway dubbed post-TLS repair. **Chapter 5** describes a study on the CRC-associated tropism of Lynch syndrome, a syndrome characterized by the mono-allelic inheritance of a faulty MMR gene. Here, PhIP, a common dietary mutagen and carcinogen relevant for the GI tract, is used to investigate (I) whether food-related agents can inactivate MMR in a Lynch-like cell-based model, (II) whether MMR deficiency affects DNA damage signaling induced by PhIP and (III) whether PhIP-induced mutagenesis is further enhanced when MMR is completely lost. Finally, **chapter 6** summarizes the findings of this thesis, discusses new questions and insights provided by the studies presented in this thesis and describes the possibilities for future research.

References

1. Ijsselstein R, Jansen JG, De Wind N. DNA mismatch repair-dependent DNA damage responses and cancer. *DNA Repair*. 2020;93:102923.
2. D'Alessandro G, d'Adda di Fagagna F. Transcription and DNA Damage: Holding Hands or Crossing Swords? *Journal of molecular biology*. 2017;429(21):3215-29.
3. Huang R, Zhou PK. DNA damage repair: historical perspectives, mechanistic pathways and clinical translation for targeted cancer therapy. *Signal Transduct Target Ther*. 2021;6(1):254.
4. Vieth R. Critique of Public Health Guidance for Vitamin D and Sun Exposure in the Context of Cancer and COVID-19. *Anticancer research*. 2022;42(10):5027-34.
5. Apalla Z, Nashan D, Weller RB, Castellsague X. Skin Cancer: Epidemiology, Disease Burden, Pathophysiology, Diagnosis, and Therapeutic Approaches. *Dermatology and therapy*. 2017;7(Suppl 1):5-19.
6. Sung H, Ferlay J, Siegel RL, Laversanne M, Soerjomataram I, Jemal A, et al. Global Cancer Statistics 2020: GLOBOCAN Estimates of Incidence and Mortality Worldwide for 36 Cancers in 185 Countries. *CA: a cancer journal for clinicians*. 2021;71(3):209-49.
7. Kylo RL, Brady KL, Hurst EA. Sebaceous carcinoma: review of the literature. *Dermatologic surgery* : official publication for American Society for Dermatologic Surgery [et al]. 2015;41(1):1-15.
8. Leiter U, Garbe C. Epidemiology of melanoma and nonmelanoma skin cancer--the role of sunlight. *Advances in experimental medicine and biology*. 2008;624:89-103.
9. Braeuer RR, Watson IR, Wu CJ, Mobley AK, Kamiya T, Shoshan E, et al. Why is melanoma so metastatic? *Pigment cell & melanoma research*. 2014;27(1):19-36.
10. Alaluf S, Atkins D, Barrett K, Blount M, Carter N, Heath A. Ethnic variation in melanin content and composition in photoexposed and photoprotected human skin. *Pigment cell research*. 2002;15(2):112-8.
11. Sinha RP, Hader DP. UV-induced DNA damage and repair: a review. *Photochemical & photobiological sciences* : Official journal of the European Photochemistry Association and the European Society for Photobiology. 2002;1(4):225-36.
12. Douki T, Reynaud-Angelin A, Cadet J, Sage E. Bipyrimidine photoproducts rather than oxidative lesions are the main type of DNA damage involved in the genotoxic effect of solar UVA radiation. *Biochemistry*. 2003;42(30):9221-6.
13. Nakamura J, Mutlu E, Sharma V, Collins L, Bodnar W, Yu R, et al. The endogenous exposome. *DNA Repair (Amst)*. 2014;19:3-13.
14. Kuluncsics Z, Perdiz D, Brulay E, Muel B, Sage E. Wavelength dependence of ultraviolet-induced DNA damage distribution: involvement of direct or indirect mechanisms and possible artefacts. *Journal of photochemistry and photobiology B, Biology*. 1999;49(1):71-80.
15. Young AR, Chadwick CA, Harrison GI, Hawk JL, Nikaido O, Potten CS. The in situ repair kinetics of epidermal thymine dimers and 6-4 photoproducts in human skin types I and II. *The Journal of investigative dermatology*. 1996;106(6):1307-13.
16. Freeman SE, Hacham H, Gange RW, Maytum DJ, Sutherland JC, Sutherland BM. Wavelength dependence of pyrimidine dimer formation in DNA of human skin irradiated in situ with ultraviolet light. *Proc Natl Acad Sci U S A*. 1989;86(14):5605-9.
17. Mouret S, Baudouin C, Charveron M, Favier A, Cadet J, Douki T. Cyclobutane pyrimidine dimers are predominant DNA lesions in whole human skin exposed to UVA radiation. *Proc Natl Acad Sci U S A*. 2006;103(37):13765-70.
18. Brash DE. UV signature mutations. *Photochemistry and photobiology*. 2015;91(1):15-26.
19. Yoon JH, Prakash L, Prakash S. Highly error-free role of DNA polymerase eta in the replicative bypass of UV-induced pyrimidine dimers in mouse and human cells. *Proc Natl Acad Sci U S A*. 2009;106(43):18219-24.
20. Bishehsari F, Mahdavinia M, Vacca M, Malekzadeh R, Mariani-Costantini R. Epidemiological transition of colorectal cancer in developing countries: environmental factors, molecular pathways, and opportunities for prevention. *World J Gastroenterol*. 2014;20(20):6055-72.
21. Chiavarini M, Bertarelli G, Minelli L, Fabiani R. Dietary Intake of Meat Cooking-Related Mutagens (HCAs) and Risk of Colorectal Adenoma and Cancer: A Systematic Review and Meta-Analysis. *Nutrients*. 2017;9(5):514.
22. Derry MM, Raina K, Agarwal C, Agarwal R. Identifying Molecular Targets of Lifestyle Modifications in Colon Cancer Prevention. *Frontiers in Oncology*. 2013;3.
23. Brenner H, Kloor M, Pox CP. Colorectal cancer. *Lancet*. 2014;383(9927):1490-502.
24. Zhu Y, Wang PP, Zhao J, Green R, Sun Z, Roebathan B, et al. Dietary N-nitroso compounds and risk of colorectal cancer: a case-control study in Newfoundland and Labrador and Ontario, Canada. *The British journal of nutrition*. 2014;111(6):1109-17.
25. Sinha R, Kulldorff M, Gunter MJ, Strickland P, Rothman N. Dietary benzo[a]pyrene intake and risk of colorectal adenoma. *Cancer Epidemiol Biomarkers Prev*. 2005;14(8):2030-4.
26. Bellamri M, Walmsley SJ, Turesky RJ. Metabolism and biomarkers of heterocyclic aromatic amines in humans. *Genes and environment* : the official journal of the Japanese Environmental Mutagen Society. 2021;43(1):29.
27. Friesen MD, Kaderlik K, Lin D, Garren L, Bartsch H, Lang NP, et al. Analysis of DNA adducts of 2-amino-1-methyl-6-phenylimidazo[4,5-b]pyridine in rat and human tissues by alkaline hydrolysis and gas chromatography/electron capture mass spectrometry: validation by comparison with ³²P-postlabeling. *Chem Res Toxicol*. 1994;7(6):733-9.

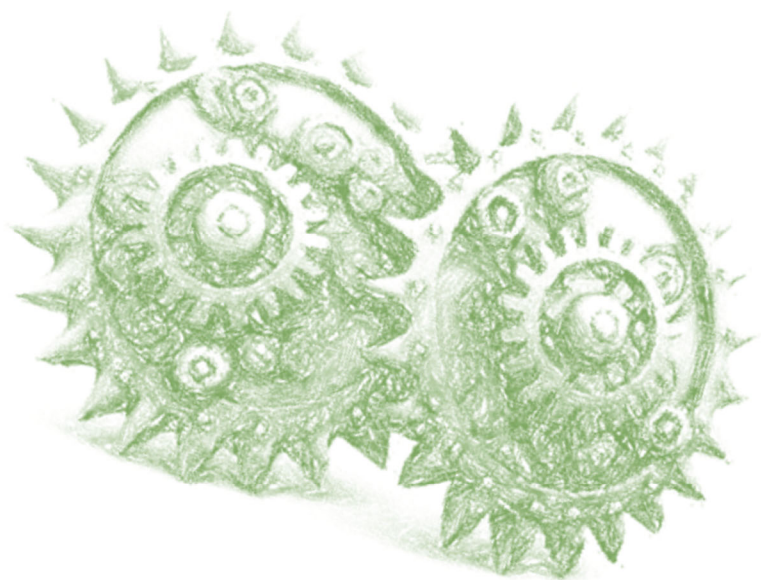
28. Brown K, Guenther EA, Dingley KH, Cosman M, Harvey CA, Shields SJ, et al. Synthesis and spectroscopic characterization of site-specific 2-amino-1-methyl-6-phenylimidazo. *Nucleic Acids Res.* 2001;29(9):1951-9.
29. Holzl-Armstrong L, Moody S, Kucab JE, Zwart EP, Bellamri M, Luijten M, et al. Mutagenicity of 2-hydroxyamino-1-methyl-6-phenylimidazo[4,5-b]pyridine (N-OH-PhIP) in human TP53 knock-in (Hupki) mouse embryo fibroblasts. *Food and chemical toxicology : an international journal published for the British Industrial Biological Research Association.* 2021;147:111855.
30. Liu Z, Zhang Y, Dang Q, Wu K, Jiao D, Li Z, et al. Genomic Alteration Characterization in Colorectal Cancer Identifies a Prognostic and Metastasis Biomarker: FAM83A|IDO1. *Front Oncol.* 2021;11:632430.
31. Bouvard V, Loomis D, Guyton KZ, Grosse Y, Ghissassi FE, Benbrahim-Tallaa L, et al. Carcinogenicity of consumption of red and processed meat. *The Lancet Oncology.* 2015;16(16):1599-600.
32. Sinha R, Rothman N. Role of well-done, grilled red meat, heterocyclic amines (HCAs) in the etiology of human cancer. *Cancer letters.* 1999;143(2):189-94.
33. Berti M, Cortez D, Lopes M. The plasticity of DNA replication forks in response to clinically relevant genotoxic stress. *Nature reviews Molecular cell biology.* 2020;21(10):633-51.
34. Zou L, Elledge SJ. Sensing DNA damage through ATRIP recognition of RPA-ssDNA complexes. *Science.* 2003;300(5625):1542-8.
35. Delacroix S, Wagner JM, Kobayashi M, Yamamoto K, Karnitz LM. The Rad9-Hus1-Rad1 (9-1-1) clamp activates checkpoint signaling via TopBP1. *Genes & development.* 2007;21(12):1472-7.
36. Blackford AN, Jackson SP. ATM, ATR, and DNA-PK: The Trinity at the Heart of the DNA Damage Response. *Mol Cell.* 2017;66(6):801-17.
37. Falck J, Coates J, Jackson SP. Conserved modes of recruitment of ATM, ATR and DNA-PKcs to sites of DNA damage. *Nature.* 2005;434(7033):605-11.
38. Lee JH, Paull TT. ATM activation by DNA double-strand breaks through the Mre11-Rad50-Nbs1 complex. *Science.* 2005;308(5721):551-4.
39. Scully R, Xie A. Double strand break repair functions of histone H2AX. *Mutat Res.* 2013;750(1-2):5-14.
40. Ziv Y, Bielopolski D, Galanty Y, Lukas C, Taya Y, Schultz DC, et al. Chromatin relaxation in response to DNA double-strand breaks is modulated by a novel ATM- and KAP-1 dependent pathway. *Nature cell biology.* 2006;8(8):870-6.
41. White D, Rafalska-Metcalf IU, Ivanov AV, Corsinotti A, Peng H, Lee SC, et al. The ATM substrate KAP1 controls DNA repair in heterochromatin: regulation by HP1 proteins and serine 473/824 phosphorylation. *Molecular cancer research : MCR.* 2012;10(3):401-14.
42. Jazayeri A, Falck J, Lukas C, Bartek J, Smith GC, Lukas J, et al. ATM- and cell cycle-dependent regulation of ATR in response to DNA double-strand breaks. *Nature cell biology.* 2006;8(1):37-45.
43. Adams KE, Medhurst AL, Dart DA, Lakin ND. Recruitment of ATR to sites of ionising radiation-induced DNA damage requires ATM and components of the MRN protein complex. *Oncogene.* 2006;25(28):3894-904.
44. Liao H, Ji F, Helleday T, Ying S. Mechanisms for stalled replication fork stabilization: new targets for synthetic lethality strategies in cancer treatments. *EMBO reports.* 2018;19(9).
45. Jones GG, Reaper PM, Pettitt AR, Sherrington PD. The ATR-p53 pathway is suppressed in noncycling normal and malignant lymphocytes. *Oncogene.* 2004;23(10):1911-21.
46. Sahu RP, Batra S, Srivastava SK. Activation of ATM/Chk1 by curcumin causes cell cycle arrest and apoptosis in human pancreatic cancer cells. *British journal of cancer.* 2009;100(9):1425-33.
47. Nik-Zainal S, Davies H, Staaf J, Ramakrishna M, Glodzik D, Zou X, et al. Landscape of somatic mutations in 560 breast cancer whole-genome sequences. *Nature.* 2016;534(7605):47-54.
48. Brambullo T, Colonna MR, Vindigni V, Piasterico S, Masciopinto G, Galeano M, et al. Xeroderma Pigmentosum: A Genetic Condition Skin Cancer Correlated-A Systematic Review. *BioMed research international.* 2022;2022:8549532.
49. Shibutani S, Takeshita M, Grollman AP. Insertion of specific bases during DNA synthesis past the oxidation-damaged base 8-oxodG. *Nature.* 1991;349(6308):431-4.
50. Fu D, Calvo JA, Samson LD. Balancing repair and tolerance of DNA damage caused by alkylating agents. *Nature Reviews Cancer.* 2012;12(2):104-20.
51. Mimmler M, Peter S, Kraus A, Stroh S, Nikolova T, Seiwert N, et al. DNA damage response curtails detrimental replication stress and chromosomal instability induced by the dietary carcinogen PhIP. *Nucleic Acids Research.* 2016;44(21):10259-76.
52. Elvers I, Johansson F, Groth P, Erixon K, Helleday T. UV stalled replication forks restart by re-priming in human fibroblasts. *Nucleic Acids Res.* 2011;39(16):7049-57.
53. Bunting SF, Nussenzweig A. End-joining, translocations and cancer. *Nature reviews Cancer.* 2013;13(7):443-54.
54. Nichols CA, Gibson WJ, Brown MS, Kosmicki JA, Busanovich JP, Wei H, et al. Loss of heterozygosity of essential genes represents a widespread class of potential cancer vulnerabilities. *Nat Commun.* 2020;11(1):2517.
55. Tilanus-Linthorst MM, Lingsma HF, Evans DG, Thompson D, Kaas R, Manders P, et al. Optimal age to start preventive measures in women with BRCA1/2 mutations or high familial breast cancer risk. *Int J Cancer.* 2013;133(1):156-63.
56. Chang DJ, Cimprich KA. DNA damage tolerance: when it's OK to make mistakes. *Nature chemical biology.* 2009;5(2):82-90.
57. Moldovan GL, Pfander B, Jentsch S. PCNA, the maestro of the replication fork. *Cell.* 2007;129(4):665-79.

58. Acharya N, Yoon JH, Gali H, Unk I, Haracska L, Johnson RE, et al. Roles of PCNA-binding and ubiquitin-binding domains in human DNA polymerase η in translesion DNA synthesis. *Proc Natl Acad Sci U S A*. 2008;105(46):17724-9.
59. Hendel A, Krijger PH, Diamant N, Goren Z, Langerak P, Kim J, et al. PCNA ubiquitination is important, but not essential for translesion DNA synthesis in mammalian cells. *PLoS Genet*. 2011;7(9):e1002262.
60. Mohiuddin M, Evans TJ, Rahman MM, Keka IS, Tsuda M, Sasanuma H, et al. SUMOylation of PCNA by PIAS1 and PIAS4 promotes template switch in the chicken and human B cell lines. *Proc Natl Acad Sci U S A*. 2018;115(50):12793-8.
61. Branzei D, Vanoli F, Foiani M. SUMOylation regulates Rad18-mediated template switch. *Nature*. 2008;456(7224):915-20.
62. Vaisman A, Woodgate R. Translesion DNA polymerases in eukaryotes: what makes them tick? *Critical reviews in biochemistry and molecular biology*. 2017;52(3):274-303.
63. McCulloch SD, Kunkel TA. The fidelity of DNA synthesis by eukaryotic replicative and translesion synthesis polymerases. *Cell Res*. 2008;18(1):148-61.
64. Fukuda H, Takamura-Enya T, Masuda Y, Nohmi T, Seki C, Kamiya K, et al. Translesional DNA synthesis through a C8-guanyl adduct of 2-amino-1-methyl-6-phenylimidazo[4,5-b]pyridine (PhIP) in Vitro: REV1 inserts dC opposite the lesion, and DNA polymerase κ potentially catalyzes extension reaction from the 3'-dC terminus. *J Biol Chem*. 2009;284(38):25585-92.
65. Washington MT, Johnson RE, Prakash L, Prakash S. Human DINB1-encoded DNA polymerase κ is a promiscuous extender of mispaired primer termini. *Proc Natl Acad Sci U S A*. 2002;99(4):1910-4.
66. Mouron S, Rodriguez-Acebes S, Martinez-Jimenez MI, Garcia-Gomez S, Chocron S, Blanco L, et al. Repriming of DNA synthesis at stalled replication forks by human PrimPol. *Nature structural & molecular biology*. 2013;20(12):1383-9.
67. Wan L, Lou J, Xia Y, Su B, Liu T, Cui J, et al. hPrimPol1/CCDC111 is a human DNA primase-polymerase required for the maintenance of genome integrity. *EMBO reports*. 2013;14(12):1104-12.
68. Garcia-Gomez S, Reyes A, Martinez-Jimenez MI, Chocron ES, Mouron S, Terrados G, et al. PrimPol, an archaic primase/polymerase operating in human cells. *Mol Cell*. 2013;52(4):541-53.
69. Bianchi J, Rudd SG, Jozwiakowski SK, Bailey LJ, Soura V, Taylor E, et al. PrimPol bypasses UV photoproducts during eukaryotic chromosomal DNA replication. *Mol Cell*. 2013;52(4):566-73.
70. Yoon JH, Johnson RE, Prakash L, Prakash S. DNA polymerase θ accomplishes translesion synthesis opposite 1,N(6)-ethenodeoxyadenosine with a remarkably high fidelity in human cells. *Genes & development*. 2019;33(5-6):282-7.
71. Yoon JH, McArthur MJ, Park J, Basu D, Wakamiya M, Prakash L, et al. Error-Prone Replication through UV Lesions by DNA Polymerase θ Protects against Skin Cancers. *Cell*. 2019;176(6):1295-309 e15.
72. Quinet A, Lerner LK, Martins DJ, Menck CFM. Filling gaps in translesion DNA synthesis in human cells. *Mutation research Genetic toxicology and environmental mutagenesis*. 2018;836(Pt B):127-42.
73. Jansen JG, Temviriyankul P, Wit N, Delbos F, Reynaud CA, Jacobs H, et al. Redundancy of mammalian Y family DNA polymerases in cellular responses to genomic DNA lesions induced by ultraviolet light. *Nucleic Acids Res*. 2014;42(17):11071-82.
74. Ziv O, Geacintov N, Nakajima S, Yasui A, Livneh Z. DNA polymerase ζ cooperates with polymerases κ and ι in translesion DNA synthesis across pyrimidine photodimers in cells from XPV patients. *Proc Natl Acad Sci U S A*. 2009;106(28):11552-7.
75. Sugiyama T, Keinard B, Best G, Sanyal MR. Biochemical and photochemical mechanisms that produce different UV-induced mutation spectra. *Mutat Res*. 2021;823:111762.
76. Temviriyankul P, van Hees-Stuivenberg S, Delbos F, Jacobs H, de Wind N, Jansen JG. Temporally distinct translesion synthesis pathways for ultraviolet light-induced photoproducts in the mammalian genome. *DNA Repair (Amst)*. 2012;11(6):550-8.
77. Yang W, Gao Y. Translesion and Repair DNA Polymerases: Diverse Structure and Mechanism. *Annual Review of Biochemistry*. 2018;87(1):239-61.
78. Friedberg EC. Suffering in silence: the tolerance of DNA damage. *Nature Reviews Molecular Cell Biology*. 2005;6(12):943-53.
79. Jansen JG, Tsaalbi-Shtylik A, de Wind N. Roles of mutagenic translesion synthesis in mammalian genome stability, health and disease. *DNA Repair (Amst)*. 2015;29:56-64.
80. Martin-Pardillos A, Tsaalbi-Shtylik A, Chen S, Lazare S, van Os RP, Dethmers-Ausema A, et al. Genomic and functional integrity of the hematopoietic system requires tolerance of oxidative DNA lesions. *Blood*. 2017;130(13):1523-34.
81. Diamant N, Hendel A, Vered I, Carell T, Reissner T, de Wind N, et al. DNA damage bypass operates in the S and G2 phases of the cell cycle and exhibits differential mutagenicity. *Nucleic Acids Res*. 2012;40(1):170-80.
82. Quinet A, Tirman S, Cybulla E, Meroni A, Vindigni A. To skip or not to skip: choosing repriming to tolerate DNA damage. *Mol Cell*. 2021;81(4):649-58.
83. Natarajan V. Regulation of DNA repair by non-coding miRNAs. *Non-coding RNA research*. 2016;1(1):64-8.
84. Peddu C, Zhang S, Zhao H, Wong A, Lee EYC, Lee M, et al. Phosphorylation Alters the Properties of Pol η : Implications for Translesion Synthesis. *iScience*. 2018;6:52-67.
85. Sabbioneda S, Bortolomai I, Giannattasio M, Plevani P, Muzi-Falconi M. Yeast Rev1 is cell cycle regulated, phosphorylated in response to DNA damage and its binding to chromosomes is dependent upon MEC1. *DNA Repair (Amst)*. 2007;6(1):121-7.

86. Pages V, Santa Maria SR, Prakash L, Prakash S. Role of DNA damage-induced replication checkpoint in promoting lesion bypass by translesion synthesis in yeast. *Genes & development*. 2009;23(12):1438-49.
87. Leung W, Baxley RM, Moldovan GL, Bielinsky AK. Mechanisms of DNA Damage Tolerance: Post-Translational Regulation of PCNA. *Genes*. 2018;10(1).
88. Baranovskiy AG, Lada AG, Siebler HM, Zhang Y, Pavlov YI, Tahirov TH. DNA polymerase delta and zeta switch by sharing accessory subunits of DNA polymerase delta. *J Biol Chem*. 2012;287(21):17281-7.
89. Pavlov YI, Frahm C, Nick McElhinny SA, Niimi A, Suzuki M, Kunkel TA. Evidence that errors made by DNA polymerase alpha are corrected by DNA polymerase delta. *Current biology : CB*. 2006;16(2):202-7.
90. Tran HT, Gordenin DA, Resnick MA. The 3'→5' exonucleases of DNA polymerases delta and epsilon and the 5'→3' exonuclease Exo1 have major roles in postreplication mutation avoidance in *Saccharomyces cerevisiae*. *Mol Cell Biol*. 1999;19(3):2000-7.
91. Bebenek K, Matsuda T, Masutani C, Hanaoka F, Kunkel TA. Proofreading of DNA polymerase epsilon-dependent replication errors. *J Biol Chem*. 2001;276(4):2317-20.
92. O'Donnell M, Langston L, Stillman B. Principles and concepts of DNA replication in bacteria, archaea, and eukarya. *Cold Spring Harb Perspect Biol*. 2013;5(7).
93. Kunkel TA. Evolving views of DNA replication (in)fidelity. *Cold Spring Harbor symposia on quantitative biology*. 2009;74:91-101.
94. Wagner R, Jr., Meselson M. Repair tracts in mismatched DNA heteroduplexes. *Proc Natl Acad Sci U S A*. 1976;73(11):4135-9.
95. Wildenberg J, Meselson M. Mismatch repair in heteroduplex DNA. *Proc Natl Acad Sci U S A*. 1975;72(6):2202-6.
96. Jiricny J. The multifaceted mismatch-repair system. *Nature reviews Molecular cell biology*. 2006;7(5):335-46.
97. Genschel J, Littman SJ, Drummond JT, Modrich P. Isolation of MutSβ from Human Cells and Comparison of the Mismatch Repair Specificities of MutSβ and MutSα. *Journal of Biological Chemistry*. 1998;273(31):19895-901.
98. Warren JJ, Pohlhaus TJ, Changela A, Iyer RR, Modrich PL, Beese LS. Structure of the human MutSα/PCNA DNA lesion recognition complex. *Mol Cell*. 2007;26(4):579-92.
99. Gradia S, Acharya S, Fishel R. The role of mismatched nucleotides in activating the hMSH2-hMSH6 molecular switch. *J Biol Chem*. 2000;275(6):3922-30.
100. Duckett DR, Drummond JT, Murchie AI, Reardon JT, Sancar A, Lilley DM, et al. Human MutSα recognizes damaged DNA base pairs containing O6-methylguanine, O4-methylthymine, or the cisplatin-d(GpG) adduct. *Proc Natl Acad Sci U S A*. 1996;93(13):6443-7.
101. Wang H, Lawrence CW, Li GM, Hays JB. Specific binding of human MSH2.MSH6 mismatch-repair protein heterodimers to DNA incorporating thymine- or uracil-containing UV light photoproducts opposite mismatched bases. *J Biol Chem*. 1999;274(24):16894-900.
102. Li GM, Wang H, Romano LJ. Human MutSα specifically binds to DNA containing aminofluorene and acetylaminofluorene adducts. *J Biol Chem*. 1996;271(39):24084-8.
103. Wu J, Gu L, Wang H, Geacintov NE, Li GM. Mismatch repair processing of carcinogen-DNA adducts triggers apoptosis. *Mol Cell Biol*. 1999;19(12):8292-301.
104. Borgdorff V, Pauw B, van Hees-Stuivenberg S, de Wind N. DNA mismatch repair mediates protection from mutagenesis induced by short-wave ultraviolet light. *DNA Repair (Amst)*. 2006;5(11):1364-72.
105. Ijsselstein R, van Hees S, Drost M, Jansen JG, de Wind N. Induction of mismatch repair deficiency, compromised DNA damage signaling and compound hypermutagenesis by a dietary mutagen in a cell-based model for Lynch Syndrome. *Carcinogenesis*. 2021.
106. Li GM. Mechanisms and functions of DNA mismatch repair. *Cell Res*. 2008;18(1):85-98.
107. Kunkel TA, Erie DA. Eukaryotic Mismatch Repair in Relation to DNA Replication. *Annual review of genetics*. 2015;49:291-313.
108. Kadyrov FA, Dzantiev L, Constantin N, Modrich P. Endonucleolytic function of MutLα in human mismatch repair. *Cell*. 2006;126(2):297-308.
109. Tran PT, Erdeniz N, Symington LS, Liskay RM. EXO1-A multi-tasking eukaryotic nuclease. *DNA Repair (Amst)*. 2004;3(12):1549-59.
110. Wei K, Clark AB, Wong E, Kane MF, Mazur DJ, Parris T, et al. Inactivation of Exonuclease 1 in mice results in DNA mismatch repair defects, increased cancer susceptibility, and male and female sterility. *Genes & development*. 2003;17(5):603-14.
111. Desai A, Gerson S. Exo1 independent DNA mismatch repair involves multiple compensatory nucleases. *DNA Repair (Amst)*. 2014;21:55-64.
112. Rikitake M, Fujikane R, Obayashi Y, Oka K, Ozaki M, Hidaka M. MLH1-mediated recruitment of FAN1 to chromatin for the induction of apoptosis triggered by O(6) -methylguanine. *Genes to cells : devoted to molecular & cellular mechanisms*. 2020;25(3):175-86.
113. Her C, Vo AT, Wu X. Evidence for a direct association of hMRE11 with the human mismatch repair protein hMLH1. *DNA Repair (Amst)*. 2002;1(9):719-29.
114. Kratz K, Artola-Boran M, Kobayashi-Era S, Koh G, Oliveira G, Kobayashi S, et al. FANCD2-Associated Nuclease 1 Partially Compensates for the Lack of Exonuclease 1 in Mismatch Repair. *Mol Cell Biol*. 2021;41(9):e0030321.

115. Goold R, Hamilton J, Menneteau T, Flower M, Bunting EL, Aldous SG, et al. FAN1 controls mismatch repair complex assembly via MLH1 retention to stabilize CAG repeat expansion in Huntington's disease. *Cell Rep*. 2021;36(9):109649.
116. Goellner EM, Putnam CD, Kolodner RD. Exonuclease 1-dependent and independent mismatch repair. *DNA Repair (Amst)*. 2015;32:24-32.
117. Kadyrova LY, Gujar V, Burdett V, Modrich PL, Kadyrov FA. Human MutLgamma, the MLH1-MLH3 heterodimer, is an endonuclease that promotes DNA expansion. *Proc Natl Acad Sci U S A*. 2020;117(7):3535-42.
118. Cannavo E, Sanchez A, Anand R, Ranjha L, Hugener J, Adam C, et al. Regulation of the MLH1-MLH3 endonuclease in meiosis. *Nature*. 2020;586(7830):618-22.
119. Chen PC, Dudley S, Hagen W, Dizon D, Paxton L, Reichow D, et al. Contributions by MutL homologues Mlh3 and Pms2 to DNA mismatch repair and tumor suppression in the mouse. *Cancer Res*. 2005;65(19):8662-70.
120. Cannavo E, Marra G, Sabates-Bellver J, Menigatti M, Lipkin SM, Fischer F, et al. Expression of the MutL homologue hMLH3 in human cells and its role in DNA mismatch repair. *Cancer Res*. 2005;65(23):10759-66.
121. Raschle M, Marra G, Nystrom-Lahti M, Schar P, Jiricny J. Identification of hMutLbeta, a heterodimer of hMLH1 and hPMS1. *J Biol Chem*. 1999;274(45):32368-75.
122. Pannafino G, Alani E. Coordinated and Independent Roles for MLH Subunits in DNA Repair. *Cells*. 2021;10(4).
123. Liu D, Keijzers G, Rasmussen LJ. DNA mismatch repair and its many roles in eukaryotic cells. *Mutation Research/Reviews in Mutation Research*. 2017;773:174-87.
124. Poulogiannis G, Frayling IM, Arends MJ. DNA mismatch repair deficiency in sporadic colorectal cancer and Lynch syndrome. *Histopathology*. 2010;56(2):167-79.
125. Lynch HT, Lynch PM, Lanspa SJ, Snyder CL, Lynch JF, Boland CR. Review of the Lynch syndrome: history, molecular genetics, screening, differential diagnosis, and medicolegal ramifications. *Clinical genetics*. 2009;76(1):1-18.
126. Lynch HT, Snyder CL, Shaw TG, Heinen CD, Hitchins MP. Milestones of Lynch syndrome: 1895–2015. *Nature Reviews Cancer*. 2015;15(3):181-94.
127. Baretti M, Le DT. DNA mismatch repair in cancer. *Pharmacology & therapeutics*. 2018;189:45-62.
128. Kunkel TA, Erie DA. DNA mismatch repair. *Annu Rev Biochem*. 2005;74:681-710.
129. Schwitalle Y, Kloor M, Eiermann S, Linnebacher M, Kienle P, Knaebel HP, et al. Immune response against frameshift-induced neopeptides in HNPCC patients and healthy HNPCC mutation carriers. *Gastroenterology*. 2008;134(4):988-97.
130. Ligtenberg MJ, Kuiper RP, Chan TL, Goossens M, Hebeda KM, Voorendt M, et al. Heritable somatic methylation and inactivation of MSH2 in families with Lynch syndrome due to deletion of the 3' exons of TACSTD1. *Nat Genet*. 2009;41(1):112-7.
131. Mangold E, Pagenstecher C, Leister M, Mathiak M, Rutten A, Friedl W, et al. A genotype-phenotype correlation in HNPCC: strong predominance of msh2 mutations in 41 patients with Muir-Torre syndrome. *J Med Genet*. 2004;41(7):567-72.
132. Lavoine N, Colas C, Muleris M, Bodo S, Duval A, Entz-Werle N, et al. Constitutional mismatch repair deficiency syndrome: clinical description in a French cohort. *Journal of Medical Genetics*. 2015;52(11):770-8.
133. Gibis M. Heterocyclic Aromatic Amines in Cooked Meat Products: Causes, Formation, Occurrence, and Risk Assessment. *Comprehensive reviews in food science and food safety*. 2016;15(2):269-302.
134. Jia W, Xie G, Jia W. Bile acid-microbiota crosstalk in gastrointestinal inflammation and carcinogenesis. *Nat Rev Gastroenterol Hepatol*. 2018;15(2):111-28.
135. Cantwell M, Elliott C. Nitrates, Nitrites and Nitrosamines from Processed Meat Intake and Colorectal Cancer Risk. *Journal of Clinical Nutrition & Dietetics*. 2017;3:4-27.
136. Marchesi F, Turriziani M, Tortorelli G, Avvisati G, Torino F, De Vecchis L. Triazene compounds: mechanism of action and related DNA repair systems. *Pharmacological research*. 2007;56(4):275-87.
137. Du H, Wang P, Li L, Wang Y. Repair and translesion synthesis of O (6)-alkylguanine DNA lesions in human cells. *J Biol Chem*. 2019;294(29):11144-53.
138. Winterbourn CC, Kettle AJ, Hampton MB. Reactive Oxygen Species and Neutrophil Function. *Annual Review of Biochemistry*. 2016;85(1):765-92.
139. Khansari N, Shakiba Y, Mahmoudi M. Chronic inflammation and oxidative stress as a major cause of age-related diseases and cancer. *Recent patents on inflammation & allergy drug discovery*. 2009;3(1):73-80.
140. Bridge G, Rashid S, Martin SA. DNA mismatch repair and oxidative DNA damage: implications for cancer biology and treatment. *Cancers*. 2014;6(3):1597-614.
141. Dizdaroglu M. Oxidatively induced DNA damage: mechanisms, repair and disease. *Cancer letters*. 2012;327(1-2):26-47.
142. Petta TB, Nakajima S, Zlatanou A, Despras E, Couve-Privat S, Ishchenko A, et al. Human DNA polymerase iota protects cells against oxidative stress. *EMBO J*. 2008;27(21):2883-95.
143. Guan J, Yu S, Zheng X. NEDDylation antagonizes ubiquitination of proliferating cell nuclear antigen and regulates the recruitment of polymerase eta in response to oxidative DNA damage. *Protein & cell*. 2018;9(4):365-79.
144. Fahrer J, Kaina B. Impact of DNA repair on the dose-response of colorectal cancer formation induced by dietary carcinogens. *Food and chemical toxicology : an international journal published for the British Industrial Biological Research Association*. 2017;106(Pt B):583-94.
145. Marteijn JA, Lans H, Vermeulen W, Hoeijmakers JH. Understanding nucleotide excision repair and its roles in cancer and ageing. *Nature reviews Molecular cell biology*. 2014;15(7):465-81.

146. Semlow DR, Walter JC. Mechanisms of Vertebrate DNA Interstrand Cross-Link Repair. *Annu Rev Biochem.* 2021;90:107-35.
147. Roy U, Scharer OD. Involvement of translesion synthesis DNA polymerases in DNA interstrand crosslink repair. *DNA Repair (Amst).* 2016;44:33-41.
148. Mehta A, Haber JE. Sources of DNA double-strand breaks and models of recombinational DNA repair. *Cold Spring Harb Perspect Biol.* 2014;6(9):a016428.
149. Cannan WJ, Pederson DS. Mechanisms and Consequences of Double-Strand DNA Break Formation in Chromatin. *Journal of cellular physiology.* 2016;231(1):3-14.
150. Sallmyr A, Tomkinson AE. Repair of DNA double-strand breaks by mammalian alternative end-joining pathways. *J Biol Chem.* 2018;293(27):10536-46.
151. Donnianni RA, Zhou ZX, Lujan SA, Al-Zain A, Garcia V, Glancy E, et al. DNA Polymerase Delta Synthesizes Both Strands during Break-Induced Replication. *Mol Cell.* 2019;76(3):371-81 e4.
152. Abbotts R, Wilson DM, 3rd. Coordination of DNA single strand break repair. *Free Radic Biol Med.* 2017;107:228-44.
153. Caldecott KW. DNA single-strand break repair. *Experimental cell research.* 2014;329(1):2-8.





Chapter 2:

DNA mismatch repair-dependent DNA damage responses and cancer

*Robbert Ijsselsteijn¹, Jacob G Jansen¹,
Niels de Wind¹*

*¹Department of Human Genetics, Leiden
University Medical Center, Leiden, The
Netherlands.*

DOI: 10.1016/j.dnarep.2020.102923

DNA Repair (Amst). 2020 Sep;93:102923

Published September 2020



Abstract

Canonical DNA mismatch repair (MMR) excises base-base mismatches to increase the fidelity of DNA replication. Thus, loss of MMR leads to increased spontaneous mutagenesis. MMR genes also are involved in the suppression of mutagenic, and the induction of protective, responses to various types of DNA damage. In this review we describe these non-canonical roles of MMR at different lesion types. Loss of non-canonical MMR gene functions may have important ramifications for the prevention, development and treatment of colorectal cancer associated with inherited MMR gene defects in Lynch syndrome. This graphical review pays tribute to Samuel H. Wilson. Sam not only made seminal contributions to understanding base excision repair, particularly with respect to structure-function relationships in DNA polymerase β but also, as Editor of DNA Repair, has maintained a high standard of the journal.

Main text

High-fidelity DNA replication is crucial to preserve the genomic integrity of eukaryotic cells and, consequently, is beneficial for organismal health. Although DNA replication by the processive DNA polymerases δ and ϵ is highly accurate, inadvertent nucleotide misincorporations occasionally do occur. Polymerase selectivity and proofreading are the first lines of defense against such misincorporations (1). When a misincorporation escapes proofreading, DNA mismatch repair (MMR) provides a last line of defense. Consequently, inactivation of any of the MMR genes causes a spontaneous mutator phenotype (2).

In addition to correcting base-base mismatches, MMR plays multiple roles in responses to a wide spectrum of DNA damage-induced mutagenic insults (Fig. 1), including methylated nucleotides, oxidative DNA lesions, interstrand crosslinks (ICLs) and helix-distorting nucleotide lesions. Helix-distorting DNA lesions include a variety of nucleotide lesion types, including intrastrand crosslinks induced by ultraviolet (UV) light and bulky nucleotide adducts induced by dietary compounds such as the heterocyclic amines 2-Amino-1-methyl-6-phenylimidazo[4,5-b]pyridine (PhIP) and the polycyclic aromatic hydrocarbon (PAH) benzo(a)pyrene (BaP) (3, 4).

The role of MMR in DNA damage responses has been described most comprehensively for monofunctional methylating agents that, amongst others, methylate the O⁶ position of guanine. When unrepaired by O⁶-Methylguanine-DNA methyltransferase (MGMT) (Fig. 2A), O⁶-methylguanine can be replicated by either the replicative polymerases δ and ϵ or by the translesion synthesis (TLS) polymerase η (5) (Fig. 2B). The methylation of guanine alters its tautomeric state, allowing it to base-pair with both cytosine and thymine during replication (6). The MMR machinery excises the thymidine in the daughter strand of O⁶-methylguanine:thymine mismatches, together with a tract of adjacent nucleotides. However, during gap filling, O⁶-methylguanine again may direct misincorporation of thymine, which results in recurrent cycling between excision and error-prone gap filling (Fig. 2C). During the next cell cycle the excision tracts lead to double stranded DNA breaks by replicative run-off (7). These double stranded DNA breaks induce apoptosis or genomic deletions and rearrangements when mis-repaired (Fig. 2D). Thus, MMR-induced damage responses ultimately prevent the accumulation of G>A transitions and, when the damage load exceeds a threshold, protects the cell from genomic instability by inducing delayed apoptosis.

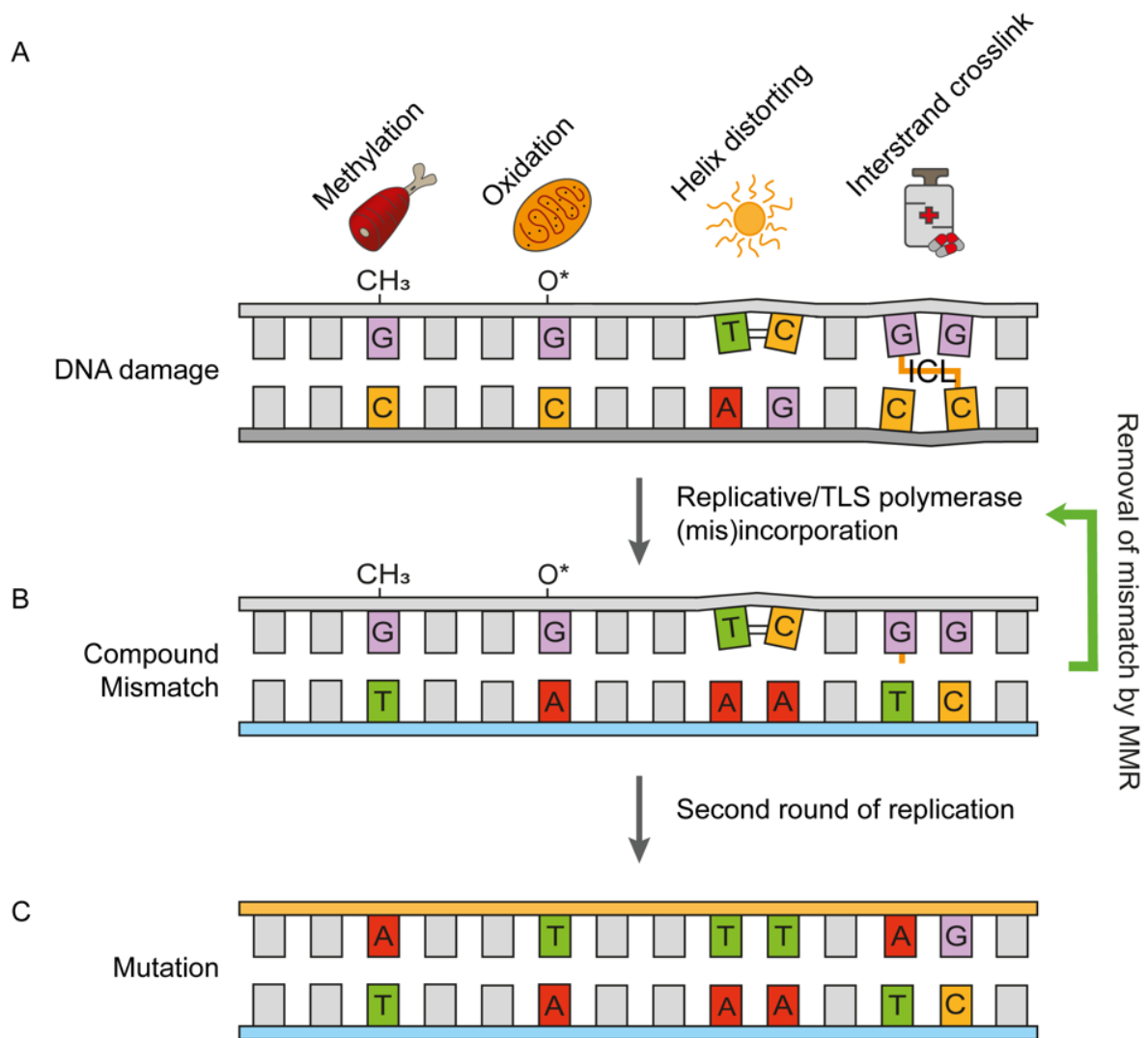


Figure 1| Replication of damaged DNA

A: DNA is continuously threatened by multiple sources of DNA damage, including diet (e.g. red meat), radical oxygen species (dysfunctional mitochondria), UV radiation (sunlight) and various (cytostatic) drugs leading to methylation (CH₃), oxidation (O*) or helix distorting DNA damage (=), as well as interstrand crosslinks (ICL). B: DNA damages are replicated by either replicative polymerases or TLS polymerases, leading to different types of compound mismatches. C: When mismatches remain in the DNA, mutation fixation occurs during successive rounds of replication. Mismatch repair/post-TLS repair may remove misincorporations, preventing DNA damage-induced mutagenesis.

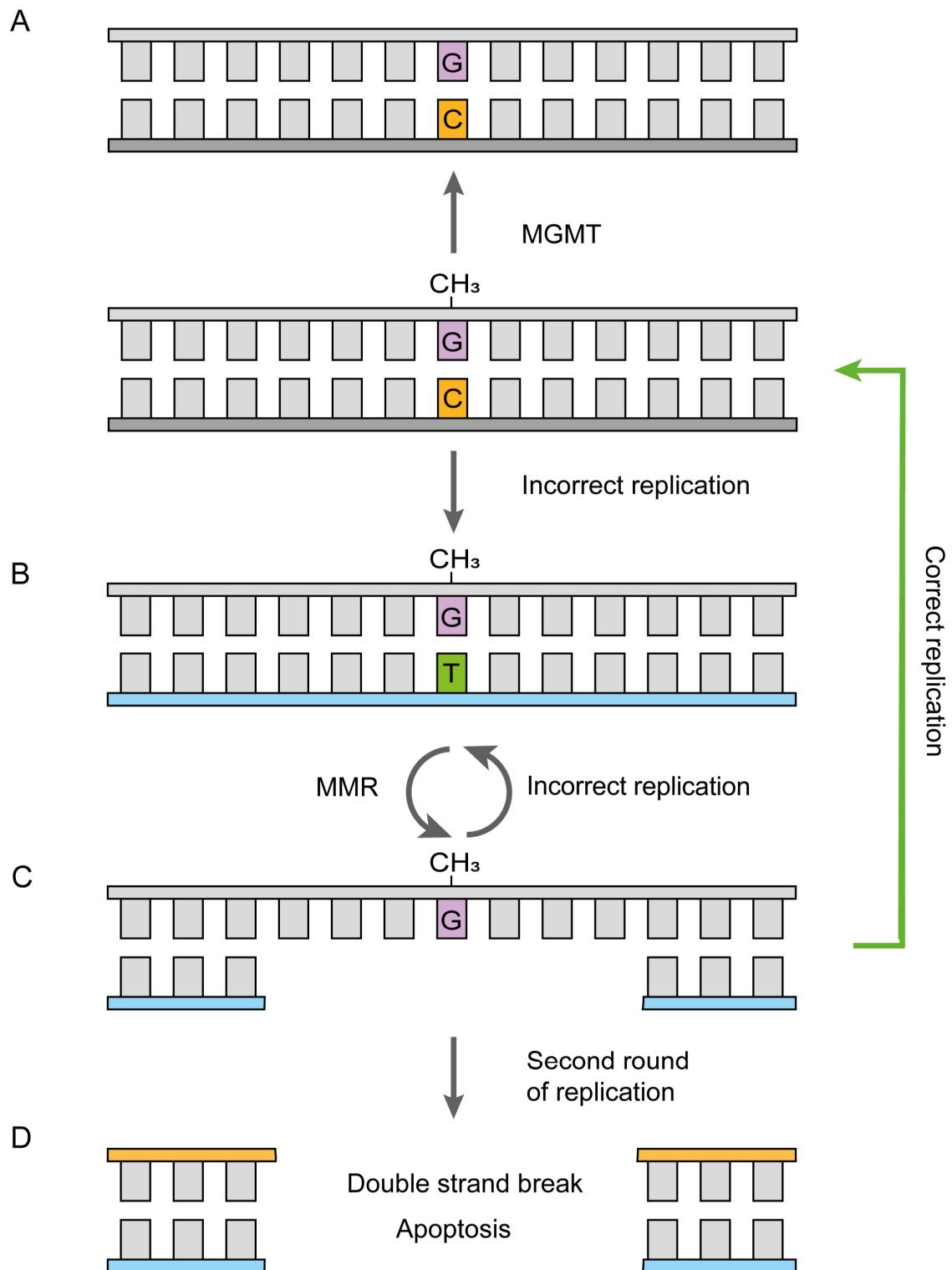


Figure 2| Roles of MMR in responses to O^6 -methylguanine

A: O^6 -methylguanine (CH_3) can be repaired by O^6 -Methylguanine-DNA methyltransferase (MGMT) leading to damage reversal. B: Replication of O^6 -methylguanine can lead to a O^6 -methylguanine.T mismatch, which can be removed by MMR resulting in a transient single stranded DNA tract. C: Gap filling can either lead to incorporation of a cytosine or to another misincorporation, that again is a substrate for MMR. D: Futile cycles of excision and misincorporation can lead to recurrent ssDNA tracts. In a subsequent round of replication these can lead to double stranded DNA breaks and consequent rearrangements or apoptosis.

Cells are under constant assault from oxidative DNA damage, induced by reactive oxygen species (ROS) (8). Again, guanines seem to be a preferred target, with 8-oxoguanine being a predominant oxidative DNA lesion (9). Similar to O⁶-methylguanine, replication of this damaged base can lead to a misincorporation, most frequently adenine (10) that can be excised by MMR and MUTYH (11) to reduce the mutagenicity of 8-oxoguanine (Fig. 3A). In addition, MMR-deficient cells retain a higher amount of oxidative lesions in the DNA than MMR-proficient cells (12). Overexpression of *MTH1*, which removes 8-oxoguanines from the nucleotide pool, reduces both spontaneous and oxidatively induced mutagenesis in MMR-deficient cells. These data indicate that MMR also excises 8-oxoguanine, incorporated from the nucleotide pool opposite adenine during replication. In contrast, removal of the template adenine by MUTYH results in mutagenesis (Fig. 3B) (13). Moreover, they suggest that oxidative DNA damage derived from the pool may significantly contribute to the spontaneous mutator phenotype of MMR-deficient cells.

In contrast to methylation and oxidative base damage, helix-distorting nucleotide lesions are poorly instructive and therefore arrest the processive DNA replication machinery. To counteract the toxicity of such lesions the cell employs specialized TLS DNA polymerases that can replicate across the damaged nucleotides, albeit in an error-prone fashion, resulting in DNA damage-directed mutagenesis (14). Interestingly, MMR can suppress this mutagenesis and increases checkpoint activation and apoptosis induced by UV, PhIP and BaP [(4, 15), Ijsselsteijn *et al.* manuscript in preparation]. In support, the MMR heterodimer MSH2-MSH6 is recruited to sites of localized UV damage (16) and selectively binds “mismatched” but not “matched” nucleotides opposite photolesions (17). The mechanistic basis for the involvement of MMR proteins in responses to such DNA lesions is not yet fully elucidated, but it has been suggested that a non-canonical MMR pathway, dubbed “post-TLS repair”, excises the nucleotide that was mis-incorporated by TLS opposite the damaged nucleotide. Thereby, post-TLS repair decreases DNA damage-induced mutagenesis while the resulting lesion-containing single-stranded DNA tracts activate DNA damage signaling (Fig. 4) (15). Another model to explain the increased mutagenesis by photolesions suggests that MMR plays a role in the recruitment of the relatively error-free TLS polymerase η , via Proliferating Cell Nuclear Antigen (PCNA) mono-ubiquitination (18, 19). However, knocking out both Polymerase η and *Msh6* in mouse embryonic stem cells shows a synergistic, rather than an epistatic, response to UV radiation in terms of mutagenesis (Ijsselsteijn *et al.* manuscript in preparation), supporting the post-TLS repair model.

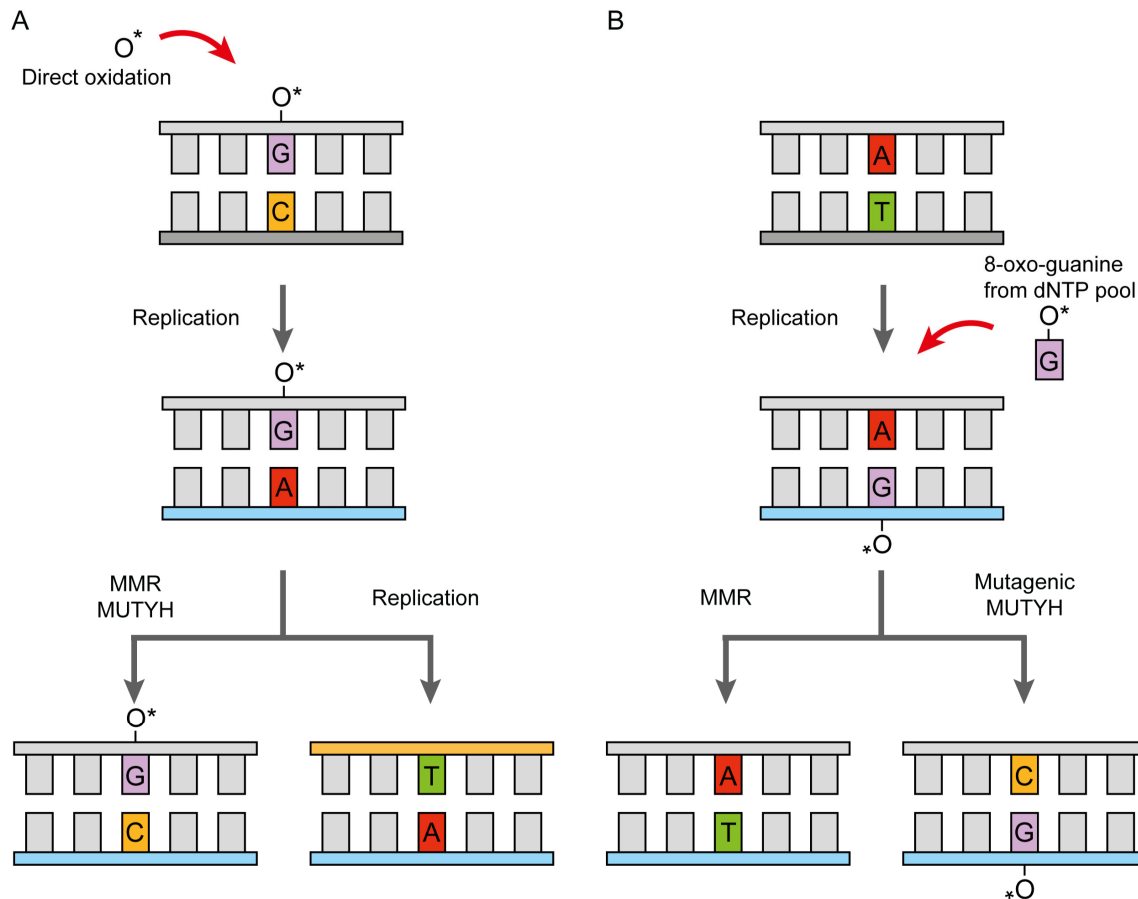


Figure 3|Processing of 8-oxoguanine. Adenine 'mispairs' by MMR and MUTYH

A: Guanines in the DNA can be oxidized by reactive oxygen species (ROS) to 8-oxoguanines (O*). Replication can lead to misincorporations of mostly adenines opposite 8-oxoguanines. When not removed by MMR and MUTYH, these misincorporations result in G>T transversions. B: Guanines that are oxidized (O*) in the free dNTP pool can be incorporated in the DNA opposite adenines. MMR recognizes these mismatches and removes the 8-oxoguanines from the DNA. In contrast, inadvertent repair of the nucleotide opposite the 8-oxoguanine by MUTYH leads to a mutation.

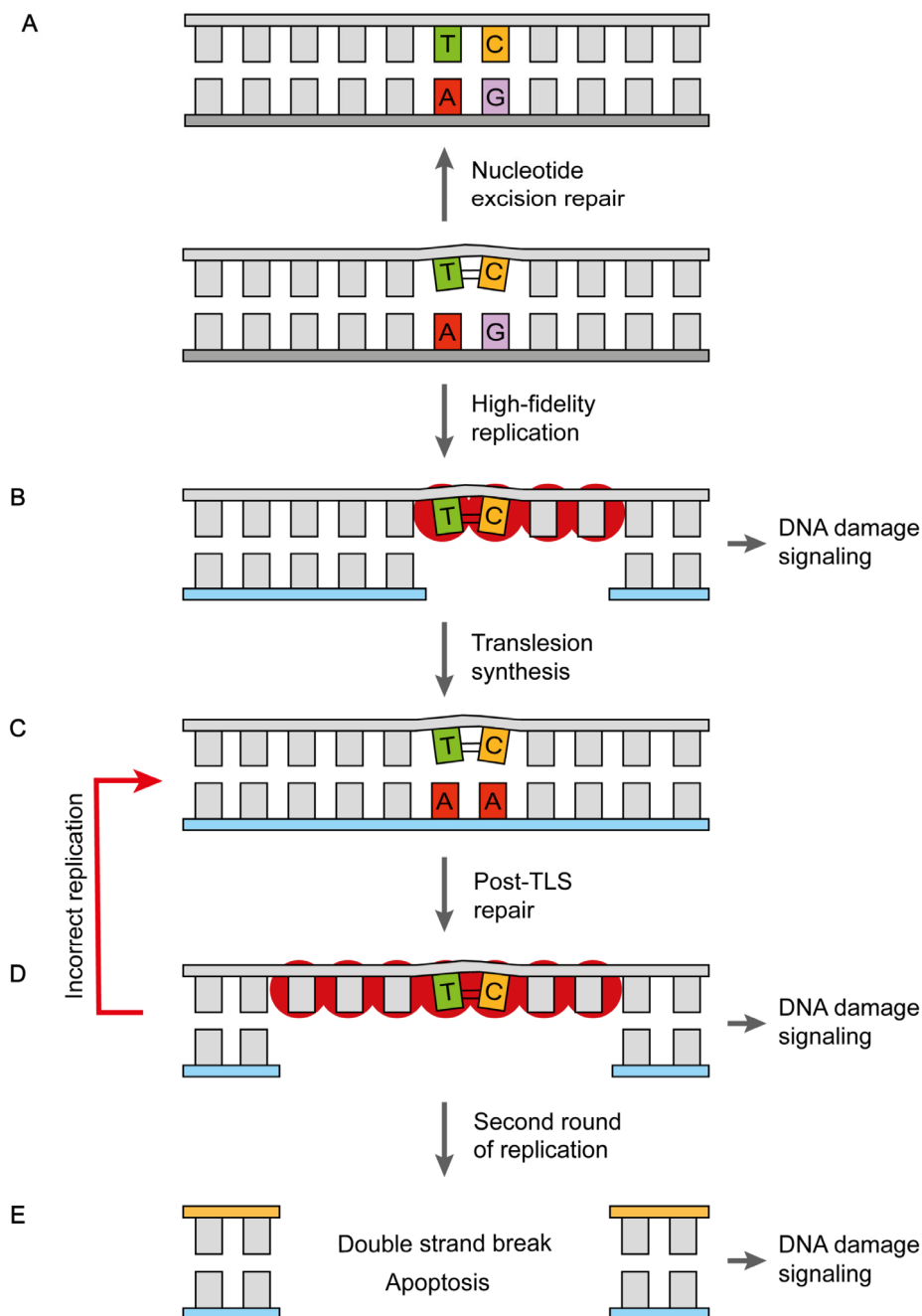


Figure 4| The role of MMR/post-TLS repair in responses to helix-distorting DNA damage

A: Exposure of DNA to sunlight (UV-light) results in helix-distorting nucleotide lesions (=) that can be repaired by nucleotide excision repair. B: Unrepaired helix-distorting nucleotide lesions arrest replicative polymerases resulting in single-stranded DNA tracts. When sufficiently long, these are coated by Replication Protein A (RPA ●) multimers, activating DNA damage signaling. TLS can replicate across the damaged nucleotides to mitigate their toxicity. C: TLS often leads to a 'misincorporation' opposite the lesion. Such a compound lesion can be recognized by post-TLS repair, likely resulting in long excision tracts. D: The resulting single-stranded DNA gap is coated by RPA multimers. Filling of these extended gaps by, successively, replicative and TLS polymerases may be a lengthy process and, therefore, underlie the strong post-TLS repair-associated DNA damage response. E: Persistent ssDNA can lead to a double stranded DNA break in the subsequent cell cycle, resulting in apoptotic signaling (3, 15).

One of the most difficult to repair DNA damages are ICLs that require a multi-step process where multiple repair pathways converge to repair the covalent linking of two opposite DNA strands. ICLs can result from aldehydes, derived from ethanol or from lipid peroxidation, from some vegetables and they are also induced by several chemotherapeutics, such as Cisplatin, used in the treatment of (amongst others) breast cancer. The repair of ICLs involves Fanconi Anemia (FA)-associated proteins, but also requires homologous recombination, TLS and in some cases nucleotide excision repair (20). It has been suggested that MMR-deficient cells display reduced sensitivity to ICL-inducing agents, indicating a role for MMR in responses to ICLs (21). 'Misincorporations', generated during gap-filling by TLS opposite the unhooked ICL might be a substrate for MMR, comparable to post-TLS repair of UV-induced intra-strand crosslinks (15). For specific ICLs, base excision repair polymerase β (Pol β) and MMR play an epistatic role. Both the toxicity and repair of ICLs are diminished in cells, knocked down for MSH2, MLH1 or Pol β , but is not further reduced in a double knock-down of Pol β and MSH2 or MLH1 (21), suggesting that the role of MMR is post-replicative and linked to Pol β .

Absence of MMR/post-TLS repair causes both a spontaneous mutator phenotype and increased DNA damage-induced mutagenesis, as well as aberrant DNA damage responses. It therefore is not surprising that loss of MMR/post-TLS repair is strongly associated with carcinogenesis (22). As mentioned before, MMR/post-TLS repair deficiency results in tolerance of various types of DNA damage and thus MMR/post-TLS repair-deficient cancers might benefit from a targeted treatment. For instance, the tolerance of MMR/post-TLS repair-deficient cells to chemotherapeutic drugs that induce O⁶-methylguanines, such as Dacarbazine and Temozolomide, indicates that these agents may be ineffective for the treatment of MMR/post-TLS repair-deficient tumors. Furthermore, exposure of MMR-proficient cells to DNA-damaging drugs might lead to selection for MMR/post-TLS repair-deficiency. For instance, glioblastomas have been shown to acquire tolerance to Temozolomide by inactivating MMR/post-TLS repair (23). Another example is provided by acute myeloid leukemia (AML), which can be a late consequence of immunosuppression by Azathioprine after organ transplantation (24). Its S⁶-(thio)guanine metabolite is methylated endogenously and induces MMR-dependent cytotoxicity, which leads to selection of MMR/post-TLS repair-deficient cells. Also, recurring AML in non-transplant patients is often MMR/post-TLS repair deficient, which might be associated with acquired tolerance to treatment of the primary AML with 6-thioguanine (25, 26). Melanomas frequently display hallmarks of MMR/post-TLS repair deficiency too (27). Sunlight, which is the major etiological agent of these tumors, induces not only intrastrand DNA crosslinks but also oxidative DNA damage (28). As described above, MMR/Post-TLS repair is associated with protective responses to both types of DNA lesions, which might provide a rationale for its loss in melanoma. Finally, MMR is lost in 15% of the sporadic colorectal cancers (CRC) (29). The mechanism of action of most chemotherapeutic treatments of CRC is based on the induction of DNA damage, leading to senescence or death of the rapidly cycling tumor cells. For instance, 5-fluoruracil (5-FU) is incorporated in RNA but also

causes nucleotide pool imbalances, while its metabolite 5-FdU can be incorporated in DNA instead of thymidine. MMR-deficient cells display a mild tolerance to 5-FU, suggesting a role for MMR in processing misincorporations due to nucleotide pool imbalances as well as misincorporations opposite 5-FdU residues (30). In support, treatment with 5-FU provides no benefit to MMR-deficient CRC (31).

Apart from the causal involvement of MMR deficiency in sporadic cancer, inheritance of a germline mutation in one allele of any of the four MMR genes is responsible for the common cancer predisposition Lynch syndrome, historically called Hereditary Non-Polyposis Colorectal Cancer (HNPCC). Carriers have an approximate 40-60% risk of developing gastrointestinal tumors and, for females, approximately 40% risk of endometrial tumors, depending on which MMR gene is mutated (32). Inheritance of a bi-allelic germline mutation in one of the MMR genes leads to constitutional MMR deficiency (cMMRd), a childhood cancer syndrome. In contrast to Lynch syndrome, cMMRd involves a wide spectrum of tumors, which is dominated by brain, hematological and intestinal cancers (33). The prevalence of sporadic MMR deficiency in CRC and the restricted cancer tropism in Lynch syndrome, as compared with cMMRd, suggest that roles of MMR/post-TLS repair in the intestine, beyond the correction of simple base-base mismatches are involved in the development of these cancers.

Cancer development requires an array of mutagenic (tumor initiation and progression) and non-mutagenic (tumor promotion and progression) events. The exposure of intestinal epithelial cells to endogenous and food-derived mutagenic compounds is pertinent to all stages of oncogenesis (34), but might be even more so in the development of MMR/post-TLS repair-deficient cancer. For instance, in gastrointestinal stem cells from individuals with Lynch syndrome, these compounds can promote the mutational inactivation of the remaining wild-type allele of the germline mutated MMR gene (Fig. 5). The resulting MMR/post-TLS repair-deficient cells may be prone to oncogenic derailment in different ways. For example, exposure to butyrate produced by the intestinal microbiome from carbohydrates, may provide a specific growth advantage to MMR-deficient crypts (35). Furthermore, exposure of these crypts to DNA methylating agents from the diet or bile (36, 37) may promote their expansion to adjacent crypts (38). Also, the signatures of spontaneous mutations caused by the MMR deficiency and those induced by helix-distorting nucleotide lesions are different (39). This increases the number of “hittable” oncogenic targets and therefore both mutagenic processes may synergize in cancer development. Furthermore, as described above, MMR/post-TLS repair-deficient cells may be intrinsically hypermutable by agents that induce helix-distorting nucleotide lesions while cell cycle arrests and apoptosis may be impaired (3, 15). These factors might further contribute to CRC development in Lynch syndrome. Moreover, intestinal mutagens such as PhIP might damage mitochondria, leading to the generation of ROS, which is another source of DNA damage (40). Finally, neoepitopes resulting from the mutator phenotypes MMR and from the exposure to intestinal mutagens in the absence of MMR/post-TLS repair may elicit an immune response (41). This immune response

may not only be tumor suppressive, but can also contribute to tumor progression, since neutrophils produce ROS that further damage the DNA (42). Given the role of MMR in responses to oxidative DNA injury, the increase of oxidatively injured DNA might provide another selective advantage to MMR-deficient cells.

In conclusion, diverse phenotypic characteristics of MMR/post-TLS repair-deficient cells can contribute to cancer development and treatment resistance. We anticipate that further understanding the involvement of MMR/post-TLS repair in responses to DNA damaging compounds may improve the prevention and management of cancers associated with inherited or somatic MMR gene defects.

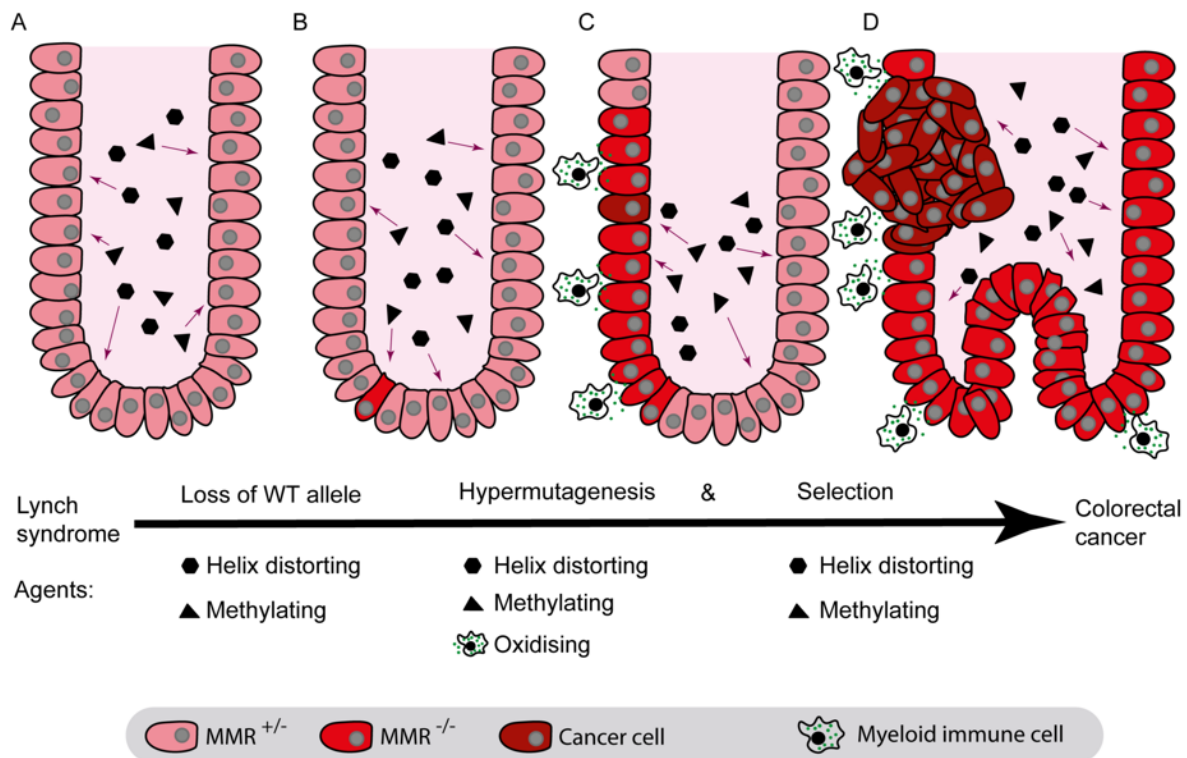


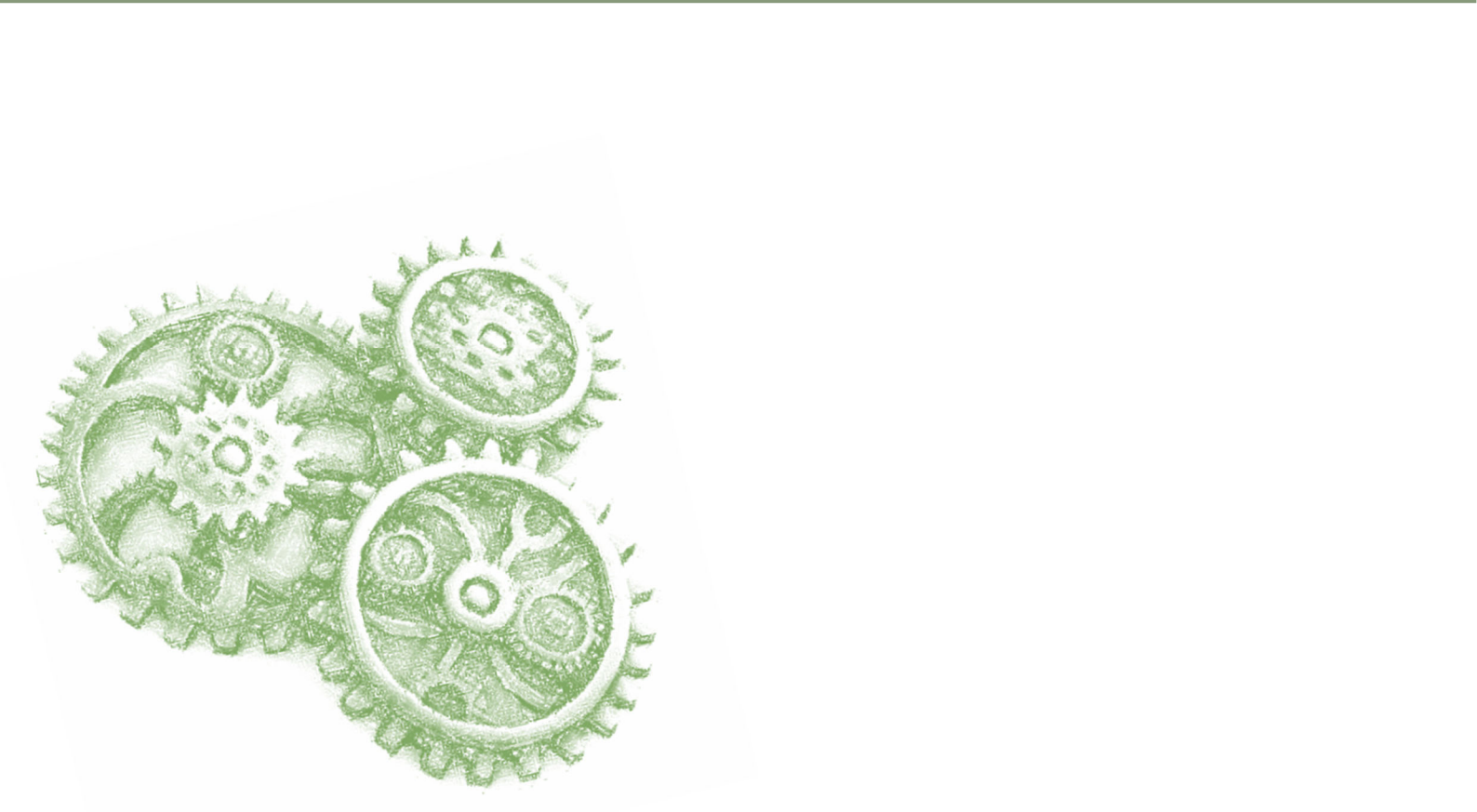
Figure 5| Etiology of cancer of the gastro-intestinal tract in Lynch syndrome

A: All gastro-intestinal crypt cells of Lynch syndrome carriers are heterozygous for an MMR gene (light red) and are continuously exposed to agents that induce methylating and helix-distorting DNA lesions. B: Methylating and helix-distorting DNA lesions can induce inadvertent loss of the wild type allele of the germ-line mutated MMR gene (bright red). C: Loss of MMR/post-TLS repair leads to hypermutagenesis, which results in the accumulation of oncogenic mutations (dark red). In addition, neoepitopes in these cells trigger the recruitment of myeloid immune cells that excrete reactive oxygen species, which may further increase mutagenesis in MMR/post-TLS repair-deficient cells. D: MMR/post-TLS repair-deficient cells also are more tolerant to methylated and to helix distorting DNA damage, which leads to their expansion. Ultimately, these selective 'advantages' can result in rapid carcinogenesis.

References

1. Rais, Johansson E. DNA Replication—A Matter of Fidelity. *Molecular Cell*. 2016;62(5):745-55.
2. Zhang Y, Yuan F, Presnell SR, Tian K, Gao Y, Tomkinson AE, et al. Reconstitution of 5'-Directed Human Mismatch Repair in a Purified System. *Cell*. 2005;122(5):693-705.
3. Smith-Roe SL, Hegan DC, Glazer PM, Buermeier AB. Mlh1-dependent suppression of specific mutations induced in vivo by the food-borne carcinogen 2-amino-1-methyl-6-phenylimidazo [4,5-b] pyridine (PhIP). *Mutat Res*. 2006;594(1-2):101-12.
4. Glaab WE, Skopek TR. Cytotoxic and mutagenic response of mismatch repair-defective human cancer cells exposed to a food-associated heterocyclic amine. *Carcinogenesis*. 1999;20(3):391-4.
5. Haracska L, Prakash S, Prakash L. Replication past O6-Methylguanine by Yeast and Human DNA Polymerase η . *Molecular and Cellular Biology*. 2000;20(21):8001-7.
6. Wyatt MD, Pittman DL. Methylating Agents and DNA Repair Responses: Methylated Bases and Sources of Strand Breaks. *Chemical Research in Toxicology*. 2006;19(12):1580-94.
7. Fu D, Calvo JA, Samson LD. Balancing repair and tolerance of DNA damage caused by alkylating agents. *Nature Reviews Cancer*. 2012;12(2):104-20.
8. Halliwell B. Free radicals, antioxidants, and human disease: curiosity, cause, or consequence? *The Lancet*. 1994;344(8924):721-4.
9. Kanvah S, Joseph J, Schuster GB, Barnett RN, Cleveland CL, Landman U. Oxidation of DNA: Damage to Nucleobases. *Accounts of Chemical Research*. 2010;43(2):280-7.
10. Van Loon B, Markkanen E, Hübscher U. Oxygen as a friend and enemy: How to combat the mutational potential of 8-oxo-guanine. *DNA Repair*. 2010;9(6):604-16.
11. Mazurek A, Berardini M, Fishel R. Activation of Human MutS Homologs by 8-Oxo-guanine DNA Damage. *Journal of Biological Chemistry*. 2002;277(10):8260-6.
12. Deweese TL, Shipman JM, Larrier NA, Buckley NM, Kidd LR, Groopman JD, et al. Mouse embryonic stem cells carrying one or two defective Msh2 alleles respond abnormally to oxidative stress inflicted by low-level radiation. *Proceedings of the National Academy of Sciences*. 1998;95(20):11915-20.
13. Russo MT, Blasi MF, Chiera F, Fortini P, Degan P, Macpherson P, et al. The Oxidized Deoxynucleoside Triphosphate Pool Is a Significant Contributor to Genetic Instability in Mismatch Repair-Deficient Cells. *Molecular and Cellular Biology*. 2004;24(1):465-74.
14. Pilzecker B, Buoninfante OA, Jacobs H. DNA damage tolerance in stem cells, ageing, mutagenesis, disease and cancer therapy. *Nucleic Acids Research*. 2019;47(14):7163-81.
15. Tsaalbi-Shtylik A, Ferras C, Pauw B, Hendriks G, Temviriyankul P, Carlee L, et al. Excision of translesion synthesis errors orchestrates responses to helix-distorting DNA lesions. *J Cell Biol*. 2015;209(1):33-46.
16. Hong Z, Jiang J, Hashiguchi K, Hoshi M, Lan L, Yasui A. Recruitment of mismatch repair proteins to the site of DNA damage in human cells. *Journal of Cell Science*. 2008;121(19):3146-54.
17. Wang H, Lawrence CW, Li GM, Hays JB. Specific binding of human MSH2.MSH6 mismatch-repair protein heterodimers to DNA incorporating thymine- or uracil-containing UV light photoproducts opposite mismatched bases. *J Biol Chem*. 1999;274(24):16894-900.
18. Zlatanou A, Despras E, Braz-Petta T, Boubakour-Azzouz I, Pouvelle C, Grant, et al. The hMsh2-hMsh6 Complex Acts in Concert with Monoubiquitinated PCNA and Pol η in Response to Oxidative DNA Damage in Human Cells. *Molecular Cell*. 2011;43(4):649-62.
19. Peña-Díaz J, Bregenhorn S, Ghodgaonkar M, Follonier C, Artola-Borán M, Castor D, et al. Noncanonical Mismatch Repair as a Source of Genomic Instability in Human Cells. *Molecular Cell*. 2012;47(5):669-80.
20. Deans AJ, West SC. DNA interstrand crosslink repair and cancer. *Nature Reviews Cancer*. 2011;11(7):467-80.
21. Sawant A, Kothandapani A, Zhitkovich A, Sobol RW, Patrick SM. Role of mismatch repair proteins in the processing of cisplatin interstrand cross-links. *DNA Repair*. 2015;35:126-36.
22. Liu D, Keijzers G, Rasmussen LJ. DNA mismatch repair and its many roles in eukaryotic cells. *Mutation Research/Reviews in Mutation Research*. 2017;773:174-87.
23. Yip S, Miao J, Cahill DP, Iafrate AJ, Aldape K, Nutt CL, et al. MSH6 Mutations Arise in Glioblastomas during Temozolomide Therapy and Mediate Temozolomide Resistance. *Clinical Cancer Research*. 2009;15(14):4622-9.
24. Offman J, Opelz G, Doehler B, Cummins D, Halil O, Banner NR, et al. Defective DNA mismatch repair in acute myeloid leukemia/myelodysplastic syndrome after organ transplantation. *Blood*. 2004;104(3):822-8.
25. Munshi PN, Lubin M, Bertino JR. 6-Thioguanine: A Drug With Unrealized Potential for Cancer Therapy. *The Oncologist*. 2014;19(7):760-5.
26. Mao G, Yuan F, Absher K, Jennings CD, Howard DS, Jordan CT, et al. Preferential loss of mismatch repair function in refractory and relapsed acute myeloid leukemia: potential contribution to AML progression. *Cell research*. 2008;18(2):281-9.

27. Kubeček O, Kopecký J. Microsatellite instability in melanoma. *Melanoma Research*. 2016;26(6):545-50.
28. Schuch AP, Moreno NC, Schuch NJ, Menck CFM, Garcia CCM. Sunlight damage to cellular DNA: focus on oxidatively generated lesions. *Free radical biology & medicine*. 2017(107):110-24.
29. Brenner H, Kloor M, Pox CP. Colorectal cancer. *Lancet*. 2014;383(9927):1490-502.
30. Meyers M, Wagner MW, Mazurek A, Schmutte C, Fishel R, Boothman DA. DNA Mismatch Repair-dependent Response to Fluoropyrimidine-generated Damage. *Journal of Biological Chemistry*. 2005;280(7):5516-26.
31. Sargent DJ, Marsoni S, Monges G, Thibodeau SN, Labianca R, Hamilton SR, et al. Defective Mismatch Repair As a Predictive Marker for Lack of Efficacy of Fluorouracil-Based Adjuvant Therapy in Colon Cancer. *Journal of Clinical Oncology*. 2010;28(20):3219-26.
32. Stoffel E, Mukherjee B, Raymond VM, Tayob N, Kastrinos F, Sparr J, et al. Calculation of Risk of Colorectal and Endometrial Cancer Among Patients With Lynch Syndrome. *Gastroenterology*. 2009;137(5):1621-7.
33. Lavoine N, Colas C, Muleris M, Bodo S, Duval A, Entz-Werle N, et al. Constitutional mismatch repair deficiency syndrome: clinical description in a French cohort. *Journal of Medical Genetics*. 2015;52(11):770-8.
34. Cross AJ, Sinha R. Meat-related mutagens/carcinogens in the etiology of colorectal cancer. *Environmental and Molecular Mutagenesis*. 2004;44(1):44-55.
35. Belcheva A, Irazabal T, Susan, Streutker C, Maughan H, Rubino S, et al. Gut Microbial Metabolism Drives Transformation of Msh2-Deficient Colon Epithelial Cells. *Cell*. 2014;158(2):288-99.
36. Jia W, Xie G, Jia W. Bile acid-microbiota crosstalk in gastrointestinal inflammation and carcinogenesis. *Nat Rev Gastroenterol Hepatol*. 2018;15(2):111-28.
37. Cantwell M, Elliott C. Nitrates, Nitrites and Nitrosamines from Processed Meat Intake and Colorectal Cancer Risk. *Journal of Clinical Nutrition & Dietetics*. 2017;3:4-27.
38. Wojciechowicz K, Cantelli E, Van Gerwen B, Plug M, Van Der Wal A, Delzenne-Goette E, et al. Temozolomide Increases the Number of Mismatch Repair-Deficient Intestinal Crypts and Accelerates Tumorigenesis in a Mouse Model of Lynch Syndrome. *Gastroenterology*. 2014;147(5):1064-72.e5.
39. Kucab JE, Zou X, Morganella S, Joel M, Nanda AS, Nagy E, et al. A Compendium of Mutational Signatures of Environmental Agents. *Cell*. 2019;177(4):821-36.e16.
40. Fang EF, Scheibye-Knudsen M, Chua KF, Mattson MP, Croteau DL, Bohr VA. Nuclear DNA damage signalling to mitochondria in ageing. *Nature Reviews Molecular Cell Biology*. 2016;17(5):308-21.
41. Dudley JC, Lin MT, Le DT, Eshleman JR. Microsatellite Instability as a Biomarker for PD-1 Blockade. *Clinical Cancer Research*. 2016;22(4):813-20.
42. Winterbourn CC, Kettle AJ, Hampton MB. Reactive Oxygen Species and Neutrophil Function. *Annual Review of Biochemistry*. 2016;85(1):765-92.





Chapter 3:

Characterizing the role of mismatch repair components in the ultraviolet light-induced post-translesion synthesis repair pathway



Robbert Ijsselsteijn¹, Gido Snaterse¹, Mark Drost¹, Jacob G Jansen¹

¹Department of Human Genetics, Leiden University Medical Center, Leiden, The Netherlands.

Abstract

DNA mismatch repair (MMR) removes base-base misincorporations that are generated by the replicative DNA polymerases delta and epsilon to prevent mutagenesis. Previous work has suggested that the apical MMR heterodimer MutS α (Msh2/Msh6) also suppresses UV-induced mutagenesis and concomitantly activates DNA damage signaling, possibly by generating ssDNA tracts covered with Replication Protein A (RPA). To identify additional MMR-related genes that may play a role in these non-canonical activities of MutS α we here analyzed responses to UV light of nucleotide excision repair (NER)-deficient mouse embryonic stem (mES) cells with an additional defect in MMR-components Mlh1 or Pms2 that form the heterodimer MutL α , in Mlh1-interacting proteins Mlh3 or Pms1, and in exonucleases Exo1 or Fan1. These experiments show that MutL α suppresses UV-induced mutagenesis to a similar extent as MutS α , however, in contrast to MutS α , MutL α is not required for activating UV-induced DNA damage signaling. Mutation spectra analyses of the Hprt gene are compatible with a model where MutS α and MutL α suppress UV-induced mutagenesis by removing misincorporations opposite photolesions at pyrimidine dimers. In contrast, Pms1, Mlh3, Fan1 and Exo1 do not play a role in the suppression of UV-induced mutagenesis or in DNA damage signaling. In conclusion, our data reveal that MutL α suppresses UV-induced mutagenesis independent of activating UV-induced damage signaling, indicating a separation of function between MutS α and its downstream actor MutL α in response to UV-induced DNA damage.

Introduction

DNA mismatch repair (MMR) is an evolutionarily conserved genome maintenance pathway best known for correcting mis-incorporations introduced by replicative DNA polymerases opposite unmodified nucleotides in DNA. The canonical MMR pathway consists of mismatch recognition, nick-dependent excision and gap filling. More specifically, eukaryotic MMR initiates with either the heterodimeric protein complex MSH2/MSH6 (MutS α) that recognizes base/base mispairs and 1-2 base pair insertion/deletion loops or with the MSH2/MSH3 (MutS β) complex that recognizes larger insertion/deletion loops. Then, recruitment of the heterodimer MLH1/PMS2 (MutL α), displaying endonucleolytic activity, is critical for the excision of the newly synthesized strand containing the mismatched nucleotide. This endonuclease can generate an incision 5' to the mismatch in the newly synthesized strand. MutL α is also important in 3' nick-directed MMR (1). Subsequently, the mis-incorporation can be removed by multiple pathways that either depend on long-range exonucleolytic resection by EXO1, continued endonucleolytic degradation by MutL α or strand displacement by replicative DNA polymerase delta followed by 5' flap cleavage (2). Any remaining single stranded DNA (ssDNA) is converted into double stranded DNA (dsDNA) by DNA polymerase delta and the remaining nick is sealed by a DNA ligase (1). Other exonucleases beside EXO1 may act redundantly in removal of misincorporations, like FANCI-associated nuclease 1 (FAN1), that is shown to interact with MSH2 and MLH1 after treatment with the MMR-inducing methylating agent N-methyl-N-nitrosourea (MNU) (3). MLH1 also interacts with MMR homologs PMS1 and MLH3 thereby forming MutL β and MutL γ , respectively. The amino acid sequence of *MLH3* is most similar to the sequence of *PMS2*, suggesting that they may display overlapping functions. Mammalian MutL γ exhibits endonuclease activity at loop-containing DNA (4) and deficiency of mouse Mlh3 leads to a low, but significant, increase of mutations at microsatellites, a phenotype indicative of defective MMR. Moreover, loss of both Pms2 and Mlh3 results in microsatellite instability comparable to loss of their binding partner Mlh1, suggesting functional redundancy between Pms2 and Mlh3 (5). The role of PMS1 is much more enigmatic and to date no clear phenotypes of PMS1 loss have been found (6).

Apart from operating in canonical MMR, several MMR proteins seem to play an important role in the response to damaged nucleotides such as bulky and helix-distorting photolesions induced by ultraviolet (UV) light. As they form strong blocks for replicative DNA polymerases, these lesions are bypassed by specialized translesion synthesis (TLS) polymerases to allow completion of DNA replication. However, due to low replication fidelity and lack of proofreading, TLS polymerases frequently misincorporate opposite UV lesions (7). Basepairing between these helix-distorting DNA lesions and 'mismatched' nucleotides is severely perturbed or absent. Nonetheless, purified MutS α is able to preferentially bind these compound structures *in vitro* (8). In addition, MSH2 and MSH6 are important for inducing an UV-induced cell cycle arrest and apoptotic responses in human melanoma cells (9), in mouse epidermal cells *in vivo*, in mouse keratinocytes and in mouse embryonic stem (mES)

cells (10, 11). Furthermore, although MutS α does not seem to play a role in the removal of photolesions, rodent cells defective for Msh2, Msh6 or Pms2 display increased UV-induced mutagenesis compared to MMR proficient cells (12-14). Mice defective for Msh2 show accelerated skin tumorigenesis following UVB exposure (15, 16), underscoring the protective role of Msh2 in genome stability in response to UV light.

In replicating cells the early responses following UV exposure are accompanied with MutS α -dependent formation of ssDNA tracts that encompass UV photolesions (11). These patches of ssDNA are coated with the ssDNA binding heterotrimeric protein Replication Protein A (RPA) that activates a signaling cascade via the sensor checkpoint kinase Ataxia Telangiectasia and Rad3-related protein (ATR), resulting in the activation of effector kinases such as Chk1 that are important for activating a cell cycle arrest (17). Based on the MutS α -dependent suppression of UV-induced mutagenesis and findings that most UV-induced mutations in MutS α -deficient cells are likely targeted at UV lesions, it has been proposed that these ssDNA patches result from MutS α -dependent removal of the 'mismatched' nucleotides opposite photolesions. Together these data led to the hypothesis of a non-canonical MMR pathway, dubbed post-TLS repair, that controls TLS-associated mutagenesis by removal of misincorporations opposite helix-distorting nucleotide lesions, whilst the excision tracts activate DNA damage signaling cascades, resulting in cell cycle arrest and apoptotic responses (11).

In the present study we asked whether MMR-related proteins other than MutS α contribute to the suppression of UV-induced mutations and the concomitant induction of cell cycle arrest and apoptotic responses. To this end isogenic mES cell lines were generated with single defects in the canonical MMR genes *Mlh1* and *Pms2*, in *Mlh3* and *Pms1* and in MMR-associated exonucleases *Exo1* and *Fan1*. These cell lines contain an additional defect in the *Xpa* gene, a core factor in nucleotide excision repair, to exclude removal of UV photolesions. We show that the generation of UV-induced ssDNA and the activation of DNA damage signaling depend on Msh6, but not on the downstream factors of canonical MMR, including MutL α . However, UV-induced mutagenesis is controlled not only by MutS α but also by Mlh1 and Pms2, indicating a role of MutL α in controlling the mutagenicity of helix-distorting DNA lesions. Mutation spectra analysis of mutations in the *Hprt* gene revealed that UV-induced mutations were dominated by C > T transitions at dipyrimidine sites, which were predominantly located in the transcribed strand, irrespective of Msh6 or Mlh1 status. Neither the Mlh1-interacting proteins Mlh3 and Pms1 nor the MMR-associated exonucleases Exo1 and Fan1 play an overt role in post-TLS repair. Taken together these data suggest an uncoupling of the DNA damage signaling induced by UV, which only depends on Msh6, from the control of UV-induced mutagenesis, which requires all of the core MMR proteins.

Materials and Methods

Cell lines and cell culture

Wild-type mES cells were used as a parental line to all cell lines acquired (18). The *Xpa* deficient cell line was previously generated by Hendriks et al. (2010) through targeted disruption of exons 3 and 4. Deficiencies for *Mlh3*, *Pms1*, *Exo1* and *Fan1* in the *Xpa* deficient cell line were introduced using CRISPR/Cas9 (Supplementary methods table 2). The *Mlh3* deficient cell lines are disrupted by a frameshifting deletion in exon 6, the *Pms1* deficient cell lines have frameshifting deletions in exon 10, the *Exo1* cell lines are disrupted in exon 5 or 6 and the *Fan1* cell lines have their entire genes deleted. The cell lines were validated using RT-PCR analysis (Fig. S1). The *Exo1* cell lines were still able to produce shortened mRNA, whereas all other cell lines did not produce stable mRNA from the disrupted gene. The MMR deficient cell lines for *Msh6*, *Mlh1* and *Pms2* were made deficient by using CRISPR/Cas9 constructs targeting exon 1-2 for *Msh6*, the entire gene for *Mlh1* and exons 5-7 for *Pms2*, respectively, and were afterwards selected for MMR deficiency following a (40 μ M) 6tG treatment for four hours. Knock-out was validated by western blot (Fig. S1). ES cells were cultured on senescent mouse embryonic fibroblast feeder cells in complete medium consisting of DMEM KO (Gibco) supplemented with 10% fetal calf serum (Bodinco/Capricorn Scientific), 1% glutamax (Gibco), 1% non-essential amino acids (Gibco), 1mM pyruvate (Gibco), 100U penicillin/100 μ g streptomycin (Gibco), 0.1mM β -mercapto-ethanol (Sigma-Aldrich) and leukemia inhibitory factor (LIF, made in house). During experiments complete medium was mixed in a 1:1 ratio with Buffalo rat liver (BRL) cell-conditioned medium called 50/50 to allow for growth on gelatin-coated culture dishes.

Determination of UV-induced DNA damage signaling

One million cells were seeded in gelatin-coated 6 wells plates with 50/50 medium one day prior to exposure with 0,75J/m² of UV-C. Following UV treatment cells were cultured in 50/50 medium. Cells were lysed using 300 μ l 2x Laemmli sample buffer 0, 2, 4 and 8 hours after UV-C exposure. In some experiments nocodazole (300 ng/ml) (Sigma Aldrich) was added immediately after UV irradiation to block cells in mitosis. Samples were loaded on SDS-PAGE using 12.5 μ l sample per slot of a 4-12% Criterion XT Bis-Tris Gel (Bio-rad). Proteins were transferred onto Protran 0.45 μ M nitrocellulose membranes (GE Healthcare) using 400mA (~70V) for 2 hours at 4°C. Then, nitrocellulose membranes were incubated with Rockland blocking reagent (Rockland) diluted 1:1 with 0.1% PBS-Tween (Rockland-PBS-T) for one hour to block non-specific antibody binding. Afterwards, membranes were incubated in Rockland-PBS-T with primary antibodies against Kap-1^P (1:1000, Bethyl, polyclonal A300-767A), Chk1^P (1:1000, Cell signaling technology, clone 133D3) or PCNA (1:8000, Santa Cruz, clone PC10) for overnight at 4°C. The next day the membranes were washed with PBS-tween (0.1%) and incubated with secondary anti-rabbit and anti-mouse HRP (1:50000 in Rockland-PBS-T) depending on the primary antibody isotype. Amersham ECL select (GE Healthcare) was used to visualize protein bands.

Subcellular fractionation and the analysis of chromatin-bound Rpa

1.5 million cells were seeded in gelatin-coated 60mm dishes in 50/50 medium and grown for a day. The cells were washed twice with PBS before exposure to 2J/m² of UV and incubated in 50/50 medium for 0 or 4 hours. Next, cells were collected by trypsinization and 2 million cells were used for fractionation using the Subcellular Protein Fractionation Kit for Cultured Cells (Thermo Fisher Scientific) according to the manufacturer's recommendation. The total amount of protein in the isolated fractions was measured using a Bradford assay (Thermo Fisher Scientific). SDS-PAGE was performed with 10µg of protein per sample using 4-12% Criterion XT Bis-Tris Gels (Bio-rad). Western blot was performed as described previously with antibodies against Histone H3 (Abcam, polyclonal) and Rpa (Cell signaling technology, Clone 4E4).

Determination of *Hprt* mutant frequency

Per condition, five million cells were seeded in 50/50 medium in a 90mm dish coated with gelatin and grown for one day. Then, cells were washed twice with PBS, exposed to 0 or 0.75J/m² UV, and 5 million cells were seeded into a new gelatin-coated dish with 50/50 medium. Cell populations were split every two days for three passages. Then, 2 million cells were equally distributed over 5 gelatin-coated 90mm dishes containing 50/50 medium with 30µM 6tG. In parallel 250 cells were seeded in gelatin-coated 60mm dishes in triplicate to determine the clone forming ability. The clones were grown 7-10 days before staining with methylene blue. The number of clones was determined by manual counting. The frequency of 6tG resistant clones per million cells was adjusted for the cloning efficiency.

Next generation sequencing of clones selected for *Hprt* inactivation

For mock treated XpaMsh6 and XpaMlh1 cells and for UV exposed Xpa, XpaMsh6 and XpaMlh1 cells approximately 400 6tG clones were collected by trypsinization and lysed in 1.6ml TRIzol reagent (Invitrogen). Total RNA was isolated following manufacturer's protocol and ultimately dissolved in 15µl TE buffer. To generate cDNA 1 µl RNA was mixed with dNTPs (0.2mM Invitrogen) and 5 µM primer 1 (Supplemental materials table 1) in a final volume of 14.5µl and incubated for 5 minutes at 65°C. Then, a mixture of 5.5µl consisting of 1µl Maxima H Minus Reverse Transcriptase (200U) (Thermo Fisher Scientific), 4µl 5x Maxima buffer and 0.5µl RNasin (20U) (Promega) was added followed by incubations at 57°C for one hour and at 85°C for 5 minutes, respectively. 2µl of cDNA was used in a PCR with 0.4U Phusion High-Fidelity DNA polymerase (Thermo Fisher Scientific), 5x Phusion PCR buffer, dNTPs (0.2mM), and a combination of forward and reverse primers (0.5µM) (Supplemental materials table 1), depending on which amplicon of *Hprt* is amplified (primers 2/3, 4/5, 6/1). Using a thermal cycler, PCR products were generated by incubating the reaction mixture for two minutes at 95°C, followed by 15 seconds at 95°C, 30 seconds at 57°C and one minute 72°C for 25 cycles, and a final elongation step of 72°C for five minutes. AMPure XP beads (Beckman Coulter) were used to purify the PCR products in 20µl deionized H₂O following manufacturer's protocol. These PCR products were used as templates for Phusion PCR with barcoded primers (primers 7/8, 9/10, 11/12, 13/14, 15/16, 17/18) as

previously described, with the exception of 8 instead of 25 cycles. Barcoded PCR products were purified with AMPure beads and the size of the purified products was measured using a Qiaxcel Advanced System (Qiagen). Finally, 50ng pooled PCR products was sequenced using Illumina Paired-End sequencing (GenomeScan).

Determination of UV-induced mutational spectra in the *Hprt* coding region

Raw next generation sequencing data was first filtered to contain reads with a maximum error probability of 0.05. Using Flash (19) paired-end reads were merged and mapped to the *Hprt* reference sequence using in-house software (20). Additional filters removed reads that did not start or end with the primer combinations that were used to obtain the PCR fragments. Finally, the mapped reads were compared to the *Hprt* sequence and annotated into WT (wild-type), single nucleotide substitution (SNS), multi nucleotide substitution (MNS), deletion or insertion. Unique mutations were considered to be real if the allele frequency was > 0.001, anything below that threshold is considered noise.

Results

UV-induced DNA damage signaling depends on MutS α , but not on MutL α

Previously, it was shown that Msh6 is important for the activation of DNA damage signaling upon UV exposure, possibly via excision of TLS-induced misincorporations opposite UV lesions (11). Here, the importance of other MMR-related genes in the activation of UV-induced damage responses was studied using *Xpa*-deficient mES cells with an additional deficiency for (i) the canonical MMR proteins and MutL α constituents Mlh1 or Pms2, that act downstream of MutS α , (ii) the Mlh1-interacting proteins Mlh3 and Pms1 and (iii) MMR-associated exonucleases Exo1 and Fan1. UV-induced DNA damage signaling was studied by western blotting for phosphorylated forms of Chk1 and Kap-1, that are substrates for the Atr/Atrip and Atm kinases, respectively. *Xpa*-deficient cells displayed significant phosphorylation of Chk1 and Kap-1, 2 to 8 hours after UV exposure, which was greatly reduced when these cells lacked *Msh6* (Fig. 1), in line with previously published work (11). UV-exposed cells deficient for *Mlh1* or *Pms2*, however, showed similar levels of phosphorylated Chk1 as the MMR proficient controls, and phosphorylation of Kap-1 appeared slightly reduced although not as much as in *Msh6* cells (Fig. 1, S2). This indicates that Mlh1 and Pms2 play a less important role than Msh6 in activating UV-induced DNA damage signaling. Similar results were found for cell lines deficient for *Mlh3*, *Pms1*, *Exo1* and *Fan1*. Together these data indicate that only MutS α plays a significant role in activating UV-induced DNA damage signaling.

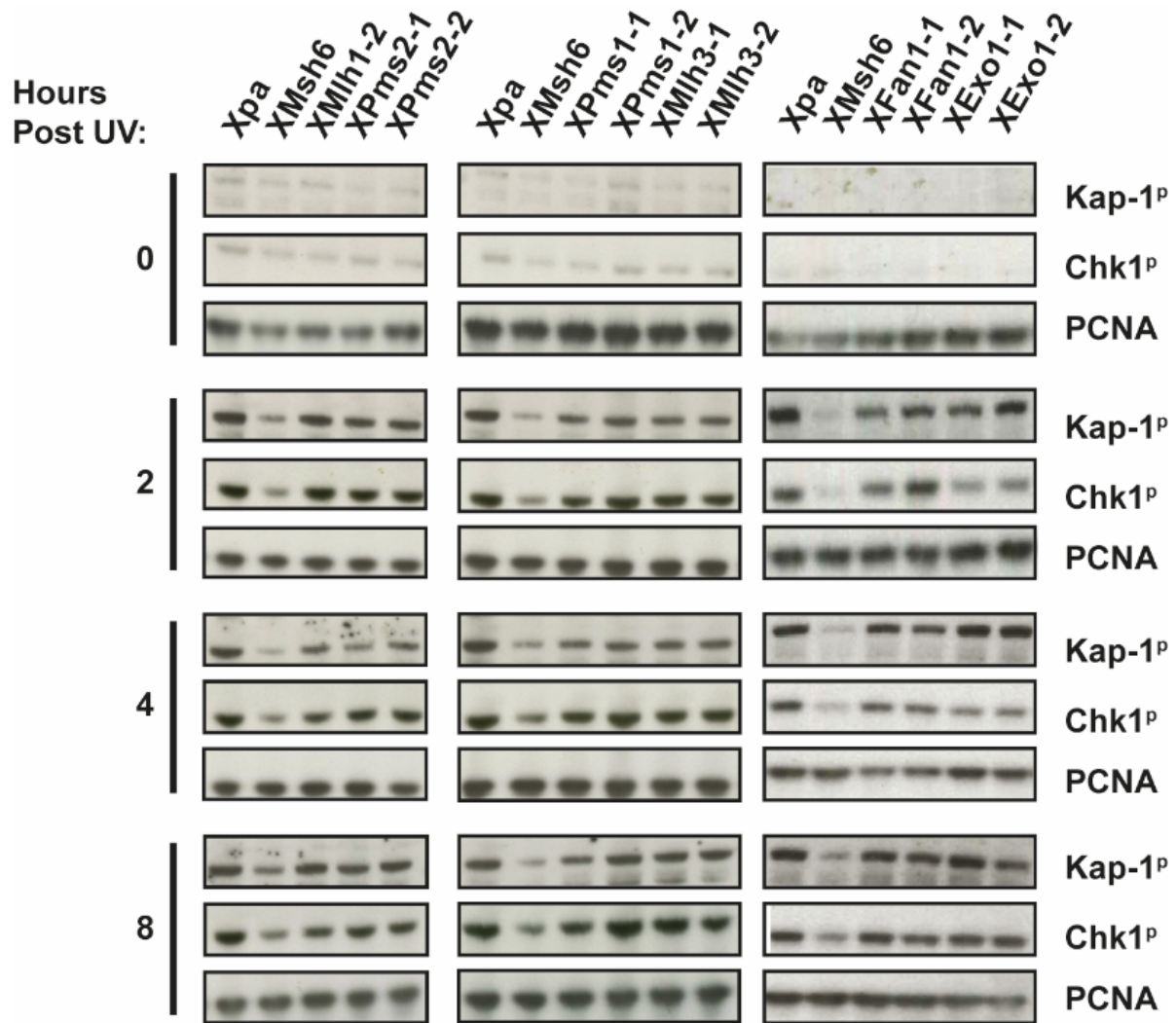


Figure 1: UVC-induced DNA damage signaling in cell lines deficient for MMR, MMR homologs and exonucleases

Western blots displaying formation of Chk1p and Kap-1p in Xpa, XMsh6, XMIh1, XPms2, XMIh3, XPms1, XExo1 and XFan1 deficient lines, 0, 2, 4 and 8 hours post UVC exposure (0,75J/M²). PCNA was used as a loading control. Cell line-1 -2, denotes independent cell lines with different inactivating mutations. Representative images of 3 independent experiments. X=Xpa deficiency.

Msh6 promotes UV-induced single stranded DNA formation and checkpoint activation independent of Mlh1

We asked whether the persistence of UV damage signaling in Mlh1-deficient cells relies on MutS α . To test this, we generated an *XpaMlh1Msh6* triple knockout cell line and compared the formation of pChk1 in *Xpa*, *XpaMsh6*, *XpaMlh1* and *XpaMlh1Msh6* cells following UV exposure. We found that UV-induced DNA damage signaling in Mlh1-deficient cells strongly depends on Msh6, since the level of pChk1 observed in UV-exposed *XpaMlh1* cells was completely absent in the *XpaMlh1Msh6* triple knock out cells (Fig. 2A). Of note, the activation of Chk1 in *Xpa* and *XpaMlh1* cells occurs during the cell cycle of UV exposure as shown by arresting UV-exposed cells at mitosis following nocodazole treatment (Fig. S3A).

MutS α may activate checkpoint signaling in different ways, *i.e.* by a direct interaction with Atr/Atrip following mismatch binding (21) or by generating patches of ssDNA, which relies on the recruitment of MutL α in case 5' nicking is required for excision (22). To distinguish between these modes of checkpoint activation, we analyzed the formation of ssDNA by western blotting for chromatin-bound RPA, a heterotrimeric protein that specifically binds to ssDNA. In the *Xpa*-deficient cell line an increase of chromatin-bound RPA was observed, 4 hours after UV irradiation. This increase completely depends on the presence of Msh6, since its loss resulted in absence of chromatin-bound RPA induced by UV (Fig. 2B-D, S3B). Conversely, *Xpa* cells deficient for Mlh1 or its binding partner Pms2 showed similar increased levels of chromatin-bound RPA as found for *Xpa* cells following UV exposure. These data suggest that the formation of UV-induced ssDNA is dependent on Msh6, but not on MutL α .

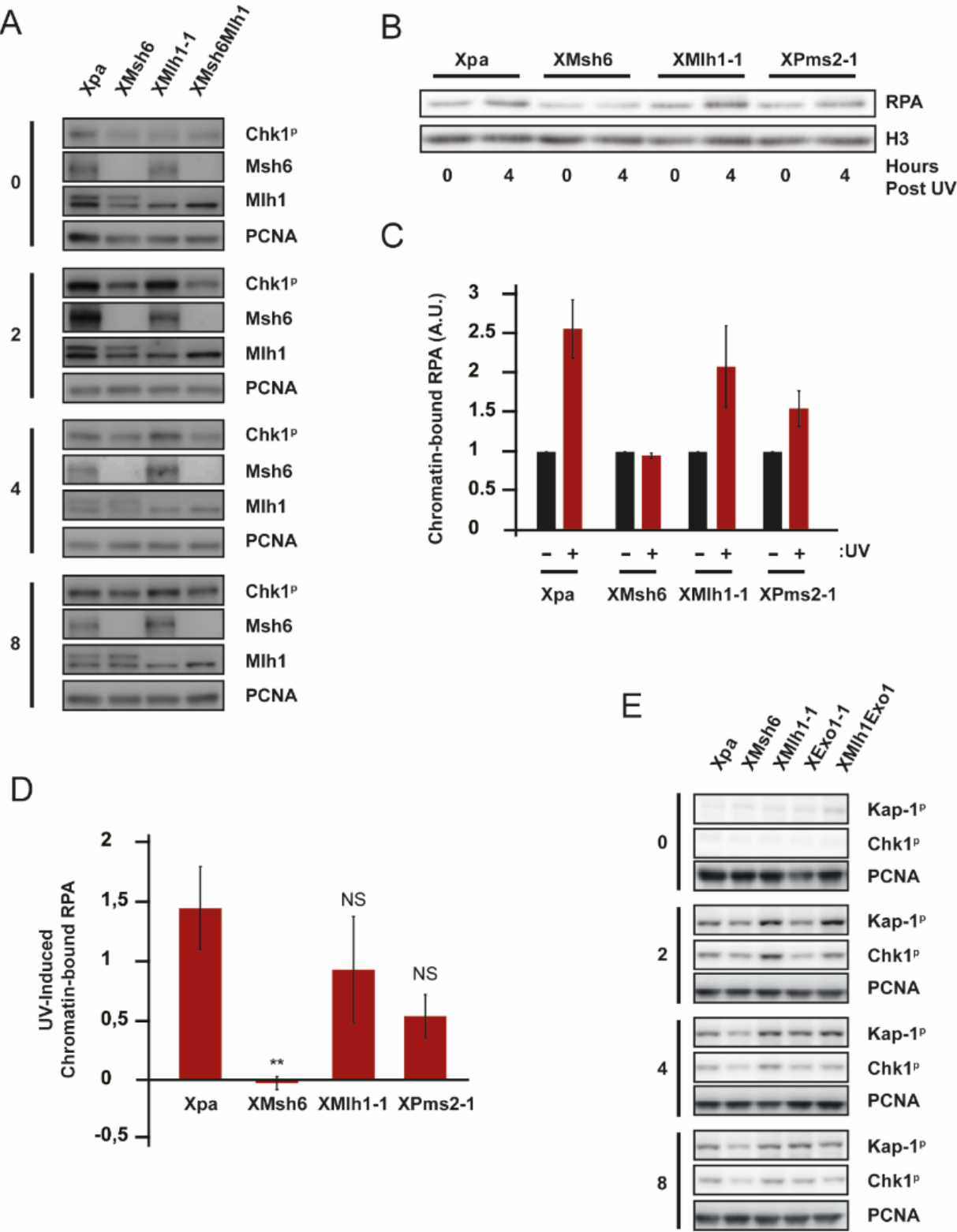


Figure 2: Msh6 dependent formation of chromatin-bound Rpa and DNA damage signaling following UVC exposure

A: Western blots showing formation of Chk1p in Xpa, XMsh6, XMIh1 and XMsh6MIh1 cell lines, 0, 2, 4 and 8 hours post UVC exposure (0,75J/M2). Msh6 and MIh1 protein status was confirmed using appropriate antibodies against Msh6 and MIh1. PCNA was used as a loading control. Representative images of 3 independent experiments. B: Western blot of chromatin-bound Rpa as a measure for the formation of single stranded DNA, 0 and 4 hours post UVC exposure (2J/M2). Histone H3 (H3) was used as a loading control. Representative image of three independent experiments. C: Quantification of chromatin-bound Rpa. Samples were normalized to the 0-hours timepoint and adjusted for the amount of Histone H3. Error-bars, SEM. D: UVC-induced chromatin-bound Rpa. Error bars, SEM. **, $P \leq 0,01$, ns, not statistically significant; unpaired T-test comparing groups to WT. E: Western blots displaying formation of Chk1p and Kap-1p in Xpa, XMsh6, XMIh1, XExo1 and XMIh1Exo1 cell lines, 0, 2, 4 and 8 hours post UVC exposure (0,75J/M2). Msh6 protein status was confirmed using Msh6 antibodies. Representative images of 3 independent experiments. X=Xpa deficiency.

Recently, it was shown that loss of Mlh1 leads to Exo1-dependent hyper-resection at DNA breaks induced by ionizing radiation, resulting in enhanced loading of RPA on DNA and, consequently, increased damage signaling (23). To test whether the UV-induced damage signaling in Mlh1-deficient cells relies on Exo1, we inactivated *Exo1* in *XpaMlh1* cells by Cas/Crispr, exposed the resulting *XpaMlh1Exo1* triple knock-out cells to UV light and determined phosphorylation levels of Chk1 and Kap-1. We found slightly increased levels of pChk1 and pKap-1 in *XpaMlh1Exo1* cells as compared to *Xpa* and *XpaMlh1* cells across most timepoints post-UV exposure (Fig. 2E), indicating that the DNA damage signaling found in *XpaMlh1*-deficient cells does not rely on *Exo1*. This result is in line with the wild type level of Chk1 phosphorylation in *XpaExo1* cells (Fig. 1 and 2E). Together these data indicate that, following UV exposure, the formation of ssDNA and concomitant activation of the RPA/Atr/Chk1 signaling cascade strongly depends on Msh6 and not on its downstream actor MutL α .

UV-induced mutagenesis is controlled by multiple MMR proteins

Msh6-dependent UV damage signaling is associated with protecting cells from UV-induced mutagenesis, possibly via the removal of TLS-induced mis-incorporations opposite UV lesions, resulting in the formation of ssDNA gaps (11). Since MutL α is not required for UV-induced checkpoint responses and formation of ssDNA, we wondered whether MutL α is dispensable for protecting against UV-induced mutagenesis as well. To address this, we determined mutant frequencies at the X-linked *Hprt* gene in mES cells deficient for the *Xpa* gene and in cells carrying an additional deficiency for *Mlh1* or *Pms2*. We also included cell lines with defects in Mlh1-interacting proteins Mlh3 or Pms1 and in exonucleases Exo1 or Fan1. *Hprt* mutants can be selected from *Hprt*-proficient cells by using 6tG as selective agent. Exposing *Xpa* cells to 0,75J/m² UV led to a minor increase of $34.02 \pm 17.76 \times 10^{-6}$ 6tG-resistant clones compared to mock-treated *Xpa* cells (Fig. 3A, S4A, S4C). Loss of *Msh6* in an *Xpa*-deficient background resulted in $108.46 \pm 22.26 \times 10^{-6}$ 6tG-resistant clones in unexposed cells, which further increased to $502.11 \pm 85,02 \times 10^{-6}$ (UV-induced: 394×10^{-6}) 6tG-resistant clones

following UV-exposure. This protection against UV-induced mutations by Msh6 is in line with previously published work (11, 24). Loss of any of the MMR-associated proteins Mlh3, Pms1, Exo1 or Fan1 in the *Xpa* background did not result in increased spontaneous mutagenesis whereas UV-induced mutagenesis in these lines was similar to that of the *Xpa* control (Fig. 3A, 3B). Interestingly, an increase in spontaneous and UV-induced 6tG-resistant clones was observed in *XpaMlh1* cell lines (Mock: 53.91 ± 0.47 and UV: 279.33 ± 36.29) and *XpaPms2* (Mock: 78.81 ± 23.23 and UV: 411.40 ± 40.72). The increase of mutagenesis resulting from UV exposure was also significantly higher than the *Xpa* control, suggesting that not only *Msh6*, but also *Mlh1* and *Pms2* control UV-induced mutagenesis (Fig. 3B, S4B, S4D).

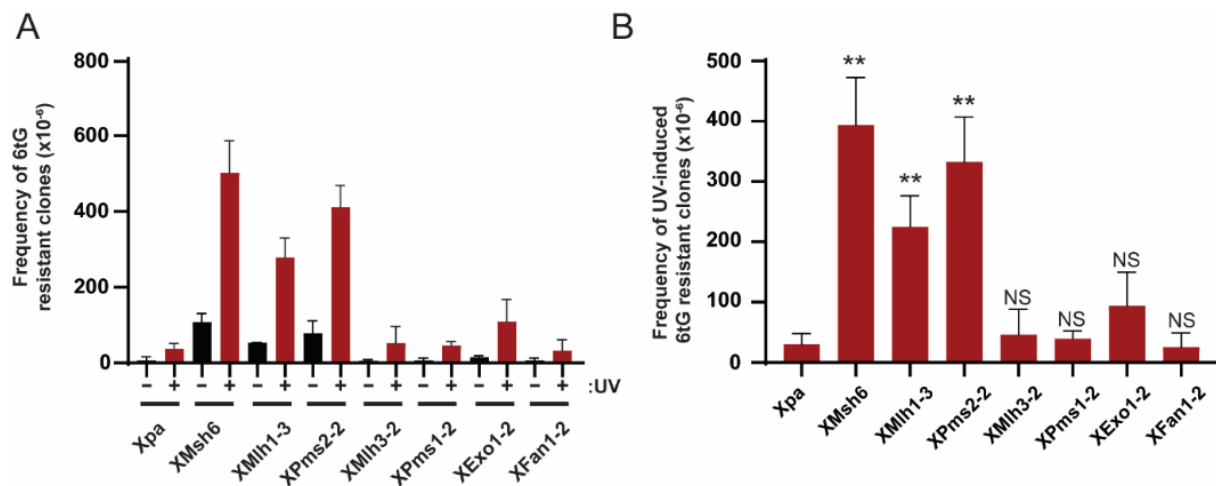


Figure 3: UV-induced mutagenesis

A: Frequency of 6tG resistant cells as a measure for mutagenesis at the *Hprt* gene following exposure to mock or 0,75J/M2 UVC. N=3. Error bars, SEM. B: Frequency of UV-induced 6tG resistant clones as a measure for mutagenesis at the *Hprt* gene. Error bars, SEM. **, $P \leq 0,01$, ns, not statistically significant; unpaired T-test comparing groups to *Xpa* cells.

Mlh1 deficient cells display a similar spectrum of UV-induced mutations as Msh6 deficient cells

So far, our data reveal the uncoupling of ssDNA formation and checkpoint responses from the protection against UV-induced mutagenesis, suggesting mechanistic differences in the control of UV-induced mutagenesis between MutS α and MutL α . To test whether this affects the spectrum of mutations induced by UV, we studied the spontaneous and UV-induced mutational fingerprints of *Xpa*, *XpaMsh6* and *XpaMlh1* cell lines. Per genetic background and exposure status, approximately 400 6tG-resistant clones were pooled to investigate what kind of mutations inactivated *Hprt*. Using a recently published sequencing analysis pipeline (20) we identified 81 unique mutations in the UV-exposed *Xpa* cells, 32 mutations in the mock treated *XpaMsh6* cells and 31 mutations in UV-exposed *XpaMsh6* cells. Moreover, we found 70 unique mutations in mock treated and 60 unique mutations in UV-exposed *XpaMlh1*-deficient cells (Table S1-5). The spectrum of spontaneous *Hprt* mutations in an *Xpa*-deficient

background could not be determined, due to the very low number of mutants that could be selected by 6tG. These data show that double nucleotide substitutions (DNS) and multi nucleotide substitutions (MNS) were mainly found in UV-exposed cell populations whilst small insertions and deletions were associated with loss of either *XpaMsh6* or *XpaMlh1* (Fig. 4A, Table 1; Table S1-5). In all conditions tested the majority of the mutations consisted of single nucleotide substitutions (SNS). To further investigate the fingerprint of SNS in these cell lines we calculated the contribution of each type of SNS to the mutant frequency (Fig. 4B, Table 1; Table S1-5). Both mock treated *XpaMsh6* and *XpaMlh1* cells displayed a signature dominated by A.T > G.C mutations and in the case of *XpaMlh1* cells also by G.C > A.T mutations). The mutation spectra of UV-exposed *XpaMsh6* and *XpaMlh1* cells mainly consisted of G.C > A.T transitions, G.C > T.A transversions and transversions at A.T base pairs. *Xpa* cells exposed to UV displayed a spectrum consisting of G.C > A.T mutations and to a lesser extent A.T > T.A transversions and G.C > T.A transversions. To determine the spectra of UV-induced mutations we subtracted the frequency of each kind of spontaneous mutation from those observed in the UV-exposed cells (Fig. 4C; Table 1; Table S1-5). Based on this analysis we concluded that both Msh6 and Mlh1 strongly protect against UV-induced G.C > A.T transitions, G.C > T.A transversions and A.T > T.A transversions. No difference in mutational strand bias was found between *Msh6* and *Mlh1*-deficient cells. For both genotypes most of the mutations were found in the transcribed strand at dipyrimidines, which are sites where photolesions are formed following UV exposure (Fig. 4D, Table S1, 3, 5). Together, these data suggest that both Msh6 and Mlh1 protect against similar mis-incorporations that are possibly provoked by photolesions in a strand-specific fashion.

In conclusion, these data show that the activation of UV-induced DNA damage signaling and the formation of UV-induced ssDNA occurs independently of MutL α . However, the formation of UV-induced ssDNA and checkpoint activation in *Mlh1*-deficient cells does rely on *Msh6*. Moreover, MutS α and MutL α are both required for controlling UV-induced mutagenicity. Mutational fingerprints of *Msh6* and *Mlh1*-deficient cells were similar, suggesting that these proteins suppress UV-induced mutagenicity via a similar mechanism, despite the difference in the formation of ssDNA gaps.

Table 1: Distribution of base pair alterations in *Xpa*, *XMsh6* and *XMLh1* deficient backgrounds

6tG resistant clones were sequenced and mutations were distributed according to base pair substitution type and condition. The absolute number of mutations, relative proportions and mutations adjusted for the mutant frequency are shown for each base pair alteration type. The number of UVC-induced mutations is calculated by subtracting the mutations found in the mock condition from the mutations found in the UV condition.

Xpa		Mock			UV			UV Induced	
		Absolute	Relative (%)	6tG resistant clones ($\times 10^{-6}$)	Absolute	Relative	6tG resistant clones ($\times 10^{-6}$)	Relative (%)	6tG resistant clones ($\times 10^{-6}$)
Transistion	G.C > A.T	0	0	0	22	46,8	26,7	46,8	26,7
	A.T > G.C	0	0	0	2	4,3	2,4	4,3	2,4
Transversion	G.C > T.A	0	0	0	9	19,1	10,9	19,1	10,9
	G.C > C.G	0	0	0	0	0,0	0,0	0,0	0,0
	A.T > T.A	0	0	0	11	23,4	13,3	23,4	13,3
	A.T > C.G	0	0	0	3	6,4	3,6	6,4	3,6
Total		0	0	0	47	100,0	57,0	100,0	57,0

XMsh6		Mock			UV			UV Induced	
		Absolute	Relative (%)	6tG resistant clones ($\times 10^{-6}$)	Absolute	Relative	6tG resistant clones ($\times 10^{-6}$)	Relative (%)	6tG resistant clones ($\times 10^{-6}$)
Transistion	G.C > A.T	4	15,4	9,4	8	38,1	231,2	40,6	221,9
	A.T > G.C	19	73,1	44,6	1	4,8	28,9	-2,9	-15,7
Transversion	G.C > T.A	1	3,8	2,3	4	19,0	115,6	20,7	113,3
	G.C > C.G	0	0,0	0,0	1	4,8	28,9	5,3	28,9
	A.T > T.A	2	7,7	4,7	4	19,0	115,6	20,3	110,9
	A.T > C.G	0	0,0	0,0	3	14,3	86,7	15,9	86,7
Total		26	100,0	61,0	21	100,0	607,0	100,0	546,0

XMLh1		Mock			UV			UV Induced	
		Absolute	Relative (%)	6tG resistant clones ($\times 10^{-6}$)	Absolute	Relative	6tG resistant clones ($\times 10^{-6}$)	Relative (%)	6tG resistant clones ($\times 10^{-6}$)
Transistion	G.C > A.T	20	37,7	38,1	17	53,1	292,7	56,6	254,6
	A.T > G.C	20	37,7	38,1	4	12,5	68,9	6,8	30,8
Transversion	G.C > T.A	4	7,5	7,6	4	12,5	68,9	13,6	61,3
	G.C > C.G	0	0,0	0,0	0	0,0	0,0	0,0	0,0
	A.T > T.A	5	9,4	9,5	5	15,6	86,1	17,0	76,6
	A.T > C.G	4	7,5	7,6	2	6,3	34,4	6,0	26,8
Total		53	100,0	101,0	32	100,0	551,0	100,0	450,0

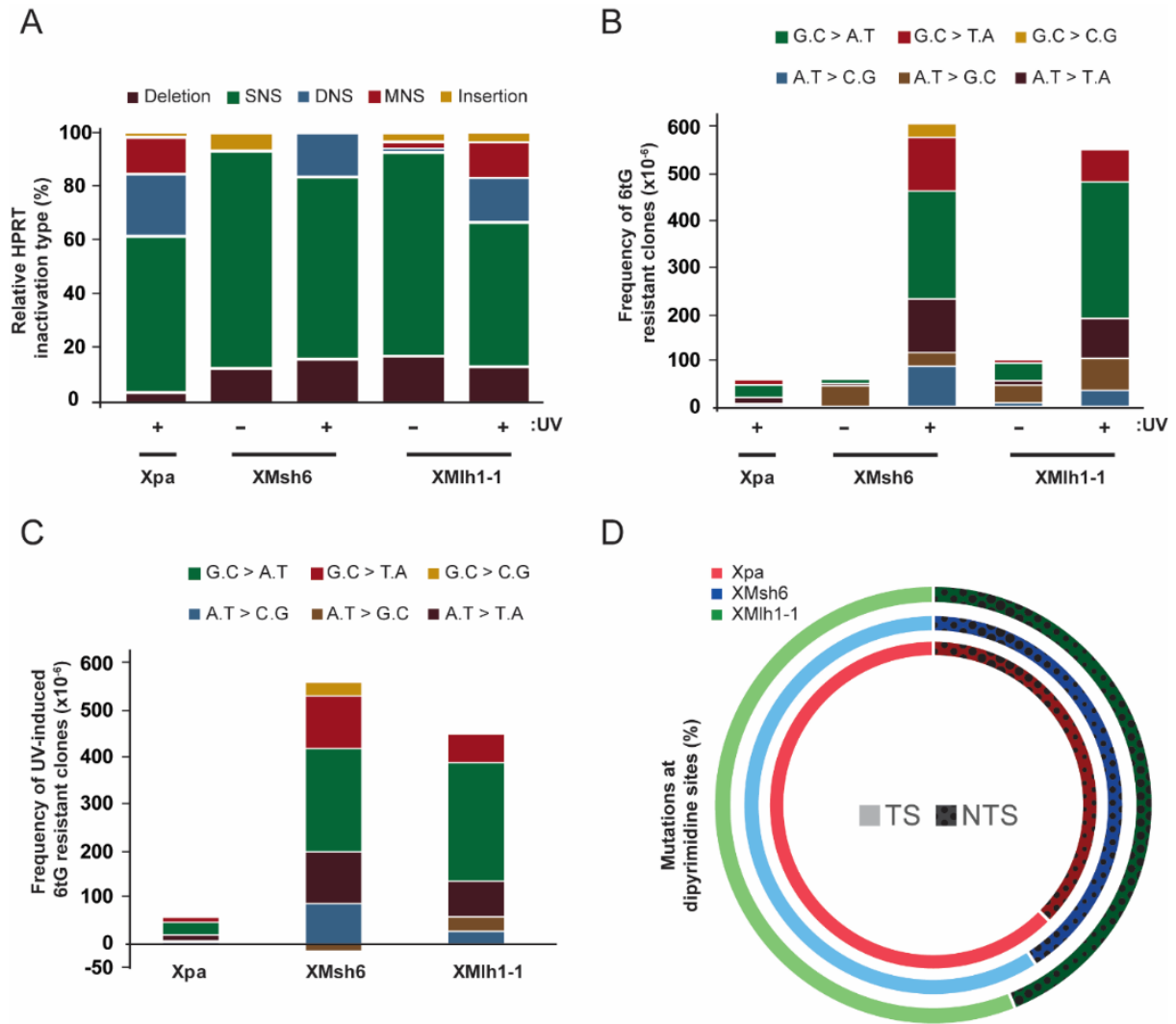


Figure 4: UVC-induced mutational fingerprints in the *Hprt* coding region of 6-thioguanine resistant cells
A: Percentage of mutational events in *Hprt* relative to the total number of unique mutants per condition. SNS, single nucleotide substitution; DNS, double nucleotide substitution; MNS, multi nucleotide substitution. B: Contribution of different base pair substitutions to the frequency of 6tG-resistant clones. C: Contribution of different base pair substitutions to the frequency of UV-induced 6tG-resistant clones. D: Mutational strand bias at *Hprt* in Xpa (red), XpaMsh6 (blue) and XpaMih1 (green) deficient cells. Light colors indicate transcriptional strand (TS), dark dotted colors indicate the non-transcribed strand (NTS).

Discussion

Previous studies have shown that MutS α suppresses UV-induced mutagenesis with concomitant generation of ssDNA tracts that activate DNA damage signaling. This led to a model in which MutS α controls UV-induced mutagenesis by removing TLS-dependent misincorporations opposite UV damages, resulting in the formation of ssDNA tracts that activate DNA damage signaling (11). In the present work we have studied the roles of other MMR-related proteins, including Mlh1 and Pms2, Mlh1-interacting proteins Mlh3 and Pms1 and exonucleases Exo1 and Fan1 cells in responses to UV light. We found that in mES cells Mlh3 and Pms1 as well as MMR-related exonucleases Exo1 and Fan1 play only limited roles in UV-induced DNA damage responses, including formation of ssDNA, activation of DNA damage signaling and mutagenesis. In addition, also Mlh1 and Pms2 seem not to be important in activating UV-induced DNA damage signaling. However, MutL α does appear to play a major role in suppressing UV-induced mutagenesis. Thus, we here provide evidence that, in contrast to MutS α , MutL α seems to suppress UV-induced mutagenesis, largely independent of generation ssDNA tracts and concomitant activation of damage signaling.

In MMR-proficient cells different mechanisms may contribute to the formation of UV-induced ssDNA tracts following stalling of replicative DNA polymerases at photolesions. These mechanisms include (i) uncoupling of leading and lagging strand DNA synthesis, (ii) repriming of DNA replication downstream of the replication-blocking DNA lesion resulting in the generation of ssDNA-dsDNA junctions (25), (iii) replication fork reversal and (iv) processing of DSBs when stalled replication forks collapse (26). In the present study we noted that the appearance of chromatin-bound RPA, a read-out for ssDNA formation, strongly correlates with phosphorylation of Chk1 and Kap1 (Figs. 1, 2B, C; Fig. S2, S3B). These data implicate that the endonuclease activity of MutL α is not essential for the generation of ssDNA in response to UV-induced DNA damage. MutS α -dependent processing of stalled or collapsed replication forks might well contribute to the formation of ssDNA in Mlh1-deficient cells exposed to UV, as reported in a recent study showing that MutS α stimulates Mre11-mediated degradation of nascent DNA strands at stalled replication forks, thereby contributing to the generation of ssDNA (27). In support, we found that the formation of chromatin-bound RPA and induction of UV damage signaling was only dependent on Msh6 and not Mlh1, presumably following binding of MutS α to “compound” lesions (*i.e.* a mismatch superimposed on a UV lesion, Fig. 2B-D). The strong correlation between formation of ssDNA and activation of damage signaling makes it less likely that MMR proteins may activate an Atr/Atm-mediated UV damage response by direct interaction with Atr (Msh2) or Atm (Mlh1) as proposed for the response to methylation- or cisplatin DNA damage (21, 28). Furthermore, complete activation of the apical DNA damage signaling protein kinases Atr and Atm, that subsequently phosphorylate Chk1 and Kap1 at multiple sites (17), requires the formation of ssDNA coated with RPA (29).

Possibly, Exo-1 dependent hyper-resection that results from runaway Exo-1 activity in the absence of Mlh1, as described previously for ionizing radiation-induced responses

(23), might also contribute to the activation of UV damage signaling in Mlh1-deficient cells. In our hands, however, knock-out of Exo1 in Mlh1-deficient cells hardly altered UV damage signaling, although in MMR-proficient cells we did observe a minor role for Exo-1 in activating an UV-induced damage response, especially at early timepoints (Fig. 1, 2E). This minor role for Exo-1 may point to a functional redundancy with other exonucleases. Of note, although Exo-1 was shown to be indispensable for MMR *in vitro* (1), it seems to be non-essential for MMR in yeast and mice, in support of our data (30).

Alternatively, the presence of 5' nicks during lagging strand synthesis may provide an important clue to how cells generate UV-induced ssDNA tracts and concomitant UV damage signaling in the absence of MutL α . During canonical MMR, it is thought that MutL α is not only important in 3' nick-directed MMR but also in the generation of incisions 5' to mismatches in the newly synthesized strand (1). However, this scenario applies primarily for misincorporations during leading strand synthesis and matured Okazaki fragments, as non-ligated Okazaki fragments in the lagging strand contain naturally occurring free 5' ends. Moreover, MutL α is dispensable for 5' nick directed mismatch repair *in vitro* (Mol Cell 12, 1077-1086 (2003); Mol Cell 15, 31-41 (2004)). Lastly, several studies indicate that eukaryotic MMR acts preferentially on the lagging strand (5, 31), which might relate, in part, to MutL α -independent MMR during lagging strand DNA synthesis. For these reasons, MutL α -independent removal of misincorporations opposite UV lesions during lagging strand synthesis might well underly the generation of ssDNA tracts and concomitant activation of UV damage signaling observed in Mlh1-defective cells. However, MutL α -independent removal of 'misincorporations' opposite UV lesions would predict a difference in strand distribution of mutagenic UV lesions between MutS α -deficient cells versus MutS α -deficient cells; a prediction that is not confirmed by our analysis of UV-induced mutations at the coding region of the endogenous *Hprt* gene in Msh6- and Mlh1-deficient cells (Fig. 6D). Nevertheless, this difference in strand bias might be obscured in part by the plasticity of DNA replication under stressful conditions (32, 33) and by transcription-associated mutagenesis at UV lesions on the transcribed strand (34, 35).

Our mutation spectra analyses also revealed that both MutS α and, albeit to a slightly lower extent, MutL α strongly protect against UV-induced G.C > A.T transitions (Fig 4B-C; Table 1), the main type of mutation induced by UV (36). However, we also noted that MutS α and MutL α protect against transversion-type mutations, including AT > TA, AT > CG and GC > TA transversions. These transversions might rely on Rev1, a TLS polymerase that is required for the bypass of UV-induced (6-4)PPs (37, 38). Thus, whereas previously published data indicate that Msh6 removes misincorporations opposite (6-4)PPs (11), the present study suggests that also MutL α may act on TLS-induced misincorporations opposite (6-4)PPs. Combined with previous studies (11) and our findings that MutS α controls UV-induced mutagenesis and concomitantly promotes the generation of ssCPD in Pol η -deficient cells (Fig. 5B, C), these data indicate that the mutagenicity of both CPDs and (6-4)PPs are controlled by MutS α and MutL α .

The spatiotemporal regulation of control of UV-induced mutagenesis by MutS α in the absence of MutL α remains to be determined. Possibly, binding of MutS α to a “compound” lesion in the absence of downstream processing by MutL α may ultimately lead to perturbed replication forks that activate DNA damage signaling. Studies using fluorescent-tagged MMR and replication proteins in replicating yeast have suggested the existence of replisome-coupled and replisome-independent (post-replicative) MutS α complexes, which recruit MutL α to perform canonical mismatch repair (5, 31). During UV-induced mutagenesis, it is thought that most mildly helix-distorting CPDs are likely bypassed by the relatively error-free TLS Pol η at the fork, whereas the bypass of strongly helix-distorting (6-4)PPs depends largely on mutagenic TLS polymerases Rev1 and ζ (39-42). Possibly, the relatively rarely occurring ‘misincorporations’ opposite CPDs might be recognized by MutS α at the replication fork that, in the absence of MutL α , will lead to stalled replication complexes resulting in ssDNA formation and activation of DNA damage signaling. On the other hand, TLS at (6-4)PPs and other helix-distorting DNA lesions might occur by post-replicative gap filling (43, 44) and will result in ‘compound’ lesions that are recognized by a subset of MutS α molecules acting in a post-replicative fashion. This mode of action allows cells to continue DNA replication and, in the absence of MutL α , might not activate DNA damage signaling (For a model see Fig. 5). The idea that MutS α acts on post-replicative TLS is supported by the finding that Msh6 also suppresses the UV-induced mutagenesis in Rev1 deficient cells (11).

At present, it is not clear which MMR factors other than MutS α and MutL α play a role in controlling UV-induced mutagenesis. Here we showed that loss of Mlh3 or Pms1 did not affect DNA damage signaling nor mutagenesis in response to UV-damage. Previous work has shown that *in vitro* MLH3 is able to slightly rescue MMR activity in the absence of PMS2, and Mlh3-loss in mouse embryonic fibroblasts slightly reduces checkpoint activation and apoptosis induced by alkylating DNA damage (5, 31). However, the latter finding is contested by studies using human cell lines (36). Possibly, in mouse cells UV-induced signaling may be differently regulated than alkylation-induced signaling. As of yet, no significant role for Pms1 in MMR has been found.

Our findings that MutL α is required for suppressing mutagenesis of helix-distorting DNA lesions may provide a plausible explanation for the observation that loss of MutL α results in severely increased risk of developing colorectal cancer (45), a cancer type that strongly correlates with exposure to food-derived genotoxins that induce helix-distorting DNA lesions (46).

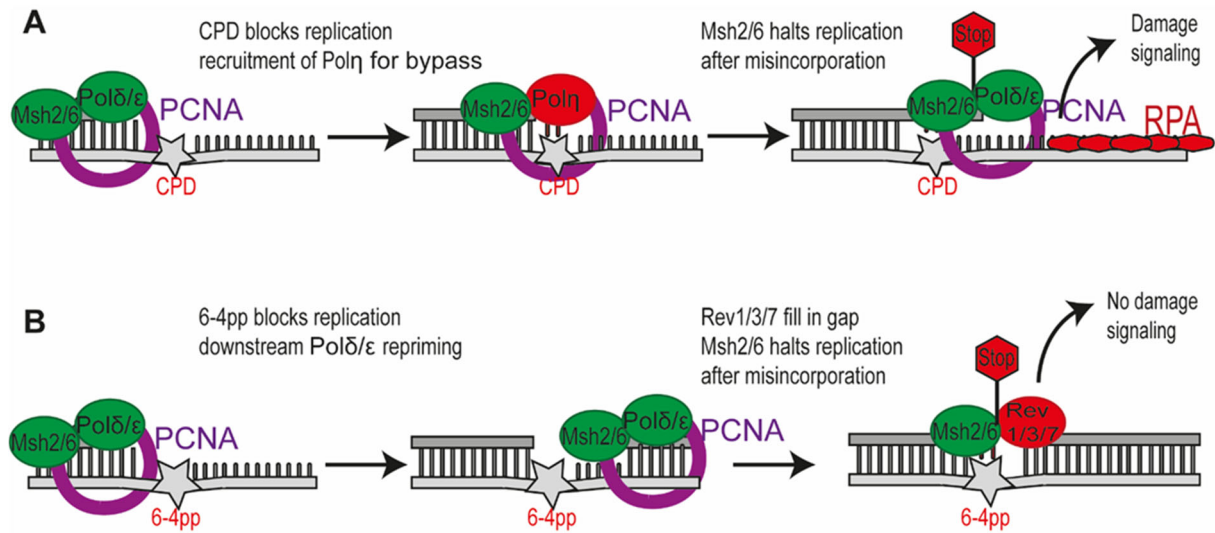


Figure 5: Different modes of bypass result in different signaling outcomes in Mlh1-deficient cells.

A: Model for the bypass of a CPD lesion in Mlh1-deficient cells. The replicative polymerases cannot continue replicating when a CPD is encountered and thus Pol η is recruited to bypass the damage “on the fly”. If done incorrectly, Msh2/6 halts the replication machinery causing persistent RPA-coated ssDNA tracts that activates damage signaling in the absence of Mlh1. B: Model for the bypass of a 6-4PP in Mlh1-deficient cells. When a replicative polymerase encounters a 6-4PP, repriming occurs downstream of the lesion which allows replication to continue. The resulting gap opposite the 6-4PP is filled by Rev1/3/7, quenching DNA damage signaling. In the absence of Mlh1/Pms2, ‘compound’ lesions are not repaired, resulting in mutation fixation in the next round of replication.

Supplemental Materials

Supplemental materials table 1: DNA sequences of PCR primers

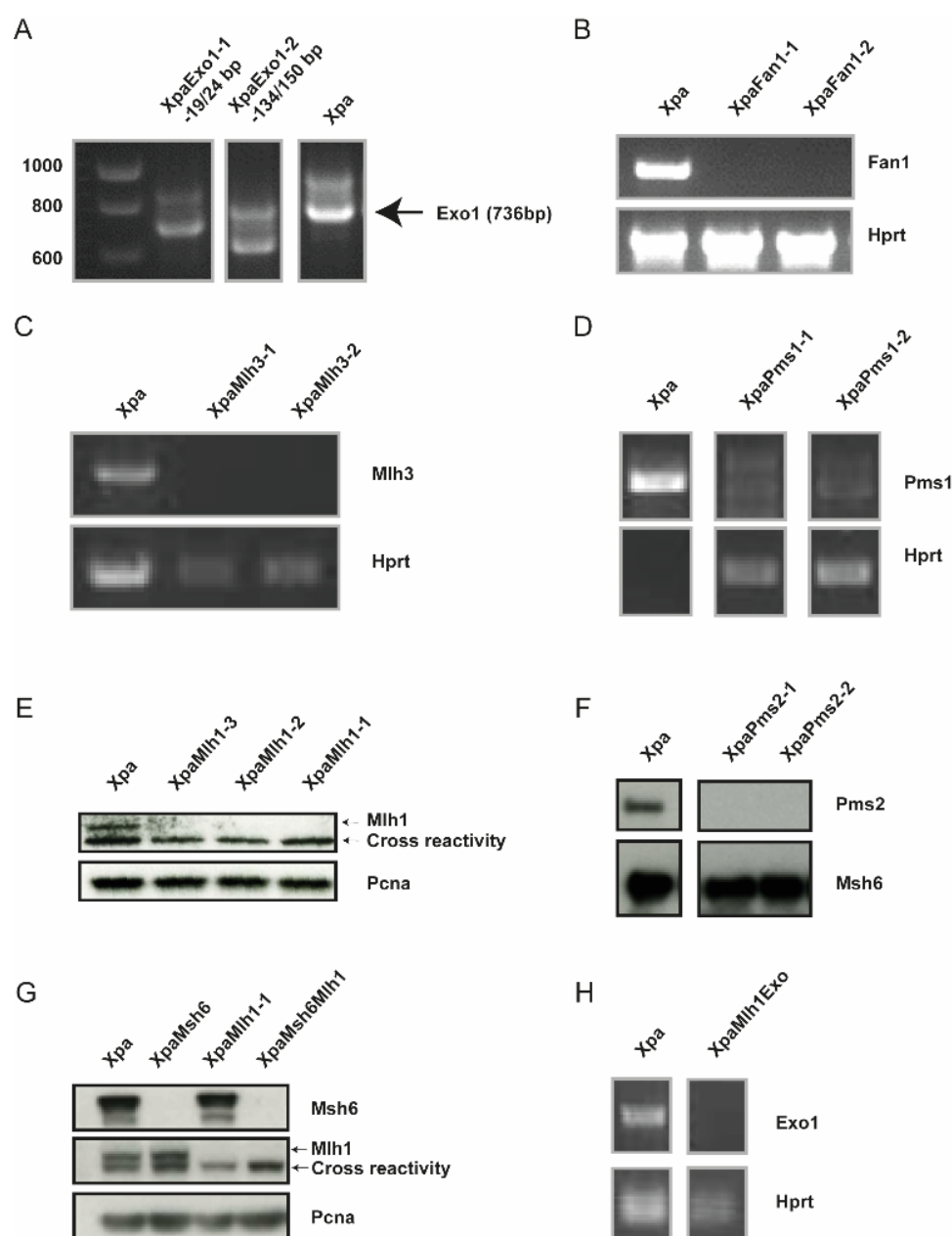
Primer:	Sequence:
1	CGTGTGCTCTTCCGATCTTTTGCAGATTCAACTTGCGCT
2	GATGTGTATAAGAGACAGCAGTCCCAGCGTCGTGATTAG
3	CGTGTGCTCTTCCGATCTATCCAGCAGGTCAGCAAAGAA
4	GATGTGTATAAGAGACAGGCCATCACATTGTGGCCCTC
5	CGTGTGCTCTTCCGATCTAGTTTGCATTGTTTTACCAGTGTC
6	GATGTGTATAAGAGACAGTGACACTGGTAAAACAATGCAA
7	AATGATACGGCGACCACCGAGATCTACACCTCTCTATTTCGTCGGCAGCGTCAGA TGTGTATAAGAGACA*G
8	CAAGCAGAAGACGGCATACGAGATagttacgtGTGACTGGAGTTCAGACGTGTGCTC TTCCGATC*T
9	AATGATACGGCGACCACCGAGATCTACACTATCCTCTTCGTCGGCAGCGTCAGA TGTGTATAAGAGACA*G
10	CAAGCAGAAGACGGCATACGAGATatacgacgGTGACTGGAGTTCAGACGTGTGCT CTTCCGATC*T
11	AATGATACGGCGACCACCGAGATCTACACAGAGTAGATCGTCGGCAGCGTCAGA TGTGTATAAGAGACA*G
12	CAAGCAGAAGACGGCATACGAGATccaactcaGTGACTGGAGTTCAGACGTGTGCT CTTCCGATC*T
13	AATGATACGGCGACCACCGAGATCTACACACTGCATATCGTCGGCAGCGTCAGA TGTGTATAAGAGACA*G
14	CAAGCAGAAGACGGCATACGAGATcgtacttcGTGACTGGAGTTCAGACGTGTGCTC TTCCGATC*T
15	AATGATACGGCGACCACCGAGATCTACACCTAAGCCTTCGTCGGCAGCGTCAGA TGTGTATAAGAGACA*G
16	CAAGCAGAAGACGGCATACGAGATgagtcacgGTGACTGGAGTTCAGACGTGTGCT CTTCCGATC*T
17	AATGATACGGCGACCACCGAGATCTACACGCGTAAGATCGTCGGCAGCGTCAGA TGTGTATAAGAGACA*G
18	CAAGCAGAAGACGGCATACGAGATgccggaacGTGACTGGAGTTCAGACGTGTGCT CTTCCGATC*T

Characterizing the role of mismatch repair components in the ultraviolet
light-induced post-translesion synthesis repair pathway

Supplemental materials table 2: guideRNA sequences used for CRISPR

CRISPR table	gRNA 1	gRNA 2	Target	Protein/mRNA	6tG selected
<i>Mlh3</i> lines	TGCCCATGAACGCATT CGTT	-	Exon 6	No mRNA	No
<i>Pms1</i> lines	AAAAAGGGCCACCAG TTCGT	-	Exon 10	No mRNA	No
<i>Exo1</i> line 1	TATCAACATCACGCAC GCC	-	Exon 5 or 6	Truncated mRNA	No
<i>Exo1</i> line 2	TTGGCCTACCTTAACA AGGC	-	Exon 5 or 6	Truncated mRNA	No
<i>Fan1</i> lines	CGAAGACGCGGGGAT CGGCT	AGGGACATCTGGCCA TCTAC	Entire gene	No mRNA	No
<i>Msh6</i> lines	GGAGCCTCCGCTTCC CGCGG	CCTTTGATGGAACGTT CAT	Exon 1-2	No protein	Yes
<i>Mlh1</i> lines	CTCCTCCGGAGTGAG CACGG	ATGCCAGATTGGACC AACTA	Entire gene	No protein	Yes
<i>Pms2</i> lines	CGGCGCGCTAGACTG GACGAGGG	GTGAAGTCCAGGCGG CAGTTAGG	Exons 5-7	No protein	Yes

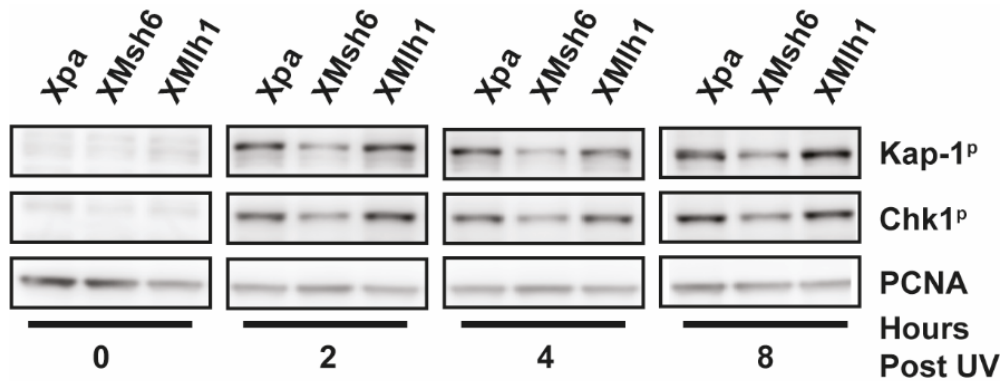
Supplemental Figures



Supplemental Figure 1: Cell line validation by mRNA and protein analysis

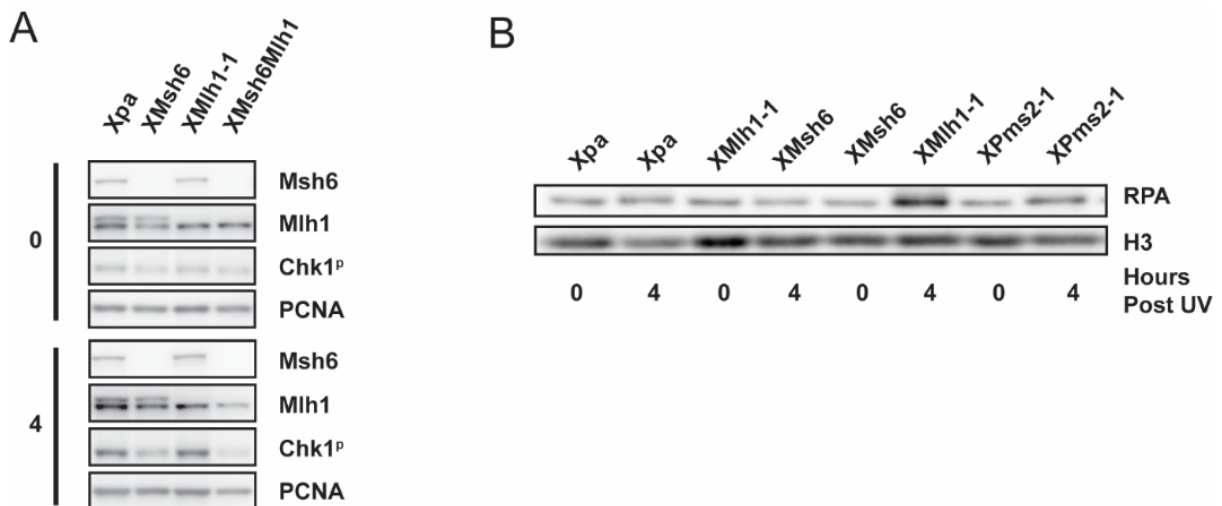
A: Knock-out of Exo1 was validated by RT-PCR. Truncated levels of mRNA were detected, sequencing analysis showed a deletion of 19/24nt for cell line 1 and 134/150bp for cell line 2, in line with the displayed fragment sizes. B: RT-PCR analysis of Fan1 cell lines show complete loss of Fan1 mRNA. Hprt was used as a control for the presence of intact RNA. C: RT-PCR analysis of Mlh3 cell lines show complete loss of Mlh3 mRNA. D: RT-PCR analysis of Pms1 cell lines show complete loss of Pms1 mRNA. E: Western blot analysis of Mlh1 knock-out cell lines shows complete depletion of Mlh1 protein. F: Western blot analysis of Pms2 knock-out cell lines show a complete depletion of Pms2 protein. Msh6 used as loading control. G: Western blot analysis of the Msh6Mlh1 knock-out cell line shows a complete depletion of both Msh6 and Mlh1. PCNA is used as a loading control. H: mRNA analysis of the Mlh1Exo1 line showed complete lack of Exo1 mRNA. Hprt is used as a control for the presence of intact mRNA.

Characterizing the role of mismatch repair components in the ultraviolet
light-induced post-translesion synthesis repair pathway



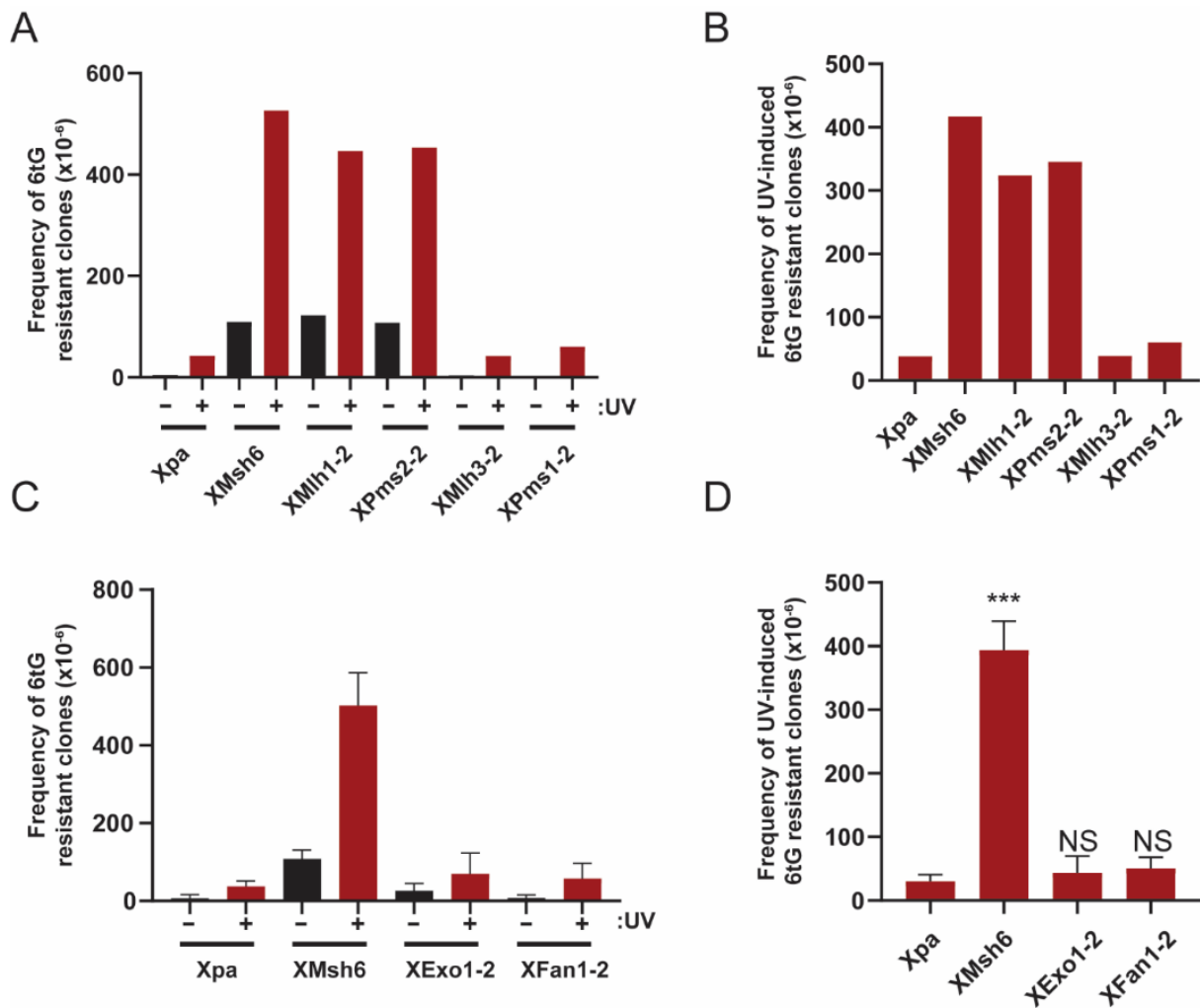
Supplemental Figure 1: UVC induced DNA damage signalling of independent cell lines

Western blots showing formation of Chk1^{P} and Kap-1^{P} in Xpa, XMsh6 and XMIh1 deficient cells, 0, 2, 4 and 8 hours post UVC exposure ($0,75\text{J/M}^2$). The XMIh1 cell line used is independent from the line used in Fig. 1. PCNA was used as a loading control. Representative images of 3 independent experiments. X=Xpa deficiency.



Supplemental Figure 2: UVC induced DNA damage signalling in nocodazole treated cells and chromatin-bound Rpa formation in independent MMR deficient clones.

A: Western blots showing formation of Chk1^{P} in Xpa, XMsh6 and XMIh1 and XMsh6MIh1 deficient cells, 0 and 4 hours post UVC exposure ($0,75\text{J/M}^2$). Nocodazole was used in all samples to prevent mitosis and ensure measured responses are in the first cell cycle. PCNA was used as a loading control. Representative images of 3 independent experiments. X=Xpa deficiency. B: Chromatin-bound fraction of Rpa indicative of ssDNA formation at 0 and 4 hours post UVC exposure (2J/M^2). Histone H3 (H3) was used as a loading control. Representative image of three independent experiments.



Supplemental Figure 3: UVC-induced mutagenesis in independent cell lines deficient for MMR, MMR homologs and exonucleases

A: Frequency of 6tG resistant cells as a measure for mutagenesis at the *Hprt* gene in MMR and MMR homolog deficient lines following exposure to mock or 0,75J/M² UVC. N=1. B: Frequency of UV-induced 6tG resistant clones as a measure for mutagenesis at the *Hprt* gene in MMR and MMR homolog deficient lines. C: Frequency of 6tG resistant cells as a measure for mutagenesis at the *Hprt* gene following exposure to mock or 0,75J/M² UVC in exonuclease deficient cell lines. XMsh6 serves as technical control. N=3. Error bars, SEM. D: Frequency of UVC-induced 6tG resistant clones as a measure for mutagenesis at the *Hprt* gene in exonuclease deficient cell lines. Error bars, SEM. ***, $P \leq 0,001$, ns, not statistically significant; unpaired T-test comparing groups to Xpa.

Table S1:

List of mutants in the Hprt gene obtained after NGS of UVC-treated Xpa deficient cells and selected with 6tG for Hprt inactivation. Flanking sequence: sequence surrounding the mutated bases, parentheses surround the mutated base, non-transcribed strand sequence is shown. Strand: strand with the dipyrimidine sequence containing the mutation. NTS, non-transcribed strand. TS, transcribed strand. Dipyrimidine: mutated dipyrimidine sequence; mutated base(s) are underscored. Ins: inserted nucleotide(s), del: deleted nucleotide(s).

	Position	Exon	Base change	Flanking Sequence	Amino acid change	Strand	Dipyrimidine
SNS	40	2	G > T	GAT(G)AAC	E > *	TS	<u>C</u> T
	51	2	T > A	TTA(T)GAC	Y > *		
	52	2	G > T	TAT(G)ACC	D > Y	TS	<u>C</u> T
	69	2	T > A	TTG(T)ATA	C > *		
	74	2	C > T	TAC(C)TAA	P > L	NTS	C <u>C</u> T
	82	2	T > A	CAT(T)ATG	Y > N	NTS	T <u>I</u>
	84	2	T > G	TTA(T)GCC	Y > *		
	95	2	T > C	ATT(T)GGA	L > S	NTS	T <u>I</u>
	109	2	A > T	TTT(A)TTC	I > F		
	110	2	T > A	TTA(T)TCC	I > N	NTS	<u>I</u> T
	113	2	C > T	TTC(C)TCA	P > L	NTS	C <u>C</u> T
	118	2	G > A	CAT(G)GAC	G > R	TS	<u>C</u> C
	119	2	G > A	ATG(G)ACT	G > E	TS	C <u>C</u> T
	125	2	T > A	TGA(T)TAT	I > N	NTS	<u>I</u> T
	125	2	T > G	TGA(T)TAT	I > S	NTS	<u>I</u> T
	134	2	G > A	ACA(G)GAC	R > K	TS	T <u>C</u> C
	145	3	C > T	AGA(C)TTG	L > F	NTS	<u>C</u> T
	149	3	C > T	TTG(C)TCG	A > V	NTS	<u>C</u> T
	151	3	C > T	GCT(C)GAG	R > *	NTS	T <u>C</u>
	170	3	T > A	AGA(T)GGG	M > K		
	202	3	C > T	GTG(C)TCA	L > F	NTS	<u>C</u> T
	208	3	G > A	AAG(G)GGG	G > R	TS	C <u>C</u> C
	209	3	G > A	AGG(G)GGG	G > E	TS	C <u>C</u> C
	239	3	A > T	TGG(A)TTA	D > V	TS	C <u>I</u>
	245	3	T > A	ACA(T)TAA	I > N	NTS	<u>I</u> T
	464	6	C > T	GCC(C)CAA	P > L	NTS	C <u>C</u> C
	482	6	C > A	TTG(C)AAG	A > E		
	527	7	C > A	GGC(C)AGA	P > Q	NTS	C <u>C</u>
	538	8	G > A	GTT(G)GAT	G > R	TS	<u>C</u> C
	539	8	G > A	TTG(G)ATT	G > E	TS	C <u>C</u> T
	544	8	G > A	TTT(G)AAA	E > K	TS	<u>C</u> T
	544	8	G > T	TTT(G)AAA	E > *	TS	<u>C</u> T
	547	8	A > T	GAA(A)TTC	I > F	TS	T <u>I</u>
	548	8	T > G	AAA(T)TCC	I > S	NTS	<u>I</u> T
	550	8	C > T	ATT(C)CAG	P > S	NTS	T <u>C</u> C
	551	8	C > A	TTC(C)AGA	P > Q	NTS	C <u>C</u>
	565	8	G > T	GTT(G)TTG	V > F		
	568	8	G > A	GTT(G)GAT	G > R	TS	<u>C</u> T
DNS	46	2	GG > TA	CCA(GG)TTA	G > Y	TS	C <u>C</u>

118	2	GG > AA	CAT(GG)ACT	G > K	TS	<u>CC</u>
169	3	AT > CA	GAG(AT)GGG	M > Q	TS	CTA
171	3	GG > AA	GAT(GG)GAG	M + G > G + R	TS	<u>CCC</u>
207	3	GG > AA	CAA(GG)GGG	K + G > K + R	TS	<u>CCC</u>
207	3	GG > AC	CAA(GG)GGG	K + G > K + R	TS	<u>CCC</u>
208	3	GG > AA	AAG(GG)GGG	G > K	TS	<u>CCCC</u>
209	3	GG > AA	AGG(GG)GGC	G > E	TS	<u>CCCC</u>
211	3	GG > AA	GGG(GG)CTA	G > N	TS	<u>CCC</u>
463	6	CC > TT	AGC(CC)CAA	P > F	NTS	<u>CCCC</u>
464	6	CC > TA	GCC(CC)AAA	P > L	NTS	<u>CCC</u>
498	7	AA > TT	GAA(AA)GGA	K + R > N + W	TS	<u>TTTC</u>
527	7	CA > AT	GGC(CA)GAC	P > H		<u>CCAG</u>
538	8	GG > AA	GTT(GG)ATT	G > K	TS	<u>CCT</u>
539	8	GA > TG	TTG(GA)TTT	G > V	TS	<u>CCT</u>
550	8	CC > TT	ATT(CC)AGA	P > L	NTS	<u>TCC</u>
568	8	GG > AA	GTT(GG)ATA	G > K	TS	<u>CCT</u>
599	8	GG > AA	TCA(GG)GAT	R > K	TS	<u>TCCC</u>
600	8	GG > AA	CAG(GG)ATT	R + D > R + N	TS	<u>CCCT</u>

	Position	Exon	Base change
MNS	44	2	CAG > AA
	113	2	CTC > TTT
	123	2	GAT > AAA
	130	2	GAC > AAA
	202	3	CTC > TTT
	229	3	GAC > AAA
	290	3	TAG > AAT
	495	7	GAAA > AAAT
	506	7	CTC > TTT
	569	8	GAT > AAA
	574	8	GCCCT > TCCCC
Insertion			
	610	9	ins AG
Deletion	486	7	del 47bp
	533	8	del 77bp
	533	8	del 21bp

Table S2:

List of mutants in the *Hprt* gene obtained after NGS of mock-treated *XMsh6* deficient cells and selected with 6tG for *Hprt* inactivation. Flanking sequence: sequence surrounding the mutated bases, parentheses surround the mutated base, non-transcribed strand sequence is shown. Dipyrimidine: mutated dipyrimidine sequence; mutated base(s) are underscored. Ins: inserted nucleotide(s), del: deleted nucleotide(s).

	Position	Exon	Base change	Flanking Sequence	Amino acid change	Dipyrimidine
SNS	122	2	T > C	GAC(T)GAT	L > P	C <u>T</u>
	131	2	A > G	TGG(A)CAG	D > G	C <u>T</u>
	140	3	A > G	CTG(A)AAG	E > G	C <u>T</u> T
	154	3	G > T	CGA(G)ATG	D > Y	T <u>C</u> T
	155	3	A > G	GAG(A)TGT	D > G	C <u>T</u>
	170	3	T > C	AGA(T)GGG	M > T	
	202	3	C > T	GTG(C)TCA	L > F	<u>C</u> T
	206	3	A > G	TCA(A)GGG	K > R	T <u>C</u> C
	220	3	T > C	AAG(T)TCT	F > L	<u>T</u> T
	233	3	T > C	ACC(T)GCT	L > P	C <u>T</u>
SNS	254	3	T > C	CAC(T)GAA	L > P	C <u>T</u>
	305	3	T > A	GAC(T)GAA	L > Q	C <u>T</u>
	446	6	T > C	CCC(T)GGT	L > P	C <u>T</u>
	491	7	T > C	TGC(T)GGT	L > P	C <u>T</u>
	495	7	G > A	GGT(G)AAA	V > V	<u>C</u> T
	526	7	C > T	AGG(C)CAG	P > S	<u>C</u> C
	530	7	A > G	CAG(A)CTT	D > G	C <u>T</u>
	533	8	T > C	ACT(T)TGT	F > S	T <u>T</u> T
	544	8	G > A	TTT(G)AAA	E > K	C <u>T</u>
	563	8	T > C	TTG(T)TGT	V > A	<u>T</u> T
	572	8	A > G	GAT(A)TGC	Y > C	
	590	8	A > T	ATG(A)GTA	E > V	C <u>T</u> C
	595	8	T > C	TAC(T)TCA	F > L	C <u>T</u> T
	598	8	A > G	TTC(A)GGG	R > G	<u>T</u> C
	611	9	A > G	ATC(A)CGT	H > R	
	614	9	T > C	ACG(T)TTG	V > A	<u>T</u> T
Insertion	103	2	ins A			
	562	8	ins T			
Deletion	323	4 / 5	del 66bp			
	345	4	del A			
	486	7	del 47bp			
	533	8	del 77bp			

Table S3:

List of mutants in the Hprt gene obtained after NGS of UVC-treated XMsh6 deficient cells and selected with 6tG for Hprt inactivation. Flanking sequence: sequence surrounding the mutated bases, parentheses surround the mutated base, non-transcribed strand sequence is shown. Strand: strand with the dipyrimidine sequence containing the mutation. NTS, non-transcribed strand. TS, transcribed strand. Dipyrimidine: mutated dipyrimidine sequence; mutated base(s) are underscored. Ins: inserted nucleotide(s), del: deleted nucleotide(s).

	Position	Exon	Base change	Flanking Sequence	Amino acid change	Strand	Dipyrimidine
SNS	53	2	A > C	ATG(A)CCT	D > A	TS	<u>CT</u>
	71	2	T > G	GTA(T)ACC	I > R		
	71	2	T > A	GTA(T)ACC	I > K		
	122	2	T > C	GAC(T)GAT	L > P	NTS	<u>CT</u>
	139	3	G > A	ACT(G)AAA	E > K	TS	<u>CT</u>
	143	3	G > T	AAA(G)ACT	R > I	TS	<u>TCT</u>
	226	3	G > C	TTT(G)CTG	A > P		
	299	3	T > G	TTA(T)CAG	I > S	NTS	<u>TC</u>
	464	6	C > A	GCC(C)CAA	P > H	NTS	<u>CCC</u>
	472	6	G > T	ATG(G)TTA	V > F	TS	<u>CC</u>
	539	8	G > A	TTG(G)ATT	G > E	TS	<u>CCT</u>
	541	8	T > A	GGA(T)TTG	F > I	NTS	<u>IT</u>
	544	8	G > A	TTT(G)AAA	E > K	TS	<u>CT</u>
	550	8	C > T	ATT(C)CAG	P > S	NTS	<u>TCC</u>
	551	8	C > T	TTC(C)AGA	P > L	NTS	<u>CC</u>
	573	8	T > A	ATA(T)GCC	Y > *		
	583	8	T > A	GAC(T)ATA	Y > N	NTS	<u>CT</u>
	589	8	G > A	AAT(G)AGT	E > K	TS	<u>CT</u>
	597	8	C > A	CTT(C)AGG	F > L	NTS	<u>TC</u>
	599	8	G > A	TCA(G)GGA	R > K	TS	<u>TCC</u>
	601	8	G > A	AGG(G)ATT	D > N	TS	<u>CCT</u>
DNS	208	3	GG > AA	AAG(GG)GGG	G > K	TS	<u>CCCC</u>
	209	3	GG > AA	AGG(GG)GGC	G > E	TS	<u>CCCC</u>
	464	6	CC > TT	GCC(CC)AAA	P > L	NTS	<u>CCC</u>
	538	8	GG > AA	GTT(GG)ATT	G > K	TS	<u>CCT</u>
	600	8	GG > AA	CAG(GG)ATT	R + D > R + N	TS	<u>CCCT</u>
Deletion	319	4	del 9bp				
	323	4 / 5	del 66bp				
	486	7	del 47bp				
	533	8	del 77bp				
	533	8	del 21bp				

Table S4:

List of mutants in the Hprt gene obtained after NGS of mock-treated XMIh1 deficient cells and selected with 6tG for Hprt inactivation. Flanking sequence: sequence surrounding the mutated bases, parentheses surround the mutated base, non-transcribed strand sequence is shown. Dipyrimidine: mutated dipyrimidine sequence; mutated base(s) are underscored. Ins: inserted nucleotide(s), del: deleted nucleotide(s).

	Position	Exon	Base change	Flanking Sequence	Amino acid change	Dipyrimidine
SNS	46	2	G > A	CCA(G)GTT	G > S	<u>TCC</u>
	46	2	G > T	CCA(G)GTT	G > C	<u>TCC</u>
	47	2	G > A	CAG(G)TTA	G > D	<u>TC</u>
	103	2	G > A	AAA(G)TGT	V > M	<u>TC</u>
	104	2	T > C	AAG(T)GTT	V > A	

Characterizing the role of mismatch repair components in the ultraviolet
light-induced post-translesion synthesis repair pathway

	113	2	C > T	TTC(C)TCA	P > L	<u>CCT</u>
	119	2	G > T	ATG(G)ACT	G > V	<u>CCT</u>
	122	2	T > G	GAC(T)GAT	L > R	<u>CT</u>
	131	2	A > G	TGG(A)CAG	D > G	<u>CT</u>
	133	2	A > G	GAC(A)GGA	R > G	<u>IC</u>
	148	3	G > A	CTT(G)CTC	A > T	
	149	3	C > T	TTG(C)TCG	A > V	<u>CT</u>
	151	3	C > T	GCT(C)GAG	R > *	<u>TC</u>
	155	3	A > G	GAG(A)TGT	D > G	<u>CT</u>
	158	3	T > G	ATG(T)CAT	V > G	<u>IC</u>
	169	3	A > G	GAG(A)TGG	M > V	<u>CT</u>
	170	3	T > C	AGA(T)GGG	M > T	
	202	3	C > T	GTG(C)TCA	L > F	<u>CT</u>
	205	3	A > G	CTC(A)AGG	K > E	<u>IT</u>
	206	3	A > G	TCA(A)GGG	K > R	<u>TIC</u>
	208	3	G > A	AAG(G)GGG	G > R	<u>CCC</u>
	209	3	G > A	AGG(G)GGG	G > E	<u>CCC</u>
	212	3	G > A	GGG(G)CTA	G > D	<u>CC</u>
	215	3	A > G	GCT(A)TAA	Y > C	
	217	3	A > G	TAT(A)AGT	K > E	<u>IT</u>
	233	3	T > C	ACC(T)GCT	L > P	<u>CT</u>
	239	3	A > T	TGG(A)TTA	D > V	<u>CT</u>
	254	3	T > C	CAC(T)GAA	L > P	<u>CT</u>
	293	3	A > T	TAG(A)TTT	D > V	<u>CT</u>
	296	3	T > C	ATT(T)TAT	F > S	<u>TIT</u>
	326	4	A > C	ATC(A)GTC	Q > P	<u>IC</u>
	344	4	A > T	TAA(A)AGT	K > I	<u>TIT</u>
	355	4	G > A	GGT(G)GAG	G > R	<u>CC</u>
	446	4	T > C	CCC(T)GGT	L > P	<u>CT</u>
	463	4	C > T	AGC(C)CCA	P > S	<u>CCC</u>
	479	4	T > G	AGG(T)TGC	V > G	<u>IT</u>
	484	4	A > G	GCA(A)GCT	S > G	<u>TIC</u>
	491	7	T > A	TGC(T)GGT	L > Q	<u>CT</u>
	499	7	A > G	AAA(A)GGA	R > G	<u>TIC</u>
	526	7	C > T	AGG(C)CAG	P > S	<u>CC</u>
	533	8	T > C	ACT(T)TGT	F > S	<u>TIT</u>
	538	8	G > A	GTT(G)GAT	G > R	<u>CC</u>
	539	8	G > A	TTG(G)ATT	G > E	<u>CCT</u>
	544	8	G > A	TTT(G)AAA	E > K	<u>CT</u>
	569	8	G > A	TTG(G)ATA	G > E	<u>CCT</u>
	572	8	A > G	GAT(A)TGC	Y > C	
	577	8	C > T	GCC(C)TTG	L > F	<u>CCT</u>
	595	8	T > A	TAC(T)TCA	F > I	<u>CTT</u>
	598	8	A > G	TTC(A)GGG	R > G	<u>IC</u>
	599	8	G > T	TCA(G)GGA	R > M	<u>TCC</u>
	599	8	G > A	TCA(G)GGA	R > K	<u>TCC</u>
	600	8	G > T	CAG(G)GAT	R > S	<u>CCC</u>
	605	8	T > C	ATT(T)GAA	L > S	<u>TI</u>
	550	8	CC > TT	ATT(CC)AGA	P > L	<u>TCC</u>

Table S4 continued:

	Position	Exon	Base change
MNS	541	8	TTT > ATA
	581	8	AC > TTTT
Insertion	96	2	ins T
	500	7	ins A
Deletion	101	2	del AA
	208	3	del 111bp
	319	4	del 9bp
	323	4 / 5	del 66bp
	337	4	G
	345	4	A
	486	7	del 47bp
	499	7	A
	533	8	del 77bp
	533	8	del 21bp
	547	8	del A
	586	8	del AAT

Table S5:

List of mutants in the Hprt gene obtained after NGS of UVC-treated XMIh1 deficient cells and selected with 6tG for Hprt inactivation. Flanking sequence: sequence surrounding the mutated bases, parentheses surround the mutated base, non-transcribed strand sequence is shown. Strand: strand with the dipyrimidine sequence containing the mutation. NTS, non-transcribed strand. TS, transcribed strand. Dipyrimidine: mutated dipyrimidine sequence; mutated base(s) are underscored. Ins: inserted nucleotide(s), del: deleted nucleotide(s).

	Position	Exon	Base change	Flanking Sequence	Amino acid change	Strand	Dipyrimidine
SNS	52	2	G > T	TAT(G)ACC	D > Y	TS	<u>CT</u>
	67	2	T > C	TTT(T)GTA	C > R	NTS	<u>TI</u>
	74	2	C > T	TAC(C)TAA	P > L	NTS	<u>CCT</u>
	118	2	G > A	CAT(G)GAC	G > R	TS	<u>CC</u>
	139	3	G > A	ACT(G)AAA	E > K	TS	<u>CT</u>
	140	3	A > T	CTG(A)AAG	E > V	TS	<u>CIT</u>
	145	3	C > T	AGA(C)TTG	L > F	NTS	<u>CT</u>
	151	3	C > T	GCT(C)GAG	R > *	NTS	<u>TC</u>
	163	3	A > T	ATG(A)AGG	K > *	TS	<u>CIT</u>
	182	3	A > T	ATC(A)CAT	H > L		-
	212	3	G > A	GGG(G)CTA	G > D	TS	<u>CC</u>
	281	3	C > A	TTC(C)TAT	P > H	NTS	<u>CCT</u>
	355	4	G > A	GGT(G)GAG	G > R	TS	<u>CC</u>
	464	4	C > T	GCC(C)CAA	P > L	NTS	<u>CCC</u>
	475	4	A > G	GTT(A)AGG	K > E	TS	<u>IT</u>
	508	7	C > T	TCT(C)GAA	R > *	NTS	<u>TC</u>
	526	7	C > T	AGG(C)CAG	P > S	NTS	<u>CC</u>
	539	8	G > A	TTG(G)ATT	G > E	TS	<u>CCA</u>
	544	8	G > A	TTT(G)AAA	E > K	TS	<u>CT</u>
	544	8	G > T	TTT(G)AAA	E > *	TS	<u>CI</u>
	547	8	A > T	GAA(A)TTC	I > F	TS	<u>TI</u>
	548	8	T > A	AAA(T)TCC	I > N	NTS	<u>TI</u>
	548	8	T > G	AAA(T)TCC	I > S	NTS	<u>TI</u>
	550	8	C > T	ATT(C)CAG	P > S	NTS	<u>TCC</u>
	569	8	G > A	TTG(G)ATA	G > E	TS	<u>CCT</u>
	574	8	G > A	TAT(G)CCC	A > T		-
	577	8	C > T	GCC(C)TTG	L > F	NTS	<u>CCT</u>
	589	8	G > A	AAT(G)AGT	E > K	TS	<u>CT</u>
	595	8	T > C	TAC(T)TCA	F > L	NTS	<u>CCT</u>
	596	8	T > G	ACT(T)CAG	F > C	NTS	<u>TTC</u>
	596	8	T > C	ACT(T)CAG	F > S	NTS	<u>TTC</u>
	597	8	C > A	CTT(C)AGG	F > L	NTS	<u>TC</u>

Table S5 continued:

	Position	Exon	Base change	Flanking Sequence	Amino acid change	Strand	Dipyrimidine
DNS	84	2	TG > AT	TTA(TG)CCG	Y + A > * + S		
	118	2	GG > AA	CAT(GG)ACT	G > K	TS	<u>CCT</u>
	157	3	GT > TA	GAT(GT)CAT	V > Y	NTS	<u>CAG</u>
	165	3	GG > AA	GAA(GG)AGA	K + E > K + K	TS	<u>TCCT</u>
	208	3	GG > AA	AAG(GG)GGG	G > K	TS	<u>CCCC</u>
	538	8	GG > AA	GTT(GG)ATT	G > K	TS	<u>CCT</u>
	568	8	GG > AA	GTT(GG)ATA	G > K		<u>CCT</u>
	573	8	TG > AT	ATA(TG)CCC	Y + A > * + S		
	600	8	GG > AA	CAG(GG)ATT	R + D > R + N	TS	<u>CCCT</u>
	611	9	AC > TT	ATC(AC)GTT	H > L		
MNS	97	2	G > AA				
	113	2	CTC > TT				
	130	2	GAC > AAA				
	202	3	CTC > TTT				
	205	3	A > CAG				
	207	3	GGG > TAA				
	229	3	GAC > AAA				
	544	8	GA > T				
Insertion	103	2	ins T				
	500	7	ins A				
Deletion	127	2	del A				
	208	3	del 111bp				
	319	4	del 9bp				
	323	4 / 5	del 66bp				
	337	4	del G				
	486	5 / 6 / 7	del 47bp				
	533	8	del 77bp				
	533	8	del 21bp				

References

1. Zhang Y, Yuan F, Presnell SR, Tian K, Gao Y, Tomkinson AE, et al. Reconstitution of 5'-Directed Human Mismatch Repair in a Purified System. *Cell*. 2005;122(5):693-705.
2. Goellner EM, Putnam CD, Kolodner RD. Exonuclease 1-dependent and independent mismatch repair. *DNA Repair (Amst)*. 2015;32:24-32.
3. Rikitake M, Fujikane R, Obayashi Y, Oka K, Ozaki M, Hidaka M. MLH1-mediated recruitment of FAN1 to chromatin for the induction of apoptosis triggered by O(6)-methylguanine. *Genes to cells : devoted to molecular & cellular mechanisms*. 2020;25(3):175-86.
4. Kadyrova LY, Gujar V, Burdett V, Modrich PL, Kadyrov FA. Human MutLgamma, the MLH1-MLH3 heterodimer, is an endonuclease that promotes DNA expansion. *Proc Natl Acad Sci U S A*. 2020;117(7):3535-42.
5. Chen PC, Dudley S, Hagen W, Dizon D, Paxton L, Reichow D, et al. Contributions by MutL homologues Mlh3 and Pms2 to DNA mismatch repair and tumor suppression in the mouse. *Cancer Res*. 2005;65(19):8662-70.
6. Prolla TA, Baker SM, Harris AC, Tsao JL, Yao X, Bronner CE, et al. Tumour susceptibility and spontaneous mutation in mice deficient in Mlh1, Pms1 and Pms2 DNA mismatch repair. *Nat Genet*. 1998;18(3):276-9.
7. Friedberg EC. Suffering in silence: the tolerance of DNA damage. *Nature Reviews Molecular Cell Biology*. 2005;6(12):943-53.
8. Wang H, Lawrence CW, Li GM, Hays JB. Specific binding of human MSH2.MSH6 mismatch-repair protein heterodimers to DNA incorporating thymine- or uracil-containing UV light photoproducts opposite mismatched bases. *J Biol Chem*. 1999;274(24):16894-900.
9. Seifert M, Scherer SJ, Edelmann W, Bohm M, Meineke V, Lobrich M, et al. The DNA-mismatch repair enzyme hMSH2 modulates UV-B-induced cell cycle arrest and apoptosis in melanoma cells. *The Journal of investigative dermatology*. 2008;128(1):203-13.
10. van Oosten M, Stout GJ, Backendorf C, Rebel H, de Wind N, Darroudi F, et al. Mismatch repair protein Msh2 contributes to UVB-induced cell cycle arrest in epidermal and cultured mouse keratinocytes. *DNA Repair (Amst)*. 2005;4(1):81-9.
11. Tsaalbi-Shtylik A, Ferras C, Pauw B, Hendriks G, Temviriyankul P, Carlee L, et al. Excision of translesion synthesis errors orchestrates responses to helix-distorting DNA lesions. *J Cell Biol*. 2015;209(1):33-46.
12. Nara K, Nagashima F, Yasui A. Highly elevated ultraviolet-induced mutation frequency in isolated Chinese hamster cell lines defective in nucleotide excision repair and mismatch repair proteins. *Cancer Res*. 2001;61(1):50-2.
13. Borgdorff V, Pauw B, van Hees-Stuivenberg S, de Wind N. DNA mismatch repair mediates protection from mutagenesis induced by short-wave ultraviolet light. *DNA Repair (Amst)*. 2006;5(11):1364-72.
14. Shin-Darlak CY, Skinner AM, Turker MS. A role for Pms2 in the prevention of tandem CC --> TT substitutions induced by ultraviolet radiation and oxidative stress. *DNA Repair (Amst)*. 2005;4(1):51-7.
15. Meira LB, Cheo DL, Reis AM, Claij N, Burns DK, te Riele H, et al. Mice defective in the mismatch repair gene Msh2 show increased predisposition to UVB radiation-induced skin cancer. *DNA Repair (Amst)*. 2002;1(11):929-34.
16. Yoshino M, Nakatsu Y, te Riele H, Hirota S, Kitamura Y, Tanaka K. Additive roles of XPA and MSH2 genes in UVB-induced skin tumorigenesis in mice. *DNA Repair (Amst)*. 2002;1(11):935-40.
17. Smith J, Tho LM, Xu N, Gillespie DA. The ATM-Chk2 and ATR-Chk1 pathways in DNA damage signaling and cancer. *Advances in cancer research*. 2010;108:73-112.
18. Hooper M, Hardy K, Handyside A, Hunter S, Monk M. HPRT-deficient (Lesch-Nyhan) mouse embryos derived from germline colonization by cultured cells. *Nature*. 1987;326(6110):292-5.
19. Magoc T, Salzberg SL. FLASH: fast length adjustment of short reads to improve genome assemblies. *Bioinformatics*. 2011;27(21):2957-63.
20. van Schendel R, Schimmel J, Tijsterman M. SIQ: easy quantitative measurement of mutation profiles in sequencing data. *NAR genomics and bioinformatics*. 2022;4(3):lqac063.
21. Wang Y, Qin J. MSH2 and ATR form a signaling module and regulate two branches of the damage response to DNA methylation. *Proc Natl Acad Sci U S A*. 2003;100(26):15387-92.
22. Ciccio A, Elledge SJ. The DNA damage response: making it safe to play with knives. *Mol Cell*. 2010;40(2):179-204.
23. Guan J, Lu C, Jin Q, Lu H, Chen X, Tian L, et al. MLH1 Deficiency-Triggered DNA Hyperexcision by Exonuclease 1 Activates the cGAS-STING Pathway. *Cancer Cell*. 2021;39(1):109-21 e5.
24. Borgdorff V, van Hees-Stuivenberg S, Meijers CM, de Wind N. Spontaneous and mutagen-induced loss of DNA mismatch repair in Msh2-heterozygous mammalian cells. *Mutat Res*. 2005;574(1-2):50-7.
25. Elvers I, Johansson F, Groth P, Erixon K, Helleday T. UV stalled replication forks restart by re-priming in human fibroblasts. *Nucleic Acids Res*. 2011;39(16):7049-57.
26. Liao H, Ji F, Helleday T, Ying S. Mechanisms for stalled replication fork stabilization: new targets for synthetic lethality strategies in cancer treatments. *EMBO reports*. 2018;19(9).
27. Zhang J, Zhao X, Liu L, Li HD, Gu L, Castrillon DH, et al. The mismatch recognition protein MutSalph promotes nascent strand degradation at stalled replication forks. *Proc Natl Acad Sci U S A*. 2022;119(40):e2201738119.
28. Wu Q, Vasquez KM. Human MLH1 protein participates in genomic damage checkpoint signaling in response to DNA interstrand crosslinks, while MSH2 functions in DNA repair. *PLoS Genet*. 2008;4(9):e1000189.
29. Shiotani B, Zou L. ATR signaling at a glance. *J Cell Sci*. 2009;122(Pt 3):301-4.

30. Li Z, Pearlman AH, Hsieh P. DNA mismatch repair and the DNA damage response. *DNA Repair (Amst)*. 2016;38:94-101.
31. Cannavo E, Marra G, Sabates-Bellver J, Menigatti M, Lipkin SM, Fischer F, et al. Expression of the MutL homologue hMLH3 in human cells and its role in DNA mismatch repair. *Cancer Res*. 2005;65(23):10759-66.
32. Yekezare M, Gomez-Gonzalez B, Diffley JF. Controlling DNA replication origins in response to DNA damage - inhibit globally, activate locally. *J Cell Sci*. 2013;126(Pt 6):1297-306.
33. Berti M, Cortez D, Lopes M. The plasticity of DNA replication forks in response to clinically relevant genotoxic stress. *Nature reviews Molecular cell biology*. 2020;21(10):633-51.
34. Hendriks G, Calleja F, Besaratinia A, Vrieling H, Pfeifer GP, Mullenders LH, et al. Transcription-dependent cytosine deamination is a novel mechanism in ultraviolet light-induced mutagenesis. *Current biology : CB*. 2010;20(2):170-5.
35. Hendriks G, Calleja F, Vrieling H, Mullenders LH, Jansen JG, de Wind N. Gene transcription increases DNA damage-induced mutagenesis in mammalian stem cells. *DNA Repair (Amst)*. 2008;7(8):1330-9.
36. Roesner LM, Mielke C, Fahnrich S, Merkhoffer Y, Dittmar KE, Drexler HG, et al. Stable expression of MutLgamma in human cells reveals no specific response to mismatched DNA, but distinct recruitment to damage sites. *Journal of cellular biochemistry*. 2013;114(10):2405-14.
37. Jansen JG, Tsaalbi-Shtylik A, Langerak P, Calleja F, Meijers CM, Jacobs H, et al. The BRCT domain of mammalian Rev1 is involved in regulating DNA translesion synthesis. *Nucleic Acids Res*. 2005;33(1):356-65.
38. Temviriyankul P, van Hees-Stuivenberg S, Delbos F, Jacobs H, de Wind N, Jansen JG. Temporally distinct translesion synthesis pathways for ultraviolet light-induced photoproducts in the mammalian genome. *DNA Repair (Amst)*. 2012;11(6):550-8.
39. Jansen JG, Fousteri MI, de Wind N. Send in the clamps: control of DNA translesion synthesis in eukaryotes. *Mol Cell*. 2007;28(4):522-9.
40. Shachar S, Ziv O, Avkin S, Adar S, Wittschleben J, Reissner T, et al. Two-polymerase mechanisms dictate error-free and error-prone translesion DNA synthesis in mammals. *EMBO J*. 2009;28(4):383-93.
41. Despras E, Daboussi F, Hyrien O, Marheineke K, Kannouche PL. ATR/Chk1 pathway is essential for resumption of DNA synthesis and cell survival in UV-irradiated XP variant cells. *Human molecular genetics*. 2010;19(9):1690-701.
42. Jansen JG, Tsaalbi-Shtylik A, Hendriks G, Gali H, Hendel A, Johansson F, et al. Separate domains of Rev1 mediate two modes of DNA damage bypass in mammalian cells. *Mol Cell Biol*. 2009;29(11):3113-23.
43. Quinet A, Martins DJ, Vessoni AT, Biard D, Sarasin A, Sary A, et al. Translesion synthesis mechanisms depend on the nature of DNA damage in UV-irradiated human cells. *Nucleic Acids Res*. 2016;44(12):5717-31.
44. Tirman S, Quinet A, Wood M, Meroni A, Cybulla E, Jackson J, et al. Temporally distinct post-replicative repair mechanisms fill PRIMPOL-dependent ssDNA gaps in human cells. *Mol Cell*. 2021;81(19):4026-40 e8.
45. Win AK, Jenkins MA, Dowty JG, Antoniou AC, Lee A, Giles GG, et al. Prevalence and Penetrance of Major Genes and Polygenes for Colorectal Cancer. *Cancer Epidemiol Biomarkers Prev*. 2017;26(3):404-12.
46. Chiavarini M, Bertarelli G, Minelli L, Fabiani R. Dietary Intake of Meat Cooking-Related Mutagens (HCAs) and Risk of Colorectal Adenoma and Cancer: A Systematic Review and Meta-Analysis. *Nutrients*. 2017;9(5):514.

Characterizing the role of mismatch repair components in the ultraviolet
light-induced post-translesion synthesis repair pathway





Chapter 4:

Elucidating the genetic entanglement of translesion synthesis and mismatch repair during the ultraviolet light-induced DNA damage response



*Robbert Ijsselsteijn¹, Jente Houweling¹,
Jacob G Jansen¹*

*¹Department of Human Genetics, Leiden
University Medical Center, Leiden, The
Netherlands.*

Abstract

Translesion synthesis (TLS) is an evolutionary conserved DNA damage tolerance pathway by which low fidelity TLS polymerases replicate across DNA helix-distorting nucleotide lesions. TLS allows completion of genomic DNA replication while quenching DNA damage signaling, thereby promoting cell survival at the expense of mutagenesis. Proteins involved in DNA mismatch repair (MMR) likely play a role in suppressing error-prone TLS. Two models have been described: (i) MMR-mediated recruitment of TLS polymerases to damaged nucleotides and (ii) the removal of TLS-induced misincorporations by MMR proteins in a pathway dubbed post-TLS repair. The latter predicts that MMR-dependent control of TLS correlates with the extent of error-prone TLS, while the former predicts an epistatic relationship between MMR and TLS. To distinguish between these two models, we generated mouse embryonic stem (mES) cells defective for Polymerase Eta (Pol η), a TLS polymerase that replicates across UV-induced cyclobutane pyrimidine dimers (CPDs) in a relatively error-free fashion. Upon UV exposure, Pol η -deficient mES cells display formation of single stranded DNA (ssDNA) gaps opposite CPDs, activation of DNA damage signaling, delayed cell cycle progression and enhanced mutagenesis resulting from increased error-prone TLS. UV-induced mutagenesis is further increased in Pol η -deficient mES cells with additional defects in the MMR genes *Msh6* or *Mlh1*. Interestingly, Msh6, but not Mlh1, is required for formation of ssDNA gaps and activation of cell cycle responses in Pol η -deficient mES cells. These results agree with Msh6-dependent excision of TLS-induced misincorporations opposite UV lesions, resulting in checkpoint activation and suppression of TLS-induced mutagenesis. Mlh1 suppresses UV-induced mutagenesis independent of DNA damage signaling and checkpoint control.

Introduction

Bulky DNA lesions that distort the helix structure of DNA form a strong block for the replicative DNA polymerases delta and epsilon. This blockage leads to stalling of replication forks that activate DNA damage signaling cascades, which contribute to fork stabilization and induce a cell cycle arrest. However, persistently stalled forks ultimately collapse, resulting in the formation of double stranded DNA breaks (DSB), gross genomic instability and cell death. To prevent replication fork collapse at helix-distorting DNA lesions, cells activate Translesion Synthesis (TLS), an evolutionary conserved DNA damage tolerance pathway that allows replication across and beyond nucleotide lesions, thereby quenching DNA damage signaling, enabling completion of DNA replication and preventing cell death (1).

Translesion synthesis is performed by a group of TLS polymerases that can be subdivided into two subfamilies: the Y-family DNA polymerases (Pol η , κ , ι and REV1) that insert nucleotides opposite the DNA lesion, forming so-called compound lesions, and the B-family DNA polymerase ζ (consisting of the catalytic subunit Rev3 and the accessory proteins Rev7, PolD2 and PolD3), important to extend DNA replication from compound DNA lesions. In contrast to DNA polymerases delta and epsilon, TLS polymerases lack the ability to perform 3'-5' proofreading. Moreover, Y-family polymerases have a more relaxed active site, allowing for the incorporation of

nucleotides opposite DNA lesions. However, the increased flexibility and the loss of proofreading lowers replication fidelity significantly (2). Consequently, replication of damaged DNA by TLS comes at the expense of mutagenesis.

Pol η is the only Y family TLS polymerase associated with human disease. Pol η is known for the relatively error-free bypass of UV-induced thymine-thymine cyclobutane dimers (CPD) due to its structure that seems uniquely suited to incorporate adenines opposite T-T CPDs (3). Mutations in *PolH*, the human gene encoding Pol η , give rise to Xeroderma Pigmentosum Variant (XPV) (4), an autosomal recessive disease, characterized by sensitivity to sunlight and strongly increased susceptibility to skin cancer formation resulting from UV-induced apoptosis and mutagenesis(5). The phenotypes of XPV highlight the two main roles Pol η performs in dealing with UV damage, namely efficient, but also relatively error-free bypass of UV-induced CPD lesions. The absence of Pol η lowers TLS processivity resulting in replication fork collapse, gross genomic instability and apoptosis. Moreover, compared to Pol η , back-up TLS polymerases are more mutagenic opposite UV lesions resulting in increased UV-induced mutagenesis and carcinogenesis (6).

As illustrated by the XPV phenotype, recruiting the ‘correct’ polymerase to bypass a nucleotide lesion is important to keep the mutagenic effects of TLS as low as possible. Control of mutagenic TLS occurs in multiple ways. Recruitment of TLS polymerases to the nucleotide lesion is a regulated process, which includes the mono-ubiquitination of PCNA, a DNA clamp that acts as a processivity factor for DNA polymerases, thereby enhancing its interaction with TLS polymerases, in particular Pol η . How the choice is made between different TLS polymerases for the bypass of various lesions is still a matter of debate, but it is clear that some polymerases will be more accurate on certain lesion types than others (7). Interestingly, replication extension from a Pol η -induced mis-incorporation is less efficient than when the correct nucleotide is incorporated (8, 9). Moreover, if Pol η halts replication when it mis-incorporates, it may hypothetically allow extrinsic exonucleases to outcompete TLS polymerases and remove the mis-incorporation, thereby controlling TLS mutagenicity. TLS-associated mutagenicity is also reported to be controlled by DNA mismatch repair (MMR). In canonical MMR, a heterodimer consisting of MSH2 and MSH6 (also known as MutS α) is required for the recognition of a base:base mismatch and the MLH1/PMS2 heterodimer (MutL α) for the subsequent nicking of the DNA and promotion of exonucleases that remove the mismatch (10). Several studies have shown that in the absence of MMR, methylation and oxidative DNA damage-induced mutagenicity is no longer suppressed (11-13), indicating that MMR also recognizes and removes mis-incorporations opposite slightly modified bases. Moreover, MMR proteins also suppress the mutagenicity of bulky helix-distorting DNA lesions induced by genotoxic agents such as UV-C light or the dietary mutagen PhIP (14, 15). The control of UV-induced mutagenesis is often accompanied with the formation of ssDNA, resulting in DNA damage signaling, cell cycle responses and apoptosis (16).

Two models are proposed to explain the suppression of UV-induced mutagenesis and DNA damage responses by MMR proteins (Fig. 1). First, the post-TLS repair model suggests that MMR proteins may perform a function reminiscent of canonical MMR, namely to reduce TLS-associated mutagenesis by removing the mis-incorporations opposite damaged DNA (17). This model is supported by the finding that MutS α binds more tightly to compound mismatches compared to correct base:lesion matches (18). Moreover, loss of Msh6 leads to increased UV-induced mutagenicity, reduced formation of ssDNA opposite UV-lesions and reduced levels of DNA damage signaling (17). Second, the role of MMR in suppressing UV-induced mutagenicity may be explained by MMR proteins that bind and recruit TLS polymerases to the lesion site. Some reports indicate that in response to various lesion types this non-canonical (nc)MMR pathway leads to MMR-dependent ubiquitination of PCNA to recruit Pol η to the site of damage (19, 20). However, another study suggests that MutS α can recruit Y family TLS polymerases to UV lesions independent of PCNA ubiquitination (21). This model suggests that when MMR is unavailable, Pol η and other Y family TLS polymerases cannot be recruited to bypass UV-lesions, thereby affecting UV mutagenesis and damage responses. Moreover, DNA damage signaling and single strand gap formation can possibly also be caused by MutS α -dependent processing of stalled forks (22) or Exo1 hyper-resection (23) as discussed in the chapter 3. These models do not explain the protective role of MMR when dealing with UV-induced mutagenesis and investigating these further falls outside the scope of this work. Similarly, MMR may be able to suppress mutagenicity by inducing DNA damage signaling thus causing cell cycle arrests allowing for DNA repair to take place or steer cells into senescence or apoptosis (24, 25), therefor preventing mutagenesis. In chapter 3, our findings revealed that Mlh1 has a protective effect against UV-induced mutagenesis, independent of the aforementioned damage signaling mechanisms. Hence, these models are unlikely to provide a plausible explanation for the observed suppression of UV-induced mutagenesis.

In this work we set out to study the relationship between TLS Pol η and MMR (Fig. 1). In particular, how MMR controls UV/TLS-associated mutagenesis and activates DNA damage signaling resulting in cell cycle arrests and apoptosis in mouse embryonic stem (mES) cells that are deficient for Pol η . The nature of the relationship between TLS and MMR could be elucidated by comparing *Polh*-deficient mES cells to *Polh*-deficient mES cells with an additional defect in *Msh6*, together with *Msh2* involved recognition of base-base mismatches, or with a defect in *Mlh1* that acts downstream of MutS α . An epistatic relationship is expected for a recruitment-based model, whereas the post-TLS repair model would be reflected by a synergistic relationship Pol η and MMR proteins. Here we show that UV-induced mutagenesis is increased in *Polh*-deficient cells and that additional deficiency for *Msh6* or *Mlh1* further exacerbates UV-induced mutagenesis. Moreover, cell cycle arrests and apoptotic responses in *Polh*-deficient cells depend on *Msh6*, but not on *Mlh1*. In line with this, DNA damage signaling and the formation of ssDNA gaps opposite UV damage only relies on Msh6.

Taken together, these data show a synergistic relationship between Pol η and the MMR proteins Msh6 and Mlh1 in support of the post-TLS repair model (26).

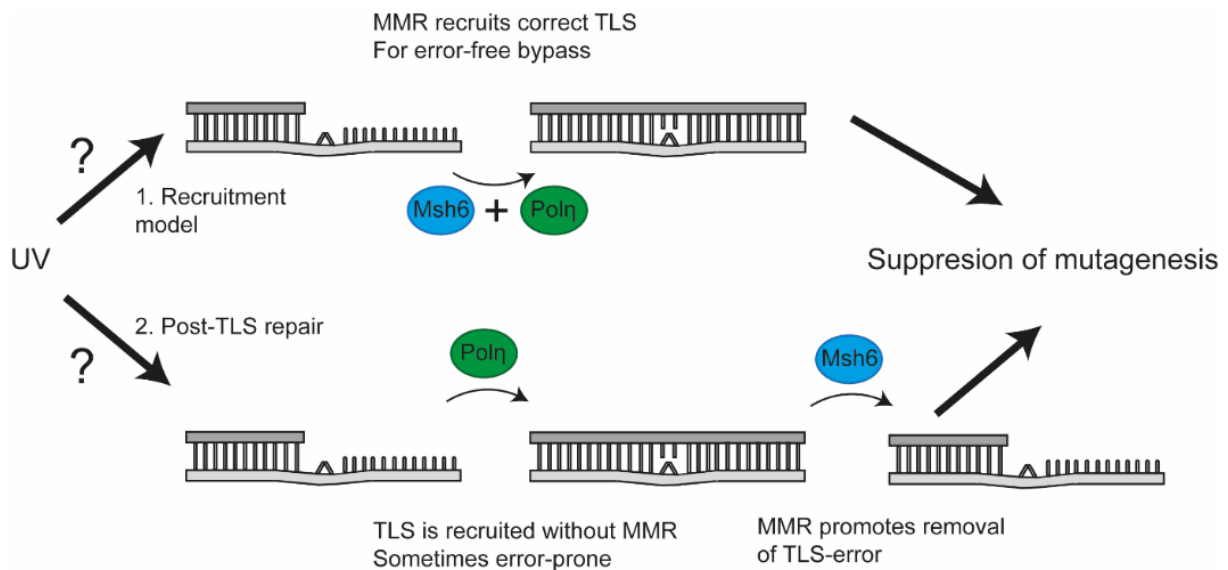


Figure 1: Recruitment and post-TLS repair models

UV radiation introduces DNA lesions (depicted by the crossed nucleotide bars) that cannot be bypassed by replicative polymerases. Pol η is recruited as a relatively error-free TLS polymerase to replicate across the damaged DNA. Two models are proposed to reduce mutagenicity of UV lesions: 1) recruitment of Pol η instead of more error-prone TLS polymerases by MMR proteins or 2) post-TLS repair, the post-replicative removal by MMR proteins of mis-incorporated nucleotides opposite DNA damage.

Materials and Methods

Mouse embryonic stem cell culture and cell lines

The generation of the wild-type mouse embryonic stem (mES) cell line is described elsewhere (27). This wild-type cell line was used as a parental cell line to generate all other cell lines in this work. The generation of the Msh6 single mutant cell line is described elsewhere (28). Cells were made deficient for *Polh* using CRISPR/Cas9 with guideRNAs targeting both the 5' and 3' region of the *Polh* gene (Supplemental methods table 1). Two independent *Polh*-deficient lines were generated which were validated by two genomic PCR strategies (Fig. 2, supplemental methods table 2). These cell lines were used for the generation of independent *PolhMsh6* and *PolhMlh1* double knockout cell lines using CRISPR/Cas9 (Supplemental methods table 1). After transfection with CRISPR/Cas9 expression constructs, the cells underwent an additional treatment with 40 μ M 6-thioguanine (6tG) for four hours to select for MMR

deficiency, which was validated on western blot (Abcam, clone 44, C-20, Santa Cruz Biotechnology for Msh6 and Mlh1, respectively). mES Cells were cultured on gelatin-coated dishes in “complete medium” which consisted of DMEM KO (Gibco) supplemented with 10% fetal calf serum (Bodinco/Capricorn Scientific), 0.1mM β -mercaptho-ethanol (Sigma-Aldrich), 1mM pyruvate (Gibco), 1% non-essential amino acids (Gibco), 1% glutamax (Gibco), 100U penicillin/ 100 μ g streptomycin (Gibco) and leukemia inhibitory factor (made in house).

Determination of UV-induced mutagenicity

Msh6, *Polh*, *PolhMsh6* and *PolhMlh1* deficient cells as well as WT cells were treated with 5mM Hypoxanthine, 20 μ M Aminopterin, 0.8 μ M Thymidine (HAT, 50x diluted, Thermo Fisher Scientific) for 6 days and afterwards with 5mM Hypoxanthine, 0.8 μ M Thymidine (HT, 50x diluted, Thermo Fisher Scientific) for 2 days to select for cells with functional *Hprt*. Next, 5 million cells per p90 culture dish were seeded and grown for a day before being exposed to 2J/m² of UV-C or mock treated. After treatment, the cells were maintained for 6 days before being seeded in a cell density of 4x10⁵ per p90 (5 p90 dishes per cell line) in the presence of 30 μ M 6tG to select for clones that have lost *Hprt*. From the same cell suspensions, 250 cells were seeded in 3 p60 culture dishes to determine the cloning efficiency of the cells. After 7-10 days the clones were stained using methylene blue and the *Hprt* mutant frequency was determined by counting the 6tG-resistant clones while adjusting for the cloning efficiency of cells.

Determination of cell cycle progression and apoptosis by FACS

Two million WT, *Msh6*, *Polh*, *PolhMsh6* and *PolhMlh1*-deficient cells were seeded in a p60 culture dish one day prior to exposure to 2J/m² of UV-C or mock treatment. After treatment, cells were incubated in medium containing 10 μ M BrdU (Merck Millipore) for 30 minutes and subsequently chased in medium containing 5 μ M thymidine (Invitrogen) until the timepoint was reached. Next, cells were trypsinized and added to the medium in which the cells were cultured. Cells were pelleted by centrifugation and fixed in ice cold 70% ethanol. For BrdU staining cells were pelleted and permeabilized/denatured using 0.5% Triton X-100 (Sigma Aldrich) in 2M HCL for 35 minutes at RT. The mixture was neutralized by adding an excess of 1M Tris (Sigma Aldrich). After centrifugation, the cells were washed once with PBS containing 0.5% Tween-20 + 5% Fetal Calf Serum (PBS-TS). Next, cells were incubated in 20 μ l mouse monoclonal anti-BrdU antibody (B44, BD Biosciences) and 30 μ l PBS-TS at 4°C for overnight. Afterwards, the cells were washed with PBS-TS and incubated with FITC-conjugated rat-anti-mouse antibody (1: 62.5, BD Pharmingen) diluted in PBS-TS for one hour in the dark. Finally, the cells were washed with PBS-TS and incubated using PBS containing propidium iodide (10 μ g/ml, Sigma Aldrich) and RNase A (100 μ g/ml, Roche Diagnostics). Cells were analyzed using a Novocyte Fluorescence Activated Cell Sorter (Acea

Biosciences) using gates for PI versus GFP. The different cell cycle phases as well as the apoptotic fraction was determined as described in supplementary figure S3.

Analysis of UV-induced DNA damage signaling

One million *Polh*, *PolhMsh6* and *PolhMlh1* deficient cells were seeded per well of a 6-wells plate one day prior to treatment. Cells were treated with 2J/m² of UV as described above and incubated in complete medium for different times. Cells were lysed in 250µl 2x Laemmli sample buffer. 12.5µl of cell lysate was used for western blot as described above. Primary antibodies against Kap-1^P (1:1000, Bethyl, polyclonal A300-767A) and Chk1^P (1:1000, Cell signaling technology, clone 133D3) were used to measure DNA damage signaling, antibodies against PCNA (1:8000, Santa Cruz, clone PC10) were used as a loading control. Antibodies against Msh6 (1:250, Abcam, clone 44) and Mlh1 (1:1000, Santa Cruz, polyclonal C20) were used for knock-out validation.

Determination of chromatin-bound Rpa

Polh, *PolhMsh6* and *PolhMlh1*-deficient cells were seeded in a cell density of 1.5x10⁶ cells per p60 culture dish, one day prior to irradiation with UV. Then, the cells were washed once with PBS and exposed to 2J/m² of UV-C. After exposure, the cells were incubated for 0 or 4 hours in complete medium. The cells were collected by trypsinization and 2 million cells were fractionated using a Subcellular Protein Fractionation Kit for Cultured Cells (Thermo Fisher Scientific) according to manufacturer's protocol. The total amount of protein in each fraction was measured using a Bradford assay (Thermo Fisher Scientific). Thirty µg of chromatin-bound protein extract was analyzed by western blot. Proteins were size-separated in 4-12% Criterion XT Bis-Tris Gels (Biorad) by gel electrophoresis using 70V for two hours followed by 120V for two hours. Next, the proteins were transferred onto 0.45µM nitrocellulose membranes (Protran, GE Healthcare) using 400mA (~70V) for two hours or at 200mA for overnight at 4°C. Protein membranes were incubated with Rockland blocking reagent (Rockland) diluted 1:1 with 0.1% PBS-tween (Rockland-PBS-T) for 1 hour at RT. Then, membranes were incubated in mixtures of Rockland-PBS-T containing primary antibodies against Histone H3 (1:14000, Abcam, polyclonal) and RPA (1:1000, Cell signaling technology, Clone 4E4) for overnight at 4°C. The membranes were washed with PBS-T and incubated with a mixture containing Rockland-PBS-T and secondary anti-mouse and anti-rabbit HRP antibodies (1:50000, Thermo Fisher Scientific) for one hours at RT. Membranes were washed again using PBS-T and the protein bands were subsequently visualized using Amersham ECL select (GE Healthcare).

Quantification of CPDs in ssDNA

One day prior to UV irradiation 5 x10⁶ *Polh*, *PolhMsh6* and *PolhMlh1* deficient cells were seeded in complete medium in p90-culture dishes. Cells were exposed to 2J/m² UV-C and incubated in complete medium containing 10µM EdU (Sigma Aldrich) for 30 minutes. Next, medium containing EdU was aspirated, and cells were incubated in medium containing 5µM Thymidine (Invitrogen) for 3.5 hours. For the 0 timepoints,

EdU labeling was done prior to UV-exposure. Subsequently, cells were collected by trypsinization, pelleted by centrifugation and washed with PBS, before incubation in ice cold CSK-Triton buffer (100 mM NaCl, 300 mM sucrose, 3 mM MgCl₂, 10 mM PIPES, 0.5% triton X-100, pH 7.2 – 7.5) for 2 minutes on ice. Afterwards, 10 ml PBS is added, cells are pelleted by centrifugation and fixed using 4% paraformaldehyde (Merck Millipore) for 20 minutes at RT. Finally, the cells were washed once more using PBS and pelleted before being resuspended in 1ml PBS. Using a cytopsin (Cytospin 4, ThermoScientific) the cells were centrifugated onto KP frost glass slides (Klinipath) and fixed onto the slides using 4% formaldehyde (Klinipath). Slides were stored in PBS until use. EdU stain was performed using Click-iT EdU Cell Proliferation Kit for Imaging 488 Dye (Thermo Fisher Scientific) following manufacturer's protocol. Afterwards, the cells were blocked in PBS containing 3% Bovine Serum Albumin (BSA) (Sigma Aldrich) and 0.1% Tween-20 (Sigma Aldrich) for 30 minutes. The slides were incubated with anti-CPD primary antibodies (1:1000, clone TDM-2, Cosmo Bio) in the dark for overnight at 4°C. Cells were then washed with five times with PBS-0.1% Tween-20 and incubated with secondary alexafluor-555 antibodies (1:1000, Thermo Fisher Scientific) for 1 hours at RT in the dark. After three times washing with PBS-0.1% Tween-20 and once with PBS, cells were mounted in anti-fade mounting medium containing DAPI (Vectashield). Cells were imaged using an AxioImagerM2 microscope (Zeiss) at 40x magnification. Quantification of integrated density was performed using ImageJ 2.1.0. The EdU-channel was binarized using the default threshold and used as a mask for the quantification of the integrated density of the CPD channel. Individual cells sized between 0.5 and 2.5 inch² were analyzed.

Results

Pol Eta deficiency: a model to study control of TLS-induced mutagenesis by MMR

Previously, MMR has been shown to reduce mutagenesis resulting from nucleotide lesions possibly by controlling TLS-associated mis-incorporations (29-31). How MMR regulates TLS fidelity has yet to be fully elucidated, but two main hypotheses are studied in this work (Fig.1): (1) MMR proteins recruit the “correct” TLS polymerases to the DNA damage (recruitment model) or (2) post-replicative removal by MMR proteins of TLS-induced mis-incorporations, dubbed post-TLS repair (17, 19-21). In this work we addressed these possibilities by generating mouse ES cells deficient for TLS *Polh* with or without an additional defect in *Msh6* or *Mlh1*. *Polh* acts relatively error-free at UV-induced CPD lesions compared to the other TLS polymerases (32). Therefore, *Polh* deficient cells are more mutable by UV-light, which allows us to more accurately study TLS-associated mutagenesis. Wild-type mES cells were made *Polh*-deficient by deleting the complete *Polh* gene using CRISPR/Cas9-induced DNA breaks at the 5' and 3' ends of the gene (Fig. 2A). We created two independent *Polh*-deficient clones as validated by a PCR using a primer pair that generates PCR fragments only when the entire gene is removed, whereas no PCR fragment was found using a primer pair that creates a PCR fragment when the gene is still present (Fig. 2B). Using CRISPR/Cas9 in combination with a positive selection for MMR-deficiency, 6TG, we

obtained *PolhMsh6* and *PolhMlh1* double knock-out clones in both *Polh*-deficient cell lines (Fig. 2C).

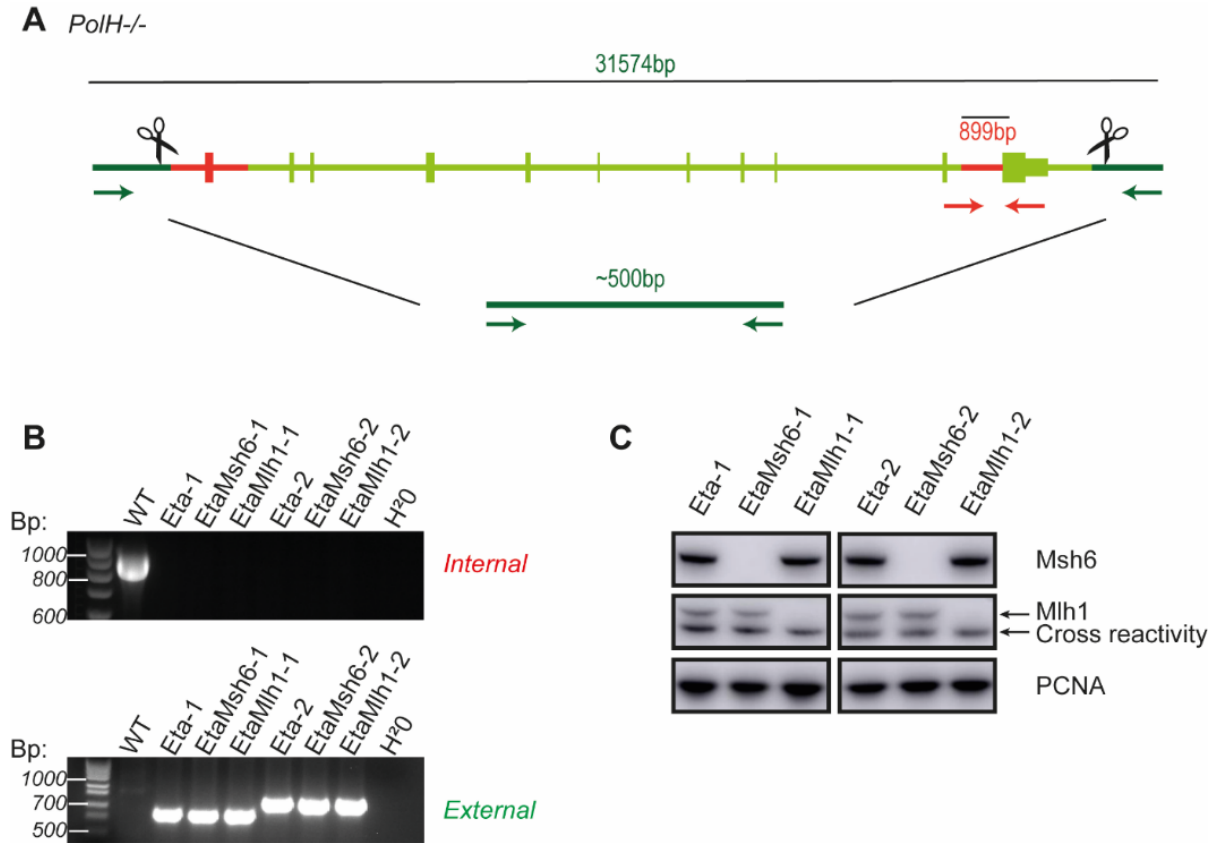


Figure 2: Generation of *Polh*-deficient cell lines

A: *Polh*-deficient cell lines were generated using CRISPR/Cas9 with guideRNAs (depicted as scissors) directing the cut slightly before and after the gene. Two sets of primers were designed to assess knock-out: a pair that targets a part of the gene to be deleted (external, red arrows) and a pair that targets the area outside of both sides of the gene (internal, green arrows). B: PCR on DNA level with the internal primer pair that is predicted to produce a 899bp product (if knock-out was unsuccessful) and a PCR with the external primer pair predicted to produce a product of approximately 500bp depending on the deletion size and method of repair (if knock-out is successful). C: Western blot was used to validate knock-out of *Msh6* and *Mlh1* in *Polh*-deficient cell lines.

Mutagenicity from UV-induced TLS-errors is controlled by both Msh6 and Mlh1

To elucidate how MMR controls TLS-associated mutagenesis, we exposed wild-type, *Msh6*, *Polh* and *PolhMsh6* double knockout cells to UV light and determined the frequency of 6tG-resistant clones, a measure for inactivating mutations at the X-linked *Hprt* gene. If MMR controls UV mutagenesis according to the recruitment model, additional knock-out of *Polh* in *Msh6* deficient cells would lead to an epistatic effect on UV mutagenesis, since the “correct” TLS polymerase is no longer recruited upon

inactivation of *Msh6*. However, in the post-TLS repair model a synergistic effect is expected between an increase of TLS-errors, due to inactivation of *Polh*, and lack of post-replicative control following *Msh6* deficiency (Fig. 1). First, we confirmed that *Polh* acts as a relatively error-free TLS polymerase at UV lesions as is described in literature (32) by subjecting wild type and *Polh*-deficient mES cells to mock and UV treatments and determine the frequency of *Hprt* mutant clones. Both cell lines show hardly any *Hprt* mutant clones following mock treatment. As expected for a role of *Polh* in error-free TLS at UV lesions, *Hprt* mutagenesis is higher in *Polh*-deficient cells than in wild-type cells (170.0×10^6 versus 81.2×10^6) following UV exposure (Fig. 3A, Fig. S1A). We also confirmed the control of UV/TLS-induced mutagenesis by *Msh6* (14) by determining *Hprt* mutagenesis in wild-type and *Msh6*-deficient cells following mock treatment and exposure to UV. As expected, mock-exposed *Msh6*-deficient cells display increased spontaneous mutagenesis compared to wild-type cells (192.1×10^6), due to loss of canonical MMR in *Msh6*-deficient cells. Following UV exposure, *Hprt* mutagenesis is strongly enhanced in *Msh6*-deficient cells, whilst in WT cells only a minor increase is observed (414.7×10^6 vs 81.2×10^6). The share of UV-induced mutagenesis, calculated by the subtraction of mutations found in the mock-exposed condition from the UV-exposed condition, is in *Msh6*-deficient cells much higher than in wild-type cells (78.2×10^6 vs 222.7×10^6) (Fig. 3B, S1B), supportive for a role of *Msh6* in controlling UV-induced mutagenesis (14). Finally, we determined UV mutagenesis in *Polh* and *Msh6* double knock-out cells and found that the frequency of UV-induced *Hprt* mutants in these cells is even higher than in *Msh6* single knock-out lines (Fig. 3C-D, Fig. S1 C-D), suggestive of synergism, rather than of epistasis, between *Polh* and *Msh6*. Interestingly, knock-out of *Mlh1* in a *Polh*-deficient background showed a similar response as *PolhMsh6*-deficient cells, suggesting that UV-induced mutagenicity is not only suppressed by *Msh6*, but also by *Mlh1*. These data show that there is a positive correlation between the extent of TLS-errors and the protection from mutagenesis by MMR, in support of the post-TLS repair model.

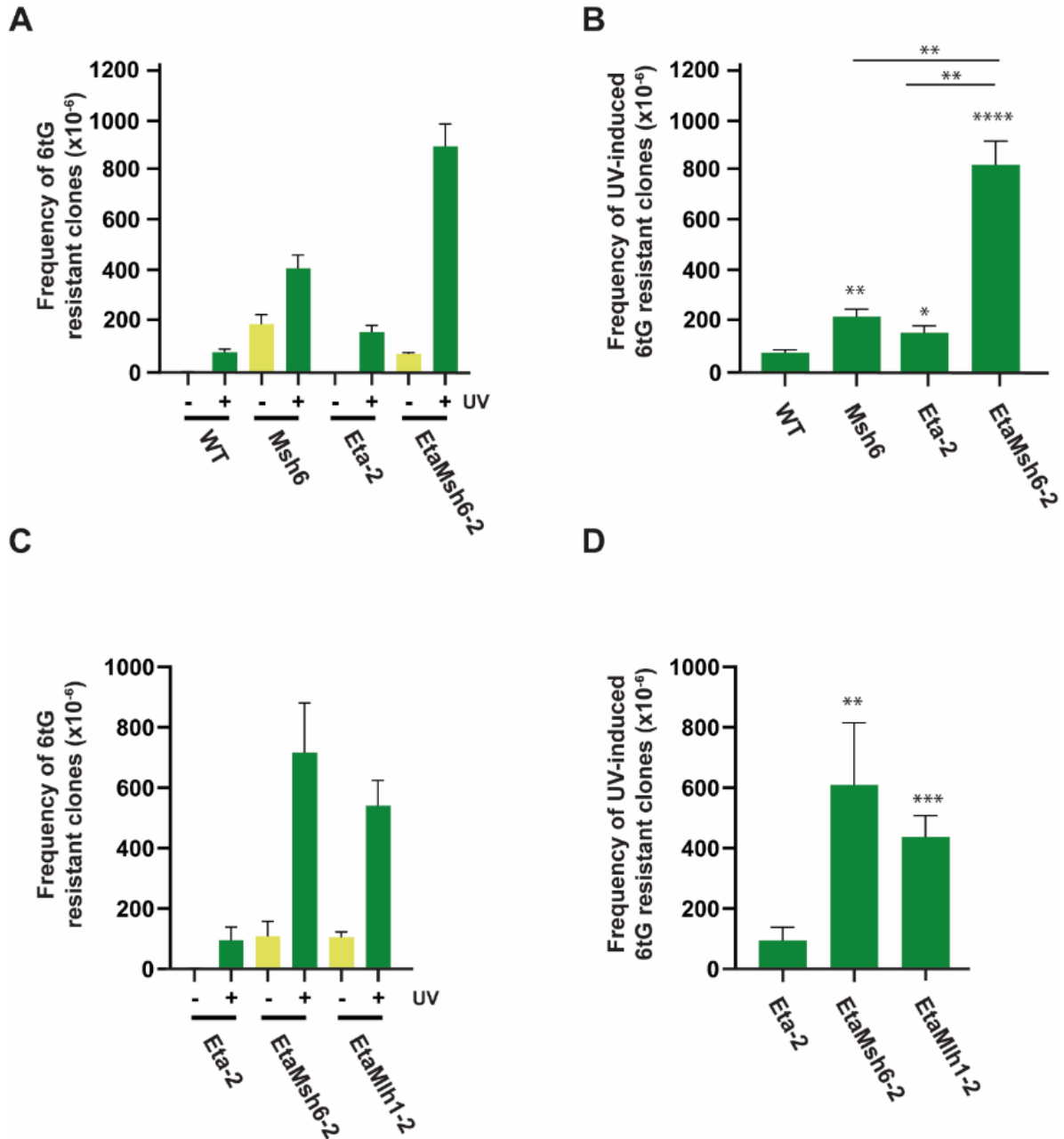


Figure 3: Mutagenicity of error-prone TLS opposed UV-damage is suppressed by Msh6 and Mlh1

A: Frequencies of 6tG-resistant clones containing inactivating Hprt mutations in spontaneous and UV-exposed WT, Msh6, Polη and PolηMsh6-deficient cells. Frequency of 6tG-resistant clones was plotted per million clone forming cells. B: Frequencies of UV-induced 6tG resistant clones in WT, Msh6, Polη and PolηMsh6-deficient cells shown per million clone forming cells. UV-induced mutagenesis was calculated by subtracting mutant frequencies of mock treated cells from those of UV-exposed cells. C: Mutagenesis in mock and UV- exposed conditions, as measured by the frequency of 6tG-resistant clones in Polη, PolηMsh6 and PolηMlh1-deficient cells shown per million clone forming cells. D: UV-induced mutagenesis as calculated by the subtraction of spontaneous mutagenesis from the mutagenesis in UV-exposed conditions in Polη, PolηMsh6 and PolηMlh1-deficient cells shown per million cells. Error bars, SEM; *, $P \leq 0,05$; **, $P \leq 0,01$; ***, $P \leq 0,001$; ****, $P \leq 0,0001$; ns, non-significant; student T-test of groups compared to WT or Polη single mutant or between EtaMsh6 and single mutants.

UV-induced cell cycle arrest and apoptosis is aggravated during error-prone TLS and requires Msh6, but not Mlh1

Suppression of UV-induced mutagenesis by MutS α is shown to be accompanied by delayed cell cycle progression due to intra-S checkpoint activation (17), which might be the result of the generation of single stranded DNA (ssDNA) tracts due to excision of TLS-induced ‘mis-incorporations’ opposite UV lesions. To investigate whether MutS α is required for an UV-induced cell cycle delay in *Polh*-deficient cells, cell cycle progression of BrdU pulse-labelled wild-type, *Msh6*-deficient, *Polh*-deficient and *PolhMsh6* doubly deficient cells was determined by FACS. As a readout we quantified the proportion of BrdU positive cells in G1/early S phase, *i.e.* cells that were replicating at the time of UV exposure or mock treatment and progressed to the subsequent cell cycle. Cell cycle progression of wild-type, *Msh6*-deficient, *Polh*-deficient and *PolhMsh6* doubly deficient cells was similar when these cells are mock-exposed (Fig. S2A-B), whereas UV exposure resulted in delayed cell cycle progression in all genotypes. However, wild-type cells and, in particular, *Polh*-deficient cells progressed much slower through the cell cycle than *Msh6*-deficient and *PolhMsh6* doubly deficient cells (Fig. S2C; compare 8 hours after UV with mock). Moreover, cell cycle progression of UV treated *Msh6*-deficient and *PolhMsh6* doubly deficient cells was almost indistinguishable from mock treated cells. These data not only confirm previous observations (11), but also strongly indicate that MutS α is essential for checkpoint activation in *Polh*-deficient cells following UV exposure. Since both *Msh6* and *Mlh1* protect *Polh*-deficient cells from UV mutagenesis to nearly the same extent (Fig. 3C, D), we wondered if *Msh6* and *Mlh1* play similar roles in UV-induced checkpoint activation. Similar to single knock-out cells, no difference in cell progression was found between double knock-out cell lines and the parental *Polh* cell lines when not exposed to UV (Fig. S3A-B). However, in stark contrast to loss of *Msh6* in *Polh*-deficient cells, deletion of *Mlh1* in *Polh*-deficient cells showed a similar or even stronger cell cycle block than *Polh* single knockout cells after UV (Fig. 4A-B). By examining the sub-G1 fraction of the cell cycle profiles we could also investigate UV-induced toxicity, as the sub-G1 cells contain a smaller amount of total DNA, which is indicative of apoptosis. Here, we show that *Polh*-deficient cell populations contain a significant fraction of apoptotic cells, starting 16 hours after UV and increasing further 24- and 32-hours post-UV (Fig. 4C, Fig. S3C). Loss of *Msh6* in *Polh*-deficient background rescues this UV sensitivity to wild-type levels at all timepoints. In contrast, *PolhMlh1* lines phenocopy the *Polh* single knock-out line and display *Polh* levels of apoptotic cells after UV-irradiation. These data show that Msh6, but not the downstream MMR factor Mlh1, is required for UV-induced cell cycle arrest and apoptosis.

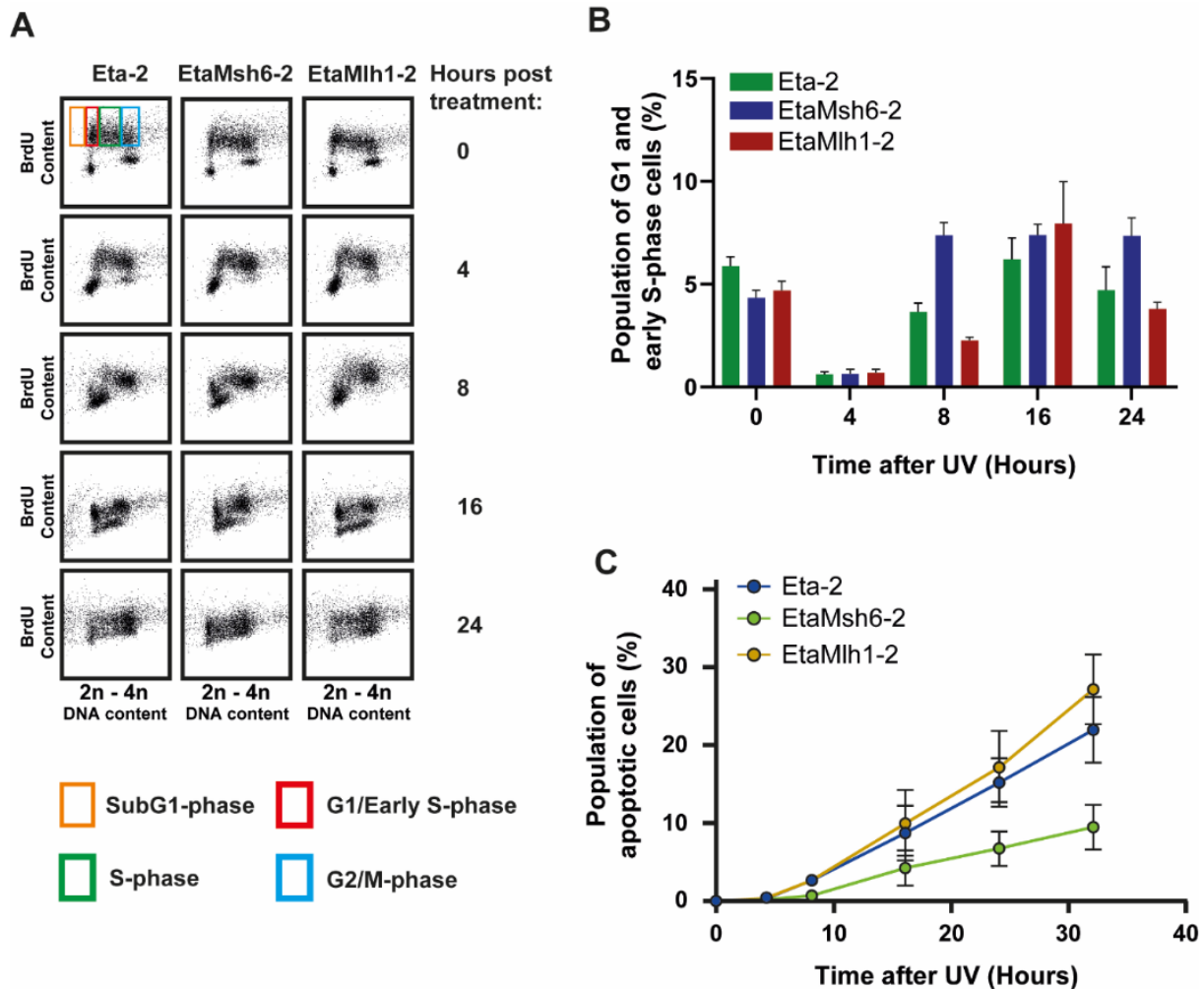


Figure 4: UV-induced cell cycle arrest and apoptosis is dependent on Msh6

A: Cell cycle profiles of Pol η , Pol η Msh6 and Pol η Mlh1-deficient cells pulse labeled with BRDU and analyzed for DNA content and BrdU content by FACS 0-24 hours after UV-exposure. B: Quantification of the mean population of G1/Early S-phase cells relative to the total amount of cells in Pol η , Pol η Msh6 and Pol η Mlh1-deficient cells, 0-24 hours post-UV. C: Quantification of the mean population of sub-G1 cells relative to the total amount of cells, 0-32 hours post-UV irradiation in Pol η , Pol η Msh6 and Pol η Mlh1-deficient conditions. Error bars, SEM.

UV-induced checkpoint responses and ssDNA formation in Pol Eta-deficient cells rely on Msh6

So far Msh6 and Mlh1 control UV mutagenesis in Pol η -deficient cells to a similar extent, while differently affecting cell cycle progression. To better understand this difference, we focused on the studying the signaling cascade that underlies the UV-induced cell cycle delay. This signaling cascade is thought to start with ssDNA formation and subsequent activation of the signaling kinase Atr/Atrp that phosphorylates a multitude of effector proteins including Chk1, which (i) controls late replication origin firing and elongation of DNA replication, (ii) stabilizes stalled replication forks and (iii) activates the G2/M checkpoint (26). Similarly, Kap-1 is phosphorylated by Atr, however, Kap-1

is also phosphorylated by Atm and as such can be used as a read-out for DSB formation (33-35). Thus, phosphorylation of Chk1 (pChk1) and of Kap-1 (pKap-1) was studied using western blot on whole protein cell extracts obtained from cells, 0, 2, 4 and 8 hours after UV exposure. Nearly undetectable levels of pChk1 and pKap-1 were observed immediately after UV exposure in *Polh*-deficient cells and MMR-deficient derivatives thereof (Fig. 5A, Fig. S4A). However, at later timepoints, levels of pChk1 and pKap-1 were clearly increased in *Polh*-deficient cells and this was significantly higher than the increase in the WT parental cell line. The *Msh6* single knock-out cell line nearly abolished all UV-induced signaling, whereas the *PolhMsh6* double knockout showed lower signaling than the *Polh* single knock-out but still markedly higher than the WT cell line (Figure S4A). In contrast, knock-out of *Mlh1* in *Polh*-deficient cells did not affect the ability to activate UV damage signaling, since these cells displayed similar levels and kinetics of pChk1 and pKap1 formation as found in *Polh*-deficient cells after UV exposure (Fig. 5A). To test the possibility that UV damage signaling in *Polh*-deficient and *PolhMlh1* doubly deficient cells relies on the formation of ssDNA rather than on 'direct signaling' by binding of MutS α to compound lesions, *i.e.* a 'mismatched' nucleotide opposite a photolesion (36), we investigated the formation of chromatin-bound Rpa, which coats ssDNA to provide stability. Western blotting revealed that *Polh*, *PolhMsh6* and *PolhMlh1*-deficient cells display similarly low levels of chromatin-bound Rpa, 0 hours after irradiation with UV (Fig. 5B, Fig. S4B). Four hours post-UV, an increase in chromatin-bound Rpa levels was seen in *Polh*-deficient cells, indicating the formation of ssDNA tracts. Additional knock-out of *Msh6* in *Polh*-deficient cells resulted in a strong decrease of chromatin-bound Rpa levels, almost as low as the 0-hour controls. *PolhMlh1* double knockout cells showed an amount of chromatin bound Rpa similar to the *Polh* single knockout.

Msh6-dependent formation of ssDNA gaps opposite CPDs

Previous work indicated that Msh6 may promote excision of misincorporations opposite pyrimidine-pyrimidone (6-4) photoproducts ((6-4)PPs), thus reducing UV-induced mutagenesis. Moreover, using cells that were genetically modified to repair specifically CPDs, it was found that Msh6 not only may act on misincorporations opposite (6-4)PPs but also opposite CPDs (17). Since *Polh*-deficient cells display enhanced UV mutagenesis (Fig. 3A-B, S1A-B), likely due to more error-prone TLS opposite CPDs, we argued that *Polh*-deficient cells and MMR-defective derivatives thereof might be a suitable model to determine gap formation opposite CPDs as a read-out for MMR-dependent excision opposite CPDs. Using an antibody that specifically recognizes CPDs in ssDNA conformation (ssCPD), we performed immunostaining under non-denaturing conditions of UV-exposed *Polh*, *PolhMsh6* and *PolhMlh1*-deficient cells. These cells were pulse labeled with EdU to identify replicating cells at the time of UV treatment (EdU+ cells). Four hours after UV treatment, a significant increase in ssCPD formation was observed for *Polh*-deficient cells and *PolhMlh1*-deficient cells, whereas a less pronounced increase is seen in *PolhMsh6* double knockout cells (Fig. 5D-E).

Taken together these data show that the formation of ssDNA in Polh deficient cells following UV exposure is dependent on Msh6, but not on Mlh1. In line with these data, UV-induced checkpoint signaling, cell cycle arrest and apoptosis all depend on the formation of ssDNA and thus requires Msh6 to be present. In contrast, not only Msh6 suppresses UV-induced mutagenesis, but Mlh1 as well. The synergistic relationship between Polh and Msh6 suggests MMR dependent post-replicative control of TLS-errors and argues against a recruitment model. However, this control may be independent of long-lived ssDNA tracts as Mlh1 similarly suppresses TLS-associated mutagenesis but does not influence ssDNA gap formation.

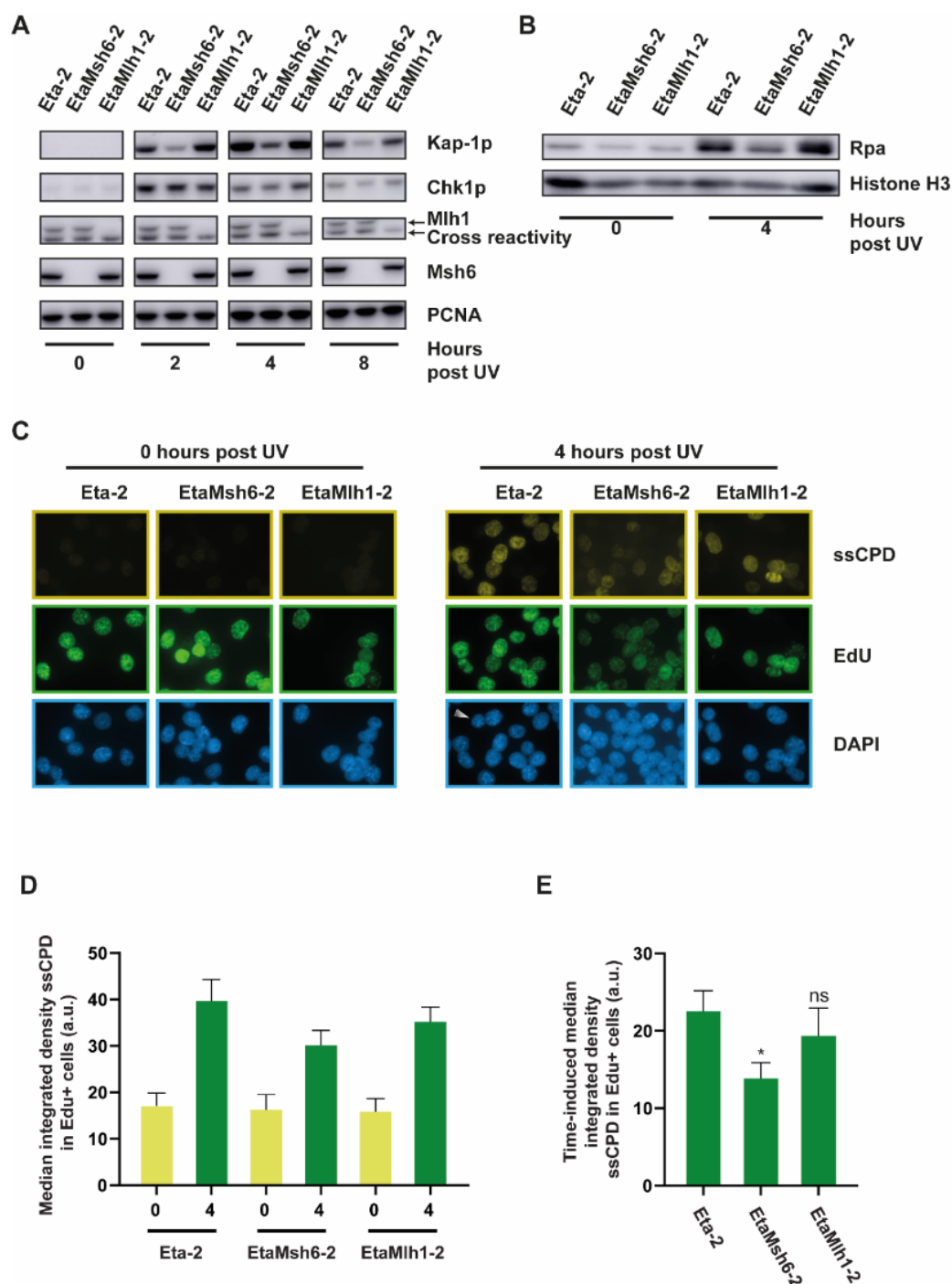


Figure 5: UV-induced checkpoint activation and ssDNA formation relies on Msh6

A: Western blots of DNA damage signaling proteins in whole protein lysates of *Polη*, *PolηMsh6* and *PolηMlh1*-deficient cells, 0-8 hours after UV exposure. Phosphorylated Chk1 and Kap-1 were assessed as a measure for ss/dsDNA break associated signaling, respectively. Antibodies against *Mlh1* and *Msh6* were used to confirm knock-out of the gene. PCNA was used as a loading control. B: Western blots of fractions of chromatin-bound proteins from *Polη*, *PolηMsh6* and *PolηMlh1* cells isolated 0 and 4 hours after UV-irradiation. Rpa was measured as a read-out for the formation of ssDNA. Histone H3 was used as a loading control. C: Immunostaining for CPD in single stranded DNA formation (ssCPD), 0- and 4-hours post-UV. EdU labeling was used to detect replicating cells at the time of UV exposure. DAPI was used as a nuclear stain. D: Quantification of the median integrated density of ssCPD in EdU+ cells. Data shown is relative to the 0 hours timepoint for each cell line. E: Normalization of the integrated density of ssCPD by subtracting the 0 hours timepoints. Error bars, IQ range; *, $P \leq 0,05$; Mann-Whitney U-test of groups compared to *Polη* single mutant.

Discussion

Translesion synthesis is a DNA damage tolerance pathway that replicates damaged DNA, thereby quenching DNA damage signaling and preventing cell death at the cost of increased mutagenesis (16). Several studies indicate that DNA damage-associated mutagenesis and DNA damage signaling can be controlled by MMR (24). Two hypotheses that may explain how MMR controls DNA damage responses are (i) the recruitment of the relatively error-free Pol η by MMR (19-21) or (ii) the removal of TLS-mis-incorporations known as post-TLS repair (17). Here we show that both Msh6 and Mlh1 are required to suppress UV-induced mutagenesis in *Polh*-deficient cells. Moreover, we provide evidence that presence of Msh6, but not Mlh1, further increases UV-induced ssDNA gap formation, DNA damage signaling, cell cycle responses and apoptosis in *Polh*-deficient cells. Finally, we reveal that UV-induced gap formation occurs opposite CPDs, extending previously published findings of Msh6-dependent UV-induced gap formation opposite 6-4PP (17).

We show that *Polh*-deficient mouse ES cells display increased UV-induced mutagenesis when compared to wild type cells, confirming previously published data (37). Pol η replicates UV-damage efficiently and relatively error-free, due to its ability to incorporate predominantly Adenines opposite both Thymidines of a T-T CPD, the most frequently induced UV lesion by UV-C light (38, 39). In the absence of Pol η , more error-prone TLS polymerases, such as polymerases kappa, iota and Rev1/Pol zeta are required for the bypass of persistent UV lesions, resulting in increased UV-induced mutagenesis and an altered spectrum of UV-induced mutations (6, 40-42). The UV mutability of *Polh*-deficient mouse ES cells is strongly affected by an additional defect in *Msh6*, since UV-induced mutagenesis in *PolhMsh6* double knockout cells is greater than the sum of UV-induced mutagenesis found in the *Polh* and *Msh6* single knockout cells. Previously, we have shown that Msh6-dependent suppression of UV-induced mutagenesis is attenuated in *Rev-1* hypomorphic cells which are hypomutable for UV (17, 43). Together, these results strongly suggest that suppression of UV-induced mutagenesis by Msh6 depends on the extent of mutagenic TLS.

Mammalian cells replicate UV-damaged DNA discontinuously by generating relatively short DNA fragments that are later converted into mature DNA molecules. This conversion is delayed in *Polh*-deficient cells (40, 44, 45). When a replicative DNA polymerase encounters a CPD, it is thought that a DNA polymerase switch is induced to enable Pol η to bypass this lesion 'on the fly', i.e. direct bypass without repriming of the replication machinery downstream of the lesion (46). This mode of lesion bypass prevents the accumulation of ssDNA and overactivation of Atr/Chk1 signaling (47). Indeed, our data indicate that *Polh*-deficiency results in the generation of ssDNA tracts as shown by enhanced formation of chromatin-bound Rpa (Fig. S5) and increased levels of unreplicated CPDs in ssDNA configuration (data not shown, unable to visualize in wild-type cells), following UV exposure. This is accompanied with strongly activated UV damage signaling, confirming previous studies (47). The ssDNA tracts found in *Polh*-deficient cells might be caused by stalled forks or repriming of the

replication machinery downstream of the photolesion. This work indicates that the formation of ssDNA tracts in *Polh*-deficient cells depends partially on Msh6, since approximately half of the ssDNA gaps that are located opposite CPDs depend on Msh6 (Fig. 5C-E). In line with this, we also found that UV-induced Atr/Chk1 signaling in *Polh*-deficient cells partially depends on Msh6. Together with the important role of Msh6 in suppressing UV-induced mutagenesis in *Polh*-deficient cells, these data suggest that UV-induced Chk1 signaling relies to a certain extent on Msh6-dependent excision of TLS mis-incorporations opposite CPDs. However, prolonged stalling of replication complexes or collapsing replication forks that occur independently of Msh6 may also contribute to Chk1 activation.

In contrast to Chk1 signaling, phosphorylation of Kap1^{S824} in *Polh*-deficient cells strongly relies on Msh6. Since Kap1 phosphorylation at S824 is reported to be mediated not only by ATM and DNA-PK, but also by ATR, the formation of Kap1^{S824p} likely depends on the generation of ssDNA tracts (ATR) and of DSBs (ATM/DNA-PK) (34, 35). Consequently, Kap1 phosphorylation is associated with the activation of cell cycle arrests and apoptosis (48), which is reflected by similar responses of *Polh*-deficient cells exposed to UV (Fig. 4, S2-3). These responses are strongly reduced in *Polh*-deficient cells with an additional deficiency in Msh6. Since the formation of Kap1^{S824p} is associated with the repair of DSBs (49-51), our data may indicate that the formation of UV-induced DSBs in *Polh*-deficient cells largely depend on Msh6. Moreover, ssDNA tracts generated by Msh6-mediated excision of TLS-errors may have a higher tendency of converting into DSBs, since the more prominent role Msh6 in phosphorylating Kap1 than in the phosphorylation of Chk1.

The present study indicates that, in contrast to Msh6, Mlh1 does not play a role in the UV-induced DNA damage response in *Polh*-deficient mouse ES cells, as shown by Mlh1-independent induction of UV damage signaling, cell cycle arrests and apoptosis. However, both Mlh1 and Msh6 suppress UV-induced mutagenesis to a similar extent. These data are in line with comparable experiments performed in mouse ES cells deficient for nucleotide excision repair (NER) (Chapter 3). Based on mutation spectra analyses, these experiments suggested that both Mlh1 and Msh6 act at 'mis-incorporations' opposite UV damage at dipyrimidine sites, although their identity remains to be determined. As stated previously, Msh6 may act on 'mis-incorporations' opposite CPDs and (6-4)PPs based on immunostainings of ssCPDs (Fig. 5C-E) and ss(6-4)PPs as well as on UV mutagenesis experiments using cells that express a CPD photolyase (17). In contrast to Msh6, Mlh1 does not seem to act on 'mis-incorporations' opposite CPDs, since similar levels of ssCPDs were found in *Polh*-deficient mouse ES cells irrespective of Mlh1 status (Fig. 5C-E). It might be that during lagging strand synthesis a proportion of 'mis-incorporations' opposite CPDs are removed in an Mlh1-independent manner, as non-ligated Okazaki fragments still contain a 5' end that allows Mlh1-independent repair. We noted that, following UV exposure, Mlh1-deficient mouse ES cells display enhanced levels of chromatin-bound Rpa (Fig. 5B, S4B), which may reflect stabilized replication forks at UV lesions. Recruitment of Rpa to stalled replication forks will deplete the pool of free Rpa, which may render cells defective in

NER (52, 53). In mouse cells, NER deficiency will affect predominantly the removal of (6-4)PPs, since CPDs are only repaired from transcribed strands of active genes (54, 55). Thus, although Msh6 and Mlh1 suppress UV-induced mutagenesis in *Polh*-deficient mouse ES cells to the same extent, they might achieve this by acting at 'mis-incorporations' opposite different subsets of UV lesions. It may be interesting to study the effect of Mlh1-deficiency in *Polh*-deficient cells on the formation of ssDNA gaps opposite 6-4PP.

In this study we aimed to investigate two seemingly conflicting models for the suppression of UV-induced mutagenesis by MMR proteins (Fig. 1), namely the recruitment model (19-21) and the post-TLS repair model (17). The former proposes a role for Msh6 by recruiting TLS polymerases to the replication-blocking UV lesion (epistasis), while the latter suggests a post-replicative role for MMR proteins due to the removal of erroneous TLS-incorporations (synergism). Apparently, our *Hprt* mutant frequency experiments in *Polh*-deficient cells with an additional *Msh6* or *Mlh1* deficiency contradicts the recruitment model, since defects in both TLS and MMR led to mutagenic synergism rather than epistasis. Yet, the post-TLS repair model cannot fully explain the present data, since loss of Mlh1 did not result in lower levels of UV-induced ssDNA which would be expected if Mlh1 is required to promote excision of TLS-induced 'mis-incorporations' across UV lesions. Instead, the two models may be interwoven (Fig. 6): In certain instances downstream repriming of the replication machinery causes UV-lesions to be bypassed erroneously by post-replicative gap filling by Rev1/Pol ζ (45). The resulting TLS-errors may be recognized and subsequently removed by the joined action of MutS α and MutL α , thus reducing mutagenesis. Following the removal, MutS α is essential to recruit relatively error-free polymerases, such as Pol η , or in its absence Polk or Poli, thereby preventing the accumulation of ssDNA and accompanied damage responses.

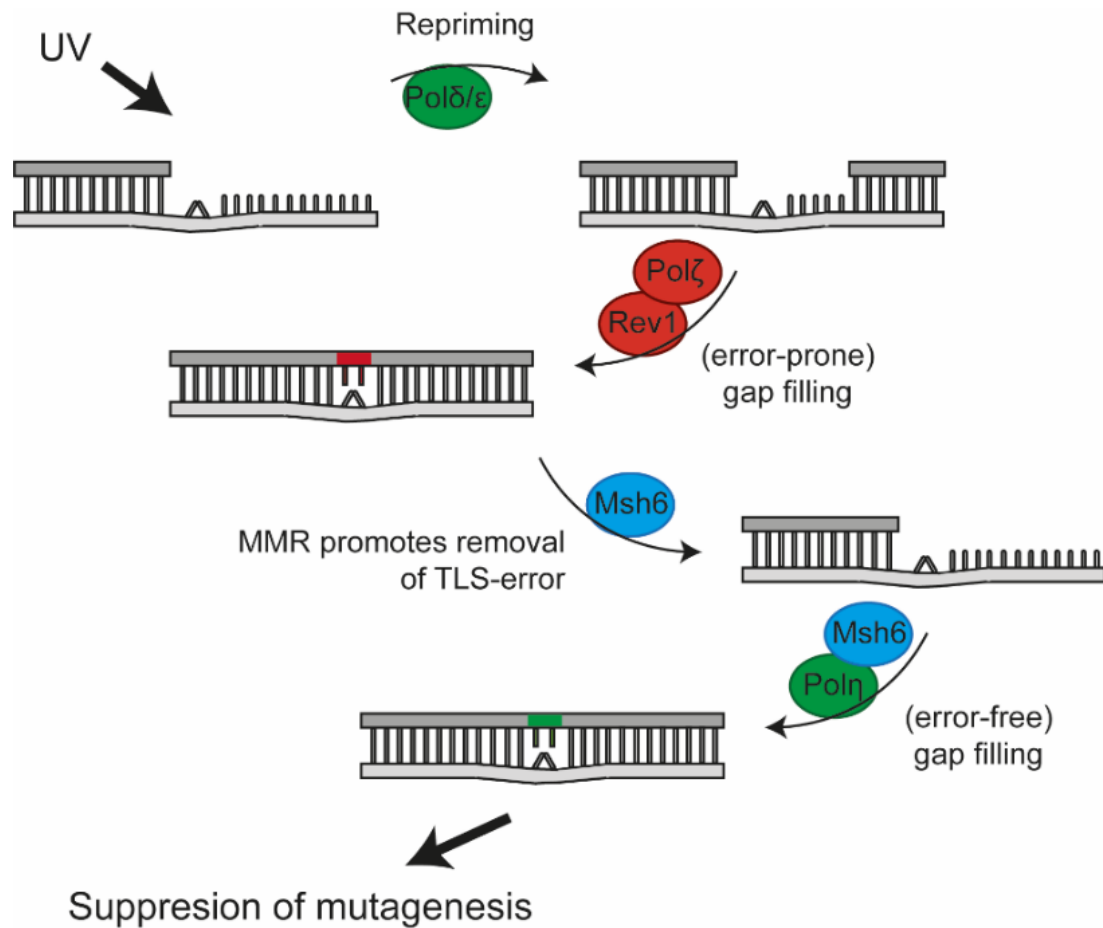


Figure 6: An integrated model where Msh6 both removes TLS errors and promotes error-free TLS

DNA exposed to UV forms intrastrand crosslinks that may sometimes cause the replication machinery to reprime downstream of the damage. For gap-filling Rev1/Pol ζ may be recruited which can cause TLS-errors. Msh6 is able to recognize these misincorporations opposite the damage and subsequently removes it. Afterwards Msh6 recruits the relatively error-free Pol η to bypass the damage, thus suppressing UV-induced mutagenesis.

Supplemental Materials

Supplemental materials table 1: guideRNA sequences used for CRISPR

<i>CRISPR table</i>	<i>gRNA 1</i>	<i>gRNA 2</i>	<i>Target</i>	<i>Protein/mRNA</i>	<i>6tG selected</i>
<i>Polη</i>	<i>CGCTGTCATTGGAC TCCGCC</i>	<i>GAATCATGTTGAC TGCTCAA</i>	<i>Entire gene</i>	<i>No mRNA</i>	<i>No</i>
<i>Msh6</i>	<i>GGAGCCTCCGCTT CCCGCGG</i>	<i>CCTTTGATGGAAC GTTCAT</i>	<i>Exon 1-2</i>	<i>No protein</i>	<i>Yes</i>
<i>Mlh1</i>	<i>CTCCTCCGGAGTG AGCACGG</i>	<i>ATGCCAGATTGGA CCAATA</i>	<i>Entire gene</i>	<i>No protein</i>	<i>Yes</i>

Supplemental materials table 2: PCR primer sequences

<i>Target:</i>	<i>Forward</i>	<i>Reverse</i>
<i>Polη external</i>	<i>AGCGTGAGTCCCAGAAGTTG</i>	<i>AGCTTGCCAGGTTCTTTATACCT</i>
<i>Polη internal</i>	<i>CAATGGGCTGGCAAGCTTTT</i>	<i>CAGGAGCCGCAGAGTTACTA</i>

Supplemental Figures

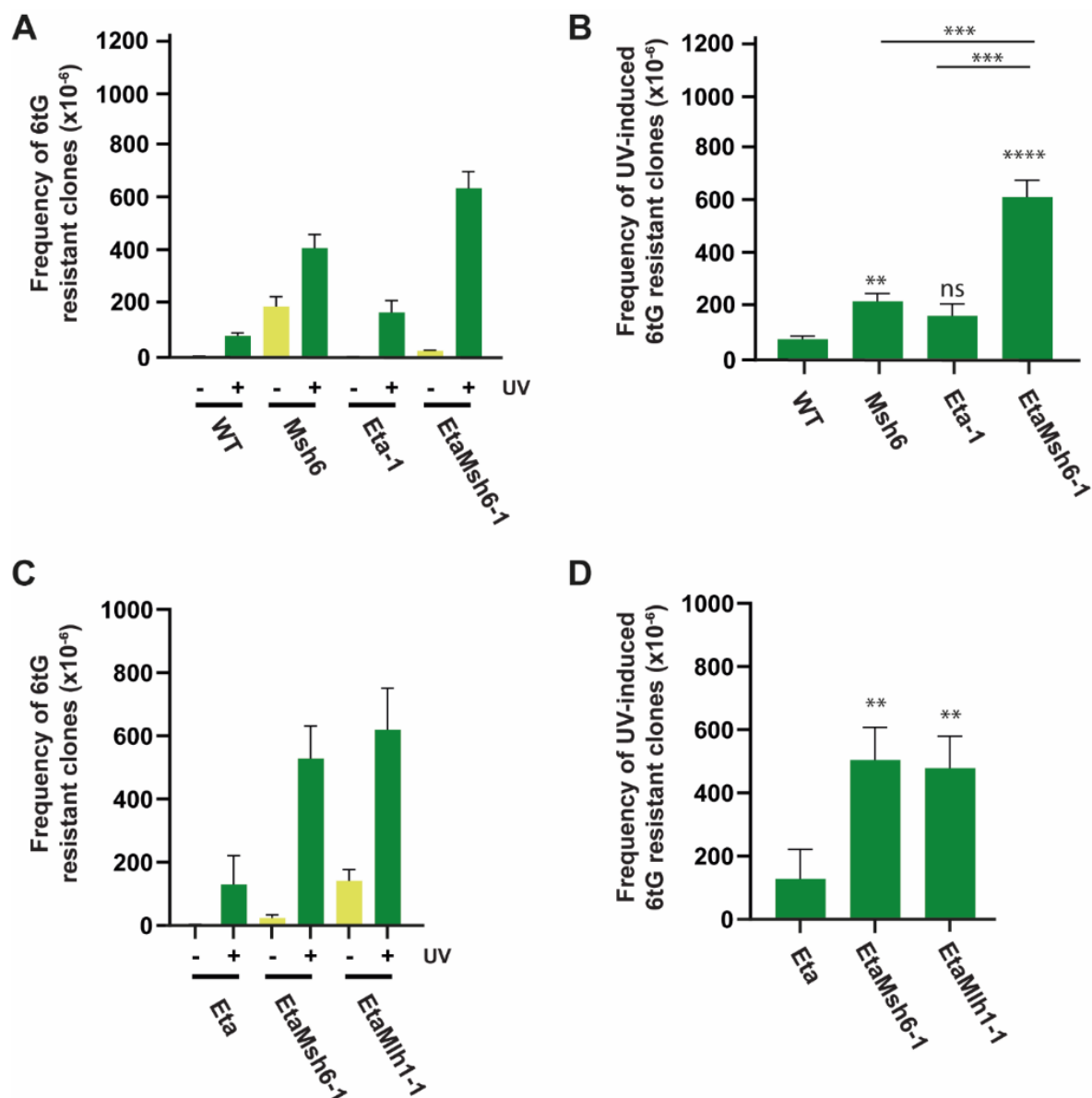
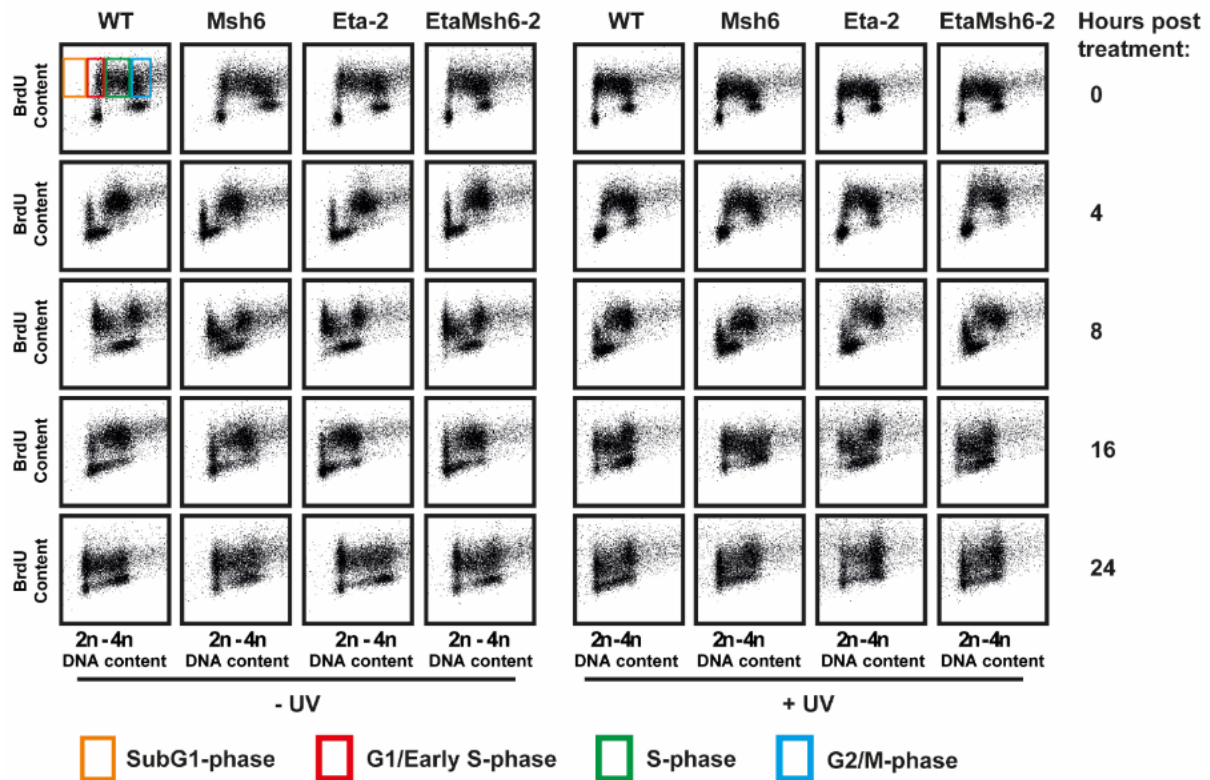


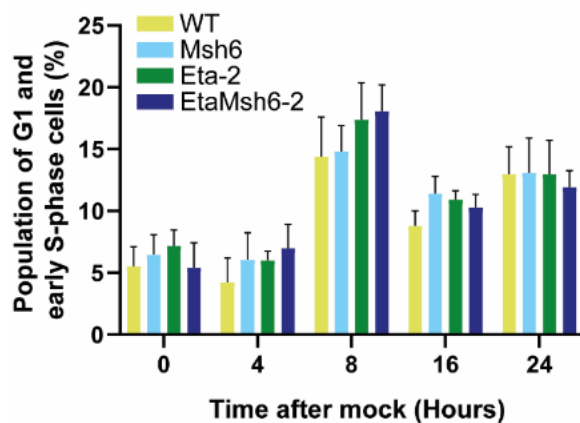
Figure S1: UV-induced mutagenesis in independent cell lines

A: Frequencies of 6tG resistant clones per million clone forming cells in mock treated and UV-exposed WT, *Msh6*, *Polη* and *PolηMsh6*-deficient cells. B: Frequencies of UV-induced 6tG resistant clones in WT, *Msh6*, *Polη* and *PolηMsh6*-deficient cells shown per million clone forming cells. C: Quantification of mutagenesis in mock and UV-conditions in *Polη*, *PolηMsh6* and *PolηMlh1*-deficient cells per million cells. D: UV-induced mutagenesis in *Polη*, *PolηMsh6* and *PolηMlh1*-deficient cells per million cells. Independent cell lines were used to validate the findings of Fig. 1. Error bars, SEM; **, $P \leq 0,01$; ****, $P \leq 0,0001$; ns, non-significant; student T-test of groups compared to WT or *Polη* single mutant or between *EtaMsh6* and single mutants.

A



B



C

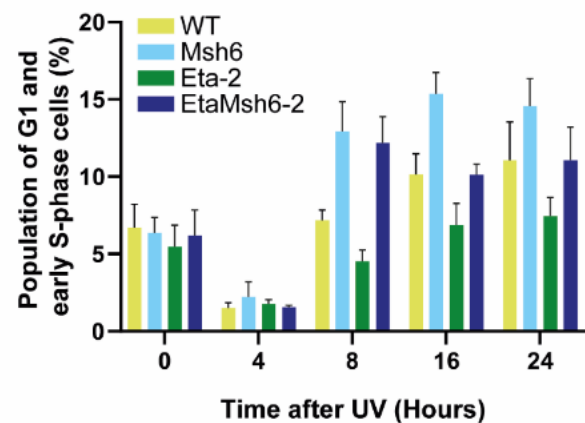


Figure S2: Cell cycle progression in WT, Msh6, Eta and EtaMsh6-deficient lines.

A: Cell cycle plots were obtained using FACS with a BRDU-FITC pulse-labeling for replicating cells plotted against total DNA content by staining with propidium iodide depicting a population of WT, Msh6, Polη and PolηMsh6-deficient cells 0-24 hours after mock or UV-exposure. B: Quantification of the mean population of G1/Early S-phase cells relative to the total amount of cells in WT, Msh6, Polη and PolηMsh6-deficient cells 0-24 hours post mock treatment. C: Quantification of the mean population of G1/Early S-phase cells relative to the total amount of cells in WT, Msh6, Polη and PolηMsh6-deficient cells 0-24 hours post mock treatment. Error bars, SEM.

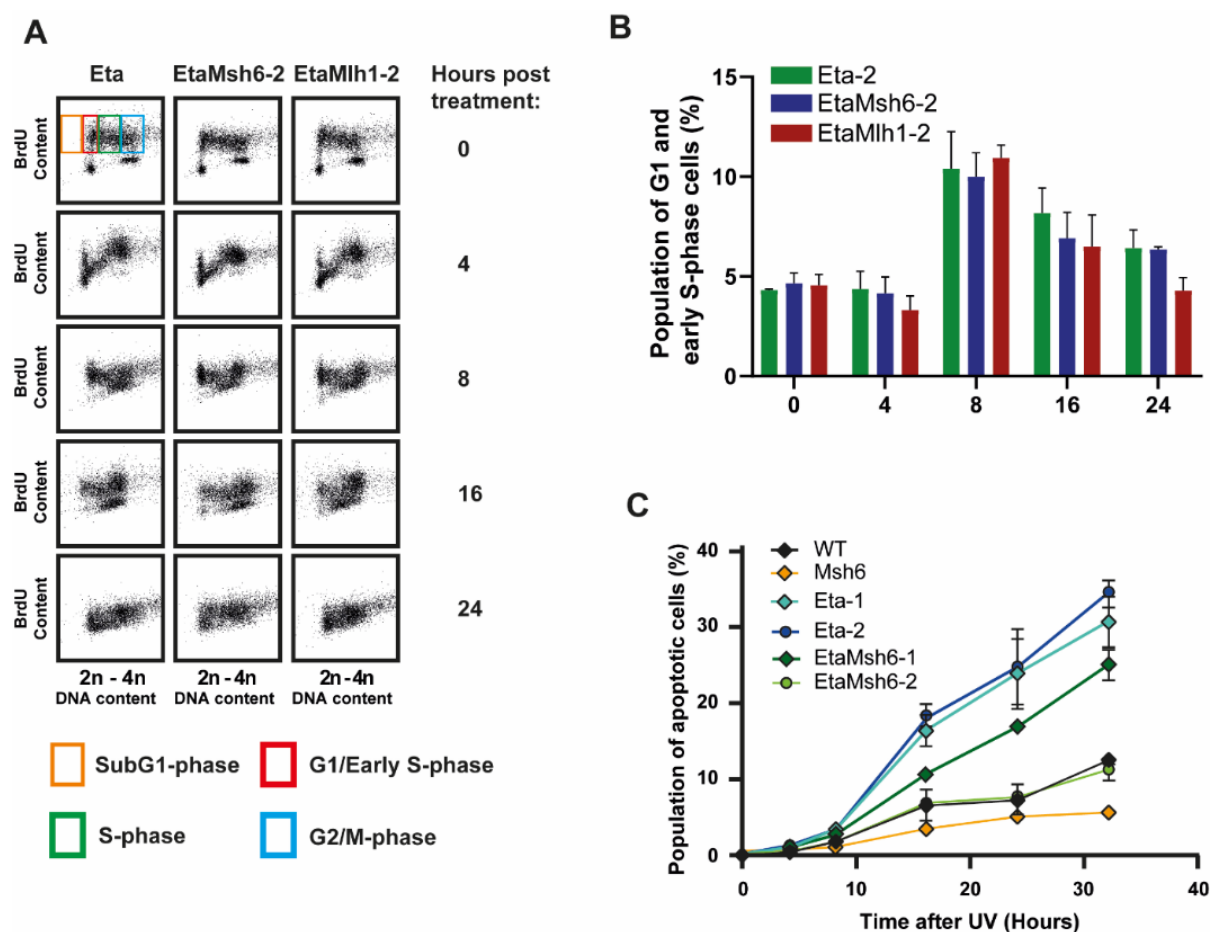


Figure S3: Cell cycle progression and apoptosis in WT, Msh6, Eta, EtaMsh6 and EtaMlh1-deficient lines. A: Cell cycle plots were obtained using FACS with a BRDU-FITC pulse-labeling for replicating cells plotted against total DNA content by staining with propidium iodide depicting a population of *Polη*, *PolηMsh6*, and *PolηMlh1*-deficient cells 0-24 hours after mock treatment. B: Quantification of the mean population of G1/Early S-phase cells relative to the total amount of cells in *Polη*, *PolηMsh6*, and *PolηMlh1*-deficient cells 0-24 hours post mock treatment. C: Quantification of the mean population of sub-G1 cells relative to the total amount of cells 0-32 hours post-UV irradiation in WT, *Msh6*, *Polη* and *PolηMsh6*-deficient conditions. Multiple lines tested to validate the results of figure 4. Error bars, SEM.

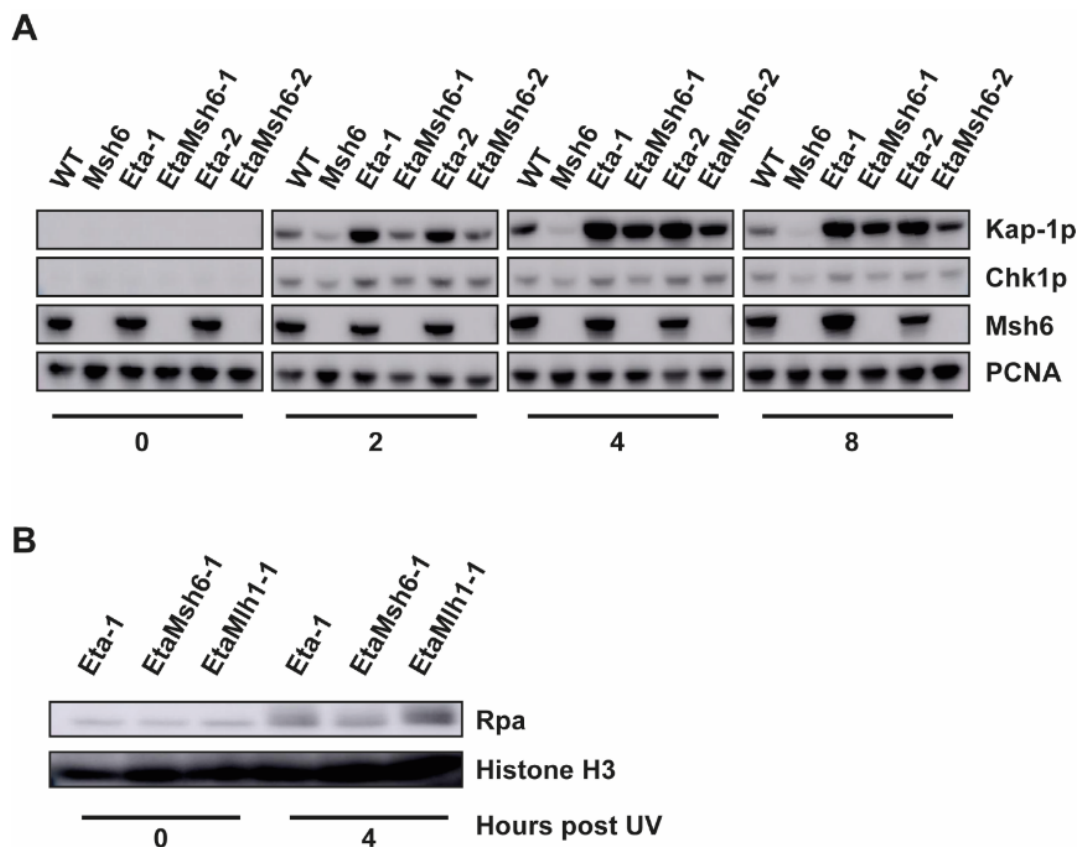


Figure S4: UV-induced DNA damage signaling and ssDNA formation in independent cell lines

A: Western blots of whole cell lysates using antibodies against phosphorylated Chk1 and Kap1. Phosphorylated Chk1 and Kap-1 were assessed as a measure for ss/dsDNA break associated signaling, respectively. Antibodies against *Msh6* were used to confirm knock-out of the gene. PCNA was used as a loading control. B: Chromatin-bound fractions of *Polη*, *PolηMsh6* and *PolηMlh1* cells were collected 0 and 4 hours after UV-irradiation. The amount of Rpa was measured as a read-out for the formation of ssDNA across the genome. Histone H3 was used as a loading control. Independent cell lines were used to validate the findings of Fig. 5.

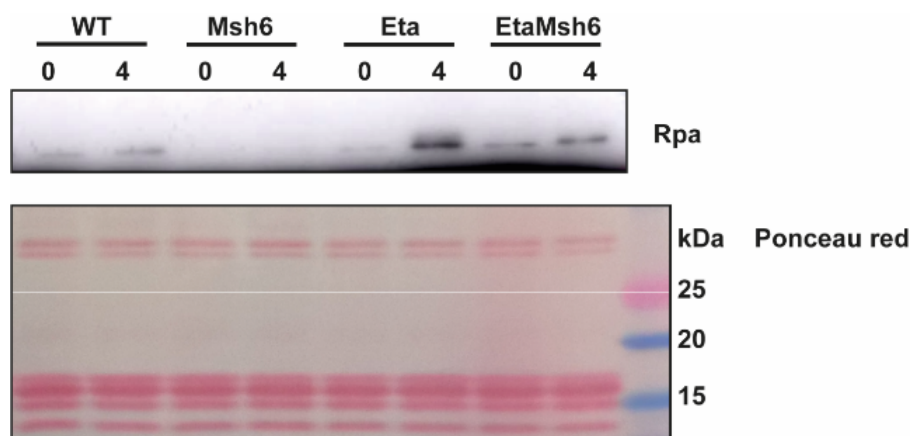


Figure S5: UV-induced ssDNA formation in independent *Eta* and *EtaMsh6*-deficient cell lines

Chromatin-bound fractions of WT, *Msh6*, *Polη* and *PolηMsh6* cells were collected 0 and 4 hours after UV-irradiation. Chromatin-bound Rpa as a read-out for the formation of ssDNA across the genome was determined by Western blot. Equal loading of proteins was verified by Ponceau red staining of the membrane after blotting.

References

1. Sale JE, Lehmann AR, Woodgate R. Y-family DNA polymerases and their role in tolerance of cellular DNA damage. *Nature reviews Molecular cell biology*. 2012;13(3):141-52.
2. Yang W, Gao Y. Translesion and Repair DNA Polymerases: Diverse Structure and Mechanism. *Annual Review of Biochemistry*. 2018;87(1):239-61.
3. Biertumpfel C, Zhao Y, Kondo Y, Ramon-Maiques S, Gregory M, Lee JY, et al. Structure and mechanism of human DNA polymerase η . *Nature*. 2010;465(7301):1044-8.
4. Masutani C, Kusumoto R, Yamada A, Dohmae N, Yokoi M, Yuasa M, et al. The XPV (xeroderma pigmentosum variant) gene encodes human DNA polymerase η . *Nature*. 1999;399(6737):700-4.
5. Gratchev A, Strein P, Utikal J, Sergij G. Molecular genetics of Xeroderma pigmentosum variant. *Experimental dermatology*. 2003;12(5):529-36.
6. Yoon JH, Prakash L, Prakash S. Highly error-free role of DNA polymerase η in the replicative bypass of UV-induced pyrimidine dimers in mouse and human cells. *Proc Natl Acad Sci U S A*. 2009;106(43):18219-24.
7. Yang W, Gao Y. Translesion and Repair DNA Polymerases: Diverse Structure and Mechanism. *Annu Rev Biochem*. 2018;87:239-61.
8. Bebenek K, Matsuda T, Masutani C, Hanaoka F, Kunkel TA. Proofreading of DNA polymerase η -dependent replication errors. *J Biol Chem*. 2001;276(4):2317-20.
9. Washington MT, Johnson RE, Prakash S, Prakash L. Mismatch extension ability of yeast and human DNA polymerase η . *J Biol Chem*. 2001;276(3):2263-6.
10. Zhang Y, Yuan F, Presnell SR, Tian K, Gao Y, Tomkinson AE, et al. Reconstitution of 5'-Directed Human Mismatch Repair in a Purified System. *Cell*. 2005;122(5):693-705.
11. Wyatt MD, Pittman DL. Methylating Agents and DNA Repair Responses: Methylated Bases and Sources of Strand Breaks. *Chemical Research in Toxicology*. 2006;19(12):1580-94.
12. Fu D, Calvo JA, Samson LD. Balancing repair and tolerance of DNA damage caused by alkylating agents. *Nature Reviews Cancer*. 2012;12(2):104-20.
13. Mazurek A, Berardini M, Fishel R. Activation of Human MutS Homologs by 8-Oxo-guanine DNA Damage. *Journal of Biological Chemistry*. 2002;277(10):8260-6.
14. Borgdorff V, Pauw B, van Hees-Stuivenberg S, de Wind N. DNA mismatch repair mediates protection from mutagenesis induced by short-wave ultraviolet light. *DNA Repair (Amst)*. 2006;5(11):1364-72.
15. Ijsselstein R, van Hees S, Drost M, Jansen JG, de Wind N. Induction of mismatch repair deficiency, compromised DNA damage signaling and compound hypermutagenesis by a dietary mutagen in a cell-based model for Lynch Syndrome. *Carcinogenesis*. 2021.
16. Friedberg EC. Suffering in silence: the tolerance of DNA damage. *Nature Reviews Molecular Cell Biology*. 2005;6(12):943-53.
17. Tsaalbi-Shitlik A, Ferras C, Pauw B, Hendriks G, Temviriyankul P, Carlee L, et al. Excision of translesion synthesis errors orchestrates responses to helix-distorting DNA lesions. *J Cell Biol*. 2015;209(1):33-46.
18. Wang H, Lawrence CW, Li GM, Hays JB. Specific binding of human MSH2.MSH6 mismatch-repair protein heterodimers to DNA incorporating thymine- or uracil-containing UV light photoproducts opposite mismatched bases. *J Biol Chem*. 1999;274(24):16894-900.
19. Zlatanou A, Despras E, Braz-Petta T, Boubakour-Azzouz I, Pouvelle C, Grant, et al. The hMsh2-hMsh6 Complex Acts in Concert with Monoubiquitinated PCNA and Pol η in Response to Oxidative DNA Damage in Human Cells. *Molecular Cell*. 2011;43(4):649-62.
20. Peña-Díaz J, Bregenhorn S, Ghodgaonkar M, Follonier C, Artola-Borán M, Castor D, et al. Noncanonical Mismatch Repair as a Source of Genomic Instability in Human Cells. *Molecular Cell*. 2012;47(5):669-80.
21. Lv L, Wang F, Ma X, Yang Y, Wang Z, Liu H, et al. Mismatch repair protein MSH2 regulates translesion DNA synthesis following exposure of cells to UV radiation. *Nucleic Acids Res*. 2013;41(22):10312-22.
22. Zhang J, Zhao X, Liu L, Li HD, Gu L, Castrillon DH, et al. The mismatch recognition protein MutS α promotes nascent strand degradation at stalled replication forks. *Proc Natl Acad Sci U S A*. 2022;119(40):e2201738119.
23. Guan J, Lu C, Jin Q, Lu H, Chen X, Tian L, et al. MLH1 Deficiency-Triggered DNA Hyperexcision by Exonuclease 1 Activates the cGAS-STING Pathway. *Cancer Cell*. 2021;39(1):109-21 e5.
24. Ijsselstein R, Jansen JG, De Wind N. DNA mismatch repair-dependent DNA damage responses and cancer. *DNA Repair*. 2020;93:102923.
25. Stojic L, Brun R, Jiricny J. Mismatch repair and DNA damage signalling. *DNA Repair (Amst)*. 2004;3(8-9):1091-101.
26. Smith J, Tho LM, Xu N, Gillespie DA. The ATM-Chk2 and ATR-Chk1 pathways in DNA damage signaling and cancer. *Advances in cancer research*. 2010;108:73-112.
27. Hooper M, Hardy K, Handyside A, Hunter S, Monk M. HPRT-deficient (Lesch-Nyhan) mouse embryos derived from germline colonization by cultured cells. *Nature*. 1987;326(6110):292-5.
28. Van Gool IC, Rayner E, Osse EM, Nout RA, Creutzberg CL, Tomlinson IPM, et al. Adjuvant Treatment for POLE Proofreading Domain-Mutant Cancers: Sensitivity to Radiotherapy, Chemotherapy, and Nucleoside Analogues. *Clin Cancer Res*. 2018;24(13):3197-203.
29. Borgdorff V, van Hees-Stuivenberg S, Meijers CM, de Wind N. Spontaneous and mutagen-induced loss of DNA mismatch repair in Msh2-heterozygous mammalian cells. *Mutat Res*. 2005;574(1-2):50-7.

30. Nara K, Nagashima F, Yasui A. Highly elevated ultraviolet-induced mutation frequency in isolated Chinese hamster cell lines defective in nucleotide excision repair and mismatch repair proteins. *Cancer Res.* 2001;61(1):50-2.
31. Glaab WE, Skopek TR. Cytotoxic and mutagenic response of mismatch repair-defective human cancer cells exposed to a food-associated heterocyclic amine. *Carcinogenesis.* 1999;20(3):391-4.
32. Sary A, Kannouche P, Lehmann AR, Sarasin A. Role of DNA polymerase η in the UV mutation spectrum in human cells. *J Biol Chem.* 2003;278(21):18767-75.
33. Ziv Y, Bielopolski D, Galanty Y, Lukas C, Taya Y, Schultz DC, et al. Chromatin relaxation in response to DNA double-strand breaks is modulated by a novel ATM- and KAP-1 dependent pathway. *Nature cell biology.* 2006;8(8):870-6.
34. White DE, Negorev D, Peng H, Ivanov AV, Maul GG, Rauscher FJ, 3rd. KAP1, a novel substrate for PIKK family members, colocalizes with numerous damage response factors at DNA lesions. *Cancer Res.* 2006;66(24):11594-9.
35. Hu C, Zhang S, Gao X, Gao X, Xu X, Lv Y, et al. Roles of Kruppel-associated Box (KRAB)-associated Co-repressor KAP1 Ser-473 Phosphorylation in DNA Damage Response. *J Biol Chem.* 2012;287(23):18937-52.
36. Wang Y, Qin J. MSH2 and ATR form a signaling module and regulate two branches of the damage response to DNA methylation. *Proc Natl Acad Sci U S A.* 2003;100(26):15387-92.
37. Maher VM, Ouellette LM, Curren RD, McCormick JJ. Frequency of ultraviolet light-induced mutations is higher in xeroderma pigmentosum variant cells than in normal human cells. *Nature.* 1976;261(5561):593-5.
38. Johnson RE, Prakash S, Prakash L. Efficient bypass of a thymine-thymine dimer by yeast DNA polymerase, Pol η . *Science.* 1999;283(5404):1001-4.
39. Washington MT, Johnson RE, Prakash S, Prakash L. Accuracy of thymine-thymine dimer bypass by *Saccharomyces cerevisiae* DNA polymerase η . *Proc Natl Acad Sci U S A.* 2000;97(7):3094-9.
40. Jansen JG, Temviriyankul P, Wit N, Delbos F, Reynaud CA, Jacobs H, et al. Redundancy of mammalian Y family DNA polymerases in cellular responses to genomic DNA lesions induced by ultraviolet light. *Nucleic Acids Res.* 2014;42(17):11071-82.
41. Ziv O, Geacintov N, Nakajima S, Yasui A, Livneh Z. DNA polymerase ζ cooperates with polymerases κ and ι in translesion DNA synthesis across pyrimidine photodimers in cells from XPV patients. *Proc Natl Acad Sci U S A.* 2009;106(28):11552-7.
42. Wang Y, Woodgate R, McManus TP, Mead S, McCormick JJ, Maher VM. Evidence that in xeroderma pigmentosum variant cells, which lack DNA polymerase η , DNA polymerase ι causes the very high frequency and unique spectrum of UV-induced mutations. *Cancer Res.* 2007;67(7):3018-26.
43. Jansen JG, Tsalbi-Shtylik A, Langerak P, Calleja F, Meijers CM, Jacobs H, et al. The BRCT domain of mammalian Rev1 is involved in regulating DNA translesion synthesis. *Nucleic Acids Res.* 2005;33(1):356-65.
44. Lehmann AR, Kirk-Bell S, Arlett CF, Paterson MC, Lohman PH, de Weerd-Kastelein EA, et al. Xeroderma pigmentosum cells with normal levels of excision repair have a defect in DNA synthesis after UV-irradiation. *Proc Natl Acad Sci U S A.* 1975;72(1):219-23.
45. Temviriyankul P, van Hees-Stuivenberg S, Delbos F, Jacobs H, de Wind N, Jansen JG. Temporally distinct translesion synthesis pathways for ultraviolet light-induced photoproducts in the mammalian genome. *DNA Repair (Amst).* 2012;11(6):550-8.
46. Edmunds CE, Simpson LJ, Sale JE. PCNA ubiquitination and REV1 define temporally distinct mechanisms for controlling translesion synthesis in the avian cell line DT40. *Mol Cell.* 2008;30(4):519-29.
47. Despras E, Daboussi F, Hyrien O, Marheineke K, Kannouche PL. ATR/Chk1 pathway is essential for resumption of DNA synthesis and cell survival in UV-irradiated XP variant cells. *Human molecular genetics.* 2010;19(9):1690-701.
48. Li X, Lee YK, Jeng JC, Yen Y, Schultz DC, Shih HM, et al. Role for KAP1 serine 824 phosphorylation and sumoylation/desumoylation switch in regulating KAP1-mediated transcriptional repression. *J Biol Chem.* 2007;282(50):36177-89.
49. Goodarzi AA, Noon AT, Deckbar D, Ziv Y, Shiloh Y, Lobrich M, et al. ATM signaling facilitates repair of DNA double-strand breaks associated with heterochromatin. *Mol Cell.* 2008;31(2):167-77.
50. Iyengar S, Farnham PJ. KAP1 protein: an enigmatic master regulator of the genome. *J Biol Chem.* 2011;286(30):26267-76.
51. Kuo CY, Li X, Stark JM, Shih HM, Ann DK. RNF4 regulates DNA double-strand break repair in a cell cycle-dependent manner. *Cell cycle.* 2016;15(6):787-98.
52. Tsalbi-Shtylik A, Moser J, Mullenders LH, Jansen JG, de Wind N. Persistently stalled replication forks inhibit nucleotide excision repair in trans by sequestering Replication protein A. *Nucleic Acids Res.* 2014;42(7):4406-13.
53. Auclair Y, Rouget R, Belisle JM, Costantino S, Drobetsky EA. Requirement for functional DNA polymerase η in genome-wide repair of UV-induced DNA damage during S phase. *DNA Repair (Amst).* 2010;9(7):754-64.
54. Ruven HJ, Berg RJ, Seelen CM, Dekkers JA, Lohman PH, Mullenders LH, et al. Ultraviolet-induced cyclobutane pyrimidine dimers are selectively removed from transcriptionally active genes in the epidermis of the hairless mouse. *Cancer Res.* 1993;53(7):1642-5.
55. Mitchell DL. The relative cytotoxicity of (6-4) photoproducts and cyclobutane dimers in mammalian cells. *Photochemistry and photobiology.* 1988;48(1):51-7.





Chapter 5:

Induction of mismatch repair deficiency, compromised DNA damage signaling and compound hypermutagenesis by a dietary mutagen in a cell-based model for Lynch syndrome

Robbert Ijsselsteijn¹, Sandrine van Hees¹,
Mark Drost¹, Jacob G Jansen¹, Niels de Wind¹

¹Department of Human Genetics, Leiden
University Medical Center, Leiden, The
Netherlands.

DOI: 10.1093/carcin/bgab108

Carcinogenesis. 2022 Mar 24;43(2):160-169

Published December 2021



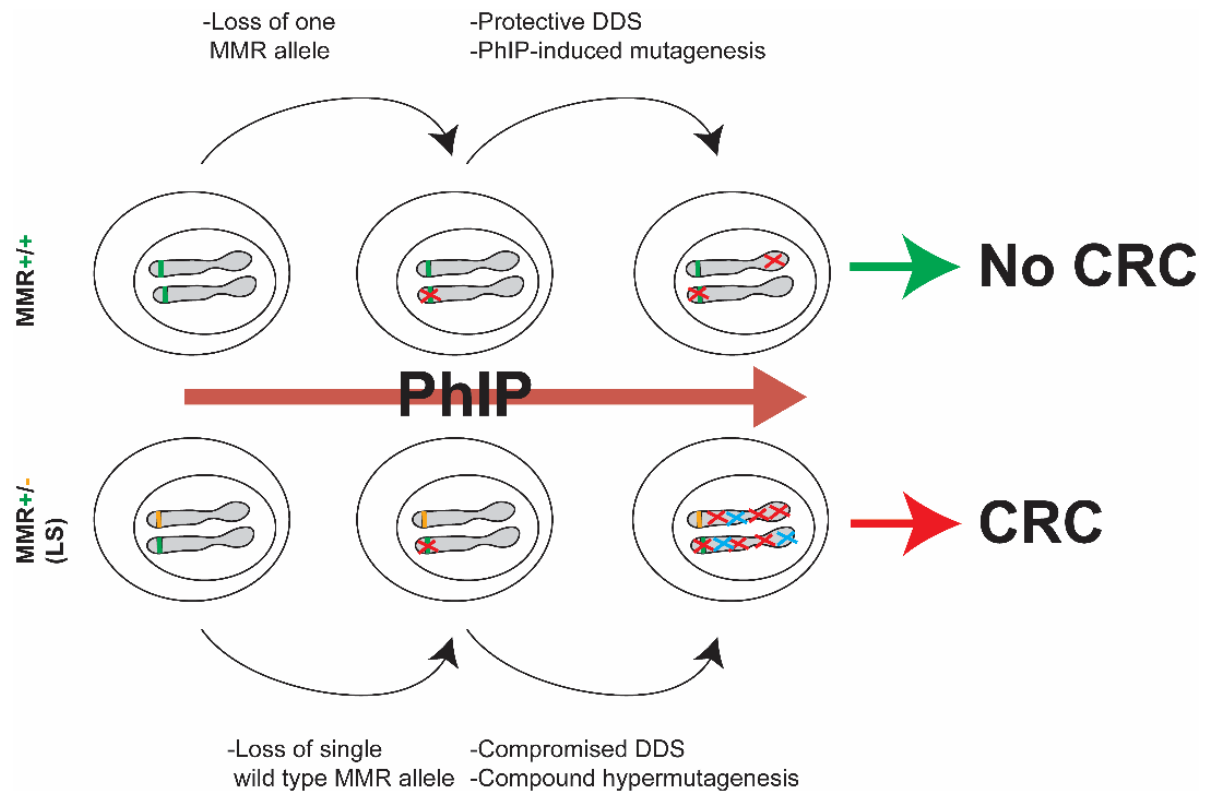
Abstract

The prevalent cancer predisposition Lynch syndrome (LS, OMIM #120435) is caused by an inherited heterozygous defect in any of the four core DNA mismatch repair (MMR) genes *MSH2*, *MSH6*, *MLH1* or *PMS2*. MMR repairs errors by the replicative DNA polymerases in all proliferating tissues. Its deficiency, following somatic loss of the wild type copy, results in a spontaneous mutator phenotype that underlies the rapid development of, predominantly, colorectal cancer (CRC) in LS. Here we have addressed the hypothesis that aberrant responses of intestinal stem cells to diet-derived mutagens may be causally involved in the restricted cancer tropism of LS. To test this we have generated a panel of isogenic mouse embryonic stem (mES) cells with heterozygous or homozygous disruption of multiple MMR genes and investigated their responses to the common dietary mutagen and carcinogen 2-amino-1-methyl-6-phenylimidazo[4,5-b]pyridine (PhIP). Our data reveal that PhIP can inactivate the wild type allele of heterozygous mES cells via the induction of either loss of heterozygosity (LOH) or intragenic mutations. Moreover, while protective DNA damage signaling (DDS) is compromised, PhIP induces more mutations in *Msh2*, *Mlh1*, *Msh6* or *Pms2*-deficient mES cells than in wild type cells. Combined with their spontaneous mutator phenotypes, this results in a compound hypermutator phenotype. Together, these results indicate that dietary mutagens may promote CRC development in LS at multiple levels, providing a rationale for dietary modifications in the management of LS.

Summary

A dietary mutagen induces loss of the wild type allele in mismatch repair gene-heterozygous cells. This results in impaired DNA damage signaling and in compound hypermutagenesis. These findings provide insights into the etiology of colorectal carcinogenesis in Lynch syndrome.

Graphical abstract



Graphical abstract. Proposed roles of dietary mutagens in the etiology of colorectal cancer in Lynch syndrome.

While individuals normally carry two intact alleles of the four MMR genes (top panel, green rectangles), LS patients carry a germ-line defect in one allele of any of these genes (bottom panel, orange cross). The single wild type allele of that gene may inadvertently be lost in stem cells in a colonic crypt, either spontaneously or induced by exposure to an intestinal mutagen, such as PhIP (red cross). This results in compromised DNA damage signaling (DDS) and, possibly, loss of protective cell cycle responses to protracted PhIP exposure. MMR deficiency not only results in a spontaneous mutator phenotype (blue crosses), but also in increased mutability by PhIP (red crosses). The consequent compound hypermutator phenotype may strongly predispose to oncogenic derailment.

Introduction

Colorectal cancer (CRC) is the third most common cancer type world-wide, with the highest incidence in developed countries (1). Many lifestyle factors increase the risk for CRC, including obesity, smoking and consumption of red, processed and cooked meat (2, 3). Ten percent of all CRC has an underlying genetic predisposition. Of these, Lynch syndrome (LS) is the most prevalent (1 in 279 individuals), accounting for 3-5% of all CRCs (4). LS is caused by an inherited heterozygous defect in one of four genes involved in DNA mismatch repair (MMR), *MSH2*, *MSH6*, *MLH1* and *PMS2*. Although LS is inherited in an autosomal dominant fashion, the wild type allele of the germ-line-defective gene must be somatically lost to procure cancer development (5).

Canonical MMR removes misincorporations by DNA polymerases during replication of undamaged DNA. Consequently, loss of MMR is associated with increased spontaneous mutagenesis. Since MMR operates in all proliferating tissues, the cause of the restricted cancer tropism of LS thus far is unclear. Interestingly, MMR-deficient cells also display aberrant mutagenic and cell cycle responses to agents that induce helix-distorting DNA lesions (6, 7). This appears paradoxical since helix-distorting DNA lesions do not induce base-base mismatches, the natural substrates for MMR. Data on responses of MMR-deficient cells to UV light have suggested the involvement of MMR proteins in the removal of misincorporations induced by DNA translesion synthesis polymerases opposite helix-distorting photolesions. This prevents their mutagenicity, while simultaneously inducing protective DNA damage signaling (DDS) (7).

Heterocyclic amines are an important class of dietary genotoxic compounds, present in meat cooked at high temperatures, that induce helix-distorting nucleotide lesions. The most abundant of these heterocyclic amines is 2-amino-1-methyl-6-phenylimidazo[4,5-b]pyridine (PhIP). Indeed, dietary intake of PhIP is positively correlated with CRC (3). Here we have investigated the hypothesis that PhIP (or similar diet-derived genotoxic compounds) may direct the development of CRC in LS at three levels (see the Graphical Abstract and Ref. 7): (i) by inducing loss of the wild type allele of the heterozygous MMR gene, (ii) by compromised PhIP-induced DDS in these MMR-deficient cells and (iii) by enhanced mutability of these cells by the mutagen. To address this tripartite hypothesis we have used mouse embryonic stem (mES) cells, heterozygous for *Msh2* or *Mlh1*, as models for colonic crypt stem cells in LS patients. We show that PhIP indeed induces loss of heterozygosity (LOH) or deleterious nucleotide substitutions, insertions, and deletions at the wild type allele. Consequently, in the resulting *Msh2*-deficient mES cells, PhIP-induced DDS is reduced. Moreover, in *Msh2*-, *Msh6*-, *Mlh1*-, or *Pms2*-deficient cells, the mutagenicity of PhIP is much higher than in wild type cells. This exacerbated mutability is additive to the spontaneous mutator phenotype of MMR-deficient cells, resulting in a compound hypermutator phenotype. These results provide support for the hypothesis that intestinal mutagens are involved at multiple levels in the development of CRC in LS and suggest the feasibility of dietary intervention as a preventive approach.

Materials and Methods

Cell culture and cell lines generated and used and their validation

mES cells were cultured on sub-lethally irradiated mouse embryonic fibroblast (MEF) feeder cells in complete medium consisting of KO DMEM supplemented with 10% fetal calf serum, 1% glutamax, 1% non-essential amino acids, 1mM pyruvate, 100U penicillin/100µg streptomycin, 0.1mM β -mercapto-ethanol and leukemia inhibitory factor. During experiments complete medium was mixed in a 1:1 ratio with Buffalo rat liver cell-conditioned medium (called 50/50) to allow for growth on gelatin-coated culture dishes.

Wild type mES cell line E14 (8) was used as a parental line to all cell lines generated and used in this study (Fig. 1A). The line was karyotyped before constructing derivative mutant mES cell lines. The *Msh2* and *Mlh1*-heterozygous mES cell lines used to study spontaneous and PhIP-induced loss of MMR (called *Msh2*-Bsd and *Mlh1*-Bsd) contain a *Blasticidin* selection cassette at the *Kcnk12* (3' of the wild type *Msh2* allele) or *Lirfip2* (3' of the wild type *Mlh1* allele) locus, respectively, introduced by classical gene targeting. The heterozygous *Msh2* and *Mlh1* deletions in these lines were generated using CRISPR/Cas9 (Supplemental Methods Table 1; manuscript in preparation). Briefly, two complementary oligonucleotides with BbsI overhangs were annealed and ligated into CRISPR-Cas9 vector PX330-Puro. mES cells were transfected with these plasmids using Lipofectamine 2000. After transfection, the introduction of a hemizygous deletion at *Msh2* or *Mlh1* was confirmed by allele-specific PCR (see below). The presence of the *Blasticidin* cassette linked to the wild type *Mlh1* or *Msh2* allele was validated by the appearance of clones, surviving 4 hours incubation with 20µM 6-thioguanine (6tG) (Sigma-Aldrich), a hallmark of MMR deficiency (9). All these spontaneous 6tG-tolerant clones had fortuitously lost the wild type allele by LOH and also the (linked) *Blasticidin* cassette, which resulted in re-acquired *Blasticidin* sensitivity (Supplemental Fig. S2 and the Results section).

The *Msh2*-1, *Msh6*-1 (10), *Mlh1*-1, *Mlh1*-s, *Pms2*-1 and *Pms2*-s knock-out cell lines (Fig. 1A) have been generated using CRISPR-Cas9, as described above (Supplemental Methods Table 1). After transfection, the cells were selected for tolerance of 6tG to more easily acquire MMR-deficient clones, with the exception of the *Pms2*-deficient lines that were identified by allele-specific PCR. Their phenotype was confirmed by Western blotting (Fig. 1B and Supplemental data only for review).

The *Msh2*-s, the *Msh6*-s and *Msh3* knock-out cell lines have been generated by conventional gene targeting (Fig. 1A) and have been published before by us (11, 12). All lines were validated prior to use by allele-specific PCR, as described (11, 12). In addition, the *Msh2*-1 and *Msh6*-1 lines were validated prior to use by testing for 6tG tolerance and by performing Western blotting (see below; Fig. 1B and Supplemental data only for review). Cell lines were validated regularly by Western blotting and/or allele-specific PCR. An overview of the origin or construction of all cell lines generated and used here and their validation/authentication are provided in Supplemental methods Table 2.

Western blotting

SDS-PAGE was performed using 4-12% Criterion XT Bis-Tris gels (Bio-rad). Proteins were transferred onto Protran 0,45µM nitrocellulose membranes (GE Healthcare). Membranes were blocked for one hour using blocking reagent (Rockland) diluted with PBS-0.1% Tween. Then, membranes were incubated overnight at 4°C with primary antibodies, diluted in Rockland-PBS-Tween. Membranes were washed using PBS-Tween (0.1%) and incubated with secondary anti-mouse and anti-rabbit HRP (ThermoFisher Scientific), depending on primary antibody isotype, diluted 1:50000 in Rockland-PBS-Tween for one hour at room temperature. Bands were visualized using Amersham ECL select western blotting detection reagent (GE Healthcare). Antibodies used: Anti-Msh2: mouse mAb (FE11, Calbiochem), anti-Msh6 (Abcam, clone 44), anti-Mlh1: rabbit polyclonal (C-20, Santa Cruz Biotechnology), anti-Pms2: mouse Ab (A16-4, BD Pharmingen), anti-Kap-1^p (Bethyl, polyclonal A300-767A), anti-Chk1^p (clone 133D3, Cell Signaling Technology) and anti-PCNA (clone PC10 clone, Santa Cruz).

Induction of MMR deficiency by PhIP

A day prior to treatment with PhIP (Apollo Scientific) or vehicle (dimethyl sulfoxide, DMSO), 5×10^6 wild type cells or cells heterozygous for *Msh2* or *Mlh1* were seeded in 50/50 medium in gelatin-coated p90 dishes. Cells were washed twice with PBS and then incubated with 18µM PhIP or DMSO in complete medium in the presence of 10% S9 rat liver extract (Trinova), for three hours. Subsequently, the cells were washed twice with PBS and 50/50 medium was added with or without 5U/ml of Blasticidin (Invivogen). After two days, the cells were trypsinized and cultured for two passages to allow fixation of mutations. Afterwards, 2×10^6 cells were seeded in a p90 dish and the next day the cells were incubated for four hours with 20µM 6tG in 50/50 medium to select for MMR-deficient clones. After one week, this selection was repeated and the cells were grown for another week in 50/50 medium to allow for the formation of clones. Clones were either stained with methylene blue and counted or picked and grown until confluency in 96-wells plates in the presence of 5mM Hypoxanthine, 20µM Aminopterin, 0.8µM Thymidine (HAT) (50x diluted, Thermo Fisher Scientific) to select against the inadvertent loss of *Hprt* that also yields 6tG resistance (albeit to a much higher concentration).

Amplification of *Msh2* and *Mlh1* for LOH analysis

Individual clones were lysed using 50µl DirectPCR lysis reagent (Viagen) with 8U/ml proteinase K (Invitrogen) for one hour at 37°C. After heat inactivation of proteinase K (5 min at 85°C), one µl of cell lysate was used in a multiplex PCR with three oligonucleotide primers to analyze LOH (Supplemental Figure 1, Supplemental Methods Table 3). LOH at *Msh2* was analyzed using primers 1 (0.4µM) and 2 (0.08µM) to amplify the intact *Msh2* allele and primers 1 and 3 (0.32µM) to amplify the disrupted *Msh2* allele. For *Mlh1*, primers 4 (0.4µM) and 5 (0.16µM) amplify the intact *Mlh1* allele and 4 (0.4µM) and 6 (0.4µM) the disrupted *Mlh1* allele. PCR products were created using GoTaq polymerase (0.625U, Promega) in GoTaq buffer with dNTPs (0,5mM) and primers during 35 cycles, each consisting of 30 sec at 95°C, 30 sec at 57°C (*Msh2*)

or 61°C (*Mlh1*) and two minutes at 72°C. A final extension was performed for 10 minutes at 72°C. DNA products were examined using 3% agarose gel electrophoresis.

Production and sequence analysis of *Msh2* and *Mlh1* cDNA

RNA was isolated from individual clones lysed in 100µl TRIzol reagent (Invitrogen) according to the manufacturer's protocol (TRIzol, Invitrogen). The RNA pellet was dissolved in 15µl TE buffer and cDNA was generated using Maxima H Minus Reverse Transcriptase (Thermo Fisher Scientific). First, a final volume of 14.5µl containing one µl RNA, OligodT primer (6.9µM, Thermo Fisher Scientific) and dNTPs (0.69mM, Invitrogen) was incubated for five minutes at 65°C. Then, 1µl Maxima Polymerase (200U/µl), 4µl of 5x Maxima buffer and 20U of RNasin (Promega) were added to a final volume of 20µl. cDNA synthesis was performed for one hour at 57°C. After heat inactivation at 85°C for five minutes, cDNA was PCR amplified using GoTaq polymerase as described above with an annealing temperature of 55°C and primers 7/8 and 9/10 for the 5' and 3' end of *Msh2* and primers 11/12 and 13/14 for both ends of *Mlh1*. PCR products were analyzed using 2% agarose gel electrophoresis. PCR products were purified using a QIAquick PCR purification kit (Qiagen) following manufacturer's protocol and eluted in a final volume of 20µl deionized H₂O. Five µl of purified PCR product was used for Sanger sequencing using 1,25µM of primer 8/10/12/15 for the 5' and 3' end of *Msh2* and *Mlh1*, respectively. Sequences were analyzed using ContigExpress from VectorNTI Suite 9. Primer sequences are listed in Supplemental Methods table 3.

Analysis of pathogenicity of PhIP-induced *Msh2* and *Mlh1* mutations

To analyze whether PhIP-induced mutations in MMR heterozygous mES cells reflect pathogenic mutations in humans, we used a combination of an *in silico* analysis (13), databases used for the classification of human MMR variants (ClinVar (14), InSiGHT (15) and COSMIC (16)), and two functional assays (CIMRA (17, 18) and reverse diagnosis catalogues ((19, 20), manuscript in preparation). For *in silico* analyses a probability of pathogenicity of less than 0.1 and more than 0.9 were used for classification as likely pathogenic or benign, respectively (13). Insertions/deletions that caused frameshifts were also classified as pathogenic, while in frame insertion/deletions are categorized as unknown.

Analysis of PhIP-induced toxicity and DDS

mES cells were seeded at a density of 5×10^4 cells per well of a 6 wells plate, one day before treatment with a dose-range of 0 to $25 \mu\text{M}$ PhIP, as described above. Cells were grown in 50/50 medium for 4 days post-treatment. The number of surviving cells was counted using a Beckman coulter counter.

The induction of DDS by PhIP was assessed as follows: one day prior to treatment with $18 \mu\text{M}$ PhIP or vehicle for one hour, 1×10^6 wild type and *Msh2*-deficient cells were seeded per well of a 6 wells plate. PhIP/vehicle treatment was performed as described above. After two washes of PBS, cells were grown for another two hours (PhIP) or five hours (PhIP or vehicle) in 50/50 medium before lysates were made in Laemmli sample buffer, gel electrophoresis and W blotting, as described above.

Determination of *Hprt*-mutant frequencies

mES cells were grown in HAT-supplemented 50/50 medium for six days to eliminate pre-existing *Hprt*-mutant cells. Then, 5×10^6 cells were seeded in p90 dishes, one day prior to PhIP or mock treatment. PhIP ($18 \mu\text{M}$) or mock treatment was performed as described above. Next, 5×10^6 cells were seeded in gelatin-coated p90 dishes and grown for six days in 50/50 medium to allow fixation of mutations. Next, 2×10^6 cells were grown 50/50 medium supplemented with 6tG ($30 \mu\text{M}$) to select *Hprt* deficient clones. In parallel, 3x250 cells were seeded in 50/50 medium in p60 dishes to determine cloning efficiencies. After 7-10 days, clones were stained with methylene blue and the *Hprt*-mutant frequency was calculated by determining the number of 6tG-resistant clones divided by the total number of clone-forming cells seeded in 6tG containing medium.

Next-generation sequencing of *Hprt*-mutant clones

Approximately 400 6tG-resistant clones from PhIP-treated wild type and *Msh2*-deficient mES cell cultures and 400 6tG-resistant clones from mock treated *Msh2* deficient ES cells were used for Next Generation Sequencing (NGS). Per experimental condition clones were pooled and cells were lysed with 1,6ml TRIzol reagent for total RNA isolation. A baseline wild type sequence was established from 8×10^6 cells, corresponding to the total number of cells of 400 6tG-resistant clones. *Hprt* cDNA was generated using Maxima Reverse Transcriptase (ThermoFisher Scientific) and *Hprt*-specific oligonucleotide primer 21. PCR products for NGS were generated in a two-step procedure. First, three separate PCRs were performed using primer combinations 16/17, 18/19 and 20/21 to amplify three overlapping amplicons of the *Hprt* cDNA. The reaction mixture of 40 μl consisted of Phusion High-Fidelity DNA polymerase (0.4U) (Thermo Fisher Scientific), Phusion polymerase reaction buffer, dNTPs ($0.4 \mu\text{M}$), Forward primer ($0.5 \mu\text{M}$), Reverse primer ($0.5 \mu\text{M}$) and two μl cDNA. Using a thermocycler, PCR products were generated by incubating the reaction mixture for two minutes at 95°C , followed by 15 seconds at 95°C , 30 seconds at 57°C and one minute 72°C for 25 cycles, and a final elongation step of 72°C for five minutes. PCR products were purified using AMPure XP beads (Beckman Coulter) following manufacturer's protocol and eluted in 20 μl deionized H_2O . Subsequently, another Phusion PCR was

performed as previously described with the exception of cycling for 8 PCR cycles instead of 25. For this PCR, forward (22-25) and reverse (26-29) primers were used with unique barcodes for each condition (Supplemental Methods table 3). Following purification using AMPure beads, the size of each PCR products was assessed using a Qiaxcel Advanced System (Qiagen). Finally, 50ng pooled PCR products was sequenced using Illumina Paired-End sequencing (GenomeScan).

Analysis of spectra of PhIP-induced mutations in the *Hprt* coding region

To detect alterations in cDNA the paired-end data was first filtered to contain exclusively high-quality reads. Thus, only reads with a maximum error probability of 0.05 were kept. Paired-end reads were merged using Flash (21) and mapped to the *Hprt* reference sequence using in-house software (van Schendel *et al.* manuscript in preparation). Additional filtering was applied to ensure each read started and ended with the primer combinations used (see above). Finally, each mapped read was compared to the reference *Hprt* sequence and annotated into wild type (no difference compared to reference), single nucleotide substitution, multi nucleotide substitution, deletion or insertion. To identify unique mutations from background noise we considered mutations to be real if the allele frequency was > 0.001 .

Results

An isogenic set of MMR gene-disrupted mES cells

mES cells are primary, diploid and display strong DNA damage responses, thus providing good models for intestinal stem cells in LS patients. We have previously described the *Msh2*-s, *Msh6*-1 and *Msh6*-s lines (10-12).

Since the mutator phenotype conferred by MMR deficiency predisposes to genetic drift, we decided to also use independently constructed isogenic mES cell lines, each carrying a targeted disruption of both alleles of one of the four genes MMR (Fig. 1A). These cell lines were generated using CRISPR-Cas9, as described in the Materials and Methods section, resulting in cell lines called *Msh2*-1, *Mlh1*-1, *Mlh1*-s, *Pms2*-1 and *Pms2*-s (Fig. 1B). As models for MMR gene-heterozygous colonic stem cells in LS patients, we employed recently generated mES cell lines, heterozygous for *Msh2* or for *Mlh1*. In these cells, the wild type *Msh2* or *Mlh1* allele was flanked by a *Blasticidin* resistance cassette (M. Drost et al, in preparation; Fig. 2A). This *Blasticidin* resistance cassette enables us to distinguish between clones that have lost the wild type allele by an intragenic mutation, since these retain the linked cassette, and clones that have undergone LOH, which results in concomitant loss of *Blasticidin* resistance. Thus, these cells allow to sensitively investigate the mechanistic basis of loss of the wild type allele in MMR gene-heterozygous cells.

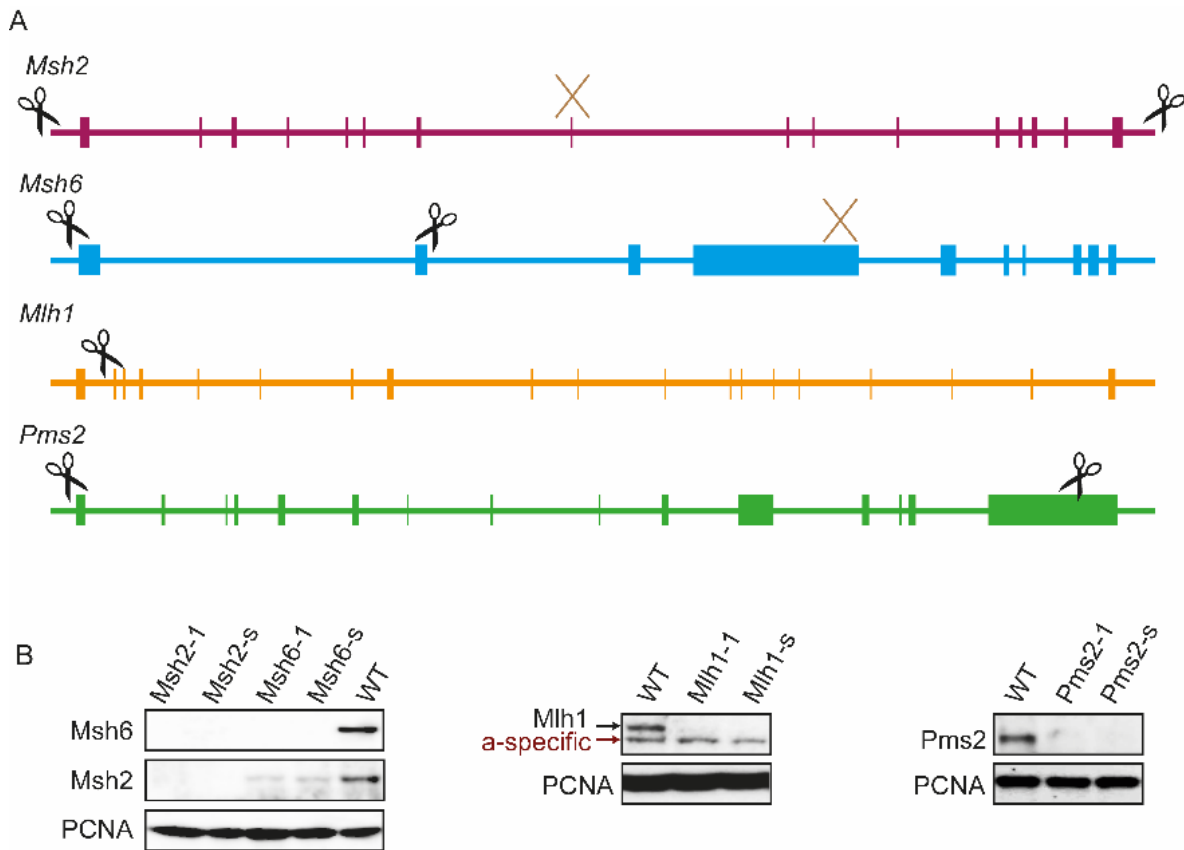


Figure 1. canonical MMR gene alleles used in this study.

(A) Graphical representation of the four core MMR genes. Vertical bars represent exons. Locations where guide RNAs directed a CRISPR-Cas9-induced break are symbolized by scissors. Brown crosses depict the sites where a hygromycin (*Msh2*) or puromycin (*Msh6*) resistance cassette was integrated to disrupt the gene to provide for completely independent knockouts. (B) Western blot validation of mES cell lines deficient for the four MMR genes. PCNA is used as a loading control. The *Msh2* and *Msh6* panels were derived from the same blot. The *Msh2-s* and *Msh6-s* lines were published before (9-11). Of note, some *Msh2* protein is visible in the *Msh6* lines, resulting from dimerization of *Msh2* with *Msh3*.

PhIP induces MMR deficiency in MMR gene-heterozygous cells

Loss of the single functional MMR allele resulting from intragenic mutations or LOH is a prerequisite for the development of CRC in LS individuals (22). We investigated whether, and how, PhIP can induce loss of the wild type allele of a heterozygous MMR gene by using the *Blasticidin* cassette-tagged mES cells, heterozygous for *Msh2* or *Mlh1*. We exploited the acquired tolerance of MMR-deficient cells to the nucleoside analog 6-thioguanine (6tG; Fig. 2A, Supplemental Fig. S1) to select individual clones that have lost the wild type allele in a MMR gene-heterozygous mES cell line (9). 6tG selection was followed by HAT counterselection to eliminate cells that inadvertently have acquired 6tG resistance by an inactivating mutation in the *Hprt* gene.

In the absence of PhIP treatment, selection of *Msh2* or *Mlh1*-heterozygous mES cell lines with 6tG yielded clones, suggesting a significant frequency of spontaneous loss of the wild type allele (Fig. 2B). These clones had all become *Blasticidin*-sensitive, indicating that the wild type allele occasionally is lost by LOH, in the absence of a

mutagen (Fig. 2C). Exposure to PhIP significantly increased the frequency of 6tG-tolerant clones in each heterozygous mES cell line (Fig. 2B-D, Supplemental table S1), suggesting that PhIP induces increased loss of the wild type allele. Of note, the frequency of both spontaneous and PhIP-induced loss of the wild type allele in *Msh2*-heterozygous cells was higher than that in *Mlh1*-heterozygous cells. This was not a consequence of higher 6tG tolerance, and therefore of more efficient selection, of *Msh2*-deficient than of *Mlh1*-deficient cells (Supplemental Fig. S1). Thus, we infer that both spontaneous and PhIP-induced allelic loss is more efficient at *Msh2* than at *Mlh1*. In each cell line, approximately 75% of the PhIP-induced 6tG-tolerant clones were Blasticidin-sensitive, indicating that PhIP predominantly induces LOH at the wild type allele. Nevertheless, about 25% of the PhIP-induced 6tG-tolerant clones had retained Blasticidin resistance, suggesting that in these clones the wild type allele was lost by a PhIP-induced intragenic mutation. To provide more evidence for the latter, we performed an allele-specific multiplex PCR on isolated clones. Indeed, all Blasticidin-resistant clones had retained one allele of *Msh2* or *Mlh1*, whereas the majority of the Blasticidin-unselected clones had undergone complete loss of the wild type allele, confirming the induction of LOH by PhIP (Supplemental Fig. S2).

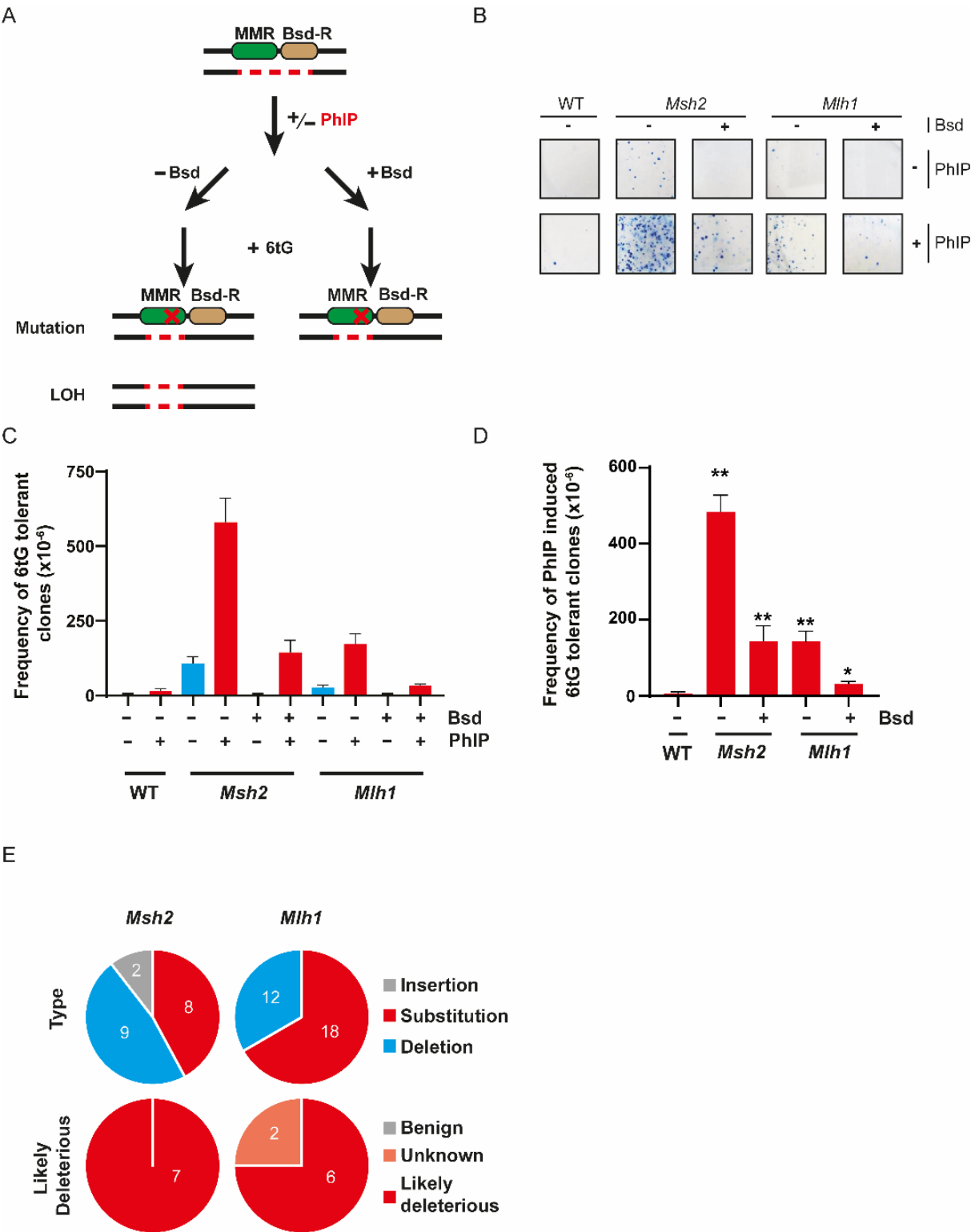


Figure 2. PhIP-induces loss of MMR in MMR gene-heterozygous mES cells.

(A) Selection pipeline to investigate PhIP-induced loss of MMR in MMR gene-heterozygous cells. One allele of either *Msh2* or *Mlh1* was deleted using CRISPR-Cas9 in mES cells (red dashes) whilst the wild type allele was marked at the 3' side with a *Blasticidin* resistance gene (Bsd-R). These cell lines were treated with PhIP to investigate the induction of loss of the wild type allele by either an intragenic mutation (which leads to preservation of Bsd resistance) or by loss of heterozygosity (LOH, which results in concomitant loss of the Bsd-R gene). 6tG was used to select for MMR-deficient cells, with or without concomitant Bsd selection. (B) Wild type, *Msh2* and *Mlh1*-heterozygous cells were exposed to PhIP or vehicle, cultured for a week, and treated with 6tG. Surviving clones were stained with methylene blue. (C) Spontaneous or PhIP-induced MMR-deficient clones (n=3). Half of the plates were also treated with *Blasticidin* (Bsd) to select for intragenic events. Error bars, SEM. (D) PhIP-induced MMR-deficient clones (after subtraction of spontaneous MMR-deficient clones). Error bars, SEM. *, $P \leq 0,05$, **, $P \leq 0,01$; unpaired T-test of groups compared to WT. (E) Upper panel: PhIP-induced mutations in *Msh2* and *Mlh1* cDNA. Lower panel: predicted pathogenicity of PhIP-induced substitution mutations. Number, number of clones.

Inactivation of the wild type allele in MMR-heterozygous cells by PhIP-induced mutations

To confirm that in these 6tG-selected, *Blasticidin*-resistant, clones the wild type *Msh2* or *Mlh1* allele was inactivated by a PhIP-induced intragenic mutation, Sanger sequencing was performed on cDNA. The results showed that for both genes the spectrum of PhIP-induced mutations consisted mostly of single nucleotide substitutions (SNS) and intragenic deletions (Supplemental Tables S2, S3). All deletions started at a guanine and SNS were dominated by G.C > T.A transversions. These data are consistent with the adduct spectrum of PhIP (typically at G nucleotides) and its mutational fingerprint (23, 24). The mutations were distributed over *Msh2* and *Mlh1* (Supplemental Fig. S3). To confirm that the mutations resulted in inactivation of the wild type allele of these genes we used *in silico* analyses, data derived from functional assays, and variant databases. These databases list human variants and thus only mutations of residues conserved between mouse and human DNA could be studied (Supplemental Tables S2, S3). In particular, an SNS was deemed likely pathogenic in case (i) the *in silico* predicted probability of pathogenicity (13) exceeded 0.9, (ii) when MMR functionality was compromised in functional assays such as the biochemical MMR (CIMRA) assay (17, 18), (iii) when the mutation was identified by large-scale genetic screens for deleterious variants ((19, 20), manuscript in preparation), (iv) when identified in LS patients as likely pathogenic or pathogenic in the ClinVar (14) or InSiGHT (15) databases, (v) when listed in the COSMIC cancer somatic database (16). Seven out of 8 and 8 out of 12 SNS in *Msh2* and *Mlh1*, respectively, comprised conserved residues and 7/7 and 6/8, respectively, were predicted pathogenic using the aforementioned analyses (Fig. 2E, Supplemental Tables S2, S3). Only in *Mlh1* two substitutions could not be classified while none of the PhIP-induced substitutions in either gene were predicted to be benign. In addition, almost all intragenic deletions that we identified were either large in size and/or frameshifting and thus also deemed pathogenic. Combined, these data show that MMR gene-heterozygous stem cells lose their wild type MMR gene by spontaneous LOH and, at a high frequency, by PhIP-induced LOH or intragenic mutations.

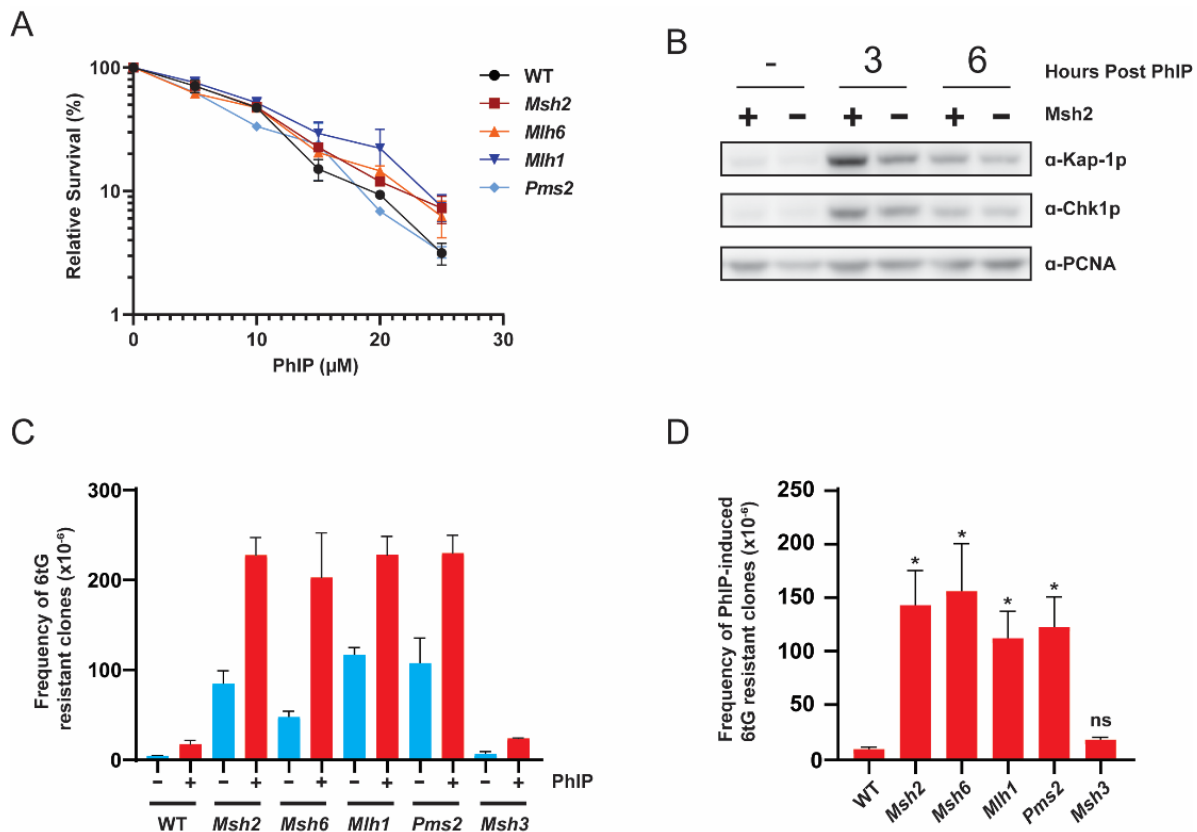


Figure 3. MMR deficient cell lines *Msh2-1*, *Msh6-1*, *Mlh-1* and *Pms2-1* are hypermutable and display reduced DDS following PhIP exposure.

(A) Cell survival after 5 days following exposure to a dose range of PhIP ($n=3$). Error bars, SEM. (B) Western blot probing for the DDS markers phosphorylated Kap-1 and phosphorylated Chk1. PCNA is used as loading control. Representative image of 3 independent experiments. (C) Frequency of *Hprt* mutants in isogenic MMR-proficient and -deficient mES cell lines following mock or PhIP treatment ($n=3$). Error bars, SEM. See Supplemental Fig. S4 for experiments using independent MMR gene mutants. (D) Frequency of *Hprt*-mutant clones induced by PhIP treatment (corrected for spontaneous mutants). Error bars, SEM. *, $P \leq 0.05$, ns, not statistically significant; unpaired T-test comparing groups to wild type.

MMR deficiency leads to impaired DDS in response to PhIP treatment

To test whether the MMR status affects the toxicity of PhIP, survival of isogenic mES cells, defective for any of the four canonical MMR genes, was determined following exposure to a dose range of PhIP. No significant difference in survival between wild type and MMR-deficient lines *Msh2-1*, *Msh6-1*, *Mlh-1* and *Pms2-1* was found (Fig. 3A). Then, we assessed the induction of DDS by PhIP in wild type and *Msh2*-deficient mES cells. This was done by western blotting using antibodies against phosphorylated Chk1 and Kap-1, DDS markers for the formation of single-stranded and double-stranded DNA breaks, respectively. In wild type cells, both markers were increased at 3 and 6 hours post PhIP addition. Deficiency of *Msh2* resulted in a significant mitigation of Kap-1 phosphorylation and a, less pronounced, decrease in Chk1 phosphorylation (Fig. 3B). These data indicate that *Msh2* is involved in provoking DDS induced by PhIP,

which suggests that *Msh2*-deficient stem cells might partially have lost protective checkpoint responses to intestinal mutagens, a result consistent with the previously observed dependence on *Msh2* of DDS and checkpoint responses induced by UV-induced DNA damage (7).

MMR-deficient cells are hypermutable by PhIP

To investigate whether the mutagenicity of PhIP is affected by MMR deficiency we quantified the frequency of mutations induced by PhIP in wild type and the mES cell lines *Msh2-1*, *Msh6-1*, *Mlh1-1* and *Pms2-1*, using the *Hprt* gene as a reporter (Fig. 3C-D, and Supplemental Figs. S4A and S4B for independent cell lines). Similar to selection of MMR-deficient clones (see above), selection for mutational inactivation of *Hprt* employs 6tG although, rather than by a pulse, selection for deleterious *Hprt* mutations is continuous and uses a higher dose. Almost no *Hprt*-mutant clones were found in vehicle-treated wild type cells or cells deficient for the minor MMR gene *Msh3*, an alternative binding partner of *Msh2* involved in repairing relatively large insertion/deletion loops (25) (Fig. 3C). PhIP treatment of these cell lines yielded a moderate increase of the mutant frequencies ranging between approximately 10 to 20 x 10⁻⁶ mutants (Fig. 3D). Whereas the MMR-deficient cell lines displayed spontaneous mutant frequencies varying between 45 and 110 x 10⁻⁶, higher frequencies of *Hprt*-mutant clones were obtained following PhIP treatment of these cell lines (approximately 220 x 10⁻⁶; Fig. 3C). Subtracting the *Hprt* mutant frequencies of the vehicle-treated cells from those of the PhIP-treated cells revealed that PhIP induced much higher frequencies of mutants in all MMR-deficient cells than in wild type or *Msh3*-deficient cells (Fig. 3D). Importantly, by using a completely independent set of isogenic mES cell lines (*Msh2-s*, *Msh6-s*, *Mlh1-s* and *Pms2-s*) we obtained identical results (Supplemental Fig. S4), excluding that secondary mutations are responsible in the observed phenotypes. Thus, in addition to suppressing the mutagenicity of spontaneous replication errors, MMR genes suppress the induction of mutations by PhIP. We conclude that the combination of spontaneous and enhanced PhIP-induced mutagenesis in MMR-deficient cells procures a compound hypermutator phenotype.

PhIP-induced mutant spectra in wildtype and MMR-deficient cells

To investigate whether MMR genes, in addition to suppressing PhIP-induced mutations, also affect the PhIP-induced mutation spectrum we treated wild type and *Msh2-1* cells with PhIP or vehicle, selected for *Hprt* mutants, and sequenced pooled *Hprt* cDNAs using an amplicon based next-generation sequencing approach to analyze most of the *Hprt* cDNA. Using a novel sequencing analysis pipeline (R. van Schendel, manuscript in preparation), 58 unique mutations in PhIP treated wild type cells, 49 mutations in mock-treated *Msh2*-deficient cells and 58 mutations in PhIP treated *Msh2*-deficient cells were identified at a 0,1% cut-off for allele frequency (Supplemental tables S4-S6). Only one spontaneous mutation was found in mock-treated wild type samples, confirming minimal sequencing noise.

In both wild type and *Msh2*-deficient cells, 75% of both spontaneous and PhIP-induced mutations were SNS (Fig. 4A). To a lesser extent, *Hprt* was inactivated by multi nucleotide substitutions (MNS, e.g. CGAT > ATTA), insertions and deletions. MNS were exclusively found in cells treated with PhIP, whereas insertions were associated with loss of *Msh2*. By multiplying the fractions of the SNS spectra (Fig. 4A) with the absolute mutant frequencies that were obtained earlier for mock and PhIP-exposed conditions (Fig 3C, 3D) we then obtained the frequency of each type of spontaneous and PhIP-induced nucleotide substitution in both cell lines (Fig. 4B, 4C, Supplemental Table S7). In wild type cells most PhIP-induced SNSs were G.C > T.A transversions, at a frequency of 12.2×10^{-6} . In mock-treated *Msh2*-deficient cells, spontaneous SNS consisted mostly of G.C > A.T and A.T > G.C transitions (at a frequency of 25.7×10^{-6} each). In *Msh2*-deficient cells treated with PhIP, mutations were mainly comprised of 104.9×10^{-6} G.C > T.A transversions, 74.0×10^{-6} G.C > A.T transitions and 61.7×10^{-6} A.T > G.C transitions. Other substitutions were very rare. Spectra of PhIP-induced SNS were determined by correcting spectra obtained after PhIP treatment for the spontaneous spectra (Fig. 4C). This revealed that *Msh2* specifically suppresses PhIP-induced G.C > T.A transversions, the dominant SNS type also induced in wild type cells. Interestingly, also the frequencies of G.C > A.T and A.T > G.C transitions, that are also part of the spontaneous mutation spectrum in MMR-deficient cells (Fig. 4B), were increased following PhIP treatment. Finally, in both PhIP-treated wild type and *Msh2*-deficient cells there was a strong bias towards nucleotide substitutions derived from guanines in the non-transcribed strand (Supplemental Fig. S5), consistent with the removal of most PhIP-adducted nucleotides from the transcribed strand by transcription-coupled nucleotide excision repair, which precludes their mutagenicity.

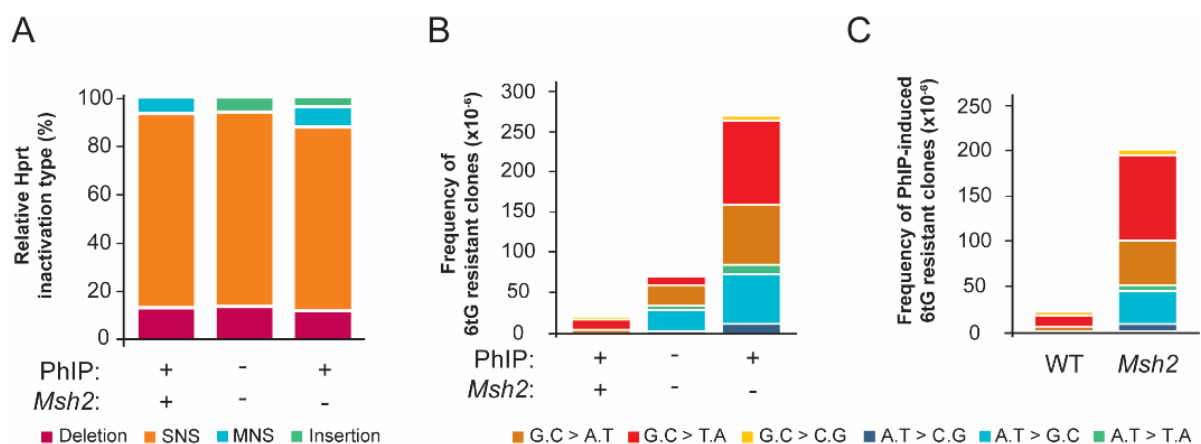


Figure 4. Analysis of PhIP-induced mutations at *Hprt* in MMR-proficient and -deficient backgrounds.

(A) Percentage of *Hprt* mutants by event type, relative to the total number of unique mutants per condition. SNS, single nucleotide substitution. MNS, multi nucleotide substitution. (B) Distribution of different single nucleotide substitutions. (C) Contribution of different nucleotide substitutions to PhIP-induced *Hprt*-mutant clones.

Discussion

Here we have generated and used isogenic panels of mES cells with targeted heterozygous deficiencies in the MMR genes *Msh2* or *Mlh1* or homozygous deficiencies in *Msh2*, *Msh6*, *Mlh1*, *Pms2* or *Msh3* as models for intestinal stem cells in LS patients and investigated responses of these cells to the prototypic heterocyclic amine PhIP.

While spontaneous LOH in *Msh2* or *Mlh1*-heterozygous cell lines was readily detectable, in both genotypes frequencies of loss of the wild type allele were strongly increased by a single exposure to PhIP (Fig. 2B-2D). Compared with *Msh2*-heterozygous cells, a lower number of MMR-deficient colonies was obtained following PhIP treatment of *Mlh1*-heterozygous cells, possibly reflecting locus-specific differences in allelic loss. The presence of a *Blasticidin* resistance cassette, linked to the wild type *Msh2* or *Mlh1* allele in these cell lines, allowed us to directly distinguish between either loss of the wild type allele by LOH (26), or by an intragenic deleterious mutation. Indeed, in approximately 25% of all MMR-deficient clones, PhIP treatment had induced inactivation of the wild type allele of *Msh2* or *Mlh1* by an intragenic mutation (Fig. 2D, Supplemental Fig. S2). The spectrum of these intragenic mutations is dominated by G.C > T.A transversions, in line with the spectrum induced by PhIP (23, 24, 27-30). Using a variety of analytical approaches we confirmed that the SNS induced by PhIP in the wild type *Msh2* or *Mlh1* alleles disrupt gene function (Fig. 2E). In support with the involvement of dietary mutagens in the induction of loss of MMR in the intestine of LS patients, our findings reflect observations in MMR-deficient tumors in LS patients where loss of the wild type allele frequently is caused by LOH (31, 32) while MMR inactivation by SNS also occurs albeit a lower frequency (33). Importantly, deleterious SNS might not result in loss of protein expression *per se*, which warrants caution as to the use of immunohistochemical staining for loss of MMR gene expression in CRC as a criterium to screen for MMR gene mutations in individuals suspected of LS (34).

Loss of DDS, that mediate protective checkpoint responses, senescence or apoptosis, is a prerequisite for early steps of carcinogenesis (35). Previous work has shown that loss of *Msh2* results in defective DDS in response to DNA damage induced by methylating agents and UV light (7, 36). We show here that also in response to PhIP, DDS of double-stranded DNA breaks (phospho-Kap-1) or (albeit to a lesser extent) persistent single stranded DNA (phospho-Chk1) partially depend on the MMR status (Fig. 3B). After exposure to a single dose of UV light, MMR-deficient cells displayed enhanced cell cycle progression compared with MMR-proficient cells (7). However, we did not observe a similar response after PhIP exposure (not shown), indicating that cell cycle responses to PhIP may only weakly be dependent on the MMR status. Nevertheless, the observed defective DDS might provide a long-term selective advantage of MMR-deficient over heterozygous intestinal stem cells when chronically exposed to PhIP or other diet-derived genotoxic agents.

Previously, we have found that *Msh2* and *Msh6*-deficient cells are hypermutable by UV light (7, 9), possibly by correcting misincorporations opposite photolesions by mutagenic translesion synthesis polymerases (37). Here we found that also the frequencies of PhIP-induced mutations are significantly higher in cells deficient for any of the four core MMR genes than in wild type cells (Fig. 3D and Supplemental Fig. S3). This exacerbated mutagenicity of helix-distorting nucleotide lesions acts in conjunction with the spontaneous mutagenesis in MMR-deficient cells, resulting in a compound hypermutagenesis phenotype. Importantly, these results were fully reproducible in an independent set of mutant cell lines (Supplemental Fig. S4). Mutational spectra analysis revealed that the frequency of the prevalent SNS induced by PhIP in wild type cells, G.C > T.A transversions, was increased most strongly in the absence of *Msh2* (Fig. 4C). This result suggests that MMR directly suppresses the mutagenicity of PhIP, possibly by removing misincorporations by translesion synthesis opposite the major lesion, dG-C8-PhIP-adducted guanines (30). This would be analogous to the proposed removal of misincorporations generated by translesion synthesis opposite UV light-induced photolesions (7).

G.C > A.T and A.T > G.C transitions dominate the spontaneous mutant spectrum of *Msh2*-deficient cells (Fig. 4B). Surprisingly, although these transitions do not represent typical PhIP-induced substitutions in wild type cells, their frequency was increased by PhIP treatment of *Msh2*-deficient cells (Fig. 4B, 4C). This might reflect the efficient activity of MMR at translesion synthesis-dependent misincorporations opposite PhIP-induced nucleotide adducts. Alternatively, the reduced DDS in the *Msh2*-deficient cells (Fig. 3B) might enable the survival of cells carrying excessive numbers of misincorporations by translesion synthesis, that otherwise would be eliminated by apoptosis. The wild-type survival of *Msh2*-deficient cells in response to PhIP (Fig. 3A), however, argues against this possibility. Finally, it cannot be excluded that in the absence of *Msh2*, mutagenic translesion synthesis is deregulated, as suggested previously (38), leading to more misincorporations in response to PhIP treatment. Irrespective of the underlying mechanism, these data show that PhIP is significantly more mutagenic in MMR-deficient cells than in MMR-proficient cells.

Taken together, our data support the possibility that dietary mutagens such as PhIP may direct CRC in LS patients at multiple levels (see the Graphical Abstract). First, PhIP exposure increases the frequency of somatic inactivation of the wild type allele in MMR-heterozygous cells by LOH or by a nucleotide substitution, resulting in MMR deficiency (Graphical Abstract). Second, the resulting MMR-deficient cells can no longer efficiently activate protective DDS in response to PhIP (Fig. 3B). Last, exposure of such MMR-deficient cells to PhIP results in compound hypermutagenesis resulting from both the spontaneous mutator phenotype at undamaged nucleotides associated with MMR deficiency (Fig. 3C, blue bars) as well as with the strongly increased mutability of these cells by PhIP as compared with wild type cells (Fig. 3D). Following validation of these observations in *in vivo* models, our findings may provide a rationale for dietary modification as a preventative strategy for LS-associated CRC.

Supplemental Materials

Supplemental Methods table 1: DNA sequences of guide RNAs.

CRISPR table	gRNA 1	gRNA 2	Target	Protein	6tG tolerant
Msh2-S	GATGAGCTACACTAGTGATG	ACACCAAAACCGCTGAGTTG	Entire gene	No protein	Yes
Msh6-1	GGAGCCTCCGCTTCCC GCGG	CCGCGGGAAGCGGAGGCTCC	Exon 1-2	No protein	Yes
Mlh1-1	GCATCAGAGTAGTTGCAA	-	Exon 2	No protein	Yes
Mlh1-S	GCATCAGAGTAGTTGCAA	-	Exon 2	No protein	Yes
Pms2-1	CGGCGCGCTAGACTGGACGAGGG	GTGAAGTCCAGGCGGCAGTTAGG	Entire gene	No protein	No
Pms2-S	TACCTGCACGTGGCCCGCGTCGG	GTGAAGTCCAGGCGGCAGTTAGG	Entire gene	No protein	No

Supplemental Methods table 2: Generation, analysis and validation of cell lines.

mES cell line	Genotype	Origin	Year of publication/creation	Validation
E14	Wild type	Ref. 8	1985	2016: Karyotyping
Msh2-Bsd	<i>Msh2</i> -heterozygous	Drost et al., in prep.	2016	2016: Fortuitous, 6tG-tolerant, Blasticidin-sensitive progeny clones; allele-specific PCR
Mlh1-Bsd	<i>Mlh1</i> -heterozygous	Drost et al., in prep.	2016	2016: Fortuitous, 6tG-tolerant, Blasticidin-sensitive progeny clones; allele-specific PCR
Msh2-1	<i>Msh2</i> -deficient	This work	2018	2018: PCR, 6tG tolerance; W blotting
Msh2-s	<i>Msh2</i> -deficient	Ref. 11	1995	2018: PCR, 6tG tolerance; W blotting
Msh6-1	<i>Msh6</i> -deficient	Ref. 10	2018	2018: 6tG tolerance; W blotting
Msh6-s	<i>Msh6</i> -deficient	Ref. 12	1998	2018: 6tG tolerance; W blotting
Mlh1-1	<i>Mlh1</i> -deficient	This work	2015	2018: 6tG tolerance; W blotting
Mlh1-s	<i>Mlh1</i> -deficient	This work	2015	2018: 6tG tolerance; W blotting
Pms2-1	<i>Pms2</i> -deficient	This work	2018	2018: PCR, W blotting
Pms2-s	<i>Pms2</i> -deficient	This work	2018	2018: PCR, W blotting
Msh3	<i>Msh3</i> -deficient	Ref. 11	1998	2019: PCR

Supplemental Methods table 3: DNA sequences of PCR primers.

Primer:	Sequence
1	CTCCTGAGAGCTGGGGTTTCAAG
2	GGGGAAAAAAGATAGTTCTTTGT
3	CCCTGGGACTCACTACGTTT
4	CCATGCACTGGTGTACGAAG
5	TCTACGAGCGGTTTGTAGGG
6	TTCCCGTCCTTGTTCTCAAC
7	ATGGCGGTGCAGCCTAAGGAG
8	GTTCTTGTTGTTGCGAAGC
9	GATCCTAACCTGAGTGAAC
10	CCCAGCTACAGACGGTAATGT
11	GACGGGCAACTCTGGCG
12	CTGGGCTGTGTCTGAAGTC
13	GTCTACGCTTACCAGATGGT
14	CCAATCCACAGGTGAAGTAC
15	GCACCAATACTGGGATACAG
16	GATGTGTATAAGAGACAGCAGTCCCAGCGTCGTGATTAG
17	CGTGTGCTCTTCCGATCTATCCAGCAGGTCAGCAAAGAA
18	GATGTGTATAAGAGACAGGCCATCACATTGTGGCCCTC
19	CGTGTGCTCTTCCGATCTAGTTTGCATTGTTTACCAGTGTC
20	GATGTGTATAAGAGACAGTGACACTGGTAAAACAATGCAA
21	CGTGTGCTCTTCCGATCTTTTGCAGATTCAACTTGCGCT
22	AATGATACGGCGACCAACCGAGATCTACACGAATTCGCTCGTCGGCAGCGTCAGATGTGTATAAGAGACAG
23	AATGATACGGCGACCAACCGAGATCTACACGCAAGCATTTCGTCGGCAGCGTCAGATGTGTATAAGAGACAG
24	AATGATACGGCGACCAACCGAGATCTACACGGCATCGATCGTCGGCAGCGTCAGATGTGTATAAGAGACA G
25	AATGATACGGCGACCAACCGAGATCTACACTAGATCGCTCGTCGGCAGCGTCAGATGTGTATAAGAGACAG
26	CAAGCAGAAGACGGCATAACGAGATAGCGTAGCGTGACTGGAGTTCAGACGTGTGCTCTTCCGATCT
27	CAAGCAGAAGACGGCATAACGAGATCAGCCTCGGTGACTGGAGTTCAGACGTGTGCTCTTCCGATCT
28	CAAGCAGAAGACGGCATAACGAGATTGCCTCTTGTGACTGGAGTTCAGACGTGTGCTCTTCCGATCT
29	CAAGCAGAAGACGGCATAACGAGATTCTCTACGTGACTGGAGTTCAGACGTGTGCTCTTCCGATCT

Supplemental Figures

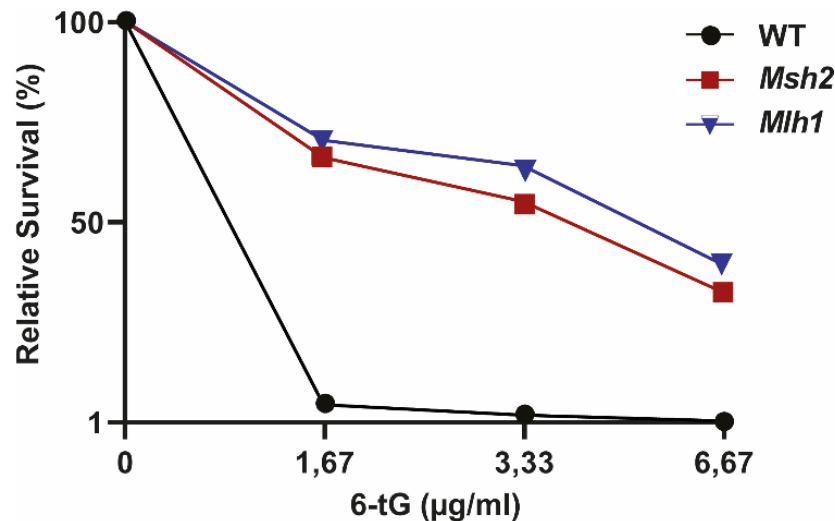


Figure S1: Tolerance of *Msh2*-1 and *Msh6*-1 mES cell lines to 6-tG

400 cells per well were seeded in triplicate in 6-well plates (day 1). The indicated concentration of 6-tG was added to the wells for four hours on days 2 and 7. Colonies were stained with methylene blue on day 10 and survival relative to untreated wells was calculated.

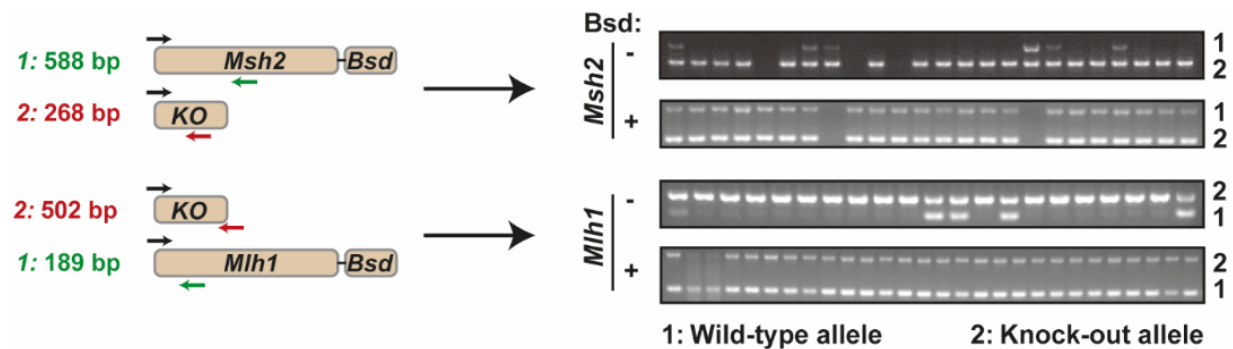


Figure S2: PCR analysis of genomic DNA from 6tG-tolerant clones that were selected with or without Blasticidin.

Primer pair 1, PCR of the wild type allele; primer pair 2, PCR of knockout allele. *Bsd*, Blasticidin. KO: knockout allele of *Msh2* or *Mlh1*.

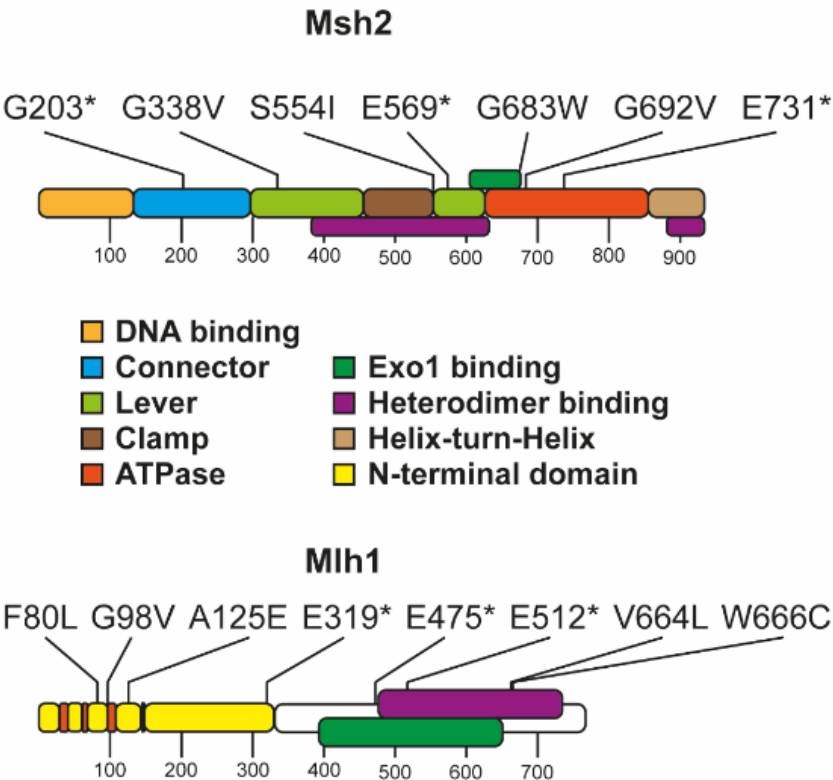


Figure S3: PhIP-induced amino acid changes in Msh2 or Mlh1 in 6tG-tolerant and Blasticidin-resistant clones. Colors depict functional domains.

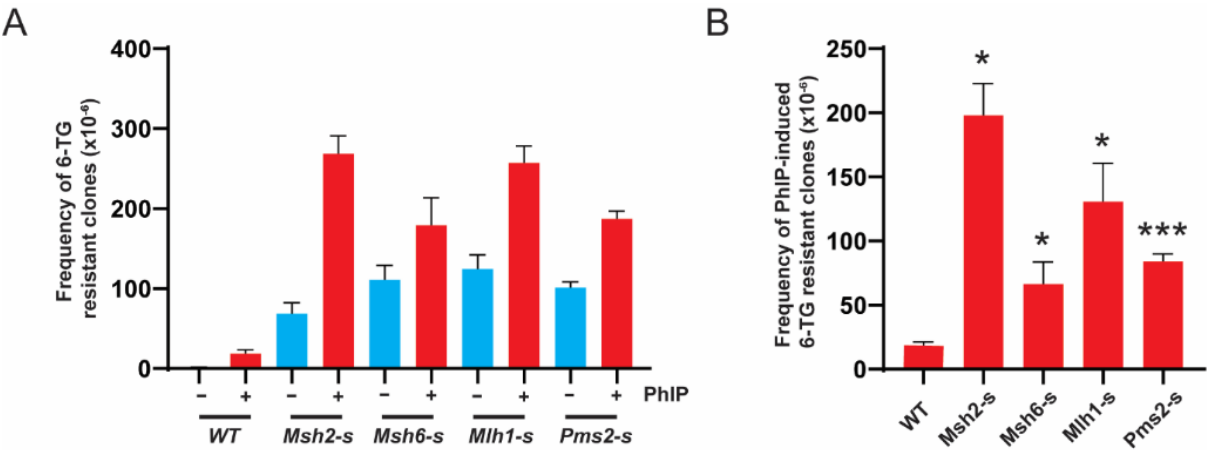


Figure S4: Spontaneous and PhIP-induced mutant frequencies in independent MMR-deficient mES cell lines

A: Cells were exposed to PhIP for 3 hours, cultured for a week in the presence of 6tG to select for clones that lost *Hprt*. Error bars, SEM. -s, independent line from those shown in Fig. 3 B: Quantification of 6tG-resistant clones induced by PhIP, corrected for spontaneous mutants. Error bars, SEM. *, $P \leq 0,05$, ***, $P \leq 0,001$; unpaired T-test of groups compared to WT.

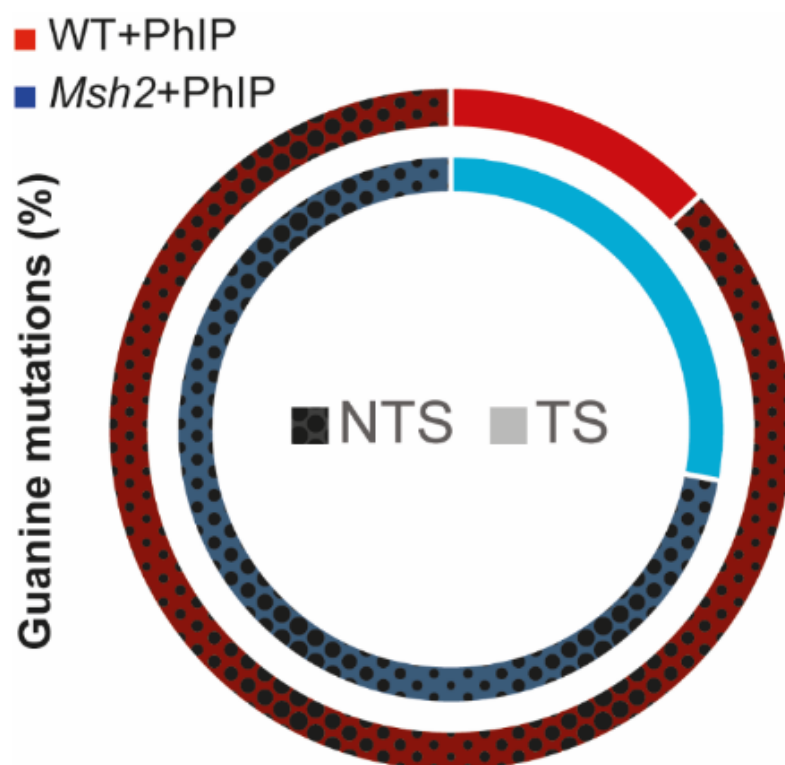


Figure S5: Strand bias of guanine mutations in PhIP-treated wild-type and Msh2-deficient cells. Dark spotted colors, non-transcribed strand (NTS); bright colors, transcribed strand (TS). Blue, Msh2-deficient cells treated without PhIP; red, Msh2-deficient cells treated with PhIP.

Supplemental Tables

Table S1: Analysis of MMR inactivation type following mock and PhIP treatment

Cells were exposed to PhIP or vehicle for 3 hours, grown for a week and pulsed with 6tG to select for clones that lost MMR. Half of the plates were also treated with Blasticidin (Bsd) to select for intragenic events opposed to LOH. Clones were stained using methylene blue and quantified. The contribution of intragenic and LOH events was calculated by subtracting the Bsd population (intragenic population) from the total amount of counted colonies. Error = SEM.

	- PhIP			+ PhIP			PhIP-induced		
	Intra genic	LOH	Total	Intra genic	LOH	Total	Intra genic	LOH	Total
WT	n/a	n/a	7.7 ± 7.2	n/a	n/	26.7 ± 22.9	n/a	n/a	19 ± 15.6
Msh 2	5 ± 1.6	192.3 ± 77.9	197.3 ± 78.2	299.6 ± 119.5	872.8 ± 243.6	1172.3 ± 215.9	294.6 ± 118.0	680.4 ± 172.4	975 ± 138.9
Mlh 1	4.2 ± 1.4	59.2 ± 30.1	63.3 ± 31.4	75.2 ± 18.9	282.8 ± 93.9	358 ± 99.6	71.1 ± 18.8	223.6 ± 66.4	294.7 ± 68.7

Induction of mismatch repair deficiency, compromised DNA damage signaling and compound hypermutagenesis by a dietary mutagen in a cell-based model for Lynch syndrome

Table S2: Inactivating mutations in Msh2 cDNA following exposure of Msh2-heterozygous mES cells to PhIP

A SNS is deemed likely pathogenic (LP) when the *in silico* prior probability exceeded 0.9 when found as (likely) pathogenic in human MMR variant databases (Insight and ClinVar), or when the functionality of the protein is disturbed in biochemical assays (CIMRA) or *in vivo* assays (Reverse Diagnosis Catalogues). Insertions or deletions are classified as likely pathogenic when these cause frameshifts, otherwise they are unknown.

Mouse			Human		Analysis of Pathogenicity						Outcome	
cDNA	Protein	Frameshift	Target sequence	cDNA	Protein	Prior probability	Insight	ClinVar	Cosmic	CIMRA	Reverse Diagnosis	Outcome
c. Δ140	p. 47	-1	GCACGAGAGAGG	N/A	N/A	N/A	N/A	N/A	N/A	N/A	N/A	LP
c. 607 G>T	p. G203*		TACCA[G]GAGGA	c. 607 G>T	p. G203*	N/A	Not found	Not found	Found	Not found	Found	LP
c. Δ213_Δ367	p. Δ71_Δ122	-2	GCAAGΔ159]CTTCT	N/A	N/A	N/A	N/A	N/A	N/A	N/A	N/A	LP
c. Δ643_789	p. Δ215_263	-2	TGAGGΔ147]CAGGT	N/A	N/A	N/A	N/A	N/A	N/A	N/A	N/A	Unknown
c. Δ791_Δ940	p. Δ264_Δ313	-2	GAATC[Δ150]AGGGT	N/A	N/A	N/A	N/A	N/A	N/A	N/A	N/A	Unknown
c. 1013 G>T	p. G338V		TCAAG[G]ACAAA	c. 1013 G>T	p. G338V	0.94	Not found	Class 3	Found	Not found	Not found	LP
c. Δ1036_Δ1046	p. Δ346_Δ349	-1	AGTGG[Δ11]GCTCA	N/A	N/A	N/A	N/A	N/A	N/A	N/A	N/A	LP
c. Δ1539	p. 513	-1	AAATGTΔGACTC	c. Δ1539	p. Δ513	N/A	N/A	N/A	N/A	N/A	N/A	LP
c. 1661 G>T	p. S554L	-1	CAACATG]TGAAT	c. 1661 G>T	p. S554L	0.55	Not found	Not found	Not found	Not found	Found	LP
c. 1661 G> 25ins	p. 554 G> 1ns(9)	-1	AACAAG]AACTT	N/A	N/A	N/A	N/A	N/A	N/A	N/A	N/A	LP
c. 1663 G>T	p. E555*	-1	ACAGT]AAATTG	Not conserved	Not conserved	N/A	N/A	N/A	N/A	N/A	N/A	N/A
c. 1705 G>T	p. E569*	-1	AAGCG]GAGTAT	c. 1705 G>T	p. E569*	N/A	Not found	Not found	Not found	Not found	Found	LP
c. Δ2008_Δ2460	p. Δ670_Δ820	-1	CTGGT]Δ453]GTC TG	N/A	N/A	N/A	N/A	N/A	N/A	N/A	N/A	Unknown
c. 2047 G>T	p. G683W	-1	AGACC]TGGGGTG	c. 2047 G>T	p. 683 G>T	0.89	Class 3	Not found	Not found	Not found	Found	LP
c. 2075 G>T	p. G692V	-1	AATCG]G]GTGT	c. 2075 G>T	p. 692 G>T	0.938875343	Class 4	Class 4	Not found	5.90%	Not found	LP
c. 2191 G>T	p. E731*	-1	TGCTG]GAGACT	c. 2191 G>T	p. E731*	N/A	Class 5	Not found	Not found	Not found	Found	LP
c. Δ2583	p. 861	-1	TCGCT]ΔGGATG	N/A	N/A	N/A	N/A	N/A	N/A	N/A	N/A	LP
c. Δ2633_2636	p. 877	-2	AAAGAG]ΔGCAJAGGTG	N/A	N/A	N/A	N/A	N/A	N/A	N/A	N/A	LP
c. 2634_2635ins ATCG	p. 878_879ins(2)	-2	AGAGAG]insATCG]CAAGGT	N/A	N/A	N/A	N/A	N/A	N/A	N/A	N/A	LP

Likely deleterious (LD)

Class 4/5

Unknown

Class 3

Benign

Class 1/2

N/A

Likely deleterious (LD) Class 4/5
 Unknown Class 3
 Benign Class 1/2
 N/A

Table S3: Inactivating mutations in *Mlh1* cDNA following exposure of *Mlh1*-heterozygous *mES* cells to *PhIP*

A SNS is deemed likely pathogenic (LP) when the *in silico* prior probability exceeded 0.9 when found as (likely) pathogenic in human MMR variant databases (Insight and ClinVar), or when the functionality of the protein is disturbed in biochemical assays (CIMRA) or *in vivo* assays (Reverse Diagnosis Catalogues). Insertions or deletions are classified as likely pathogenic when these cause frameshifts, otherwise they are unknown.

Mouse			Human		Analysis of Pathogenicity							
cDNA	Protein	Frameshift	Target sequence	cDNA	Protein	Prior probability	Insight	ClinVar	Cosmic	CMRA	Reverse Diagnosis	Outcome
c. 240 C>A	p. F80L		AGGTTCTACTAC	c. 240 C>A	p. F80L	0.70	Not found	Not found	Not found	Not found	Found	LP
c. 293 G>T	p. G98V		CTATGTCGCTTTC	c. 293 G>T	p. G98V	0.94	Not found	Not found	Not found	Not found	Not found	LP
c. 374 C>A	p. A125E		ATGTGTCGTACA	c. 374 C>A	p. A125E	0.97	Not found	Class 3	Not found	13% Found	Not found	LP
c. Δ453_Δ544	p. Δ151_Δ181	-2	ATCAC[92]GGTAT	N/A	N/A	N/A	N/A	N/A	N/A	N/A	N/A	N/A
c. 520 G>T	p. G174*		AGTAC[9]GAAAA	Not Conserved	Not conserved	N/A	N/A	N/A	N/A	N/A	N/A	N/A
c. Δ531_Δ545	p. Δ177_Δ182		ATTTT[15]GTATT	N/A	N/A	N/A	N/A	N/A	N/A	N/A	N/A	Unknown
c. Δ589_Δ592	Δ197	-1	AAAAA[CAAG]GTGAG	c. 955 G>T	p. E319*	N/A	Class 5	Class 5	Not found	Not found	Found	LP
c. 955 G>T	p. E319*		TGCAC[9]AGGAG	Not Conserved	Not conserved	N/A	N/A	N/A	N/A	N/A	N/A	N/A
c. 1243 C>T	p. R415*		CTGTGTCGAGGG	Not Conserved	Not conserved	N/A	N/A	N/A	N/A	N/A	N/A	N/A
c. 1281 G>T	p. T427T		GCCAC[9]CGGGA	c. 1423 G>T	p. E475*	N/A	Not found	Not found	Not found	Not found	Not found	Unknown
c. 1435 G>T	p. E479*		ATCGG[9]AGGAC	c. 1534 G>T	p. E512*	N/A	Class 5	Class 5	Found	Not found	Not found	LD
c. 1546 G>T	p. E516*		AGGAA[9]AGATT	N/A	N/A	N/A	N/A	N/A	N/A	N/A	N/A	LP
c. Δ1597_Δ1598	p. 532	-2	ACCATTC[9]CTTTG	N/A	N/A	N/A	N/A	N/A	N/A	N/A	N/A	LP
c. Δ1613_Δ1614	p. 537_538	-2	CTGTGTCGTAATCC	N/A	N/A	N/A	N/A	N/A	N/A	N/A	N/A	LP
c. 2002 G>C	p. V668L		CTGAG[9]TGAAAT	c. 1990 G>C	p. V664L	0.59	Class 3	Not found	Not found	Not found	Not found	Unknown
c. 2010 G>T	p. W670C		AATTG[9]GATGA	c. 1998 G>T	p. W666C	0.94	Not found	Not found	Not found	Not found	Not found	LP
c. Δ2040_Δ2153	p. Δ680_Δ717	-2	AGTCTT[114]GACTGT	N/A	N/A	N/A	N/A	N/A	N/A	N/A	N/A	Unknown
c. 2276 G>T	p. R759L		TGAGC[9]GTGTT	Not Conserved	Not conserved	N/A	N/A	N/A	N/A	N/A	N/A	N/A

Likely deleterious (LD) Class 4/5
 Unknown Class 3
 Benign Class 1/2
 N/A

Induction of mismatch repair deficiency, compromised DNA damage signaling and compound hypermutagenesis by a dietary mutagen in a cell-based model for Lynch syndrome

Table S4: List of mutations in the *Hprt* gene in PhIP-treated wild type cells.

Flanking sequence; sequence surrounding the mutated bases, parentheses surround the mutated base, non-transcribed strand sequence is shown. Strand; in which strand the mutated guanine is found, the base which is known to be mutable by PhIP. NTS, non-transcribed strand. TS, transcribed strand. Ins: inserted nucleotide(s), del: deleted nucleotide(s).

	Position	Exon	Base change	Flanking Sequence	Amino acid change	Strand
SNS	40	2	G > U	GAT(G)AAC	E > *	NTS
	47	2	G > A	CAG(G)TTA	G > D	NTS
	74	2	C > G	TAC(C)TAA	P > R	TS
	88	2	G > U	GCC(G)AGG	E > *	NTS
	97	2	G > U	TTG(G)AAA	E > *	NTS
	113	2	C > U	TTC(C)TCA	P > L	TS
	118	2	G > U	CAT(G)GAC	G > *	NTS
	119	2	G > C	ATG(G)ACT	G > A	NTS
	119	2	G > U	ATG(G)ACT	G > V	NTS
	134	2	G > U	ACA(G)GAC	R > M	NTS
	134	2	G > A	ACA(G)GAC	R > K	NTS
	135	3	G > U	CAG(G)ACT	R > S	NTS
	139	3	G > A	ACT(G)AAA	E > K	NTS
	145	3	C > U	AGA(C)TTG	L > F	TS
	148	3	G > A	CTT(G)CTC	A > T	NTS
	149	3	C > U	TTG(C)TCG	A > V	TS
	172	3	G > U	ATG(G)GAG	G > *	NTS
	208	3	G > U	AAG(G)GGG	G > W	NTS
	208	3	G > C	AAG(G)GGG	G > R	NTS
	209	3	G > A	AGG(G)GGG	G > E	NTS
	211	3	G > C	GGG(G)GCT	G > R	NTS
	212	3	G > A	GGG(G)CTA	G > D	NTS
	212	3	G > U	GGG(G)CTA	G > V	NTS
	222	3	C > A	GTT(C)TTT	F > L	TS
	229	3	G > U	GCT(G)ACC	D > Y	NTS

Table S4: Continued

	Position	Exon	Base change	Flanking Sequence	Amino acid change	Strand
SNS	238	3	G > U	CTG(G)ATT	D > Y	NTS
	463	4	C > A	AGC(C)CCA	P > T	TS
	464	4	C > A	GCC(C)CAA	P > H	TS
	482	4	C > A	TTG(C)AAG	A > E	TS
	500	7	G > U	AAA(G)GAC	R > M	NTS
	527	7	C > A	GGC(C)AGA	P > Q	TS
	539	8	G > U	TTG(G)ATT	G > V	NTS
	539	8	G > A	TTG(G)ATT	G > E	NTS
	551	8	C > A	TTC(C)AGA	P > Q	TS
	565	8	G > C	GTT(G)TTG	V > L	NTS
	568	8	G > U	GTT(G)GAT	G > *	NTS
	568	8	G > C	GTT(G)GAT	G > R	NTS
	569	8	G > U	TTG(G)ATA	G > V	NTS
	569	8	G > A	TTG(G)ATA	G > E	NTS
	580	8	G > U	CTT(G)ACT	D > Y	NTS
	582	8	C > A	TGA(C)TAT	D > E	TS
	599	8	G > A	TCA(G)GGA	R > K	NTS
	600	8	G > C	CAG(G)GAT	R > S	NTS
	601	8	G > U	AGG(G)ATT	D > Y	NTS
	610	9	C > A	AAT(C)ACG	H > N	TS
	612	9	C > G	TCA(C)GTT	H > Q	TS
MNS	152	3	GAGA > TG			
	236	3	TGG > CTGA			
	555	8	CA > G			
	597	8	CA > AT			
Deletion	208	3	del 111bp			
	319	4, 5	del 84bp			
	323	4, 5	del 66bp			
	337	4	del G			
	486	7	del 47bp			
	533	8	del 77bp			
	533	8	del 21bp			
	557	8	del A			

Induction of mismatch repair deficiency, compromised DNA damage signaling and compound hypermutagenesis by a dietary mutagen in a cell-based model for Lynch syndrome

Table S5: List of mutations in the *Hprt* gene in mock-treated *Msh2*-deficient cells.

Flanking sequence; sequence surrounding the mutated bases, parentheses surround the mutated base, non-transcribed strand sequence is shown. Strand; in which strand the mutated guanine is found, the base which is known to be mutable by PhIP. NTS, non-transcribed strand. TS, transcribed strand. Ins: inserted nucleotide(s), del: deleted nucleotide(s).

	Position	Exon	Base change	Flanking Sequence	Amino acid change
SNS	58	2	G > T	CTA(G)ATT	D > Y
	74	2	C > A	TAC(C)TAA	P > H
	103	2	G > A	AAA(G)TGT	V > M
	104	2	T > C	AAG(T)GTT	V > A
	119	2	G > A	ATG(G)ACT	G > E
	122	2	T > C	GAC(T)GAT	L > P
	130	2	G > T	ATG(G)ACA	D > Y
	131	2	A > G	TGG(A)CAG	D > G
	134	2	G > T	ACA(G)GAC	R > M
	134	2	G > A	ACA(G)GAC	R > K
	151	3	C > T	GCT(C)GAG	R > *
	158	3	T > C	ATG(T)CAT	V > A
	170	3	T > C	AGA(T)GGG	M > T
	172	3	G > T	ATG(G)GAG	G > *
	202	3	C > T	GTG(C)TCA	L > F
	208	3	G > A	AAG(G)GGG	G > R
	209	3	G > A	AGG(G)GGG	G > E
	212	3	G > A	GGG(G)CTA	G > D
	220	3	T > C	AAG(T)TCT	F > L
	233	3	T > C	ACC(T)GCT	L > P
	245	3	T > A	ACA(T)TAA	I > N
	248	3	A > G	TTA(A)AGC	K > R
	254	3	T > C	CAC(T)GAA	L > P
	295	3	T > C	GAT(T)TTA	F > L
	305	3	T > G	GAC(T)GAA	L > R

Table S5: Continued

	Position	Exon	Base change	Flanking Sequence	Amino acid change
SNS	358	4	G > T	GGA(G)ATG	D > Y
	446	4	T > C	CCC(T)GGT	L > P
	464	4	C > T	GCC(C)CAA	P > L
	527	7	C > T	GGC(C)AGA	P > L
	548	8	T > A	AAA(T)TCC	I > N
	550	8	C > T	ATT(C)CAG	P > S
	563	8	T > C	TTG(T)TGT	V > A
	572	8	A > C	GAT(A)TGC	Y > S
	574	8	G > A	TAT(G)CCC	A > T
	577	8	C > T	GCC(C)TTG	L > F
	595	8	T > A	TAC(T)TCA	F > I
	610	9	C > T	AAT(C)ACG	H > Y
	611	9	A > G	ATC(A)CGT	H > R
	614	9	T > C	ACG(T)TTG	V > A
Insertion	103	2	ins A		
	126	2	ins GAT		
	562	8	ins T		
Deletion	323	4, 5	del 66bp		
	345	4	del A		
	486	7	del 47bp		
	533	8	del 77bp		
	533	8	del 21bp		
	585	8	del TA		
	586	8	del AAT		

Induction of mismatch repair deficiency, compromised DNA damage signaling and compound hypermutagenesis by a dietary mutagen in a cell-based model for Lynch syndrome

Table S6: List of mutations in the *Hprt* gene in PhIP-treated *Msh2*-deficient cells.

Flanking sequence; sequence surrounding the mutated bases, parentheses surround the mutated base, non-transcribed strand sequence is shown. Strand; in which strand the mutated guanine is found, the base which is known to be mutable by PhIP. NTS, non-transcribed strand. TS, transcribed strand. Ins: inserted nucleotide(s), del: deleted nucleotide(s).

	Position	Exon	Base change	Flanking Sequence	Amino acid change	Strand
SNS	47	2	G > A	CAG(G)TTA	G > D	NTS
	47	2	G > T	CAG(G)TTA	G > V	NTS
	119	2	G > A	ATG(G)ACT	G > E	NTS
	122	2	T > C	GAC(T)GAT	L > P	
	130	2	G > C	ATG(G)ACA	D > H	NTS
	134	2	G > A	ACA(G)GAC	R > K	NTS
	135	3	G > T	CAG(G)ACT	R > S	NTS
	143	3	G > T	AAA(G)ACT	R > I	NTS
	149	3	C > T	TTG(C)TCG	A > V	TS
	166	3	G > T	AAG(G)AGA	E > *	NTS
	170	3	T > C	AGA(T)GGG	M > T	
	208	3	G > T	AAG(G)GGG	G > W	NTS
	208	3	G > A	AAG(G)GGG	G > R	NTS
	209	3	G > A	AGG(G)GGG	G > E	NTS
	212	3	G > A	GGG(G)CTA	G > D	NTS
	212	3	G > T	GGG(G)CTA	G > V	NTS
	220	3	T > C	AAG(T)TCT	F > L	
	223	3	T > A	TTC(T)TTG	F > I	
	229	3	G > T	GCT(G)ACC	D > Y	NTS
	233	3	T > C	ACC(T)GCT	L > P	
	238	3	G > T	CTG(G)ATT	D > Y	NTS
	296	3	T > C	ATT(T)TAT	F > S	
	358	4	G > T	GGA(G)ATG	D > Y	NTS
	365	4	T > G	ATC(T)CTC	L > R	

Table S6: Continued

	Position	Exon	Base change	Flanking Sequence	Amino acid change
SNS	446	6	T > C	CCC(T)GGT	L > P
	463	6	C > A	AGC(C)CCA	P > T
	464	6	C > T	GCC(C)CAA	P > L
	472	6	G > T	ATG(G)TTA	V > F
	478	6	G > T	AAG(G)TTG	V > F
	491	7	T > C	TGC(T)GGT	L > P
	495	7	G > A	GGT(G)AAA	V > V
	501	7	G > T	AAG(G)ACC	R > S
	536	8	T > G	TTG(T)TGG	V > G
	539	8	G > T	TTG(G)ATT	G > V
	553	8	G > T	CCA(G)ACA	D > Y
	554	8	A > G	CAG(A)CAA	D > G
	569	8	G > T	TTG(G)ATA	G > V
	574	8	G > A	TAT(G)CCC	A > T
	586	8	A > G	TAT(A)ATG	N > D
	599	8	G > A	TCA(G)GGA	R > K
	601	8	G > A	AGG(G)ATT	D > N
	612	9	C > A	TCA(C)GTT	H > Q
	614	9	T > C	ACG(T)TTG	V > A
	614	9	T > A	ACG(T)TTG	V > D
MNS	112	2	CCT > GCC		
	210	3	GG > AT		
	486	7	CT > AG		
	491	7	TGG > GGA		
	553	8	GAC > TAA		
Insertion	103	2	ins A		
	562	8	ins T		
Deletion	48	2, 3	del 88bp		
	319	4	del 9bp		
	323	4, 5	del 66bp		
	486	7	del 47bp		
	533	8	del 77bp		
	533	8	del 21bp		
	535	8	del G		

Table S7: Frequencies of PhIP-induced single base pair substitutions in wild type and Msh2-deficient backgrounds (corrected for spontaneous substitutions).

WT		Mock			PhIP			PhIP-induced	
		Absolute	Relative (%)	6tG-resistant clones (x10 ⁻⁶)	Absolute	Relative	6tG-resistant clones (x10 ⁻⁶)	Relative (%)	6tG-resistant clones (x10 ⁻⁶)
Transitions	G.C > A.T	0	0	0	12	26,1	5,6	26,1	5,6
	A.T > G.C	0	0	0	0	0,0	0,0	0,0	0,0
Transversions	G.C > T.A	0	0	0	26	56,5	12,2	56,5	12,2
	G.C > C.G	0	0	0	8	17,4	3,8	17,4	3,8
	A.T > T.A	0	0	0	0	0,0	0,0	0,0	0,0
	A.T > C.G	0	0	0	0	0,0	0,0	0,0	0,0
Total		0	0	0	46	100,0	21,6	100,0	21,6

Msh2 ^{-/-}		Mock			PhIP			PhIP induced	
		Absolute	Relative (%)	6tG-resistant clones (x10 ⁻⁶)	Absolute	Relative	6tG-resistant clones (x10 ⁻⁶)	Relative (%)	6tG-resistant clones (x10 ⁻⁶)
Transitions	G.C > A.T	14	35,9	25,7	12	27,3	74,0	24,2	48,3
	A.T > G.C	14	35,9	25,7	10	22,7	61,7	18,0	36,0
Transversions	G.C > T.A	6	15,4	11,0	17	38,6	104,9	47,0	93,9
	G.C > C.G	0	0,0	0,0	1	2,3	6,2	3,1	6,2
	A.T > T.A	3	7,7	5,5	2	4,5	12,3	3,4	6,8
	A.T > C.G	2	5,1	3,7	2	4,5	12,3	4,3	8,7
Total		39	100,0	71,6	44	100,0	271,5	100,0	199,8

References

1. IARC. Globocan 2018: Cancer Fact Sheets - Colorectal Cancer http://gco.iarc.fr/today/data/factsheets/cancers/10_8_9-Colorectum-fact-sheet.pdf2018.
2. Derry MM, Raina K, Agarwal C, Agarwal R. Identifying Molecular Targets of Lifestyle Modifications in Colon Cancer Prevention. *Frontiers in Oncology*. 2013;3.
3. Chiavarini M, Bertarelli G, Minelli L, Fabiani R. Dietary Intake of Meat Cooking-Related Mutagens (HCAs) and Risk of Colorectal Adenoma and Cancer: A Systematic Review and Meta-Analysis. *Nutrients*. 2017;9(5):514.
4. Win AK, Jenkins MA, Dowty JG, Antoniou AC, Lee A, Giles GG, et al. Prevalence and Penetrance of Major Genes and Polygenes for Colorectal Cancer. *Cancer Epidemiol Biomarkers Prev*. 2017;26(3):404-12.
5. Lynch HT, Snyder CL, Shaw TG, Heinen CD and Hitchins MP Milestones of Lynch syndrome: 1895-2015. *Nat. Rev. Cancer* 2015;15(3):181-194.
6. Ijsselstein R, Jansen JG, De Wind N. DNA mismatch repair-dependent DNA damage responses and cancer. *DNA Repair*. 2020;93:102923.
7. Tsaalbi-Shtylik A, Ferras C, Pauw B, Hendriks G, Temviriyankul P, Carlee L, et al. Excision of translesion synthesis errors orchestrates responses to helix-distorting DNA lesions. *J Cell Biol*. 2015;209(1):33-46.
8. Hooper M, Hardy K, Handyside A, Hunter S, Monk M. HPRT-deficient (Lesch-Nyhan) mouse embryos derived from germline colonization by cultured cells. *Nature*. 1987;326(6110):292-5.
9. Borgdorff V, van Hees-Stuivenberg S, Meijers CM, de Wind N. Spontaneous and mutagen-induced loss of DNA mismatch repair in Msh2-heterozygous mammalian cells. *Mutat Res*. 2005;574(1-2):50-7.
10. Van Gool IC, Rayner E, Osse EM, Nout RA, Creutzberg CL, Tomlinson IPM, et al. Adjuvant Treatment for POLE Proofreading Domain-Mutant Cancers: Sensitivity to Radiotherapy, Chemotherapy, and Nucleoside Analogues. *Clin Cancer Res*. 2018;24(13):3197-203.
11. de Wind N, Dekker M, Berns A, Radman M, te Riele H. Inactivation of the mouse Msh2 gene results in mismatch repair deficiency, methylation tolerance, hyperrecombination, and predisposition to cancer. *Cell*. 1995;82(2):321-30.
12. de Wind N, Dekker M, Claij N, Jansen L, van Klink Y, Radman M, et al. HNPCC-like cancer predisposition in mice through simultaneous loss of Msh3 and Msh6 mismatch-repair protein functions. *Nat Genet*. 1999;23(3):359-62.
13. Thompson BA, Greenblatt MS, Vallee MP, Herkert JC, Tessereau C, Young EL, et al. Calibration of multiple in silico tools for predicting pathogenicity of mismatch repair gene missense substitutions. *Hum Mutat*. 2013;34(1):255-65.
14. Landrum MJ, Lee JM, Benson M, Brown GR, Chao C, Chitipiralla S, et al. ClinVar: improving access to variant interpretations and supporting evidence. *Nucleic Acids Res*. 2018;46(D1):D1062-D7.
15. Thompson BA, Spurdle AB, Plazzer JP, Greenblatt MS, Akagi K, Al-Mulla F, et al. Application of a 5-tiered scheme for standardized classification of 2,360 unique mismatch repair gene variants in the InSiGHT locus-specific database. *Nat Genet*. 2014;46(2):107-15.
16. Tate JG, Bamford S, Jubb HC, Sondka Z, Beare DM, Bindal N, et al. COSMIC: the Catalogue Of Somatic Mutations In Cancer. *Nucleic Acids Res*. 2019;47(D1):D941-D7.
17. Drost M, Zonneveld JBM, Van Hees S, Rasmussen LJ, Hofstra RMW, De Wind N. A rapid and cell-free assay to test the activity of lynch syndrome-associated MSH2 and MSH6 missense variants. *Human Mutation*. 2012;33(3):488-94.
18. Drost M, Zonneveld JEBM, Van Dijk L, Morreau H, Tops CM, Vasen HFA, et al. A cell-free assay for the functional analysis of variants of the mismatch repair protein MLH1. *Human Mutation*. 2010;31(3):247-53.
19. Drost M, Lutzen A, van Hees S, Ferreira D, Calleja F, Zonneveld JB, et al. Genetic screens to identify pathogenic gene variants in the common cancer predisposition Lynch syndrome. *Proc Natl Acad Sci U S A*. 2013;110(23):9403-8.
20. Drost M, Tiersma Y, Glubb D, Kathe S, van Hees S, Calleja F, et al. Two integrated and highly predictive functional analysis-based procedures for the classification of MSH6 variants in Lynch syndrome. *Genet Med*. 2020;22(5):847-56.
21. Magoc T, Salzberg SL. FLASH: fast length adjustment of short reads to improve genome assemblies. *Bioinformatics*. 2011;27(21):2957-63.
22. Sekine S, Mori T, Ogawa R, Tanaka M, Yoshida H, Taniguchi H, et al. Mismatch repair deficiency commonly precedes adenoma formation in Lynch Syndrome-Associated colorectal tumorigenesis. *Modern Pathology*. 2017;30(8):1144-51.
23. Zhang S, Lloyd R, Bowden G, Glickman BW, De Boer JG. Msh2 DNA mismatch repair gene deficiency and the food-borne mutagen 2-amino-1-methyl-6-phenylimidazo [4,5-b] pyridine (PhIP) synergistically affect mutagenesis in mouse colon. *Oncogene*. 2001;20(42):6066-72.

24. Smith-Roe SL, Hegan DC, Glazer PM, Buermeier AB. Mlh1-dependent suppression of specific mutations induced in vivo by the food-borne carcinogen 2-amino-1-methyl-6-phenylimidazo [4,5-b] pyridine (PhIP). *Mutat Res.* 2006;594(1-2):101-12.
25. Genschel J, Littman SJ, Drummond JT, Modrich P. Isolation of MutS β from Human Cells and Comparison of the Mismatch Repair Specificities of MutS β and MutS α . *Journal of Biological Chemistry.* 1998;273(31):19895-901.
26. Thiagalingam S, Laken S, Willson JK, Markowitz SD, Kinzler KW, Vogelstein B, et al. Mechanisms underlying losses of heterozygosity in human colorectal cancers. *Proc Natl Acad Sci U S A.* 2001;98(5):2698-702.
27. Lynch AM, Gooderham NJ, Davies DS, Boobis AR. Genetic analysis of PHIP intestinal mutations in MutaTMMouse. *Mutagenesis.* 1998;13(6):601-5.
28. Stuart GR, Thorleifson E, Okochi E, De Boer JG, Ushijima T, Nagao M, et al. Interpretation of mutational spectra from different genes: analyses of PhIP-induced mutational specificity in the lacI and cII transgenes from colon of Big Blue® rats. 2000;452(1):101-21.
29. Yadollahi-Farsani M, Gooderham NJ, Davies DS, Boobis AR. ACCELERATED PAPER: Mutational spectra of the dietary carcinogen 2-amino-1-methyl-6-phenylimidazo[4,5- b]pyridine (PhIP) at the Chinese hamster hprt locus. 1996;17(4):617-24.
30. Carothers AM, Yuan W, Hingerty BE, Broyde S, Grunberger D, Snyderwine EG. Mutation and repair induced by the carcinogen 2-(hydroxyamino)-1-methyl-6-phenylimidazo[4,5-b]pyridine (N-OH-PhIP) in the dihydrofolate reductase gene of Chinese hamster ovary cells and conformational modeling of the dG-C8-PhIP adduct in DNA. *Chem Res Toxicol.* 1994;7(2):209-18.
31. Ollikainen M, Hannelius U, Lindgren CM, Abdel-Rahman WM, Kere J, Peltomäki P. Mechanisms of inactivation of MLH1 in hereditary nonpolyposis colorectal carcinoma: a novel approach. *Oncogene.* 2007;26(31):4541-9.
32. Zhang J, Lindroos A, Ollila S, Russell A, Marra G, Mueller H, et al. Gene conversion is a frequent mechanism of inactivation of the wild-type allele in cancers from MLH1/MSH2 deletion carriers. *Cancer Res.* 2006;66(2):659-64.
33. Lu SL, Akiyama Y, Nagasaki H, Nomizu T, Ikeda E, Baba S, et al. Loss or somatic mutations of hMSH2 occur in hereditary nonpolyposis colorectal cancers with hMSH2 germline mutations. *Jpn J Cancer Res.* 1996;87(3):279-87.
34. Shia J. Immunohistochemistry versus microsatellite instability testing for screening colorectal cancer patients at risk for hereditary nonpolyposis colorectal cancer syndrome. Part I. The utility of immunohistochemistry. *The Journal of molecular diagnostics : JMD.* 2008;10(4):293-300.
35. Bartkova J, Hořejší Z, Koed K, Krämer A, Tort F, Zieger K, et al. DNA damage response as a candidate anti-cancer barrier in early human tumorigenesis. *Nature.* 2005;434(7035):864-70.
36. Jiricny J. The multifaceted mismatch-repair system. *Nature reviews Molecular cell biology.* 2006;7(5):335-46.
37. Pilzecker B, Buoninfante OA, Jacobs H. DNA damage tolerance in stem cells, ageing, mutagenesis, disease and cancer therapy. *Nucleic Acids Research.* 2019;47(14):7163-81.
38. Lv L, Wang F, Ma X, Yang Y, Wang Z, Liu H, et al. Mismatch repair protein MSH2 regulates translesion DNA synthesis following exposure of cells to UV radiation. *Nucleic Acids Res.* 2013;41(22):10312-22.





Chapter 6: Discussion and future perspectives



DNA replication is a complex process that can lead to mutagenesis and disease when performed incorrectly. This thesis aimed to investigate how mutagenesis induced by bulky, helix-distorting DNA damage is regulated with a particular focus on DNA mismatch repair (MMR), a pathway that removes replication errors made by replicative DNA polymerases. Contrary to undamaged DNA, helix-distorting DNA lesions are replicated by translesion synthesis (TLS) polymerases with a significantly lower fidelity. This led to the hypothesis that besides its canonical function, MMR may also control TLS-related DNA damage responses.

The work presented in **chapters 3 to 5** show that the four main MMR subunits, Msh2, Msh6, Mlh1 and Pms2, all participate in reducing mutagenesis caused by ultraviolet (UV) radiation and the dietary mutagen 2-Amino-1-methyl-6-phenylimidazo(4,5-b)pyridine (PhIP). Moreover, it was shown that loss of the Msh2/Msh6 heterodimer, also known as MutS α , resulted in loss of UV and PhIP-induced DNA damage signaling and a reduction in DNA damage-induced ssDNA formation. Interestingly, loss of the Mlh1/Pms2 heterodimer, also known as MutL α , showed no such phenotype, revealing an uncoupling of DNA damage signaling and mutagenesis induced by UV-light. The data in **Chapter 4** shows that the gene *Polh*, which encodes for the TLS polymerase eta (Pol η), and *Msh6* or *Mlh1* act synergistically with respect to suppressing UV-induced mutagenesis. Moreover, **Chapter 4** indicates that in *Polh*-defective cells *Mlh1* is not required for activating UV damage responses or for the formation of ssDNA, supporting the findings of **Chapter 3**.

This chapter aims to discuss these findings and to put them in a broader biological perspective. Thus, this chapter will discuss why only the four canonical MMR proteins are significantly involved in the DNA damage response, but not other MMR-related factors, such as the exonucleases and MMR homologs. Next, the findings regarding the uncoupling of UV-induced damage signaling and UV-induced mutagenesis are discussed, what role the two different MMR heterodimers, MutS α and MutL α , may play in these processes and how these findings relate to the observed cancer predisposition associated with defects in the four canonical MMR proteins. Furthermore, additional models are presented how MMR may control the DNA damage response, via (i) controlling the recruitment of TLS polymerases, (ii) reducing the mutagenicity of TLS, or (iii) controlling the activity of error-free template switching. Sporadic or inherited loss of MMR genes is associated with an increased risk of developing colorectal and endometrial cancer. As of yet, it remains unclear what causes this specific cancer tropism, since MMR should be important for suppressing mutagenesis in each replicating cell of the body. This chapter will elaborate on the possible causes of the cancer tropism associated with loss of MMR. Finally, this chapter closes with concluding remarks and advises carriers of dysfunctional MMR genes and their physicians to be mindful of the dangers of DNA damaging compounds.

Identifying genes involved in suppressing DNA damage-associated mutagenesis

Cells in the human body accumulate at least 50000 endogenous DNA lesions per day (1) and are also exposed to exogenous agents that induce DNA damage. In the past, numerous studies have been done to characterize the DNA damage response of the canonical MMR proteins Msh2, Msh6, Mlh1 and Pms2. It has been shown, using a variety of models, that MMR proteins are important in suppressing mutagenicity resulting from a broad range of DNA lesion types, including small base modifications due to methylation, ethylation and oxidation, but also from DNA lesions that distort the DNA helix, such as bulky lesions and intrastrand crosslinks (table 1). Together, these studies suggest that MMR proteins play an important role in protecting cells from the genotoxic effects of a wide variety of persistent base damages. The study described in **Chapter 3** extends these findings by measuring UV-induced mutagenesis in *Mlh1* and *Pms2*-deficient mouse embryonic stem cells (mESC). It was found that all four core MMR genes, *Msh2*, *Mlh1*, *Msh6* and *Pms2*, are important for suppressing UV-induced mutagenesis. However, canonical MMR requires not only the activity of these four core proteins, but often also requires exonuclease activity (2). Inactivating mutations in the exonucleases *Exo1* and *Fan1* did not increase UV-induced mutagenesis either. It was previously shown that deficiency for *Exo1* leads to upregulation of other exonucleases, such as Mre11, Artemis and Fan1 (3). Extensive redundancies among these exonucleases may be the reason that there is no apparent UV-induced phenotype in the *Exo1* deficient cells. Knock-out of any single exonuclease may be complemented with increased activity of the others. To that end, it may also be interesting to create double and even triple knock-out cell lines to study the role of exonucleases in the UV-induced damage response.

Table 1: Summary of known literature regarding the role of MMR in dealing with DNA damage induced mutagenesis (mutagenesis) and tumorigenesis (tumorigenesis).

Agent	DNA lesions	MMR defect	Cells	Reporter gene	Muta	Tumor	Ref
MMS	methylation	Mlh1	Human cancer cell line	<i>HPRT</i>	↑		(66, 67)
		Msh6	Human cancer cell line	<i>HPRT</i>	↑		(66, 67)
Temozolomide	methylation	Msh2	Mice			↑	(68)
MNNG	methylation	Msh6	Human cancer cell line	<i>HPRT</i>	↑		(69)
ENU	ethylation	Msh2	Mice and Mouse cells	<i>Hprt</i>	↑	↑	(70)
EMS	ethylation	Pms2	Mouse kidney cell line	<i>Aprt</i>	↑		(71)
H ₂ O ₂	oxidative	Pms2	Mouse kidney cell line	<i>Aprt</i>	↑		(71)
Cisplatin	crosslink	Msh2	Human cancer cell line	Acquired resistance assay	↑		(72)
Cisplatin	crosslink	Mlh1	Human cancer cell line	Acquired resistance assay	↑		(72)
UV	Intrastrand crosslink	Msh6	Chinese hamster cell line	Acquired resistance assay	↑		(73)
		Pms2	Chinese hamster cell line	Acquired resistance assay	↑		(73)
		Pms2	Mouse kidney cell line	<i>Aprt</i>	↑		(71)
		Msh2	Chinese hamster cell line	Acquired resistance assay	↑		(73)
		Msh2	Mice			↑	(74)
		Msh2	Mouse embryonic fibroblasts	<i>Hprt</i>	↑		(75)
		Msh6	Mouse embryonic stem cells	<i>Hprt</i>	↑		(11)
PhIP	bulky	Msh2	Human cancer cell line	<i>HPRT</i>	↑		(46)
		Mlh1	Human cancer cell line	<i>HPRT</i>	↑		(46)
		Msh6	Human cancer cell line	<i>HPRT</i>	↑		(46)
		Msh2	Mouse intestine in vivo	<i>lacI</i>	↑		(76)
		Mlh1	Mouse intestine in vivo	<i>cII</i>	↑		(77)
B[a]P	bulky	Msh2	Mice			↑	(78)

Exo1 is known to have both catalytic and structural domains that are suggested to play a role in the DNA damage response and MMR, respectively (4). It is important to note that the *Exo1* mutants in this thesis were generated by disrupting the catalytic domain resulting in mutants that still expressed mRNA which might encode for a truncated protein containing the structural domain. However, these *Exo1* mutants display tolerance to methylating agents such as N-methyl-N'-nitro-N-nitrosoguanidine (MNNG) (5), indicative for defective canonical MMR. Thus, the *Exo1* mutants described in this thesis are most likely functionally deficient for *Exo1*. For unknown reasons, however, an experiment to generate cell lines with a complete knock-out of the *Exo1* gene using CRISPR did not produce any viable clones.

Additionally, Pms1 and Mlh3 are MMR homologs that can bind to Mlh1 and may also play a role in the UV-induced DNA damage response (6). Previous publications have shown that the yeast ortholog of Pms1 co-localizes with Msh2/Msh6 and is important in activation of platinum-induced DNA damage responses (7). Moreover, a dominant *PMS1* mutation was found that conferred a mutator phenotype in human cells (8). For *Mlh3* it was previously observed that mice with an *Mlh3*-deficiency develop colon cancer at an increased rate (9) and that Mlh3 also seems to relocate to sites of UV-damage (10). **Chapter 3** investigated the role of these proteins and found that deficiency of either *Mlh3* or *Pms1* caused no apparent phenotype in mESC, thus these genes are seemingly not involved in any significant UV-induced DNA damage response. Previous work has also shown that the phenotypes induced by *Mlh3*-deficiency are minor and are exacerbated by additional loss of *Pms2* (9). Therefore, it may be that Mlh3 still plays a minor backup role for Pms2 and that a double knock-out cell line may reveal this additional functionality. Additionally, it may be of interest to investigate other MMR binding partners with respect to their role in the DNA damage response. For instance, it has previously been shown that in human cancer cell lines the MCM9 helicase was important for canonical MMR activity (11) and thus may be similarly involved in the MMR-mediated DNA damage responses. Likewise, the bloom helicase BLM binds directly to both human MSH6 and MLH1. Although BLM does not seem to be important for canonical MMR (12, 13), it may be involved in MMR-mediated DNA damage responses. Finally, it may also be of interest to study the role of DNA2, a nuclease that is known to play a role in Exo1-independent MMR and may also play a role in the MMR-mediated DNA damage response (14).

The uncoupling of DNA damage signaling and mutagenesis in MMR-deficient cells: consequences for colorectal cancer development?

Chapters 3 and 4 show that both MutS α and MutL α participate in the suppression of UV-induced mutagenesis. To obtain mechanistical insights in how these MMR genes control UV-induced mutagenesis, the spectrum of UV-induced mutations at the *Hprt* coding region in cell lines deficient for *Msh6* or *Mlh1* was studied (**chapter 3**). No difference was observed between the *Msh2* and *Mlh1*-deficient cell lines in terms of the kinds and types of mutations induced by UV light. Most of these mutations were

located at dipyrimidine sites, suggestive of *Msh6* and *Mlh1* working on misincorporations opposite UV lesions. However, also in unexposed cells most mutations occurred at dipyrimidine sites. Thus, from these data it cannot be concluded that UV-induced mutations were actually targeted at UV lesions. These mutational spectra analyses were restricted to the exons of the *Hprt* reporter gene encompassing a coding sequence of only 654 nucleotides. Therefore, studying the UV-induced mutational profile of MMR-deficient cells by using whole genome sequencing may be more informative. Nevertheless, previous work with *Msh6*-deficient cells showed that UV-induced mutations are predominantly targeted to a site-specific 6-4PP in a replicating plasmid (15). In addition, it has been shown that MutS α more strongly binds to incorrectly paired 6-4PPs rather than 6-4PPs that are paired with the correct bases (16, 17). Moreover, using antibodies that recognize CPDs (**Chapter 4**) or 6-4PPs (15) in ssDNA configuration, it was shown that loss of Msh6 resulted in less ssDNA gaps opposite UV-lesions, suggesting Msh6-mediated excision of ssDNA opposite UV-damaged DNA. Taken together, these data argue for a model in which misincorporations opposite UV lesions are removed by MMR, thereby suppressing UV-induced mutagenesis. To further evaluate the hypothesis that MMR excises replication errors opposite damaged DNA, additional experiments are of interest. Previous studies have shown that MutS α is able to bind various damaged DNA substrates, including those containing ‘mismatches’ opposite UV photolesions (16, 17) and O⁶-methylguanines (18) and substrates that contain cisplatin intrastrand crosslinks (18), deoxyguanosine adducts of aminofluorene and acetylaminofluorene (19), benzo[a]pyrene-7,8-hydrodiol-9,10-epoxide adducts at guanines (20) and benzo[c]phenanthrene adenines (21). It would be interesting to analyze whether MutS α can also recognize replication errors opposite PhIP-damaged guanines to support the findings summarized in **chapter 5**. Moreover, it would be of interest to study the structure of such a binding using crystallography to better understand how and why MutS α binds to (mis-)paired PhIP adducts. It would also be valuable to study MMR activity in the panel of MMR-deficient cell lines described in this thesis by using a replicating plasmid containing a site-specific UV-lesion or PhIP adduct, similar to what was previously published in *Msh6*-deficient cells (15). Finally, it may be of interest to perform *in vitro* experiments to measure MMR activity in nuclear extracts using a nicked DNA substrate that contains ‘matched’ or ‘mismatched’ nucleotides opposite a photolesion or PhIP adduct, reminiscent of the cell-free *in vitro* MMR activity (CIMRA) assay that measures G-T mismatch repair in a test tube (22).

The generation of UV-induced mutations is the outcome of a cellular response to unrepaired photolesions that includes, amongst others, the activation of the Atr/Chk1 and the Atm/Chk2 signaling axes, induced by the formation of ssDNA and double strand DNA breaks (DSB), respectively (23). While studying the phosphorylation of Chk1 and Kap-1 as markers for ssDNA and DSB-induced activation of DNA damage signaling (24, 25), an interesting observation was made: while loss of MutS α resulted in reduced UV-induced phosphorylation of Chk1 and Kap-1, loss of MutL α showed no such phenotype. This result suggests that MutS α mediates both formation of ssDNA

and DSB upon UV-irradiation, independent of MutL α . This suggestion was supported by studies on the UV-induced formation of chromatin-bound Rpa, indicative for the generation of ssDNA (**chapters 3 and 4**). Combined with an investigation of the level of UV lesions in ssDNA configuration, as a more direct measure of ssDNA gap formation opposite UV lesions, the results indicated that knock-out of *Mlh1* did not reduce the formation of UV-induced ssDNA. Taken together these data suggest an uncoupling of UV-induced mutagenesis and ssDNA formation in the case of *Mlh1* and *Pms2*-deficient cells. This is a puzzling finding, since in the canonical MMR model mutagenesis is controlled by removing the misincorporation, thus by generating ssDNA, in which MutL α is an important factor. The possible mechanisms that may explain the UV-induced activation of the Atr/Chk1 and the Atm/Chk2 signaling axes in the absence of MutL α are extensively discussed in **chapters 3 and 4**. These mechanisms include Msh2-dependent stimulation of Mre11-mediated degradation of nascent DNA at stalled replication forks, Mlh1-independent removal of misincorporations in the lagging strand and Exo1 hyper-excision of DNA in the absence of Mlh1. The latter was tested experimentally by inactivating *Exo1* in *Mlh1*-deficient cells. However, these double knock-out cells displayed only slightly reduced UV-induced damage signaling as compared to *Mlh1*-deficient cells (**Chapter 3**), indicating that Exo1 hyper-excision only slightly contributes to the activation of checkpoint signaling after UV exposure. Thus, additional experiments and considerations are required to better understand how MutL α controls UV-induced mutagenesis independent of activation of UV damage signaling.

Counterintuitively, the MutL α -independent activation of protective DNA damage signaling pathways contrasts strongly with the observation that germ line mutations in MLH1 or MSH2 are associated with a higher penetrance and earlier mean age of cancer onset than MSH6 or PMS2 mutations (26). In addition, **Chapter 5** shows that there is no significant difference among the four core MMR proteins in the level of protection against diet-derived PhIP-induced mutagenesis, which is thought to play a role in the development of CRC (see below). However, **chapter 5** also reveals that loss of Msh2 results in reduced PhIP-induced DNA damage signaling which may give Msh2-deficient cells a growth advantage. Thus, one interesting experiment for the future could be to grow a mixed population of wild-type and *Msh2*-deficient cells in the presence of a chronic low-dose of PhIP and monitor if *Msh2*-deficient cells will dominate the culture of cells over time. Recently, others have shown that a defect in MSH2 in colonic organoids or human embryonic stem cells results in reduced replication stress as well as a growth advantage compared to MMR-proficient cells (27). Reduced DNA damage signaling, hypermutability and a growth advantage of MSH2 defective cells may possibly explain the strong contribution of MSH2 carriers in the population of LS patients. In contrast to loss of MSH2, which renders cells completely defective in MMR, loss of MSH6 leads to a somewhat milder phenotype as these individuals still express the MSH2/MSH3 heterodimer involved in the recognition and removal of insertion-deletion loops. Possibly, for this reason carriers with a MSH6 mutation are less likely to contract CRC as compared to carriers with a MSH2 mutation.

But what about MLH1? As mentioned before, contrary to *Msh2* deficiency, *Mlh1*-deficient cells do activate DNA damage signaling (**Chapters 3 and 4**) that can result in decreased cell cycle progression (see also **chapter 4**), increased DNA repair and increased senescence or apoptosis in order to prevent mutagenesis and, consequently, tumorigenesis (28). Yet, *Mlh1*-deficient cells display hypermutability after exposure to UV light and other DNA damaging agents (**Chapters 3-5**, Table 1) and *Mlh1*-deficient mice show enhanced mutagenesis following PhIP exposure (Table 1). Together these data suggest that tumorigenesis in the absence of Mlh1 may occur more frequently, despite the activation of DNA damage signaling. This paradoxical phenotype is somewhat reminiscent of that found in UV-exposed mice containing a defect in TLS polymerase Rev1. Although a *Rev1* defect results in enhanced replication stress, increased DNA damage signaling and reduced mutagenesis (29), UV-exposed *Rev1*-mutated mice develop skin tumors much more rapidly than *Rev1*-proficient mice. This is accompanied with hyperproliferation in the skin and increased expression of IL-6, a cytokine that can stimulate cell proliferation in a paracrine fashion (29). Apparently, enhanced cell proliferation compensates for increased DNA damage signaling and reduced mutagenesis in the *Rev1*-mutant mouse skin. Interestingly, IL-6 signaling is triggered by the presence of cytosolic DNA (30) resulting from processing of ssDNA and DSB. Since *Mlh1*-deficient cells generate increased levels of ssDNA, and likely also DSB, following the formation of bulky and helix-distorting DNA damage (**chapters 3 and 4**), processing of ssDNA and DSB may result in the formation of cytosolic DNA (31). Consequently, it might be possible that Mlh1-deficient cells compensate for the anti-proliferative effects of checkpoint signaling by enhancing cell proliferation via the expression of cytokines such as IL-6. Thus, the higher risk for developing CRC in carriers with an *MLH1* mutation might be explained by (i) DNA damage-induced hypermutagenesis in *Mlh1*-deficient cells and (ii) enhanced cell proliferation that is promoted following the formation of cytosolic DNA derived from processed ssDNA and collapsed replication forks.

Post-replicative control of DNA damage-induced mutagenesis

Persistent DNA damage induces mutations in the genome via different routes. Unreplicated ssDNA formations may become DSB resulting in genomic alterations when repaired in an error-prone fashion (32), DNA repair pathways can be error-prone (33) and DNA damage tolerance pathways may bypass the damaged DNA incorrectly (34). **Chapter 4** investigated how MMR may control the mutagenicity of TLS and two hypotheses were formulated: MMR-dependent recruitment of the “correct” TLS polymerases or MMR-dependent excision of TLS errors. **Chapter 4** concluded that neither model is an exact fit and that the two models may be interwoven; MMR-mediated excision of TLS-induced misincorporations will activate DNA damage signaling, cell cycle arrest and DNA repair to prevent excessive mutagenesis in surviving cells, whilst post-excision recruitment of “correct” TLS polymerases by MutSα may quench DNA damage signaling and, in addition, prevent mutagenesis.

As an alternative to TLS, cells can employ replication fork reversal and template switching to bypass replication-blocking DNA lesions. Template switching prevents DNA damage-induced mutagenesis and involves recombination of a nascent strand with the complementary, newly synthesized strand of the sister chromatid. Although template switching in mammalian cells is still poorly understood, template switching in yeast depends on the Rad5 protein (35). Rad5 is an E3 ubiquitin ligase as well as a DNA helicase that catalyzes fork reversal and strand invasion. Recently, it was not only shown that both yeast Msh2 and Mlh1 interact with Rad5 but also that the human homologs of Rad5, HLTf and SHPRH, are binding partners of MSH2 and MLH1, respectively (36). Although the biological relevance of these interactions is still unclear, it should be noted that HLTf and SHPRH prevent mutagenesis in a DNA damage-specific manner: HLTf suppresses UV-induced mutagenesis, whereas SHPRH contributes in suppressing methylation-induced mutagenesis (37, 38). Experimental evidence suggests that (i) HLTf might stimulate the recruitment of Pol η to allow relatively error-free bypass of UV damage, (ii) HLTf might prevent the interaction of SHPRH with error-prone Pol κ at UV damage, and (iii) SHPRH can interact with Pol κ , which acts relatively error-free at methylation damage (38). In addition, HLTf, like Rad5, can reverse stalled replication forks resulting in chicken foot structures that allow bypass of DNA damage in an error-free fashion. Furthermore, HLTf promotes strand invasion and D-loop formation that are intermediates during template switching (39). The interactions of MMR proteins with HLTf and SHPRH could play two important roles in suppressing DNA damage-induced mutagenesis. First, following the recognition of 'compound lesions' caused by error-prone TLS across nucleotide lesions, MMR proteins may stimulate error-free TLS by recruiting Pol η or Pol κ via HLTf or SHPRH. Second, recognition of 'compound lesions' by MutS α may activate HLTf-mediated fork reversal or template switching. It may be of interest to perform follow-up studies by knocking-out HLTf and SHPRH in MMR-proficient mESC as well as in cells defective for MutS α or MutL α and analyze mutagenic and signaling responses following UV irradiation.

Aberrant responses to food-derived DNA damage and the Lynch syndrome tropism

The narrow colorectal/endometrial cancer tropism of LS is an interesting phenomenon. Lynch syndrome is caused by loss of MMR in individuals who inherited one dysfunctional copy of an MMR gene (26). In principle, tissue types with many proliferating cells should all be affected as these tissues will garner many replication errors that are substrate for MMR. Yet, cancer in the hematopoietic system, where cells are constantly dividing to create mature blood and immune cells (40), is infrequently found in LS patients. To make matters even more interesting, inheriting not one but two faulty copies of a MMR gene (also known as constitutional MMR deficiency) does predispose carriers to a large range of cancers in highly dividing tissues, including the hematopoietic system and the (still developing, young) brain (41).

The answer to what causes the LS tropism may be found in what sets the gastro-intestinal tissue apart from the others: cells of the gastro-intestinal tract are continuously exposed to DNA reactive metabolites derived from food substances. In LS patients these DNA damaging agents may inactivate the remaining, functional, copy of the MMR gene and thus kickstart hyper-mutagenesis in intestinal cells. This hypothesis was tested in **chapter 5** in which a mESC model that mimics the LS cell situation was used to investigate whether the diet-derived mutagen PhIP may inactivate MMR. Indeed, exposing cells, hemizygous for *Msh2* or *Mlh1*, to PhIP resulted in a significantly higher frequency of MMR-deficient cells than PhIP-exposed wild-type cells. This finding may already partly explain the tropism found in LS individuals. However, the gastro-intestinal tract is not the only rapidly dividing tissue exposed to DNA damaging agents. The skin is also a rapidly dividing tissue and often exposed to UV light from solar radiation. So why do individuals with LS not develop skin malignancies? In fact, approximately 10% of individuals with LS do develop sebaceous skin tumors, a syndrome called Muir-Torre (42). Moreover, constitutional MMR deficiency is associated with sunlight-induced skin cancer in mice (43). The difference in incidence between skin and colorectal tumors in LS may be caused by the rate of cell division, which will invariably influence the rate of replication-associated mutagenesis. In normal epidermis the cell proliferation rate is approximately one cell division every 13 days (44), whereas colonic stem cells divide roughly every 2 days (45). As such MMR may play a much more important role in protecting against DNA damage-induced mutagenesis in the colorectal tract than in the skin.

Apart from inactivating MMR, PhIP may also play a role in increasing the mutational burden in MMR-deficient cells, thus further accelerating carcinogenesis. Previously, it was found by Glaab *et al.* that MMR-deficient cancer cell lines had increased levels of PhIP-induced mutagenesis compared to MMR-proficient cancer cell lines (46). **Chapter 5** further corroborates and expands upon this finding by exposing a complete panel of MMR-deficient mESC lines to PhIP. It was shown that under the experimental conditions used, 50 to 90% of all PhIP-induced mutations are suppressed by the four core MMR proteins, indicating a major role for the pathway in protecting against diet-induced mutagenesis. In contrast, *Msh3* played no significant role in suppressing PhIP-induced mutagenesis. The mutational profile described in **chapter 5** shows that the PhIP-induced mutations were primarily G>T and G>A mutations, in line with previously published literature (46). Interestingly, a recent publication showed that LS tumors contain mutations mainly encompassing the COSMIC mutational fingerprints SBS1, SBS20 and SBS44 (47), which are largely characterized by G>T and G>A mutations. As such, these mutational fingerprints may be in part attributed to PhIP-exposure. Yet, other signatures are sometimes found as well, such as SBS5 that shows a mutational profile which is not at all dominated by one or two types of SBS, but is instead more varied (47). It is important to realize that the gastro-intestinal tract is not solely exposed to PhIP, but also to other mutagens from the diet (48), the microbiome (49) and bile (50, 51). This complicates the effort to correlate a spectrum of mutation in colorectal tumor DNA with exposure to specific mutagenic agents, especially considering the

status of DNA repair pathways, differential cell proliferation rates and pre-existing mutations. Therefore, a one-to-one mapping of a single genotoxin to a mutational profile should be avoided.

If exposure of colonic cells to DNA damaging agents is at the root of the Lynch tropism, what then underlies the formation of endometrial cancers (EC) associated with LS? Endometrial cells are often exposed to high levels of hormones, such as estrogen, that are known to indirectly damage the DNA (52-54). Upon oxidation, estrogens can be converted in reactive quinones that bind to guanine and adenine bases (52, 55). These base modifications are chemically unstable resulting in non-instructive abasic sites (55), which can lead to mutations upon bypass by TLS (56). In addition, estrogen quinones can induce oxidative DNA damage which may provoke mutagenesis (52). Possibly, estrogen-induced misincorporations might be recognized and excised by MMR, similar to the excision of misincorporations opposite other lesions such as those induced by PhIP and UV light. As such MMR may play an important role in suppressing estrogen-induced mutagenesis. For this reason, loss of MMR in endometrial cells may explain the high incidence of endometrial cancers in LS carriers. Moreover, previous studies have also shown that exposure to estrogen upregulates MLH1 expression, suggesting a role for MMR in regulating the outcomes of estrogen exposure (57).

Taken together, as stated in **chapter 5**, food-derived DNA damage may influence the LS cancer tropism by a three-step process: (i) PhIP-induced mutational inactivation of the remaining wild-type MMR gene, (ii) reduced DNA damage signaling as a consequence of MutS α deficiency and (iii) loss of protective MMR resulting in PhIP-induced hypermutagenesis. However, further studies should be done to corroborate these findings and place them in a broader biological perspective. The work of this thesis was performed using mESCs, but it is important to validate the findings in different models to assess their biological relevance. For instance, now that human inducible pluripotent stem cells have been more widely adopted, this model may also be used to create Lynch-like cell lines. Indeed, it would be valuable to investigate whether PhIP can cause MMR-deficiency and accelerate mutagenesis in cells originating from an actual LS patient. Cell models are important tools in biological research, yet they will always lack the complexity of tissues, *i.e.* the 3D structures, different cell types and immune micro-environments. Thus, it would be important to reproduce the experiments with PhIP using *in vivo* mouse models to increase the biological relevance of the findings described in **chapter 5** even further. These findings can also be further expanded upon by performing epidemiological studies. Previously it was already shown that intake of red and processed meat increases the risk of developing CRC (58, 59). Furthermore, some studies have shown that in LS carriers dietary patterns, such as diets with high amounts of fat or meat, may slightly influence CRC incidence (60) or cancer incidence in general (61), whereas others find no significant differences (62). As such, it would be valuable to further investigate which dietary patterns are influencing cancer incidence in LS carriers by doing more extensive population studies with LS carriers and tracking their lifestyles in-depth.

Concluding remarks

The work presented in this thesis showed that the core MMR genes are invaluable for suppressing DNA damage-induced mutagenesis and as such safeguard the genome against the harmful consequences of TLS errors. Moreover, this thesis investigated what other genes are important in the suppression of DNA damage-induced mutagenesis and showed how MMR might contribute to activate DNA damage signaling. Here, an interesting new model is presented that may answer long standing questions about how MMR regulates DNA damage responses, namely, that suppression of DNA damage-induced mutagenesis is the result of MMR-mediated excision of TLS errors in combination with MMR-dependent recruitment of “correct” TLS polymerases or with MMR-dependent promotion of error-free template switching.

The work presented here also studied the DNA damage responses induced by MMR in a more clinically relevant setting by investigating the effect of PhIP, an intestinal mutagen, in a cell-based model of LS. Diet-derived mutagens accelerated the loss of the remaining wild-type copy of the affected MMR gene in Lynch-like cells. Subsequently, complete loss of MMR further increased mutagenesis coming from the same diet-derived mutagen and quenched the protective DNA damage signaling. This fundamental work may also have important implications for carriers of LS, which are at greater risk of losing the MMR pathway and are predisposed to develop colorectal cancer. To minimize the risk of developing colorectal cancer, these individuals may be advised to modulate their lifestyles in order to reduce the exposure to DNA damaging agents, for instance found in the diet. It may be of interest for individuals affected by LS to adopt a vegetarian lifestyle, but to also avoid other products known to contain DNA damaging agents, such as aflatoxins found in long storage food products, e.g. nuts and dried fruits (63). Moreover, if meat is consumed, preparation is key. Using the right herbs and cooking the meat at low temperatures reduces the amount of DNA damaging agents (64). Interestingly, a recent study has shown that consumption of resistant starch, found in for instance bananas, potatoes and grains, reduced extracolonic tumor formation in LS patients (61). Resistant starch is hypothesized to reduce total bile acid levels, a known mutagen that induces oxidative DNA damage (51), and as such the negative effect of post-TLS repair deficiency may be reduced (65). Collecting such studies about diet and lifestyle factors into one large compendium may be an interesting venture for further research to better advise LS carriers.

References

1. Nakamura J, Mutlu E, Sharma V, Collins L, Bodnar W, Yu R, et al. The endogenous exposome. *DNA Repair (Amst)*. 2014;19:3-13.
2. Zhang Y, Yuan F, Presnell SR, Tian K, Gao Y, Tomkinson AE, et al. Reconstitution of 5'-Directed Human Mismatch Repair in a Purified System. *Cell*. 2005;122(5):693-705.
3. Desai A, Gerson S. Exo1 independent DNA mismatch repair involves multiple compensatory nucleases. *DNA Repair (Amst)*. 2014;21:55-64.
4. Schaezlein S, Chahwan R, Avdievich E, Roa S, Wei K, Eoff RL, et al. Mammalian Exo1 encodes both structural and catalytic functions that play distinct roles in essential biological processes. *Proc Natl Acad Sci U S A*. 2013;110(27):E2470-9.
5. Klapacz J, Meira LB, Luchetti DG, Calvo JA, Bronson RT, Edelmann W, et al. O6-methylguanine-induced cell death involves exonuclease 1 as well as DNA mismatch recognition in vivo. *Proc Natl Acad Sci U S A*. 2009;106(2):576-81.
6. Kolodner RD, Marsischky GT. Eukaryotic DNA mismatch repair. *Curr Opin Genet Dev*. 1999;9(1):89-96.
7. Durant ST, Morris MM, Illand M, McKay HJ, McCormick C, Hirst GL, et al. Dependence on RAD52 and RAD1 for anticancer drug resistance mediated by inactivation of mismatch repair genes. *Current biology : CB*. 1999;9(1):51-4.
8. Reyes GX, Zhao B, Schmidt TT, Gries K, Kloor M, Hombauer H. Identification of MLH2/hPMS1 dominant mutations that prevent DNA mismatch repair function. *Communications biology*. 2020;3(1):751.
9. Chen PC, Dudley S, Hagen W, Dizon D, Paxton L, Reichow D, et al. Contributions by MutL homologues Mlh3 and Pms2 to DNA mismatch repair and tumor suppression in the mouse. *Cancer Res*. 2005;65(19):8662-70.
10. Roesner LM, Mielke C, Fahnrich S, Merkhoffer Y, Dittmar KE, Drexler HG, et al. Stable expression of MutLgamma in human cells reveals no specific response to mismatched DNA, but distinct recruitment to damage sites. *Journal of cellular biochemistry*. 2013;114(10):2405-14.
11. Traver S, Coulombe P, Peiffer I, Hutchins JR, Kitzmann M, Latreille D, et al. MCM9 Is Required for Mammalian DNA Mismatch Repair. *Mol Cell*. 2015;59(5):831-9.
12. Pedrazzi G, Bachrati CZ, Selak N, Studer I, Petkovic M, Hickson ID, et al. The Bloom's syndrome helicase interacts directly with the human DNA mismatch repair protein hMSH6. *Biol Chem*. 2003;384(8):1155-64.
13. Langland G, Kordich J, Creaney J, Goss KH, Lillard-Wetherell K, Bebenek K, et al. The Bloom's syndrome protein (BLM) interacts with MLH1 but is not required for DNA mismatch repair. *J Biol Chem*. 2001;276(32):30031-5.
14. Kadyrova LY, Dahal BK, Gujar V, Daley JM, Sung P, Kadyrov FA. The nuclease activity of DNA2 promotes exonuclease 1-independent mismatch repair. *J Biol Chem*. 2022;298(4):101831.
15. Tsaalbi-Shlylik A, Ferras C, Pauw B, Hendriks G, Temviriyankul P, Carlee L, et al. Excision of translesion synthesis errors orchestrates responses to helix-distorting DNA lesions. *J Cell Biol*. 2015;209(1):33-46.
16. Wang H, Lawrence CW, Li GM, Hays JB. Specific binding of human MSH2.MSH6 mismatch-repair protein heterodimers to DNA incorporating thymine- or uracil-containing UV light photoproducts opposite mismatched bases. *J Biol Chem*. 1999;274(24):16894-900.
17. Mu D, Tursun M, Duckett DR, Drummond JT, Modrich P, Sancar A. Recognition and repair of compound DNA lesions (base damage and mismatch) by human mismatch repair and excision repair systems. *Mol Cell Biol*. 1997;17(2):760-9.
18. Duckett DR, Drummond JT, Murchie AI, Reardon JT, Sancar A, Lilley DM, et al. Human MutSalphalpha recognizes damaged DNA base pairs containing O6-methylguanine, O4-methylthymine, or the cisplatin-d(GpG) adduct. *Proc Natl Acad Sci U S A*. 1996;93(13):6443-7.
19. Li GM, Wang H, Romano LJ. Human MutSalphalpha specifically binds to DNA containing aminofluorene and acetylaminofluorene adducts. *J Biol Chem*. 1996;271(39):24084-8.
20. Wu J, Gu L, Wang H, Geacintov NE, Li GM. Mismatch repair processing of carcinogen-DNA adducts triggers apoptosis. *Mol Cell Biol*. 1999;19(12):8292-301.
21. Wu J, Zhu BB, Yu J, Zhu H, Qiu L, Kindy MS, et al. In vitro and in vivo modulations of benzo[c]phenanthrene-DNA adducts by DNA mismatch repair system. *Nucleic Acids Res*. 2003;31(22):6428-34.
22. Drost M, Zonneveld J, van Dijk L, Morreau H, Tops CM, Vasen HF, et al. A cell-free assay for the functional analysis of variants of the mismatch repair protein MLH1. *Hum Mutat*. 2010;31(3):247-53.
23. Lanz MC, Dibitetto D, Smolka MB. DNA damage kinase signaling: checkpoint and repair at 30 years. *EMBO J*. 2019;38(18):e101801.
24. Smith J, Tho LM, Xu N, Gillespie DA. The ATM-Chk2 and ATR-Chk1 pathways in DNA damage signaling and cancer. *Advances in cancer research*. 2010;108:73-112.
25. Federico MB, Vallerga MB, Radl A, Paviolo NS, Bocco JL, Di Giorgio M, et al. Chromosomal Integrity after UV Irradiation Requires FANCD2-Mediated Repair of Double Strand Breaks. *PLoS Genet*. 2016;12(1):e1005792.
26. Lynch HT, Snyder CL, Shaw TG, Heinen CD, Hitchins MP. Milestones of Lynch syndrome: 1895–2015. *Nature Reviews Cancer*. 2015;15(3):181-94.
27. Madden-Hennessey K, Gupta D, Radecki AA, Guild C, Rath A, Heinen CD. Loss of mismatch repair promotes a direct selective advantage in human stem cells. *Stem cell reports*. 2022;17(12):2661-73.
28. Blackford AN, Jackson SP. ATM, ATR, and DNA-PK: The Trinity at the Heart of the DNA Damage Response. *Mol Cell*. 2017;66(6):801-17.

29. Tsaalbi-Shtylik A, Verspuy JW, Jansen JG, Rebel H, Carlee LM, van der Valk MA, et al. Error-prone translesion replication of damaged DNA suppresses skin carcinogenesis by controlling inflammatory hyperplasia. *Proc Natl Acad Sci U S A*. 2009;106(51):21836-41.
30. Hong C, Schubert M, Tijhuis AE, Requesens M, Roorda M, van den Brink A, et al. cGAS-STING drives the IL-6-dependent survival of chromosomally unstable cancers. *Nature*. 2022;607(7918):366-73.
31. Guan J, Lu C, Jin Q, Lu H, Chen X, Tian L, et al. MLH1 Deficiency-Triggered DNA Hyperexcision by Exonuclease 1 Activates the cGAS-STING Pathway. *Cancer Cell*. 2021;39(1):109-21 e5.
32. Liao H, Ji F, Helleday T, Ying S. Mechanisms for stalled replication fork stabilization: new targets for synthetic lethality strategies in cancer treatments. *EMBO reports*. 2018;19(9).
33. Bunting SF, Nussenzweig A. End-joining, translocations and cancer. *Nature reviews Cancer*. 2013;13(7):443-54.
34. Chang DJ, Cimprich KA. DNA damage tolerance: when it's OK to make mistakes. *Nature chemical biology*. 2009;5(2):82-90.
35. Motegi A, Liaw HJ, Lee KY, Roest HP, Maas A, Wu X, et al. Polyubiquitination of proliferating cell nuclear antigen by HLTf and SHPRH prevents genomic instability from stalled replication forks. *Proc Natl Acad Sci U S A*. 2008;105(34):12411-6.
36. Miller AK, Mao G, Knicely BG, Daniels HG, Rahal C, Putnam CD, et al. Rad5 and Its Human Homologs, HLTf and SHPRH, Are Novel Interactors of Mismatch Repair. *Frontiers in cell and developmental biology*. 2022;10:843121.
37. Seelinger M, Sogaard CK, Otterlei M. The Human RAD5 Homologs, HLTf and SHPRH, Have Separate Functions in DNA Damage Tolerance Dependent on The DNA Lesion Type. *Biomolecules*. 2020;10(3).
38. Lin JR, Zeman MK, Chen JY, Yee MC, Cimprich KA. SHPRH and HLTf act in a damage-specific manner to coordinate different forms of postreplication repair and prevent mutagenesis. *Mol Cell*. 2011;42(2):237-49.
39. Kondratyck CM, Washington MT, Spies M. Making Choices: DNA Replication Fork Recovery Mechanisms. *Semin Cell Dev Biol*. 2021;113:27-37.
40. Orkin SH, Zon LI. Hematopoiesis: an evolving paradigm for stem cell biology. *Cell*. 2008;132(4):631-44.
41. Lavoine N, Colas C, Muleris M, Bodo S, Duval A, Entz-Werle N, et al. Constitutional mismatch repair deficiency syndrome: clinical description in a French cohort. *Journal of Medical Genetics*. 2015;52(11):770-8.
42. Le S, Ansari U, Mumtaz A, Malik K, Patel P, Doyle A, et al. Lynch Syndrome and Muir-Torre Syndrome: An update and review on the genetics, epidemiology, and management of two related disorders. *Dermatol Online J*. 2017;23(11).
43. Young LC, Thulien KJ, Campbell MR, Tron VA, Andrew SE. DNA mismatch repair proteins promote apoptosis and suppress tumorigenesis in response to UVB irradiation: an in vivo study. *Carcinogenesis*. 2004;25(10):1821-7.
44. Weinstein GD, McCullough JL, Ross P. Cell proliferation in normal epidermis. *The Journal of investigative dermatology*. 1984;82(6):623-8.
45. Potten CS, Kellett M, Rew DA, Roberts SA. Proliferation in human gastrointestinal epithelium using bromodeoxyuridine in vivo: data for different sites, proximity to a tumour, and polyposis coli. *Gut*. 1992;33(4):524-9.
46. Glaab WE, Skopek TR. Cytotoxic and mutagenic response of mismatch repair-defective human cancer cells exposed to a food-associated heterocyclic amine. *Carcinogenesis*. 1999;20(3):391-4.
47. Lee BCH, Robinson PS, Coorens THH, Yan HHN, Olafsson S, Lee-Six H, et al. Mutational landscape of normal epithelial cells in Lynch Syndrome patients. *Nat Commun*. 2022;13(1):2710.
48. Cantwell M, Elliott C. Nitrates, Nitrites and Nitrosamines from Processed Meat Intake and Colorectal Cancer Risk. *Journal of Clinical Nutrition & Dietetics*. 2017;3:4-27.
49. Belcheva A, Irrazabal T, Susan, Streutker C, Maughan H, Rubino S, et al. Gut Microbial Metabolism Drives Transformation of Msh2-Deficient Colon Epithelial Cells. *Cell*. 2014;158(2):288-99.
50. Jia W, Xie G, Jia W. Bile acid-microbiota crosstalk in gastrointestinal inflammation and carcinogenesis. *Nat Rev Gastroenterol Hepatol*. 2018;15(2):111-28.
51. Bernstein H, Bernstein C, Payne CM, Dvorak K. Bile acids as endogenous etiologic agents in gastrointestinal cancer. *World J Gastroenterol*. 2009;15(27):3329-40.
52. Yager JD. Endogenous estrogens as carcinogens through metabolic activation. *Journal of the National Cancer Institute Monographs*. 2000(27):67-73.
53. Rodriguez AC, Blanchard Z, Maurer KA, Gertz J. Estrogen Signaling in Endometrial Cancer: a Key Oncogenic Pathway with Several Open Questions. *Hormones & cancer*. 2019;10(2-3):51-63.
54. Caldon CE. Estrogen signaling and the DNA damage response in hormone dependent breast cancers. *Front Oncol*. 2014;4:106.
55. Convert O, Van Aerden C, Debrauwer L, Rathahao E, Molines H, Fournier F, et al. Reactions of estradiol-2,3-quinone with deoxyribonucleosides: possible insights in the reactivity of estrogen quinones with DNA. *Chem Res Toxicol*. 2002;15(5):754-64.
56. Thompson PS, Cortez D. New insights into abasic site repair and tolerance. *DNA Repair (Amst)*. 2020;90:102866.
57. Lu JY, Jin P, Gao W, Wang DZ, Sheng JQ. Estrogen enhances mismatch repair by induction of MLH1 expression via estrogen receptor-beta. *Oncotarget*. 2017;8(24):38767-79.
58. Sinha R, Rothman N. Role of well-done, grilled red meat, heterocyclic amines (HCAs) in the etiology of human cancer. *Cancer letters*. 1999;143(2):189-94.

59. Bouvard V, Loomis D, Guyton KZ, Grosse Y, Ghissassi FE, Benbrahim-Tallaa L, et al. Carcinogenicity of consumption of red and processed meat. *The Lancet Oncology*. 2015;16(16):1599-600.
60. Botma A, Vasen HFA, Van Duijnhoven FJB, Kleibeuker JH, Nagengast FM, Kampman E. Dietary patterns and colorectal adenomas in Lynch syndrome. *Cancer*. 2013;119(3):512-21.
61. Mathers JC, Elliott F, Macrae F, Mecklin JP, Moslein G, McDonald FE, et al. Cancer Prevention with Resistant Starch in Lynch Syndrome Patients in the CAPP2-Randomized Placebo Controlled Trial: Planned 10-Year Follow-up. *Cancer Prev Res (Phila)*. 2022;15(9):623-34.
62. Eijkelboom AH, Brouwer JGM, Vasen HFA, Bisseling TM, Koornstra JJ, Kampman E, et al. Diet quality and colorectal tumor risk in persons with Lynch syndrome. *Cancer epidemiology*. 2020;69:101809.
63. Macri AM, Pop I, Simeanu D, Toma D, Sandu I, Pavel LL, et al. The Occurrence of Aflatoxins in Nuts and Dry Nuts Packed in Four Different Plastic Packaging from the Romanian Market. *Microorganisms*. 2020;9(1).
64. Gibis M. Heterocyclic Aromatic Amines in Cooked Meat Products: Causes, Formation, Occurrence, and Risk Assessment. *Comprehensive reviews in food science and food safety*. 2016;15(2):269-302.
65. Ijsselstein R, Jansen JG, De Wind N. DNA mismatch repair-dependent DNA damage responses and cancer. *DNA Repair*. 2020;93:102923.
66. Glaab WE, Tindall KR, Skopek TR. Specificity of mutations induced by methyl methanesulfonate in mismatch repair-deficient human cancer cell lines. *Mutat Res*. 1999;427(2):67-78.
67. Glaab WE, Risinger JI, Umar A, Barrett JC, Kunkel TA, Tindall KR. Cellular resistance and hypermutability in mismatch repair-deficient human cancer cell lines following treatment with methyl methanesulfonate. *Mutat Res*. 1998;398(1-2):197-207.
68. Wojciechowicz K, Cantelli E, Van Gerwen B, Plug M, Van Der Wal A, Delzenne-Goette E, et al. Temozolomide Increases the Number of Mismatch Repair-Deficient Intestinal Crypts and Accelerates Tumorigenesis in a Mouse Model of Lynch Syndrome. *Gastroenterology*. 2014;147(5):1064-72.e5.
69. Goldmacher VS, Cuzick RA, Jr., Thilly WG. Isolation and partial characterization of human cell mutants differing in sensitivity to killing and mutation by methylnitrosourea and N-methyl-N'-nitro-N-nitrosoguanidine. *J Biol Chem*. 1986;261(27):12462-71.
70. Claij N, van der Wal A, Dekker M, Jansen L, te Riele H. DNA mismatch repair deficiency stimulates N-ethyl-N-nitrosourea-induced mutagenesis and lymphomagenesis. *Cancer Res*. 2003;63(9):2062-6.
71. Shin-Darlak CY, Skinner AM, Turker MS. A role for Pms2 in the prevention of tandem CC → TT substitutions induced by ultraviolet radiation and oxidative stress. *DNA Repair (Amst)*. 2005;4(1):51-7.
72. Lin X, Howell SB. Effect of loss of DNA mismatch repair on development of topotecan-, gemcitabine-, and paclitaxel-resistant variants after exposure to cisplatin. *Molecular pharmacology*. 1999;56(2):390-5.
73. Nara K, Nagashima F, Yasui A. Highly elevated ultraviolet-induced mutation frequency in isolated Chinese hamster cell lines defective in nucleotide excision repair and mismatch repair proteins. *Cancer Res*. 2001;61(1):50-2.
74. Meira LB, Cheo DL, Reis AM, Claij N, Burns DK, te Riele H, et al. Mice defective in the mismatch repair gene Msh2 show increased predisposition to UVB radiation-induced skin cancer. *DNA Repair (Amst)*. 2002;1(11):929-34.
75. Borgdorff V, Pauw B, van Hees-Stuivenberg S, de Wind N. DNA mismatch repair mediates protection from mutagenesis induced by short-wave ultraviolet light. *DNA Repair (Amst)*. 2006;5(11):1364-72.
76. Zhang S, Lloyd R, Bowden G, Glickman BW, de Boer JG. Msh2 DNA mismatch repair gene deficiency and the food-borne mutagen 2-amino-1-methyl-6-phenylimidazo [4,5-b] pyridine (PhIP) synergistically affect mutagenesis in mouse colon. *Oncogene*. 2001;20(42):6066-72.
77. Smith-Roe SL, Hegan DC, Glazer PM, Buermeyer AB. Mlh1-dependent suppression of specific mutations induced in vivo by the food-borne carcinogen 2-amino-1-methyl-6-phenylimidazo [4,5-b] pyridine (PhIP). *Mutat Res*. 2006;594(1-2):101-12.
78. Zienolddiny S, Ryberg D, Svendsrud DH, Eilertsen E, Skaug V, Hoyer A, et al. Msh2 deficiency increases susceptibility to benzo[a]pyrene-induced lymphomagenesis. *International Journal of Cancer*. 2006;118(11):2899-902.





Chapter &: Summary, Samenvatting, Curriculum Vitae, Dankwoord



Summary

Mutagenesis, the process that generates alterations in the DNA sequence, underlies many serious illnesses plaguing mankind, most notably cancer. Mutagenesis often occurs during DNA replication and **Chapter 1** discusses in detail the workings of this process. In short: during the replication of double-stranded DNA, the DNA double-helix is unwound allowing for the duplication of both strands by replicative DNA polymerases. When a replicative polymerase incorporates an incorrect nucleotide during DNA replication a 'mismatch' is generated which can lead to a mutation in the next replication cycle. DNA mismatch repair (MMR) can detect and remove these mismatches thereby preventing mutations in the DNA. **Chapter 1** describes how the MMR process on base-base mismatches works: the MMR-proteins MSH2 and MSH6 form a heterodimer that is able to recognize mismatches and subsequently recruit a heterodimer consisting of MLH1 and PMS2 to generate a nick in the DNA-strand containing the misincorporation. Finally, EXO1 is recruited to excise a part of the newly generated strand, including the mismatch. However, the necessity of EXO1 in the MMR pathway is being debated as other nucleases, amongst which FAN1, could possibly substitute for EXO1 if EXO1 is not available. Other proteins may also play a role in the MMR pathway, such as PMS1 and MLH3. These proteins are homologs of MLH1 and PMS2, but their exact role is, as of yet, unclear. Furthermore, loss of PMS1 or MLH3 does not lead to MMR-deficiency. In essence, there are four MMR core-genes, *MSH2*, *MSH6*, *MLH1*, *PMS2*. Loss of any of these genes leads to MMR-deficiency resulting in hyper-mutagenesis and an increased risk of cancer. Furthermore, **Chapter 1** describes the different types of DNA damage and the associated DNA repair pathways. DNA damage alters the DNA structure, and when left unrepaired, it leads to replicative blocks that activate DNA damage signaling, and ultimately results in cell death. However, DNA damage signaling can also activate DNA damage tolerance mechanisms, such as translesion synthesis (TLS). TLS is performed by so-called TLS polymerases that can replicate damaged DNA thereby quenching DNA damage signaling and preventing cell death. However, TLS polymerases are error-prone which leads to increased mutagenesis. Our cellular DNA is constantly threatened by DNA damaging agents, for instance found in the diet, thus it is advantageous to suppress TLS-induced mutagenicity as much as possible. This thesis investigated whether the MMR pathway could be involved in reducing mutagenesis from DNA damaging agents by controlling TLS and DNA damage responses.

Chapter 2 is a graphical review that summarizes the role of MMR in dealing with responses associated with DNA damage. MMR plays an unmistakable role in four different lesion types: alkylation, oxidation, interstrand crosslinks, and helix-distorting. Loss of MMR can result in increased resistance to these various lesion types and often leads to increased mutagenicity. Additionally, **Chapter 2** details the implications of loss of MMR for cancer development and treatment. DNA-damaging agents are commonly used to combat cancer, but loss of MMR may increase resistance to such drugs and may even result in an environment where pre-cancerous MMR-deficient cells can thrive, leading to the formation of new tumors. Furthermore, in **Chapter 2** it is

hypothesized that individuals with Lynch syndrome (LS), a cancer predisposition syndrome caused by the inheritance of one dysfunctional copy of an MMR gene, are at greater risk from the adverse effects of DNA-damaging agents.

Chapter 2 described the important role of MMR in reducing the adverse effects of DNA damaging agents, such as mutagenesis and loss of DNA damage signaling. However, several questions remained: (i) how does MMR reduce mutagenesis from DNA damaging agents, (ii) how does MMR contribute to activation of damage signaling, and (iii) which MMR-related proteins play a role in dealing with DNA damage? The aim of **Chapter 3** was to answer these questions by generating a panel of isogenic mouse embryonic stem cell lines deficient for *Msh6*, *Mlh1*, *Pms2*, *Exo1*, *Fan1*, *Mlh3* or *Pms1* and exposing these cells to mutagenic ultraviolet (UV) radiation. All these cell lines contained an additional *Xpa*-deficiency to prevent the repair of UV lesions. **Chapter 3** describes that *Msh6*, *Mlh1*, and *Pms2* protect against UV-induced mutagenesis, but the other investigated genes do not show such a phenotype. In the case of *Exo1* and *Fan1*, this may be because these genes are redundant with other exonucleases. The same can be said for the MMR homologs *Mlh3* and *Pms1*; these genes may share functional redundancy with *Pms2*. Moreover, **Chapter 3** confirmed previously published data that *Msh6*-deficient cells have greatly reduced UV-induced DNA damage signaling and associated single-stranded DNA formation compared to wild-type cells. These data led to the hypothesis that Msh6 (together with Msh2) may control the DNA damage response by removing TLS replication errors, thereby generating single-stranded DNA tracts that activate DNA damage signaling. However, **Chapter 3** also shows that, in contrast to loss of Msh6, loss of Mlh1 or Pms2 does not result in the reduction of damage signaling and single-stranded DNA formation, which may suggest that some Mlh1/Pms2-independent processes take place that generate these ssDNA gaps. Taken together, the data in **Chapter 3** suggest that all four canonical MMR genes, *Msh2*, *Msh6*, *Mlh1* and *Pms2*, play a role in suppressing UV-induced mutagenesis.

Chapter 4 investigates the hypothesis that the control of UV light-induced mutagenesis by MMR correlates with the extent of error-prone TLS replication. To this end, *Polymerase H* (*Polh*)-deficient cells were generated and analyzed. *Polh* encodes for TLS Polymerase eta, which can bypass UV damage in a relatively error-free manner. When *Polh* is lost, more error-prone TLS polymerases bypass UV lesions, resulting in enhanced UV-induced mutagenesis. Thus, if MMR reduces mutagenicity resulting from TLS errors, then loss of MMR must be even more detrimental in *Polh*-deficient cells than in *Polh*-proficient cells. To evaluate this hypothesis, *PolhMsh6* and *PolhMlh1* double knock-out cell lines were generated. In support, loss of Msh6 or Mlh1 in *Polh*-deficient cells further increased UV-induced mutagenesis, even higher than the sum of UV-induced mutagenesis in the single knock-out cell lines. Additionally, the removal of TLS errors by MMR would result in single-stranded DNA tracts and concomitant induction of DNA damage signaling. Loss of Msh6 in *Polh*-deficient cells led to reduced UV-induced single-stranded DNA formation and damage signaling. Consistent with the results described in **Chapter 3**, a deficiency for *Mlh1* in a *Polh*-deficient background

did not result in the loss of single-stranded DNA formation and damage signaling. Interestingly, previously published works have shown that MMR proteins Msh2/Msh6 can recruit TLS polymerases to the site of damage and, in addition, might be involved in promoting error-free template switching to bypass a DNA lesion. These findings together with the work presented in **Chapter 4** may provide a model to explain the control of the DNA damage response by MMR in a two-step process: (i) MMR removes TLS errors, thereby preventing mutagenesis and promoting DNA damage signaling and checkpoint activation, and (ii) Msh2/Msh6 subsequently promotes error-free bypass either by TLS or by template switching which will quench DNA damage signaling and checkpoint activation.

Patients with LS display a remarkable restricted cancer tropism as most LS patients develop colon cancer. **Chapter 5** aimed to investigate the hypothesis that cells containing one dysfunctional copy of an MMR gene, such as intestinal stem cells of LS patients, are at greater risk from the adverse effects of food-derived genotoxic compounds. To test this hypothesis, mouse embryonic stem cell models were generated that resemble LS cells by containing only one wild type allele of either the MMR gene *Msh2* or *Mlh1*. These cells were exposed to 2-Amino-1-methyl-6-phenylimidazo(4,5-b)pyridine (PhIP), a mutagen found in meat grilled at high temperatures that induces helix-distorting DNA lesions. **Chapter 5** shows that *Msh2* or *Mlh1* heterozygous cells lost MMR at a significantly higher frequency than WT cells when exposed to PhIP. Moreover, previous literature has shown that loss of MMR may result in aggravated hypermutagenesis from various DNA-damaging agents. In **Chapter 5**, these findings were corroborated by showing that defects in either one of the four core MMR genes (*Msh2*, *Mlh1*, *Msh6* and *Pms2*) enhanced PhIP-induced mutagenesis in mouse embryonic stem cell lines. Finally, loss of *Msh2* resulted in the loss of protective DNA damage signaling, which may give these MMR-deficient cells a growth advantage. Taken together, the data in **Chapter 5** suggest that PhIP may drive oncogenesis in LS patients on three levels: (i) by increasing the frequency at which MMR-heterozygous cells become MMR-deficient; (ii) the resulting MMR-deficient cells have lost the capability to suppress PhIP-induced mutagenesis; and (iii) they have also lost protective DNA damage signaling. As such, this data may be important in advising LS individuals to adopt a lifestyle that reduces exposure to DNA-damaging agents, such as those found in unhealthy diets. Moreover, the findings in **Chapter 5** may explain why LS patients predominantly develop colon cancer, as this tissue type is constantly exposed to dietary DNA-damaging agents.

In conclusion, this thesis shows the importance of MMR in the regulation of DNA-damage induced mutagenesis and the implications of these findings for both healthy individuals and LS-patients. This thesis describes a pathway in which MMR is first required to remove the misincorporation opposite a DNA damage and is subsequently required to facilitate the (error-free) bypass of the DNA lesion by recruiting either TLS polymerases or template switch components. **Chapter 6** discusses the results and models described in this thesis in more detail and in light of previously published works. Moreover, **Chapter 6**, describes possible next steps for the research presented in this

thesis, such as the continued investigation of which proteins, for example exonucleases other than Exo1 and Fan1, are involved in MMR-activity on damaged DNA. Another interesting next step would be to investigate how MMR recognizes and removes misincorporations opposite damaged DNA. For instance, this could involve measuring MMR activity on substrates with a misincorporation opposite a DNA damage. Additionally, studying the binding of Msh2/Msh6 to a PhIP-adduct containing mismatch would provide valuable insights. Finally, this thesis shows that DNA damage is particularly hazardous for individuals that have lost MMR partially or completely and **Chapter 6** discusses the clinical implications of this finding in detail. Altering the diet to minimize DNA damaging agents in the colon would be good advice for patients with an MMR-defect.

Samenvatting

Mutagenese, het proces dat veranderingen in de DNA-sequentie veroorzaakt, is de onderliggende oorzaak van veel ziektes die we als mensheid te voorduren hebben, de meeste bekende daarvan is kanker. Mutagenese ontstaat vaak tijdens DNA-replicatie en **hoofdstuk 1** bespreekt in detail hoe dit proces werkt. In het kort: tijdens de replicatie van dubbelstrengs DNA worden de beide DNA strengen van elkaar gescheiden om te worden verdubbeld door replicatieve DNA polymerases. Wanneer een replicatieve DNA-polymerase tijdens het verdubbelen van het DNA een foutieve nucleotide inbouwt ontstaat er een 'mismatch' die tijdens een volgende ronde van replicatie een mutatie kan worden. DNA-mismatch herstel (mismatch repair, MMR) kan deze mismatches detecteren en opruimen waardoor een mutatie in het DNA voorkomen wordt. In **hoofdstuk 1** wordt beschreven hoe het MMR-proces werkt: de MMR-eiwitten MSH2 en MSH6 vormen een dimeer wat mismatches kan herkennen en MSH2/MSH6 rekruteren vervolgens een dimeer bestaande uit MLH1 en PMS2 om een enkelstrengs breuk in de DNA-streng met de verkeerd ingebouwde nucleotide aan te brengen. Ten slotte kan EXO1, een exonuclease, gerekruteerd worden om een gedeelte van de nieuw gegeneerde DNA-streng te verwijderen, inclusief de mismatch. De noodzaak van EXO1 in het MMR-proces staat ter discussie omdat andere (exo)nucleases, waaronder FAN1, mogelijk de rol van EXO1 kunnen overnemen als EXO1 niet beschikbaar is. Andere eiwitten spelen mogelijk ook een rol in het MMR-proces, zoals PMS1 en MLH3. Deze eiwitten lijken op MLH1 en PMS2, maar hun exacte functie is tot op heden onduidelijk. Daarnaast leidt verlies van PMS1 of MLH3 niet tot een grote verstoring in het MMR-proces. In principe zijn er dus vier 'kern'-genen in het MMR-systeem, namelijk *MSH2*, *MSH6*, *MLH1* en *PMS2*. Verlies van één van deze genen leidt tot een niet-functionerend MMR-proces, resulterend in een verhoogde mutagenese en een verhoogd risico op kanker. Naast MMR beschrijft **hoofdstuk 1** ook de verschillende soorten DNA-schades en de bijbehorende DNA-herstelsystemen. Niet opgeruimde DNA-schade kan de DNA-dubbele helix zo vervormen dat replicatieve DNA polymerases het DNA niet meer kunnen verdubbelen. Als dit gebeurt activeert de cel de DNA-schadesignalering wat er uiteindelijk voor kan zorgen dat de cel doodgaat, maar het kan er ook voor zorgen dat mechanismen die DNA-schade kunnen tolereren geactiveerd worden, denk bijvoorbeeld aan de rekrutering van translesie synthese (TLS) polymerases. TLS polymerases kunnen beschadigd DNA repliceren waardoor de DNA-schadesignalering wordt afgeschaald en celdood vermeden wordt. Echter, TLS polymerases maken relatief veel fouten wat vaak leidt tot een verhoging van de mutagenese. Ons DNA wordt continue aangevallen door DNA-beschadigende stoffen, substanties die bijvoorbeeld in ons dieet zitten, waardoor het erg belangrijk is om uit te vinden of en hoe mutagenese door TLS polymerases gecontroleerd en beperkt wordt. In dit proefschrift is onderzocht of TLS en DNA-schade responsen gecontroleerd worden door MMR waardoor de DNA-schade geïnduceerde mutagenese beperkt blijft.

In **hoofdstuk 2** wordt de rol van MMR in de DNA-schade respons beschreven. Uit dit literatuuroverzicht blijkt dat MMR een onmiskenbare rol speelt in de reactie op DNA-

schades die veroorzaakt worden door agentia die de DNA-helix structuur verstoren, het DNA alkyleren, het DNA oxideren of de DNA strengen covalent verbinden (interstrand crosslinken). Verlies van MMR kan resulteren in verhoogde cellulaire resistentie tegen deze verschillende DNA-schades. Verlies van MMR leidt vaak ook tot een verhoging van de mutagenese. **Hoofdstuk 2** laat verder zien wat de implicaties zijn van het verlies van MMR voor de ontwikkeling en de behandeling van kanker. DNA beschadigende stoffen worden namelijk vaak gebruikt om kanker te behandelen, maar verlies van MMR kan kankercellen juist resistent maken tegen zulke medicijnen. Sterker nog, deze medicijnen kunnen ervoor zorgen dat er in het voorstadium van kanker een omgeving ontstaat waarin cellen met een defect in MMR juist heel goed gedijen wat tot nieuwe tumoren kan leiden. Verder wordt in **hoofdstuk 2** verondersteld dat DNA beschadigende stoffen extra gevaarlijk zijn voor mensen met Lynch syndroom (LS), een erfelijk overdraagbare ziekte veroorzaakt door een dysfunctioneel MMR gen.

Hoofdstuk 2 beschreef de belangrijke rol van MMR in het beperken van mutagene effecten van DNA beschadigende stoffen en in de activatie van DNA-schade responsen. Een paar belangrijke vragen bleven echter onbeantwoord: (i) hoe vermindert MMR de mutagenese veroorzaakt door DNA beschadigende stoffen, (ii) hoe activeert het vervolgens de DNA-schade signalering en (iii) welke andere eiwitten, die mogelijk een rol spelen bij MMR, zijn bij deze processen betrokken? In **hoofdstuk 3** wordt getracht deze vragen te beantwoorden met behulp van een panel van muis embryonale stamcellijnen, die deficiënt gemaakt zijn voor MMR-eiwitten Msh6, Mlh1 of Pms2, voor de exonucleases Exo1 of Fan1 en voor de MMR-homologen Mlh3 of Pms1. Als DNA-beschadigend agens is ultraviolet type C (UV) licht gebruikt, omdat UV licht zeer goed gekarakteriseerde mutagene en cytotoxische DNA-schades veroorzaakt die model staan voor DNA-schades veroorzaakt door een scala van mutagene chemische stoffen waaraan de mens kan worden blootgesteld. Al deze cellijnen bevatte nog een additioneel defect in *Xpa* wat ervoor zorgt dat de UV-schades niet tussentijds gerepareerd worden. De resultaten uit **hoofdstuk 3** laten duidelijk zien dat Msh6, Mlh1 en Pms2 beschermen tegen UV-geïnduceerde mutagenese, maar voor de andere onderzochte eiwitten werd dit fenotype niet gevonden. Voor Exo1 en Fan1 kan dit komen omdat hun functie overgenomen kan worden door andere (exo)nucleases. Hetzelfde kan gezegd worden Mlh3 en Pms1, die beiden kunnen binden aan Mlh1; deze eiwitten delen mogelijk hun functie met *Pms2*. **Hoofdstuk 3** beschrijft tevens dat *Msh6*-deficiente cellen, in vergelijking met wild-type cellen, een flinke vermindering laten zien in UV-geïnduceerde enkelstrengs DNA-formaties en de daarmee geassocieerde DNA-schadesignalering. Hetzelfde kan echter niet gezegd worden voor *Mlh1* en *Pms2*, wat kan betekenen dat *Mlh1/Pms2*-onafhankelijke processen kunnen zorgen voor deze enkelstrengs DNA-formaties. Samenvattend, de resultaten in **hoofdstuk 3** suggereren dat *Msh2*, *Msh6*, *Mlh1* en *Pms2*, die essentieel zijn bij het opruimen van mismatches ontstaan door replicatieve DNA polymerases, tevens een rol spelen in het onderdrukken van UV-schade geïnduceerde mutagenese. Deze resultaten leidden tot de hypothese dat MMR TLS-geassocieerde

replicatiefouten verwijderd, wat vervolgens leidt tot de waargenomen enkelstrengs DNA-formaties en de activatie van DNA-schade responsen.

In **hoofdstuk 4** zijn studies beschreven met muis embryonale stamcellen die deficiënt zijn gemaakt voor *Polymerase H (Polh-)*, het gen dat codeert voor polymerase Eta (Pol η). Deze cellen zijn gebruikt om te onderzoeken of MMR beschermt tegen TLS-geassocieerde replicatiefouten en op die manier UV-geïnduceerde mutagenese beperkt. Pol η is een TLS polymerase dat UV-beschadigd DNA juist relatief foutloos kan repliceren. Als *Polh* niet meer aanwezig is, kunnen andere TLS polymerases het UV-beschadigde DNA te repliceren. Echter deze andere TLS polymerases maken vaker fouten wat leidt tot een verhoging van de UV-geïnduceerde mutagenese. Als het beschermend effect van MMR op UV-geïnduceerde mutagenese gecorreleerd is aan de mate van TLS replicatiefouten, dan zou het verlies van MMR in deze *Polh*-deficiënte cellen moeten zorgen voor een nog hogere UV-geïnduceerde mutagenese dan in *Polh*-proficiënte cellen. Om deze stelling te onderzoeken zijn er *PolhMsh6* en *PolhMlh1*-deficiënte cellen gemaakt en deze zijn vervolgens blootgesteld aan UV-straling. De resultaten lieten zien dat UV-geïnduceerde mutagenese hoger is in deze dubbelmutanten dan in de enkelmutanten, zelfs als de getallen van de enkelmutanten bij elkaar worden opgeteld. Verder lieten de resultaten in **hoofdstuk 4** zien dat verlies van *Msh6* in een *Polh*-deficiënte achtergrond ook resulteert in een verlaging van de UV-geïnduceerde enkelstrengs DNA-formaties en geassocieerde DNA-schade signaleringen. Consistent met de resultaten in **hoofdstuk 3**, zorgde het verlies van *Mlh1*, ook in *Polh*-deficiënte achtergrond, niet voor een vermindering van enkelstrengs DNA en DNA-schade signalering. Een verklaring hiervoor zou gevonden kunnen worden in eerder gepubliceerd werk wat laat zien dat *Msh2/Msh6*, en niet *Mlh1/Pms2*, verantwoordelijk zijn voor de rekrutering van TLS polymerases naar beschadigd DNA. Ander werk laat zien dat *Msh2/Msh6* juist zorgen voor de activatie van template switching, een route om tijdens replicatie DNA-schades foutloos te passeren. Deze twee waarnemingen en de resultaten beschreven in **hoofdstuk 4** suggereren dat MMR in twee stappen DNA-schade responsen controleert: (i) MMR verwijderd TLS fouten waardoor DNA-schade signalering wordt geactiveerd en mutagenese wordt voorkomen en (ii) *Msh2/Msh6* rekruteert vervolgens TLS polymerases om de DNA schade mogelijk foutloos te repliceren of *Msh2/Msh6* zorgt voor de activatie van het foutloze template switching om op die manier mutagenese te voorkomen en DNA-schade signalering uit te doven.

Ondanks dat alle lichaamscellen van LS-patiënten heterozygoot zijn voor een MMR-gen, ontwikkelen de meeste LS-patiënten voornamelijk darmkanker. Het onderzoek beschreven in **Hoofdstuk 5** was er opgericht om de vraag te beantwoorden of cellen die één disfunctionele kopie van een MMR-gen bevatten, zoals de darmcellen van LS-patiënten, een groter risico lopen op de nadelige effecten van genotoxische verbindingen uit voedsel dan wild-type cellen. Om dit te onderzoeken werden muis embryonale stamcel modellen gegenereerd die lijken op LS-cellen doordat ze 1 werkende en 1 defecte kopie van het *Msh2* of *Mlh1*-gen hebben. Deze cellen werden vervolgens blootgesteld aan 2-Amino-1-methyl-6-phenylimidazo(4,5-b)pyridine (PhIP),

een mutagene stof dat wordt gevormd tijdens het grillen van vlees op een hoge temperatuur en dat helix-verstorende DNA-schades veroorzaakt. **Hoofdstuk 5** laat zien dat cellen heterozygoot voor Msh2 of Mlh1 met een hogere frequentie deficiënt werden voor MMR dan wild-type cellen wanneer deze blootgesteld werden aan PhIP. Eerder gepubliceerd werk liet zien dat cellen die MMR zijn verloren extra vatbaar waren voor mutagenese geïnduceerd door verschillende types van DNA-schade. In **hoofdstuk 5** werden deze bevindingen bevestigd door in muis embryonale stamcellen aan te tonen dat PhIP-geïnduceerde mutagenese wordt versterkt door defecten in een van de vier MMR-kerngenen (*Msh2*, *Mlh1*, *Msh6* en *Pms2*). Ten slotte resulteerde het verlies van Msh2 in verminderde DNA-schade signalering als gevolg van PhIP blootstelling. Dit kan ervoor zorgen dat MMR-deficiënte cellen een groeivoordeel hebben ten opzichte van MMR-proficiënte cellen als ze blootgesteld worden aan PhIP. Alles bij elkaar genomen suggereren de gegevens in **hoofdstuk 5** dat PhIP de oncogenese bij LS-patiënten op drie niveaus kan stimuleren: (i) door de frequentie te verhogen waarmee cellen, die heterozygoot zijn voor een van de MMR-kerngenen, MMR compleet verliezen; (ii) doordat de MMR-deficiënte cellen het vermogen hebben verloren om PhIP-geïnduceerde mutagenese te onderdrukken; en (iii) doordat deze cellen ook de DNA-schade signaleringsmechanismen zijn verloren waardoor de MMR-deficiënte cellen een groeivoordeel verkrijgen en normale cellen wegconcurreren. Als zodanig kunnen deze gegevens belangrijk zijn om LS-patiënten te adviseren een levensstijl aan te nemen waardoor ze zoveel mogelijk DNA beschadigende stoffen vermijden, stoffen die bijvoorbeeld veelvuldig voorkomen in bepaalde ongezonde diëten. Verder kunnen de bevindingen in **hoofdstuk 5** verklaren waarom LS-patiënten voornamelijk darmkanker ontwikkelen, doordat dit weefsel constant blootgesteld wordt aan DNA beschadigende stoffen uit het dieet.

Samenvattend laat dit proefschrift zien dat MMR een belangrijke rol speelt bij het reguleren van DNA-schade geïnduceerde mutagenese en wat de implicaties daarvan zijn voor gezonde individuen maar ook voor LS-patiënten. Dit proefschrift beschrijft een mechanisme waarin MMR eerst de misincorporatie verwijdert tegenover een DNA-schade, maar ook belangrijk kan zijn om vervolgens (error-free) bypass van de DNA-schade te faciliteren middels rekrutering van TLS polymerases of template switching componenten. **Hoofdstuk 6** bespreekt de resultaten en modellen beschreven in dit proefschrift in detail en in het licht van eerder gepubliceerde artikelen. Verder bespreekt **hoofdstuk 6** ook mogelijke vervolgstappen voor het onderzoek dat gepresenteerd wordt in dit proefschrift, zoals het verder onderzoeken van de verschillende eiwitten die bij het MMR-proces op beschadigd DNA betrokken kunnen zijn, zoals andere nucleases. Een andere interessante vervolgstap zou kunnen zijn om te onderzoeken hoe MMR-mismatches tegenover beschadigd DNA herkent en verwijdert. Dit kan bijvoorbeeld onderzocht worden door MMR-activiteit te meten op voor-geprepareerde DNA-substraten met DNA-schade of door de binding tussen Msh2/Msh6 en een mismatch met PhIP-schade te bestuderen. Tot slot laat dit proefschrift zien dat DNA-schade bijzonder gevaarlijk kan zijn voor mensen met disfunctionele kopieën van MMR-genen en **hoofdstuk 6** bespreekt de klinische

implicaties van deze conditie in meer detail. Het aanpassen van het dieet zodat er minder DNA-beschadigende verbindingen in de darmen terechtkomen zou een goed advies zijn voor patiënten met een MMR-beperking.

Curriculum Vitae

Robbert IJsselsteijn, geboren op 19 januari 1992, groeide op in Gouda, waar hij in 2009 de middelbare school afrondde. Tijdens zijn middelbare schooltijd ontwikkelde hij een grote interesse in biologie en scheikunde en startte daarom in 2010 met de studie Life Science and Chemistry aan de Hogeschool Utrecht. In 2013 bestudeerde hij het belang van microRNA's op de ontwikkeling van hoofd- en nekanker aan de Universiteit van Maastricht, en in 2014 onderzocht hij de regulatie van primaire ciliogenese door microRNA's aan de Université de Liège. Na het behalen van zijn HBO-diploma in 2014 zette hij zijn studie voort door te beginnen aan de master Molecular and Cellular Life Sciences aan de Universiteit Utrecht. Tijdens zijn master heeft hij aan de Universiteit Utrecht onderzoek gedaan naar de rol van oxysterol-bindende eiwitten bij de replicatie van enterovirussen, en vervolgens heeft hij bij de afdeling Humane Genetica van het Leids Universitair Medisch Centrum (LUMC) varianten van onzekere betekenis in het *BRCA2*-gen bestudeerd en geholpen bij het opzetten van een vergelijkbaar onderzoeksprotocol voor *BRCA1*-varianten. In 2016 behaalde hij zijn masterdiploma en in 2017 begon hij aan een promotieonderzoek bij de afdeling Humane Genetica van het LUMC. Tijdens zijn promotieonderzoek onderzocht hij of en hoe Mismatch Repair-eiwitten DNA-schade-responsen controleerden onder begeleiding van zijn co-promotor Dr. J.G. Jansen en projectleider Dr. N. de Wind. Tijdens zijn promotieonderzoek heeft hij ook verschillende script-, coderings- en data science-cursussen gevolgd, waardoor hij zijn passie voor IT-werk ontdekte. Na zijn vierjarige PhD-contract begon hij als IT-trainee bij Qquest en zette hij zijn IT-carrière voort als DevOps Engineer bij Eneco.

Dankwoord

Het leven kan soms een beetje voelen als een avontuur uit een boek, en ook al zijn we niet allemaal protagonisten op het wereldtoneel, we zijn wel de hoofdpersonen van ons eigen verhaal. Hierbij wil ik graag alle helden, mentoren, vertrouwelingen en anti-helden bedanken die een rol hebben gespeeld tijdens mijn promotietraject.

Allereerst wil ik graag alle leden van groep de Wind bedanken. We hebben mooie tijden gehad en interessante discussies gevoerd. De verscheidenheid aan hobby's, achtergronden en meningen hebben me veel geleerd over de wereld en hoe mensen deze waarnemen. Niels, onze groepsleider, ik heb je altijd bewonderd om je standvastigheid en dat je echt vecht voor je overtuigingen. Zonder jou zou ik niet zo sterk zijn als ik vandaag de dag ben. Jaap, mijn promotietraject zou niets zijn zonder jouw begeleiding. Bedankt voor alle tijd en moeite die je in mij gestoken hebt om me te leren hoe ik netjes kan werken en hoe ik mijn schrijfvaardigheden kan verbeteren, zelfs lang nadat mijn contract was afgelopen. Mark, ook jou wil ik bedanken voor je begeleiding. Jij was de balans die onze groep nodig had en ik heb je altijd bewonderd voor je luchtige houding, maar dat je tegelijkertijd ook heel serieus kon zijn wanneer dat nodig was. Sandrine, samenwerken met jou vond ik ontzettend leuk en gezellig. Je hebt me veel geleerd, niet alleen over het laboratorium, maar ook over het leven zelf. Aan alle huidige en voormalige leden van de feestkamer T3-11, ik kijk met veel plezier terug op de gezellige borrels, de escaperooms/gevangenissen en themaparken die we hebben bezocht.

Het promotietraject kan enorm veeleisend en stressvol zijn. Daarom wil ik graag ons afdelingshoofd, Silvère van der Maarel, mijn promotor Marcel Tijsterman en Frits Koning, de vertrouwenspersoon voor promovendi, bedanken voor hun hulp tijdens een zeer moeilijke periode.

Vaak loopt een promotietraject ook veel langer dan het standaard 4-jarige PhD contract. Ik was overdonderd en ben enorm dankbaar voor de ongelooflijke steun die mijn collega's bij Qquest en Eneco mij hebben gegeven in de periode na mijn LUMC-contract. Bedankt voor jullie steun, geduld en zelfs ingrijpen wanneer de situatie te veel voor me werd.

Een hele speciale dank aan mijn paranimf Renuka Ramlal, je bent er altijd voor me geweest tijdens de hoogte- en dieptepunten van mijn promotietraject. Samen hebben we gelachen en gehuild, en ik kan me niet voorstellen hoe ik het zonder jou had overleefd.

Aan mijn lieve familie, jullie snapte niet altijd wat ik deed of de keuzes die ik maakte. Desalniettemin hebben jullie me wel altijd gesteund. Enorm bedankt dat jullie er altijd voor me zijn.

Aan mijn vriendin, mijn beste vriend, mijn collega-wetenschapper, mijn paranimf en mijn vrouw, Marieke Erica Ijsselsteijn. Al 15 jaar lang ben jij de hoeksteen van mijn leven, zonder jou zou niets mogelijk zijn. Als een echte wetenschapper vond je steeds nieuwe en innovatieve manieren om me op te vrolijken wanneer het werk me verdrietig maakte. Tijdens de goede tijden stimuleerde je me om ambitieus te zijn en zei je dat ik mijn dromen moest najagen. Ik zal dit advies ter harte nemen en jou overal voor altijd op de voet volgen.

